A Mineralogical and Geochemical Study of the Tin Deposit at NAD-Mine in the Rooiberg Tin Field.

by

Karin Naudé

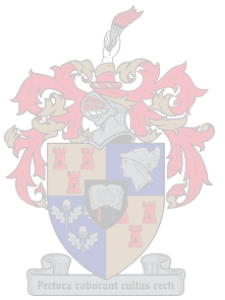

Thesis presented in partial fulfilment of the requirements for the degree Master of Science at the University of Stellenbosch.

June 1994

Study Leader: Professor D.K. Hallbauer

Declaration:

I, the undersigned, hereby declare that the work contained in this thesis is my own original work and has not previously in its entirety or in part been submitted at any university for a degree.

Stellenbosch

Karin Naudé Date

Acknowledgements

The writer is indebted to Gold Fields of South Africa Limited for permission to conduct this study on the NAD tin mine in the Rooiberg tin field. She would also like to extend her thanks to Mr J. Misiewicz for the accompanied underground visits.

The W.P. de Kock and Stellenbosch 2000 bursaries enabled the writer to commence this study and she would like to thank the authorities who made it possible. Also, an overseas study visit would not have materialized without a contribution from the Harry Crossley Fund; it created a wonderful opportunity to work with Prof. D. Wolf of the Bergakademie Freiberg in Germany and with Mr M. Cuney of CREGU in France. The discussions and guidance from these expert scientists were of great value. Without the valuable help and discussions with her study leader, Prof. D.K. Hallbauer, completion of this study would not have been possible. The encouragement from and discussions with other staff-members at the Geology Department of the University of Stellenbosch are not forgotten.

She would also like to thank Mr E.H. Basson of EMATEK, CSIR in Pretoria for his help and patience and time spent on the sophisticated computers and computer software at the CSIR, during compilation of the diagrams in the thesis. Thank you to Ms M. Wiesner for her contribution towards the correction of grammatical errors and style of the thesis.

Heartfelt gratitude is extended towards the writer's family for the opportunity to study, and for encouragement and support throughout these studies. A special word of thanks to Mr G.F. van der Merwe who spent many a late night with the writer and who was always ready to discuss matters.

Abstract

The NAD deposit forms part of the A-Mine Complex in the Rooiberg tin field in the north-western Transvaal. Mining started in 1986 and the mine was closed recently following a decline of tin prices and metallurgical problems with ore recovery.

The deposit is hosted by the Boschoffsberg Quartzite Member of the Pretoria Group sediments and is structurally controlled within the so-called Tin Zone. Extensive alteration of the original host rocks occurred during the mineralisation event. Potassic remobilisation and redistribution appear to have taken place pervasively. The nature of the original host rock was altered to such an extent that it cannot be classified correctly. Previous workers refer to the host rock as an arkose because of its feldspathic nature. Wall rock alteration in the hanging- and foot wall of the different ore lodes (fractures) is generally similar. Very little change is observed in whole rock chemistry away from the lodes.

The mineral chemistry of the ore lode minerals is indicative of fluid composition and mineralising conditions in the NAD deposit. The FeO/(FeO + MgO) ratio of tourmalines indicates deposition at a distance from the source of the mineralising fluids. Pyrite trace element chemistry differs from that of the Leeuwpoort deposit, indicating changing fluid chemistry. Contrary to previous assumptions that the carbonate present is ankerite, abundant siderite occurrences were found. Pyrite may co-precipitate with siderite under specific physico-chemical conditions. Cassiterite is generally trace element poor and relatively enriched in Fe.

Hydraulic brecciation of the fractures as well as the tourmaline chemistry are strong indicators of a hydrothermal origin for the NAD deposit. However, the origin of the hydrothermal fluids is still uncertain.

Opsomming.

Die NAD- tinafsetting vorm deel van die A-Myn-kompleks in die Rooiberg tinveld in die noord-wes Transvaal. Die myn is in 1986 geopen en is onlangs gesluit weens swak tinpryse en metallurgiese ertsherwinningsprobleme.

Die tinafsetting kom voor in die Boschoffsberg Kwartsiet lid van die Pretoria Groep sedimente. Dit is struktureel gekontroleer binne die sogenaamde Tin Sone.

Vorige navorsers het na die waardgesteente as 'n arkose verwys op grond van die hoë veldspaat-inhoud. Intensiewe en uitgebreide verandering van die oorspronklike waardgesteentes het plaasgevind tydens mineralisasie. Deurdringende kalium-hermobilisering en -herverspreiding het plaasgevind. Die aard van die oorspronklike waardgesteente is egter tot so 'n mate verander, dat dit chemies nie korrek geklassifiseer kan word nie. Wandrotsverandering van die verskillende ertsskeute in beide die voet- en dakgesteentes is baie soortgelyk. Die heelrotsgeochemie van die wandgesteentes verskil baie min weg van die ertsskeute af.

Die mineraalchemie van die ertsskeut-minerale is aanduidend van die vloeistofsamestelling en mineralisasietoestande van die NAD-tinafsetting. Die FeO/(FeO + MgO) verhouding van toermalyne dui daarop dat afsetting op 'n afstand vanaf die bron van die mineralisasie-vloeistowwe plaasgevind het. Die spoor-elementchemie van die NAD-piriete verskil van die piriete van die Leeuwpoort tinafsetting, wat verandering in vloeistofsamestelling aandui. In teenstelling met vorige aannames dat die karbonate in die Rooiberg tinafsettings as ankeriet bekend staan, is daar volop sideriet gevind. Piriet kristalliseer dikwels saam met sideriet onder spesifieke fisiese en chemiese toestande. Kassiteriet is meestal arm aan spoor-elemente, maar is relatief verryk in Fe.

Hidroliese breksiëring van die skeute en die toermalyn-chemie dui sterk op 'n hidrotermale oorsprong vir die NAD afsetting. Die bron van die vloeistowwe is nog nie definitief vasgestel nie.

A Mineralogical and Geochemical Study of the Tin Deposit at NAD-Mine in the Rooiberg Tin Field.

CONTENTS

1. **Chapter 1. Introduction.**

1.1. Aims of Investigation. 1.1

1.2. Classification of World-wide Tin Deposits. 1.2

1.3. The Rooiberg Tin Field. 1.9

2. **Chapter 2. Regional Geology of the Rooiberg Fragment.**

2.1. The Bushveld Tin Deposits. 2.1

2.2. The Structure of the North-Western Bushveld. 2.4

2.3. The Rooiberg Fragment. 2.5

2.3.1. The Stratigraphy of the Rooiberg Fragment. 2.5

2.3.1.1. The Boschoffsberg Quartzite Member. 2.5

2.3.1.2. The Blaauwbank Shale Member. 2.7

2.3.1.3. The Smelterskop Formation. 2.7

2.3.1.4. The Rooiberg Felsites. 2.7

2.3.1.5. The Rashoop Granophyre Suite. 2.8

2.3.1.6. The Lebowa Granite Suite. 2.8

2.3.2. The Structure of the Rooiberg Fragment. 2.9

2.4. The Rooiberg Tin Deposits. 2.12

2.5. Major Structures in the NAD Deposit. 2.14

3. **Chapter 3. Sampling Techniques and Analytical Methods.** 3.1

4. **Chapter 4. Mineralogy and Geochemistry of the NAD Deposit.**

4.1. Previous Work on the Rooiberg Tin Deposits. 4.1

4.2. The Tin Zone Hypothesis. 4.4

4.3. Mineralogy and Petrography of the NAD Deposit. 4.7

4.3.1. Macroscopic Examination of the NAD Lodes. 4.7

4.3.2. Observations on the NAD Deposit. 4.10

4.3.3. Microscopic Examination of the NAD Deposit. 4.12

4.3.3.1. The Host Rock. 4.12

4.3.3.2. The Ore Lodes. 4.16

4.4. Geochemistry of the NAD Deposit. 4.17

5. **Chapter 5. Mineral Chemistry.**

5.1. Cassiterite Chemistry. 5.1

5.2. Tourmaline Chemistry. 5.4

5.3. Carbonate Chemistry. 5.13

5.4. Sulphide Chemistry. 5.17

6. **Chapter 6. The Chemical Nature of the Mineralising Fluids and Factors related to Ore Deposition.** 6.1

7. Chapter 7. Conclusions.

7.1. Discussion on the Formation of the NAD Deposit. 7.1

7.2. Recommendations. 7.3

References.

Appendices.

A. Sample Localities and Features.

B. Petrography: Paragenetic Tables.

C. Colour Plates.

D. Geochemistry Data.

- D.1. Major Element Whole Rock Chemistry.
- D.2. Trace Element Whole Rock Chemistry.
- D.3. Single Grain Mineral Chemistry.
  - D.3.1. Cassiterite Chemistry (SX50 and Camebax Data).
  - D.3.2 Tourmaline Chemistry.
  - D.3.3. Carbonate Chemistry.
  - D.3.4. Sulphide Chemistry.

Chapter 1 .

1. Introduction.

1.1. Aims of the Investigation.

This is a mineralogical and geochemical study of part of the Rooiberg tin field with special reference to the ore lode minerals (cassiterite, tourmaline, carbonate and sulphides), wall rock alteration and the chemical nature of the mineralising fluid as it occurs in the NAD mine. Since no formal mineralogical or geochemical studies have been conducted on the NAD deposit and because it exhibits steep fracture mineralisation, the NAD mine was an ideal case study of this type of mineralisation in the Rooiberg tin field. With the tin economy at a constant low this was possibly a last opportunity to study the tin deposits of the Rooiberg tin field, before closure of the mines.

The study is aimed at determining the extent of hydrothermal alteration within and away from the ore lodes, but within the general tin zone. No samples were available from outside the recognised tin zone, so that the extent of alteration within the tin zone cannot be compared directly to unaltered host rock. Data from the literature had to be used to exemplify possible fresh (unaltered) host rock.

The ore lodes are structurally controlled in NAD, and are identified as the Union-, Bonus-, Cotton-, B-, C-, T- and U-lodes. The positions of these fractures are illustrated in map A (folder). The lodes consist mainly of carbonate, tourmaline, cassiterite, pyrite and chalcopyrite. Some free quartz occurs, but is no major constituent of the ore lodes.

The fractures in the NAD deposit seem to be hydraulically brecciated fractures (appendix C, plate 10) with replacement bodies on hairline fractures

leading from the main ore lodes (fractures). During crystallisation of the Bushveld granite, volumetric shrinkage caused tensional conditions in the Rooiberg Fragment. This produced near-horizontal tensional fractures, forming bedded lodes such as in the Leeuwpoort tin deposit. Tensional fracturing influenced the NAD lodes to such an extent that the brecciated fragments within the lodes support each other, so that the fragments do not sink to the bottom of the fracture. This leaves a highly permeable fracture open for the mineralising fluid, and creates the impression that the brecciated fragments "float" within the carbonaceous matrix.

The study of cassiterite, tourmaline, carbonate and the sulphides in conjunction with wall rock alteration is also aimed at determining the chemical nature of the mineralising fluids. It was hoped to determine the physico-chemical conditions from the ore lode mineral paragenesis and from trace element chemistry which will reflect the conditions of fluid transportation and ore deposition. The NAD deposit will also be discussed within the framework of existing tin deposition models for the Rooiberg tin field.

The fine-grained nature of the NAD deposit probably indicates that it was among the last phases of mineralisation. NAD could therefore add valuable information to the crystallisation history of the Rooiberg tin deposits.

1.2. Classification of Worldwide Tin Deposits.

Taylor (1979) studied tin deposits world-wide, and classified them according to regional province, age, economic significance and the general environment (tables 1.1 and 1.2). This is a global classification and cannot be applied to smaller deposits within a larger tin province.

TABLE 1.1.
CLASSIFICATION OF TIN PROVINCES OF THE WORLD.

TYPE	REGION PROVINCE	AGE	ECONOMIC SIGNIFICANCE	GENERAL ENVIRONMENT
1	**North America**			
	Seward Peninsula - Alaska	Upper Cretaceous - Lower Tertiary	Minor P	P O, I
	New Brunswick Canada	Lower Carboniferous	Minor P	P O, I V
2	**South and Central America**			
	Bolivia	Tertiary (and Upper Triassic)	Major P	P O I VVV
	Mexico	Tertiary	Minor P - A	P O VVV (mostly)
	Brazil, Rondonia	(a) Precambrian	Intermediate A	F - V?
		(b) Precambrian	Minor P	C - G?
3	**Europe**			
	Cornwall, England	Upper Carboniferous - Permian	Intermediate P	P O I
	Erzgebirge Germany / Czechoslovakia	Lower Carboniferous	Intermediate P	P O I
	West Iberia, Spain, Portugal	Carboniferous - Permian	Minor P	P O I
	France, Massif Central Brittany	Carboniferous - Permian	Minor P	P O I
4	**Africa**			
	Nigeria	(a) Jurassic	Major A	F VV
		(b) Precambrian	Minor P	C G?
	Central Africa: Zaire Rwanda, Burundi, Uganda, Tanzania	Precambrian	Intermediate A P	C G - G?
	South Africa: Bushveld	Precambrian	Minor P	Part of BIC
	Zimbabwe, Zambia	Precambrian	Minor P	C G?
	Namibia	(a) Jurassic Cretaceous	Minor P	F V?
		(b) Precambrian	Minor P	C G?
	Swaziland	Precambrian	Minor P	C G
5	**South East Asia**			
	Thailand, Malaysia, Indonesia	Upper Carboniferous Tertiary (mostly Upper Triassic)	Major A	P O I
	Japan, Honshu	Upper Cretaceous - Tertiary	Minor P	P O VV

(continue)

TABLE 1.1. (Continued)
CLASSIFICATION OF TIN PROVINCES OF THE WORLD.

TYPE	REGION PROVINCE	AGE	ECONOMIC SIGNIFICANCE	GENERAL ENVIRONMENT
6	**Australia**			
	NW Tasmania	Middle-Upper Devonian	Intermediate A	P O I
	Herberton - Mt Garnet, Queensland	Upper Permian	Intermediate A P	P O I V (mostly I)
	NE Tasmania	Upper Devonian	Intermediate P	P O I
	New England, New South Wales	Upper Permian	Minor - Intermediate A	P O I
	Cooktown, Queensland	Permian	Minor A	P O I V (mostly I)
	Albury - Ardlethan, New South Wales	Upper Devonian	Minor A P	P O I
	Kangaroo Hills, Queensland	Carboniferous - Permian	Minor P	P O I (V?)
	Greenbushes, W Australia	Precambrian	Minor A	C - G?
	Pilbara, W Australia	Precambrian	Minor A	C - G
	Northern Territory	Precambrian	Minor P	P O? - I?
	Broken Hill, New South Wales	Precambrian	Minor P	C - G
7	**USSR**			
	Yakutia & Kolmya	Upper Jurassic - Lower Cretaceous	Intermediate - Major ? A P	P O I V (mostly I)
	Southern Maritime Territory (Sikhote Alin)	Upper Cretaceous - Lower Tertiary	Intermediate - Major P	P O VVV
	Chukotka			
	Transbaikal	Middle Jurassic - Lower Tertiary	Intermediate - Major ? A P	P O V
	East Kazakstan	Upper Jurassic - Lower Cretaceous	Intermediate - Major P	P O I VV
	Maly Khingan	Permian	Intermediate P?	P O I V (mostly I)
	Miao Chang - Komsomol'sk	Upper Cretaceous - Lower Tertiary	Minor - Intermediate P	P O VVV
	Central Asia Group	Upper Cretaceous	Minor P	P O I
	East Sayan	Upper Carboniferous? - Permian?	Minor P	P O I
	Ladoga-Karelia, Baltic	Precambrian	Minor P	C - G
		Precambrian	Minor P	C - G
8	**China**	Late Mesozoic: no details available		
	Kwangsi-Kwangtang, Hunan Province			
	Coastal Zone			
	Kochiu			
	Hainan			

(after Taylor 1979)

Footnote

Some minor provinces in the USSR have been merged and details concerning China are unknown.

Symbols utilised:

P Predominately Primary

A Predominately Alluvial

PO Post-orogenic
Deposits associated with granitoids emplaced in close relationship with a major period of orogeny (i.e. folding, fracturing and uplift). Granitoid emplacement predominantly post-dates major folding

I Intrusive
Deposits associated with granitoids show no direct evidence of a volcanic association.

V Volcanic
Deposits associated with granitoids which are spatially and temporally linked with acid volcanic extrusives, VVV indicates strong volcanic association

F Fracture
Deposits associated with granitoids emplaced along major zones of fracturing in a non-orogenic setting (i.e. not associated with a major period of fold development).

C Cratonic
Deposits associated with ancient cratonic shield areas. Geological details concerning connection with major orogeny uncertain. Spatial association with granitoids ranges from close (G) to uncertain (G?).

The NAD deposit forms part of the Rooiberg tin field, which in turn forms part of the Bushveld tin province. The Bushveld tin province is a unique deposit. There are, however, small differences between the tin deposits in the Bushveld tin province. All the deposits are related to the Bushveld Complex, but some are endogranitic (occurring within the mineralising granite such as at Zaaiplaats) and others are exogranitic (occurring in the surrounding rocks of the mineralising granite such as at Rooiberg). Further differences are mineralogical: Zaaiplaats is a fluorine- and boron-enriched deposit, while Rooiberg is a boron-enriched deposit. These differences imply different formation and deposition conditions for the various deposits, even though they are all related to the Bushveld granites. Table 1.1 indicates four major trends in the tin provinces world-wide, as described by Taylor (1979).

1. Tin occurrences range from the Precambrian to the Tertiary in age.
2. Four tin bearing environments can be identified from table 1.1:
   a. Granitoids associated with layered igneous complexes of the Bushveld type.
      (1 province)
   b. Anorgenic granitoids associated with major fracturing - rifting of stable cratonic zones.
      (3 provinces)
   c. Precambrian cratonic shields excluding types (a) & (b) above.
      (11 provinces)
   d. Granitoids normally associated with post Precambrian mobile zones and periods of major orogeny (i.e. post orogenic emplacement within fold belts).
      (30 provinces)
3. Provinces classified as of major to intermediate economic significance are mostly within the orogenic group (d) (13/16). Precambrian concentrations are usually of minor economic significance (11/13) and are rarely exploited without alluvial enrichments.
4. The major orogenic grouping is reflected by clustering around periods of major crustal orogeny.

Early concepts from the USSR stressed classification based on mineralogical characteristics. More recently, Itsikson (1960 in Taylor 1979) related tin deposits to different types of batholithic regions produced at different stages in the development of fold belts. Table 1.2 represents an expansion of the Itsikson approach and has been compiled from provincial data contained in Taylor (1979). The magmatic environments represented by orogenic fold belt provinces can be conveniently categorised into volcanic, sub-volcanic hypabyssal and plutonic. This arrangement is better conceptualised as an overlapping spectrum of environments that form a complete series.

TABLE 1.2.
ENVIRONMENTS CONTAINING SIGNIFICANT PRIMARY CONCENTRATIONS OF TIN

	GENERAL ENVIRONMENT	ASSOCIATED IGNEOUS ROCKS	COMPOSITION OF IGNEOUS ROCKS	EXAMPLES
1	**FOLD BELT TYPE** Tin deposits associated with granitoids showing close spatial and temporal relationship with a major period of orogeny. Granitoid emplacement predominantly post major folding.			
a	Tin concentrations associated predominantly with extrusives and pyroclastics. Minor related intrusives.	Terrestrial lava flows, tuffs, volcanic breccias. Minor stocks- dykes and intrusive sheets with volcanic, non porphyritic to minor porphyritic textures.	Predominantly rhyolites with andesites, dacites and latites.	Mexico
b	Tin concentrations associated with intrusive complexes of sub-volcanic nature occurring in association with terrestrial extrusives.	Small stocks, pipes and irregularly shaped intrusives. Often steep walled and funnel shaped at depth. Associated dykes, dyke swarms, sills, breccia pipes.	Diverse composition with porphyritic textures predominating. Granite porphyry, quartz porphyry, dacite, quartz latite porphyry, quartz diorite, granodiorite, granite. Aplites and pegmatites are very rare. Volcanics are predominantly rhyolites and andesites.	Bolivia (south) Southern Maritime Territory USSR Ardlethan-Albury, Australia Japan Maly Kinghan, USSR Miao Chang, USSR
c	Tin concentrations associated with intrusive complexes of mixed character, i.e. representing a deep volcanic to high plutonic environment. Extrusive rocks mostly absent, but may be present.	Wide diversity in form ranging from small stocks to large scale intrusive complexes. Major massifs-batholiths are often very complex and contain a large number of intrusive phases. Active repeated intrusion prevails over a more passive environment. At upper levels garlands or rosary chains of small granitoids associated with regional fractures reflect the deeper batholith structures. Geochemically specialised granitoids are often present and may form clear end members of granodiorite-granite differentiation sequence. Dykes and swarms are normally abundant, although often irregularly distributed. Aplites and pegmatites are uncommon.	Diverse composition, granites and granitoids prevail with minor monzonites, diorites. Evidence of hybridism occurs in some provinces resulting in "diorites", andesine granites. Plutonic textures prevail over porphyritic.	Herberton, Australia Kangaroo Hills, Australia Chukotka, USSR Yakutia, USSR New England, Australia ? Northern Territory, Australia Transbaikal, USSR New Brunswick, Canada.

(continue)

TABLE 1.2. (continued)
ENVIRONMENTS CONTAINING SIGNIFICANT PRIMARY CONCENTRATIONS OF TIN

	GENERAL ENVIRONMENT	ASSOCIATED IGNEOUS ROCKS	COMPOSITION OF IGNEOUS ROCKS	EXAMPLES
d	Tin occurrence associated with intrusive complexes of plutonic character. Extrusives absent. Dykes and dyke swarms are minor.	Intermediate to large scale intrusive complexes. Massif-batholiths generally contain a small number of individual plutons. Differentiation sequences are often well established between phases, and a relatively passive intrusion environment is suggested. Geochemically specialised granites are common, and often form minor phase end members of a granodiorite - granite sequence.	Predominantly granites, granodiorites with minor alaskites, leucogranites and other specialised intrusives. Plutonic textures prevail. Aplites and pegmatites common.	Bolivia (north) Erzgebirge, Czechoslovakia - GDR Cooktown, Australia Massif Central - Brittany, France Central Asia ?? Thailand-Malaysia-Indonesia ? Seward Peninsula, Alaska NE Tasmania
2	**ANOROGENIC TYPE** Tin deposits associated with granitoids emplaced via major zones of fracturing in cratonic shield areas. Granitoids are anorogenic.	Small ovate-circular intrusive ring complexes. Minor stocks; ring dykes are often capped by sheets. Minor volcanics. Groups of complexes show strong linear alignments.	Predominantly granite, microgranite and rhyolite. Alkali granites present in Nigeria. Plutonic and porphyritic textures present	Nigeria Brazil - Rondonia Namibia ?
3	**PRECAMBRIAN PEGMATITIC TYPE** Tin deposits associated with pegmatites in metamorphic terrains. Association with granitoids ranges from well established to uncertain. In many regions the geology is uncertain. Subtypes may be present.	Wide range of intrusive forms, e.g. batholiths domed complexes, stocks, sills. Plutonic and gneissic textures predominate. Geology is often uncertain.	Predominantly granites with minor alaskites. Pegmatites, aplites and granophyric phases are common.	Central Africa Pilbara, Australia Greenbushes, Australia Broken Hill, Australia Brazil, shield area Nigeria, shield area Zimbabwe Swaziland Namibia East Sayan, USSR
4.	**PRECAMBRIAN RAPAKIVI** Tin deposits associated with rapakivi granites in ancient metamorphic cratonic areas. May also be considered as a subtype of (3).	Massif-stocks of polyphase granitoids. Plutonic to porphyritic textures. Late phase of massifs is geochemically specialised for tin and associated with tin mineralisation.	Predominantly granite with porphyritic and pegmatitic phases. Pegmatites common.	Lodoga-Karalia, USSR
5.	**BUSHVELD TYPE** Tin deposits associated with granitoid members in ancient metamorphic cratonic terrains. Unique to the Bushveld Complex, South Africa.	Stratiform granitic sheet associated with felsitic extrusions and pyroclastics. Intruded by stocks of granite and underlain by sheets of gabbro and norite. Wide textural variation (plutonic to granophyric).	Predominantly granite - plutonic, porphyritic and granophyric.	Bushveld district, South Africa

Adapted from Taylor (1979)

1.3. The Rooiberg Tin Field.

The first reports on the Rooiberg tin fields date back to 1905, when the ancient tin workings were discovered. Mining in the Rooiberg tin fields started about 500 to 3000 years ago during the late Southern African Iron Age. This early mining activity ended in the mid-19th century. An estimated 2 000 tons of metallic tin were produced from 30 000 tons of ore. Modern mining began early in the 20th century, with Rooiberg Minerals Development Company registered in 1908. The Leeuwpoort Tin Mines Limited was formed in 1911 but was liquidated in 1932 when the mineral rights over the property were acquired by the Rooiberg Company. The Rooiberg Minerals Development Company was incorporated by the Gold Fields of SA Group in 1960. Several small mining companies were operative before 1960, and have been incorporated by the Rooiberg Minerals Development Company. The Rooiberg mines have all closed down recently (1993) due to the low tin price and poor economic viability.

The Rooiberg tin field is hosted by the Rooiberg Fragment, West-Central-Transvaal (figure 1.1, Rozendaal *et al* 1986). The Rooiberg Fragment lies approximately 60 km west of Warmbaths in the western lobe of the Bushveld Complex.

The Rooiberg Fragment is roughly triangular-shaped and consists of the Rooiberg Group (felsites) which is underlain by the rocks of the Pretoria Group sediments of the Upper Transvaal Sequence. The Transvaal Sequence has been dated at ca. 2350 to 2125 Ma (Walraven & Hattingh 1993), when it was deposited on the Archean Kaapvaal Craton in an elongate, east-west trending basin (Button 1976). The intrusion of the Bushveld Complex at ca. 2060 to 2049 Ma (Walraven & Hattingh 1993) had presumably detached the upper portion of the Transvaal Sequence from the bottom portion. Figure 1.2 (Stear 1977) displays this presumed detached roof-portion (the Rooiberg Fragment) within the surrounding Lebowa Granite

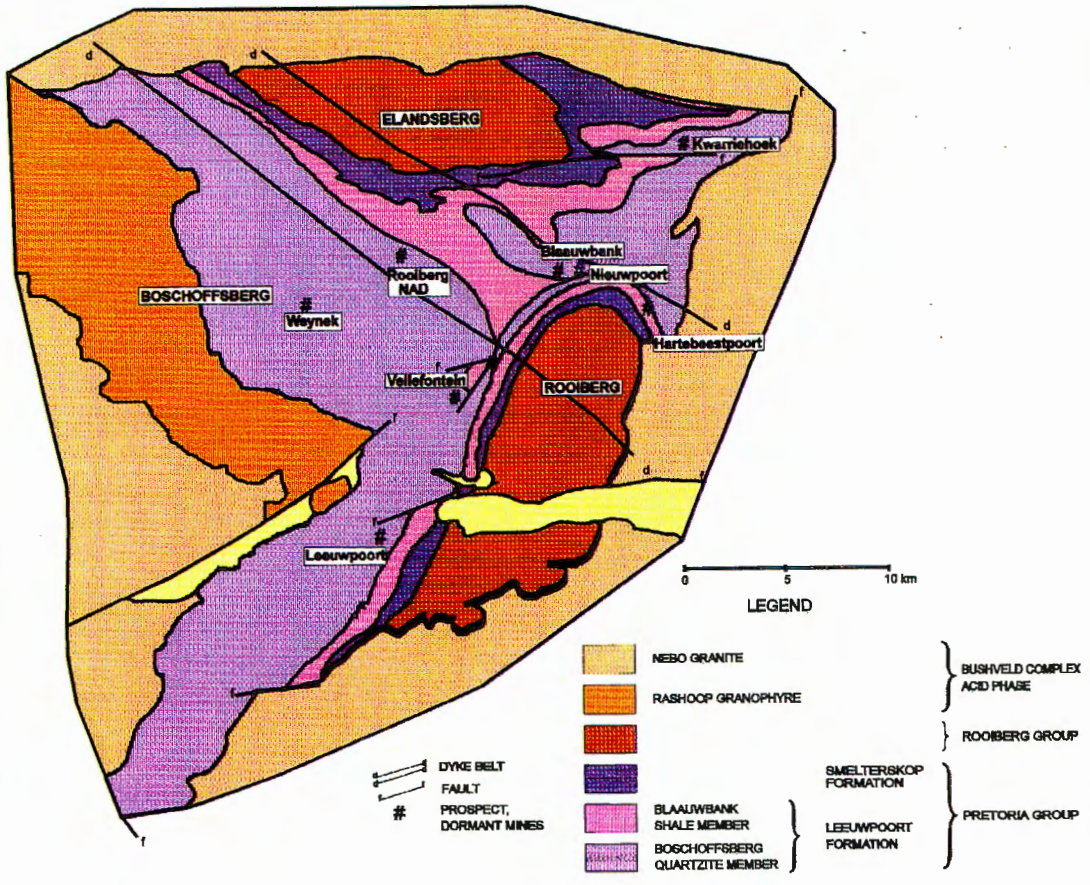

Figure 1.1. The general geology of the Rooiberg Fragment (after Rozendaal *et al* 1986).

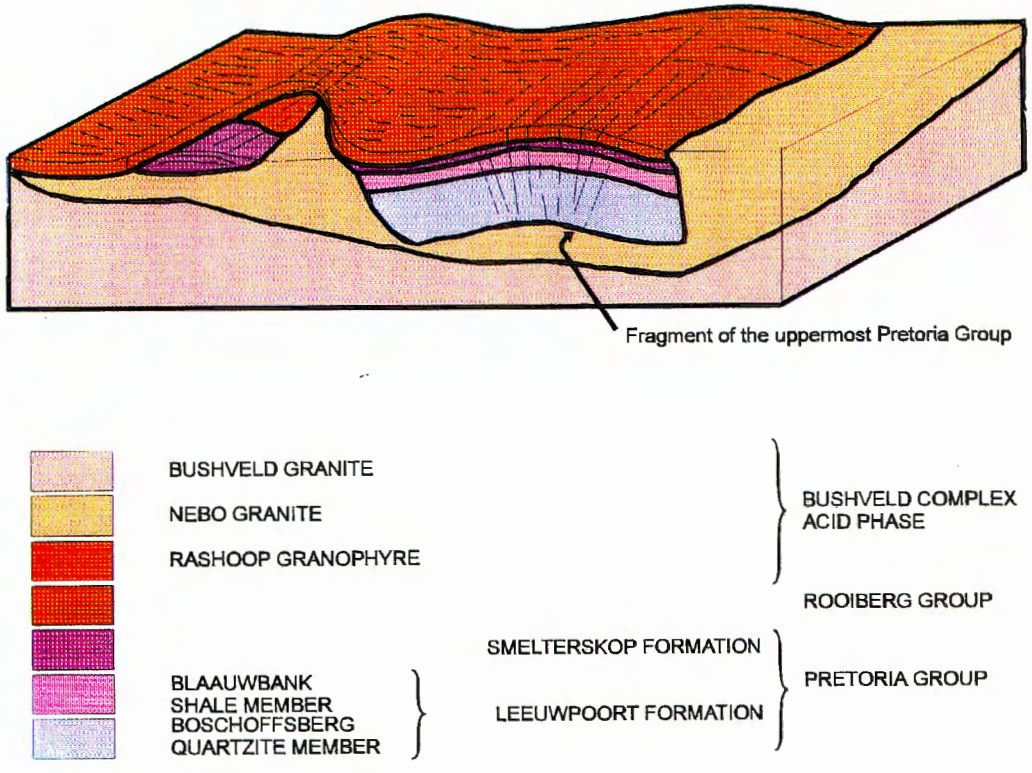

Figure 1.2. An idealised model of the drifting sediments of the Rooiberg Fragment (after Stear 1977).

Suite. Tin mineralisation is hosted in the Boschoffsberg Quartzite Member at the bottom of the Pretoria Group. The Nebo granite (dated to ca. 2054.4 ± 1.8 Ma), appears to be responsible for the tin mineralisation. Mineralisation was structurally controlled and evidence of a tin zone exists within structural boundaries.

The Rooiberg tin field consists of the Rooiberg A Mine Complex, Blaauwbank, Nieuwpoort, Hartebeestpoort, Weynek, Vellefontein and Leeuwpoort deposits. Leeuwpoort (C mine) was until recently (1993) the only productive mine, with NAD mine having been closed down earlier. The NAD deposit forms part of A Mine Complex (figure 1.3, unpubl. rep. Roberts 1983), and lies in close proximity to the Rooiberg town.

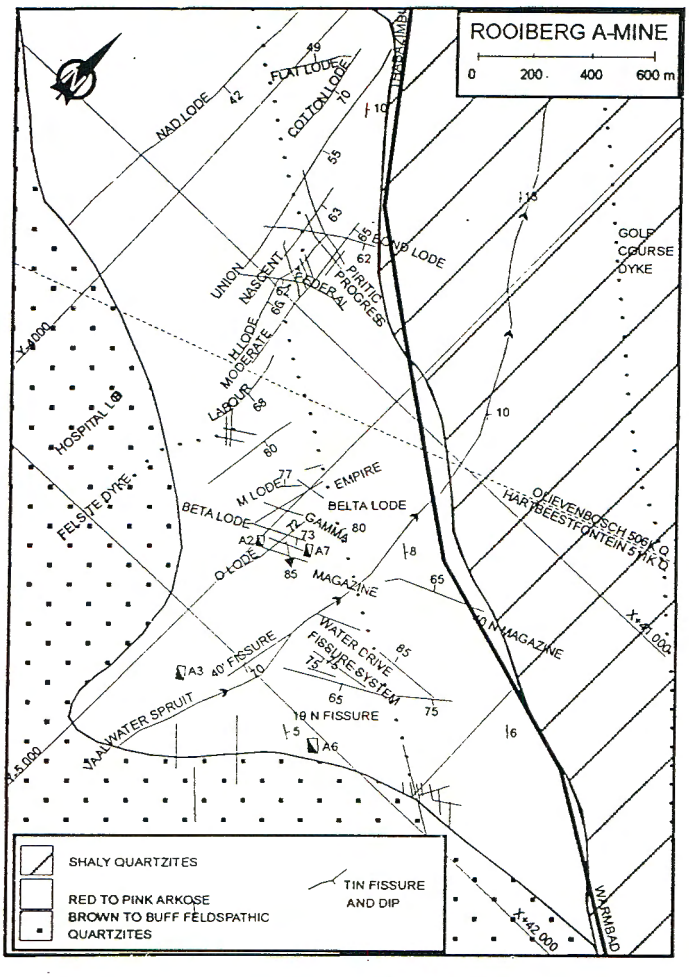

Figure 1.3. The Rooiberg A Mine Complex (unpubl. rep. Roberts 1983).

Chapter 2 .

2. Regional Geology of the Rooiberg Fragment.

2.1. The Bushveld tin deposits.

Lenthall (1974) grouped the economic tin deposits of the Bushveld into six discrete tin fields. The tin occurrences can be defined as being either exogranitic or endogranitic. Exogranitic deposits are defined as deposits formed by granitic fluids outside the main granitic body, while endogranitic deposits are formed by granitic fluids within the granitic body. These tin fields are depicted in figure 2.1 and are briefly discussed below.

Mineralisation in the **Rooiberg tin field** was exogranitic and deposition was widespread within the Boschoffsberg quartzites. The mineralising fluids are assumed to have originated from the surrounding granites. All the mineralisation occurs directly below the Blaauwbank shale member, which appears to have trapped the mineralising fluids. Mineralisation was structurally controlled and in some locations evidence of a structurally controlled tin zone is to be found. The ore deposits were formed by replacement of the host rock as well as by fissure filling.

Mineralisation in the **Zaaiplaats tin field** is endogranitic within a late granitic differentiate (McCarthy & Fripp 1980), termed the Bobbejaankop Granite, where mineralisation was restricted to the upper parts of the granite. The ore can be mainly subdivided into disseminated and pipe-like deposits.

Mineralisation in the **Nylstroom tin field** is exogranitic and associated with a shaly sedimentary horizon within the Rooiberg Felsite (Phillips 1982). The ore deposits are replacement type mineralisation, located in close proximity to the fractures, without actually filling them.

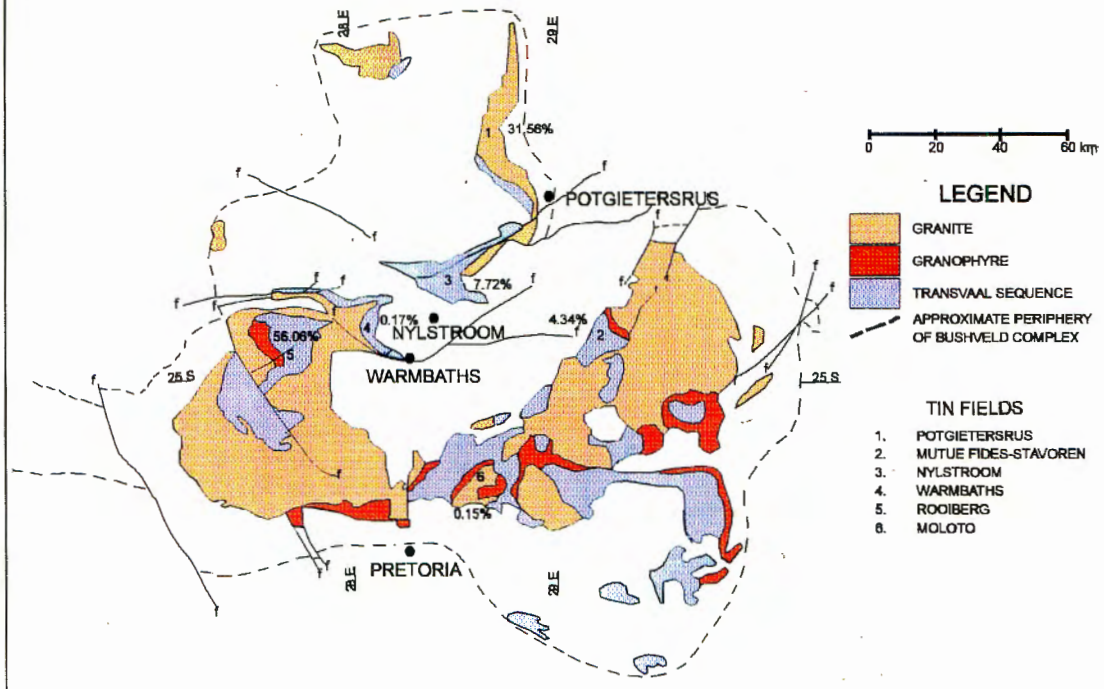

Figure 2.1. The distribution of tin fields in relation to the acid phase of the Bushveld Complex (after Lenthall 1974, Rozendaal *et al* 1986).

Mineralisation in the **Olifants tin field** is endogranitic (Mutue Fides), and exogranitic in the overlying granophyres (Stavoren) and sediments (Vlakfontein) (Lenthall 1974). Cassiterite occurs as disseminated ore, as well as pipe-like bodies in the granite.

Mineralisation in the **Elands tin field** NW of Warmbaths, takes the form of irregular pipe-like bodies, associated with pegmatitic sheets and aplite dykes and disseminated deposits within the granites. In the felsites cassiterite occurs as replacement bodies.

Mineralisation in the **Moloto tin field** occurs as disseminated deposits in the granite and individual ore-bodies are related to fissures.

Table 2.1 gives the production figures from the individual tin fields within the Bushveld Complex (Lenthall 1974), and shows that the Rooiberg tin field had by far the largest production.

TABLE 2.1.

Tin production figures from the individual tin fields within the Bushveld Complex

	CONCENTRATES	% OF TOTAL	METALLIC TIN	% OF TOTAL
Rooiberg tin field	62 365.983	56.43	39 149.484	56.06
Zaaiplaats tin field	31 287.865	28.32	21 948.337	31.56
Nylstroom tin field	11 599.402	10.50	5 395.256	7.72
Olifants tin field	4 861.795	4.40	3 033.451	4.34
Elands tin field	222.251	0.20	118.138	0.17
Moloto tin field	169.567	0.15	103.730	0.15
	110 506.863	100.00	69 748.396	100.00

(Modified after Lenthall 1974)

2.2. Structure of the North-Western Bushveld.

In order to understand the structure, the Rooiberg Fragment should be viewed in a regional context with the north-western part of the Bushveld Complex, as described by Stear (1976, 1977). The region referred to as the north-western Bushveld is the Thabazimbi-Loubad-Crocodile River area. The structural evolution of this area involved three major periods of deformation: emplacement of the Bushveld Complex, and tectonism during and after deposition of the Waterberg and Karoo sedimentary sequences. The most prominent structures have east-north-east and north-west orientations.

According to Stear (1976), Verwoerd (1963) and Leube (1960) post-Transvaal deformation related to the intrusion of the Bushveld Complex essentially by horizontal compression producing force fields of varying orientations. This led to superimposed folding, faulting and thrusting in the enclosed Transvaal country rocks. Meinster (in Stear 1977) regards the original fault- and fracture pattern in the Thabazimbi-Loubad-Crocodile River area as representing block-faulting in Bushveld times, resulting from tensional fracturing during regional subsidence with the Rooiberg Fragment in the centre. This implies displacement of crustal blocks in response to vertical tectonics. Field and underground evidence show that regionally significant block-faulting due to vertical tectonics was unlikely at the time of Bushveld granite emplacement, since most planes of movement indicate displacements resulting from horizontal forces (Stear 1977).

Post-Karoo faulting is displayed by graben-like structures such as the Crocodile River fault. These faults are generally east-north-east trending and are often filled by dolerite dykes.

2.3. The Rooiberg Fragment.

The geological succession of the Rooiberg Fragment is best explained by Table 2.2, adapted from Rozendaal *et al* (1986).

2.3.1. Stratigraphy of the Rooiberg Fragment.

2.3.1.1. The Boschoffsberg Quartzite Member.

The Boschoffsberg quartzite member, previously also known as the Main quartzite, hosts the tin deposits at Rooiberg. The sediments dip about 15° E and show thin conglomerate layers towards the base. This succession reaches a thickness of about 1320 m to 1400 m and is intruded by the Bushveld granites and Rashoop granophyre. It is transitional into the shaly beds overlying the quartzite.

The quartzite has an exceptionally high feldspar content and can thus not strictly be classified as a quartzite. Leube and Stumpfl (1963) use the term "arkose" or "arkosite" to accommodate the high percentage of feldspar according to the Pettijohn classification system for sediments. Phillips (1982), however, prefers the term feldspathic arenite or meta-arkose, since he believes the feldspar content in the quartzite is mostly due to alteration and metasomatic processes. The mineralogy of the arenites has been changed dramatically by metasomatism and recrystallisation of individual crystals into an interlocking texture. The unmineralized quartzite is of lighter colour (almost white to greenish), with the mineralised quartzite varying from greenish-pink to red. The quartzite closest to the mineralised lodes and in the so-called tin zone is more extensively metasomatised. Recrystallisation, sericitisation, chloritisation and tourmalinisation affected the original sediment. Strauss (1947) and Labuschagne (1970) found that the red colour is due to minute specks of limonite or hematite in the potash feldspar, which have been introduced during alteration and metasomatism of the white quartzite.

Table 2.2.

The geological succession of the Rooiberg Fragment.

Bushveld Complex	Lebowa Granite Suite	Nebo Granite: a grey to red, coarse, equigranular, in places porphyritic granite Mineralogy: quartz, feldspar, biotite, amphibole.
	Rashoop Granophyre suite	Red to grey granophyric quartz-feldspar rocks, medium- to coarse-grained, locally with country rock xenoliths
Rooiberg Group	258 - 1100 m	Quartz porphyry at the top, banded felsite (flow banding), porphyritic felsite, massive fine-grained felsite at the base. Agglomerate occurs locally towards the base. Primary features; flow banding
Pretoria Group	Smelterskop Quartzite Formation 275 - 550 m	Lenticular pink to red feldspathic quartzites and tuffaceous shales with interbedded andesitic volcanics. Local development of conglomerates, pebble bands, grits and agglomerates. Primary features; trough cross-bedding, tabular cross-bedding, ripple bedding, mud-flake layers, slump structures. Andesites show amygdales, flow banding, pillow structures.
	Leeuwpoort Formation	*Blaauwbank Shale Member 190 - 300 m.* Thinly bedded shales and sandstones with facies variation to massive mudstone and siltstones. Shaly-quartzite; a transition zone typified by lenticular arkoses and sandstones interbedded with shales and siltstones, upward fining. Primary features; ripple marks, flaser bedding, scour channels, slump and ball-and-pillow structures clay-pellet conglomerates, mud-cracks, cross-bedding (tabular, trough), ripple laminations. *Boschoffsberg Quartzite Member 1320 - 1400 m* Cross-bedded feldspathic quartzites and arkoses, upward-fining sequence. Coarse-grained units with interbedded conglomerate and pebble bands at the base grade to trough crossbedded arkoses with shale layers in places towards the top. Primary features; trough and planar crossbedding; slumping diapiric structures; load casts, ball-and-pillow structures, clay pellets, current lineation, mud cracks, shale-flake conglomerates, ripple marks (asymmetrical and symmetrical)

(After Rozendaal *et al* 1986).

Cross-bedding is present, although it is noticed with difficulty, except where later alteration had taken place. Sericitisation and tourmalinisation both enhance the cross-bedding. Since there is no easily identifiable marker horizon present, it is difficult to recognise any stratigraphic sequence. Paleocurrent studies conducted by both Stear (1976) and Phillips (1982) imply that transportation was from a northerly direction. Phillips (1982) speculates on the possibility that the Makoppa Dome constitutes the source of the feldspathic sediments.

2.3.1.2. The Blaauwbank Shale Member.

The Blaauwbank shale member overlies the Boschoffsberg quartzite member. A shaly quartzite layer forms a transitional zone between the two members. This layer is composed of alternating bands of mudstone and sandstone. The transitional zone is overlain by a shale zone of varying thickness. Parting planes were formed by slight folding between the members and were sometimes filled by the rising mineralisation fluids that crystallised there. The shale member, however, is devoid of mineralisation and seemingly acted as a barrier to contain the ore-forming fluids in the quartzite.

2.3.1.3. The Smelterskop Formation.

The Smelterskop formation conformably overlies the Blaauwbank shales. The Smelterskop formation is a mixed sedimentary (feldspathic arenite) and pyroclastic succession, with interbedded amygdaloidal high-magnesia basalts. This succession represents a distinct stratigraphic interval. Sedimentation ended before the extrusion of the Rooiberg felsites and is of little economic importance.

2.3.1.4. The Rooiberg Felsites.

The Rooiberg felsites overlie the Smelterskop Formation conformably. Labuschagne (1970) identified four types of felsite in the Rooiberg Fragment:

Quartz porphyry
Banded felsite
Porphyritic felsite
Non-porphyritic felsite

The contacts between the different felsites are never sharp and display both banding and mottling. The felsite is not known to carry cassiterite in economic concentrations, but does contain visible amounts of manganese oxide minerals, tourmaline and pyrite.

2.3.1.5. The Rashoop Granophyre Suite.

According to Walraven (1976) the granophyric rocks around the Rooiberg Fragment form part of the Rashoop Granophyre Suite of the Bushveld Complex. Two types of granophyre can be identified:

a thick sheet that constitutes part of the Boschoffsberg, and

narrow zones on the contact between the granite and felsite.

Ianello (1971) considered the granophyre as an intermediate stage in the granitisation of the feldspathic quartzites of the Rooiberg Fragment. Phillips (1982), however, considers the intrusive contact between the granophyre and the Rooiberg Fragment, coupled with the intrusive granite contact below it, as evidence that the granophyre was intruded and consolidated prior to the intrusion of the granites.

2.3.1.6. The Lebowa Granite Suite.

The Lebowa Granite Suite occurs as sheet-like bodies within the central part of the Bushveld Complex. It displays rough layering consisting of a coarse grey hornblende granite at the base, grading up through medium-grained red and grey biotitic granites, red granophyric granite to granophyre that is commonly overlain by felsites or sediments of the Transvaal Supergroup (Phillips, 1982).

The geochemistry of the Bushveld granites was studied by several workers. Trace-element geochemistry shows that despite consistency in the granites of the Zaaiplaats area, the different granites represent a fractionation sequence. This fractionation was discussed by McCarthy and Hasty (1976) in terms of the three elements barium, strontium and rubidium. These elements were chosen because of the strong compatibility of barium and strontium versus the incompatibility of rubidium with the crystal lattices of major silicate minerals. Their study confirmed the *in situ* fractional crystallisation of a single

parent magma. The element concentrations concerned are shown in table 2.3.

Barium and strontium decrease in concentration in later magmatic fractions while rubidium increases. Since the melt tends to become impoverished with respect to titanium due to its incorporation into hornblende and later into biotite, titanium also decreases in later magmatic fractions.

Table 2.3.

Trace-element geochemistry of the Bushveld granites in the Zaaiplaats area.

	Ba	Sr	Rb
Residual melt	250 ppm	5 ppm	750 ppm
Parent magma	1200 ppm	40 ppm	240 ppm
Water saturation	± 700 ppm		

(McCarthy in Phillips 1982)

Phillips (1982) showed by his traverse across the differentiated granites east of Leeuwpoort that the Rooiberg granites fit the model proposed by McCarthy and Hasty (1976).

2.3.2. Structure of the Rooiberg Fragment.

The Rooiberg Fragment was subjected to three different tectonic phases during the emplacement of the Bushveld Complex. Stear (1976) describes the structural form of the Rooiberg Fragment as being "a broad arch with a cross-trending saddle-like structure in the Blaauwbank area where the depression of this regional antiform is cut by a belt of parallel-trending dykes".

The product of the first tectonic event recognised, is the open anticline with axial orientation ENE (070°), coinciding with a westward extrapolation of the Murchison trend (Stear 1976). It is unknown whether the granite intruded an

existing anticlinal structure or whether it deformed the sedimentary roof rocks into an arch. According to Verwoerd (1962) the N-S compression of the Transvaal sequence in the Crocodile River Fragment was caused by horizontal stresses during granite emplacement. Hartzer (1989), however, explains the tectonic development of the Crocodile River Fragment by means of an updoming model. During updoming compressional forces led to the development of folds with northwest striking axial planes, followed by east-northeast striking folds. There is, however, no confirmation that the same regional effects apply to the Rooiberg Fragment.

A second major tectonic episode occurred during the emplacement of the Bushveld granites. Compressive forces acted in a NE-SW direction, giving rise to the formation of a large strike-slip fault (the Kwarriehoek wrench) and several fold structures. According to Stear (1976) it is possible that these structures are part of an interference fold pattern formed when the compressive stress acted obliquely to the original arch. The resultant geometrical form of the structure seems to be a mushroom-shaped interference fold, apparent in the north-eastern corner of the Rooiberg Fragment. The Blaauwbank syncline forms the synclinal feature on the hinge zone of the dome whilst the Kwarriehoek anticline and Elandsberg syncline are secondary fold features on the southern limb of the dome. Theoretically an anticline should lie next to the Rooiberg syncline, but the rocks composing it could have been assimilated by the intruding granite. Figure 2.2 (Stear 1976) depicts the first two major tectonic phases in the Rooiberg Fragment, as well as the basic controls of mineralisation at Rooiberg A Mine.

The intermediate principal stress of the second phase (along a NW-SE (140°) direction), became the maximum principal stress during the next phase of compression and resulted in thrusting along the eastern margin of the fragment. This thrust-system (the South Parallel Thrust), is described by Stear (1976) as a fault-complex in which certain structural features controlled the type of fault. "The apparent inclination of the maximum principal stress,

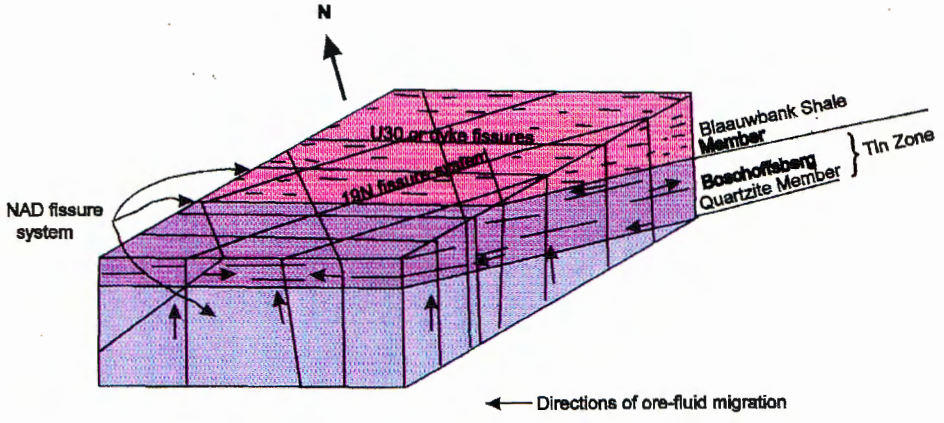

Stratabound tin mineralisation at a stratigraphic contact zone. Mineralising solutions transported by a system of fissures and master joints, migrated along bedding-planes in cross-bedded arkosite and formed cassiterite-bearing ore-bodies in a stratabound tin zone (Stear 1977).

Figure 2.2. Basic controls of mineralisation at Rooiberg A Mine. Note the fissure system formed by tectonic deformation (after Stear 1977).

the disposition of the Rooiberg syncline and the orientation of the sedimentary stratification were controlling factors determining whether low-angled thrusting or high-angled reverse-faulting occurred". This system extends from Kwarriehoek to the South of Vellefontein where it apparently dissipates into the stratification as a series of bedding-plane thrusts. Figure 2.3 (Stear 1976) shows the effects of the third major tectonic phase.

Apart from the possible intrusion of dykes into re-activated block-faults and fractures within and parallel to the Blaauwbank syncline, the intensive deformation of post-Waterberg tectonism to the north of the Fragment did not noticeably affect the tin field. Post-Karoo deformation produced tensional conditions resulting in graben-like structures in particularly the southern portion of the tin field. Faulting and fracturing occurred along the older structural lines, following E-W, ENE and NE directions. Stear (1976) recorded block-faulting and step-faulting to the south-east.

2.4. The Rooiberg Tin Deposits.

Tin mineralisation generally occurs within the uppermost 300 m of the Boschoffsberg Quartzite, where the 'shaly quartzite' and Blaauwbank Shale Member obstructed the mineralising fluids. The Weynek and Vaalwater deposits are the only deposits within the shales. Mineralisation is strongly related to the fracture system in the Rooiberg Fragment. Open space filling and early replacement mineralisation depended on the nature of the fractures. All the deposits are related to a major fault, caused by near-horizontal tectonism.

Rozendaal, Toros and Anderson (1986) reviewed the Rooiberg tin deposits. They found that the deposits are stratabound, being confined to the upper Boschoffsberg Quartzite Member and shaly quartzites of the Blaauwbank Shale Member. The deposits are classified as being either conformable or

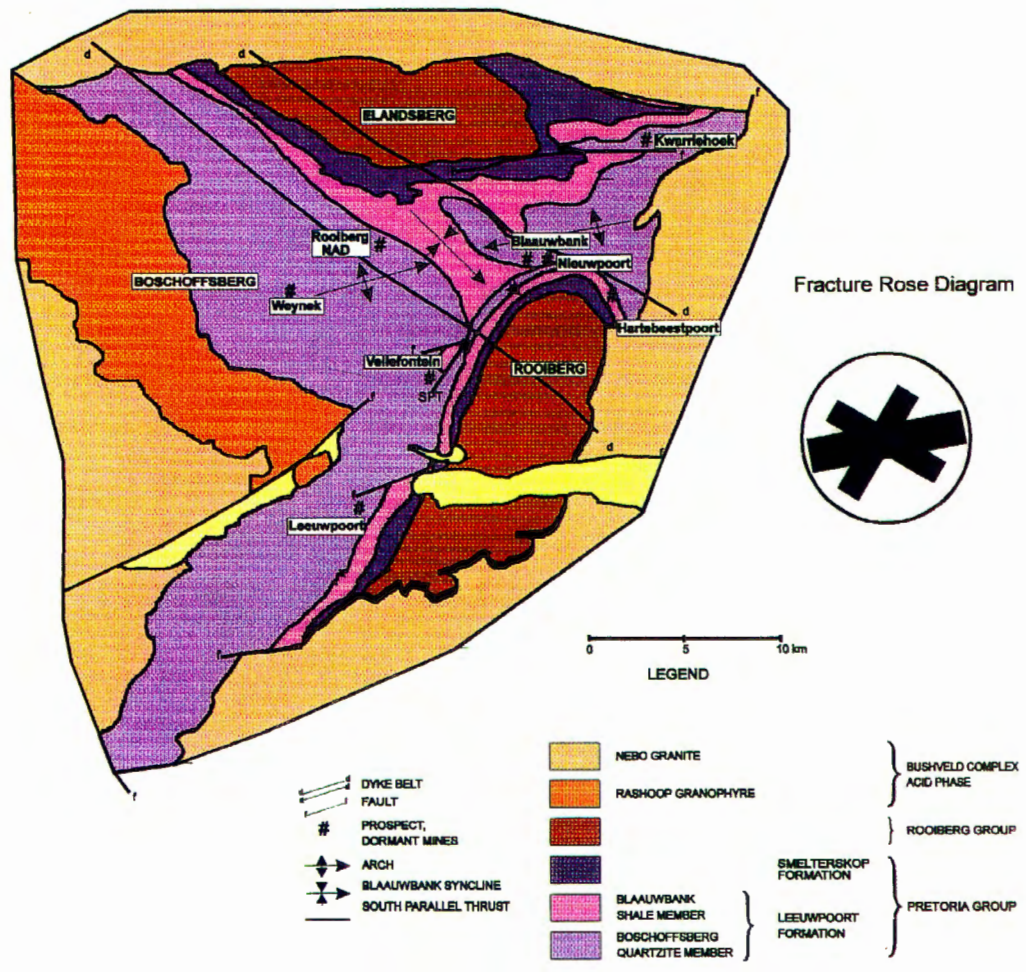

Figure 2.3. The third major tectonic phase in the Rooiberg Fragment (after Stear 1977).

unconformable, depending on their relation to the stratigraphy. Conformable deposits are pocket mineralisation, bedding plane mineralisation, bedded lodes and bedded stringer mineralisation. Unconformable deposits occur as prominent steep-dipping lodes parallel to the major fracture directions.

The common mineral paragenesis at A Mine and Vellefontein is cassiterite, tourmaline, carbonate, sericite and pyrite in contrast to the mineral paragenesis of cassiterite, chlorite and haematite at C Mine. Quartz and red potassic feldspars are the most common gangue minerals.

There is evidence from the pervasive alteration of the host rocks that a complex hydrothermal system operated on a large scale within the Rooiberg Fragment over a long period. The low niobium content in the cassiterites from the various mines indicates a low temperature genesis, which is consistent with the abundance of sulphides and carbonates in the ore lodes. Quartz fluid inclusion studies (Olilla 1981) from the Leeuwpoort area also indicate a low temperature of formation (174 to 220°C).

Phillips (1982) compared the major tin deposits in the Rooiberg tin field in table 2.4. The NAD deposit is also included.

2.5. Major Structures in the NAD Deposit.

Swan (1985) contoured the NAD tin zone from borehole data and the geology in the NAD Decline. The contours divide the NAD deposit into two major zones: the Western zone and the Eastern zone, with the Union lode dividing them. It appears that the Union lode is the only fracture displaying movement, since it displaced a dyke across the Union lode.

Table 2.4.

Comparison of the Major Tin Ore Deposits in the Rooiberg Tin Field.

DEPOSIT	RELATED THRUST OR WRENCH	TYPE OF MINERALISATION	
		BEDDED	STEEP FRACTURE
Leeuwpoort	'South Parallel' or Fault Lode fracture	# Large lodes: open space filling, e.g. Spruit Lode. Replacement rare, e.g. in Blaauwbank Shale Formation and as precursors to open space fillings, e.g. Spruit Lower and Gap Lower Lodes.	Open space filling is important, e.g. 1200' fissure. Replacement or pocket mineralisation is rare, e.g. New Strike Fracture conduct mineralisation up into Smelterskop Formation.
Vellefontein	'South Parallel'	# Large lodes: open space filling, e.g. Parker Lode.	Minor open space filling, rare replacement or pocket mineralisation.
Rooiberg A Mine	Elandsberg	Important bedded replacement, e.g. Whiskey Stope. Note - thrusting caused surfaces of dislocation since destroyed by mineralisation. Bedded open space lodes very rare.	Important open space filling, e.g. Moderate Lode. ** Replacement mineralisation, e.g. 19N area. Pocket mineralisation (Dinsdale 1982).
Nieuwpoort	'South Parallel'	Important bedded replacement and open space filling, e.g. Main Lode.	** Major replacement and stockwork, e.g. Stewart Ore Body.
Blaauwbank	'South Parallel' and Elandsberg	# Replacement, eg. Mill Lode.	Replacement, pocket mineralisation
NAD-mine	Elandsberg	Bedded open space replacement absent. Some bedded replacement	Important open space filling, e.g. Union lode, Bonus lode. Replacement, Disseminated Tin area and pocket mineralisation.

(after Phillips 1982)

\# Greater importance of replacement due to lack of open spaces for infilling
** Greater intensity of faulting and open space formation

The Eastern zone is the most extensive with a general N-S strike, varying locally between NW-SE and N-S. The dip tends to vary considerably on local scale: to the south the dip is > 30° and further north it decreases to 20°, but increases to 35° in the east.

The western zone displays a wider range in strike, varying from NNW-SSE to almost E-W. The dip is slightly more constant, varying from 8° to 16°.

Chapter 3 .

3. Sampling Techniques and Analytical Methods.

3.1. Sampling Techniques.

Sampling was limited by technical and managerial constraints to four underground visits, accompanied by the chief geologist at Rooiberg, Mr J. Misiewicz. At first only the lode material was sampled, as those were of greatest interest. During the last two visits both the wall rock and the lodes were sampled. The writer tried to spread sample localities along a line in each specific lode to compare the different localities in a lode, as well as the extent of alteration into the wall rock, and also to compare lodes with one another. Five samples were taken at each locality: two each in both the foot and hanging wall of the lode and one in the lode. The wall rock samples were taken at approximately 0.25 m and 0.50 m perpendicular to the lode to study wall rock alteration and geochemical changes away from the fractured lodes.

The locality map (map A, folder) indicates the spread of samples in the mining area of NAD mine as in February 1991.

3.2. Analytical Methods.

3.2.1. X-Ray Fluorescence.

The samples selected for XRF analysis were chosen for their homogeneity in hand specimen, in order to avoid analysing atypical samples. The rock samples were crushed, and then powdered in the 'Siebtechnik' mill to -300 mesh. Acetone was added whilst milling, to prevent Fe-oxidation. About 30 g of sample is needed to make duplicate powder briquettes and fusion disks for

analysis on the Phillips Wavelength Dispersive X-Ray Spectrometer PW 1404. The analyses were conducted by Ms A. Uttley of the Department of Geology, University of Stellenbosch.

The laboratory makes use of the Norrish and Hutton (1969) technique of sample preparation for powder briquettes and fusion disks. The powder briquettes are used for trace element analysis and the fusion discs for major element analysis.

a. Preparation of Powder Briquettes.

0.16g of Mowiol is added to 8g of powdered sample, after which it is milled together on the 'Siebtechnik' mill for two minutes. About 20 drops of de-ionised water is added, it is well mixed in an agate mortar and dried in an oven at 60°C for approximately an hour. It is then grounded again in an agate mortar until fine. The mixture is now pressed for one minute under 7 tons pressure. If the briquette is too brittle, it should be remade and the sample not dried completely. These briquettes are handled carefully and the analysing surface not touched to avoid contamination.

b. Preparation of Norrish Fusion Disks.

2g of powdered sample is weighed into a "vitreosil" crucible, after which it is heated at 110°C for 4 hours to determine (H_2O^-). The sample is then ignited at 1000°C, normally overnight, but for a minimum of 4 hours; loss on ignition (- % H_2O + CO_2 + FeO > Fe_2O_3 +) is now determined. For the actual fusion process, the flux (Spectroflux 105 with 47.0% lithium tetraborate, 36.7% lithium carbonate, and 16.3% lanthanum oxide) is dried overnight at 450°C and kept in a desiccator.

The fusion mixture (1.50000g - 0.002g flux and 0.3000g - 0.002g ignited sample) is transferred to a Pt-crucible. The mixture is heated over a Bunsen flame (980°C minimum) for about 15 minutes and gently stirred until completely melted. A graphite holder and Al-plunger are kept on a hot plate

at 240°C with two asbestos plates next to it at 220°C. The molten sample is now collected on the edge of the crucible over the flame. The complete melt is now poured onto the graphite holder and the plunger brought down firmly, but gently. The melt now spreads over the surface to form a glass disc. The disc can then be transferred to the asbestos plates to cool down with the analysing surface to the bottom. These discs are not handled on the analysing surface, to avoid contamination.

The ten major element oxides analysed on the fusion discs were SiO_2, Al_2O_3, K_2O, Na_2O, Fe_2O_3(tot), MgO, MnO, CaO, TiO_2, and P_2O_5. The analysis was conducted using a Geol target Mo-Sc tube, while the trace elements (including Sn) were analysed with a Rh tube. The actual values were calculated using international geological reference material such as the USGS standards.

3.2.2. Electron Microprobe.

Single grain analyses were conducted on the ore minerals by means of the electron microprobe. Since the ore minerals are intimately intergrown, electron microprobe analyses were best suited to the samples. Polished thin sections prepared for microscope work were used after being carbon coated. Each thin section was covered by a thin layer of carbon (peacock coloured on brass) to ensure conductivity of electrons.

Although the detection limits for trace elements are relatively high (table 3.1), significant amounts of trace elements could be recognised in most samples. Table 3.2 lists the minerals analysed on the electron microprobe. The analyses were done at the University of Nancy, France, on both the SX50 and Camebax microprobes under supervision of Mr J.M. Claude; and at the University of Cape Town on a Camebax microprobe under supervision of Mr D. Rickard.

The detection limits are LLD + 2σ:

$$LLD = 6/m \sqrt{\frac{\text{Background c/s}}{\text{Total counting time}}}$$

where m = nett counts/sec per %

$$2\sigma = \sqrt{\frac{\frac{\text{Peak c/s}}{\text{Peak time}} + \frac{\text{Background c/s}}{\text{Background time}}}{\text{Peak c/s} - \text{Background c/s}}}$$

TABLE 3.1.

Detection Limits for the Trace Elements and Oxides Analysed on the Electron Microprobe.

CASSITERITE		TOURMALINE		SULPHIDES	
TiO_2	685 ppm	K_2O	900 ppm	Co	340 ppm
WO_3	4200 ppm	Cr_2O_3	1600 ppm	Ni	340 ppm
Nb_2O_5	2200 ppm	MnO	3300 ppm	Pb	1700 ppm
Ta_2O_5	4200 ppm	CaO	1500 ppm	Ag	580 ppm
MnO	1200 ppm	TiO_2	1700 ppm	As	760 ppm
		NiO	3000 ppm	Zn	670 ppm
				Mn	2500 ppm
				Cu	780 ppm

TABLE 3.2.

Minerals Analysed on the Electron Microprobe.

MINERAL	ELEMENTS ANALYSED	MICROPROBE	MICROPROBE CONDITIONS
Cassiterite	Sn, W, Fe, Ti, Ca, Mn, Ta, Nb	SX50, Camebax: Nancy Camebax: UCT	20 kV 25 kV
Tourmaline	Fe, Na, K, Si, Mn, Ca, Ni, Al, Ti, Cr, Mg	Camebax: Nancy	15 kV
Carbonate	Ca, Mg, Fe, Mn, Sr	Camebax: UCT	15 kV
Pyrite	As, Co, Mn, Ni, Pb, Cu, Fe, S	Camebax: UCT	25 kV
Chalcopyrite	As, Co, Mn, Ni, Pb,Cu, Fe, S	Camebax: UCT	25 kV
Feldspar	Na, K, Si, Al, Fe, Mg, Ca	Camebax: UCT	15 kV
Mica	F, Cl, Na, K, Si, Ti, Al, Cr, Fe, Mn, Mg, Ca, Ba, Sr	Camebax: UCT	15 kV

3.2.3. Optical Emission Spectrography.

Detection limits are much lower than with the electron microprobe, and are ideally suited to mono-mineralic analysis for trace elements. The spectrographic analyses were carried out at the Bergakademie Freiberg, Germany under supervision of Prof. D. Wolf and Dr. U. Kempe. Sample preparation was done according to the method of Schrön *et al* (1978 & 1983). Mono-mineralic samples were selected and crushed in an agate mortar to -63 mesh. The samples were then mixed with non-compacting carbon powder containing Ge or Pd as an internal standard in a ratio of 1 : 2, for example: [sample: C((EK2/O) + Ge, Pd) = 70 mg: 140 mg].

The samples were then arced on a Plane Grid Spectrograph (PGS-2). The spectrographic conditions were:

Volatilisation:	occurs from an anode linked to a carrier electrode.
Generation:	direct current continuous arc, 220 V; 8.5 A; SBG-30.
Light supply:	intermediate image; intermediate apertures 5; step filter III.
Exposure time:	120 s (total volatilisation).
Photographic plates:	Orwo WU 3
Developer:	Orwo MH-28: H2O = 1:4; agitated development (4 min).

The standards for silicate analysis are made up from a synthetic mix of Al, Ca, Fe, K, Mg, Na and Si oxides; for pyrite analysis from a synthetic mix of carbonyl iron and sulphur; and for cassiterite analysis from a synthetic mix of SnO_2 and carbon powder. The photographic plates are then scanned for the spectral lines of the specific elements, and the internal standard of Ge or Pd is used as the correction factor.

Because of the intimate intergrowth of the ore minerals, it was difficult to select clean, mono-mineralic samples. Those analysed appeared clean under the stereo microscope, but the results indicated that micro-intergrowths had probably been included. It was especially difficult to separate clean cassiterite from tourmaline, and pyrite from chalcopyrite. The pyrite contains microscopic exsolution lamellae of chalcopyrite, which can be seen in the analyses.

Chapter 4 .

4. Mineralogy and Geochemistry of the NAD Deposit.

4.1. Previous work on the Rooiberg Tin Deposits.

Strauss (1947) considered the original wall rock to be a white coloured quartzo-feldspathic sediment that discoloured to a reddish hue after introduction of alkalis to the system by hydrothermal metasomatism. He considered the overall alteration process from original quartzite to altered feldspathic quartzite to be one of desilication and the introduction of alkali-feldspars. Table 4.1 (Phillips 1982) summarizes Strauss' sequence of unaltered to most altered material from the Rooiberg Fragment.

Table 4.1.

Feldspathisation of the Boschoffsberg Quartzite.

Element wt %	Normal Quartzite	Mobilised Quartzite	Leptite	Red Quartzite	White Quartzite
SiO_2	89.01	81.89	76.14	73.08	68.80
TiO_2	-	-	0.27	0.48	0.39
Al_2O_3	6.22	10.64	12.63	14.29	16.47
Fe_2O_3	0.56	0.56	1.32	0.82	1.33
FeO	0.07	0.07	0.43	0.28	0.85
MnO	-	-	-	-	-
MgO	0.50	0.64	0.49	0.30	0.69
CaO	0.39	.034	0.23	0.60	0.82
Na_2O	2.73	4.81	1.59	3.46	4.48
K_2O	0.25	0.37	5.67	5.73	3.78
P_2O_5	-	-	tr.	0.23	0.24
H2O+	0.53	0.37	0.47	0.33	1.07
H2O-	-	0.06	0.20	0.22	0.32
F	-	-	0.01	0.07	0.04
CO_2	-	-	0.53	0.35	0.53
Totals	100.26	99.80	99.71	100.24	100.17
Locality	DE - MOND - VAN BLOKSPRUIT			LOSKOP 148	
ID Numbers	CPA21	CPA22	CPA23	CPA24	CPA25

(After Strauss (1947) in Phillips 1982)

As none of the writer's samples correspond to the original unaltered wall rock, the sample from Strauss' collection will be taken to represent the original wall rock for comparison with altered and mineralised material. The change of the original feldspathic quartz-rich sediment to a rock with granite-like composition, can be described as a process very similar to greisenisation. Though weakly developed, Ianello (1971) considered the granophyric rocks surrounding the meta-sediments to have been greisenised. The relatively minor Bobbejaankop type granites are the only true granites recognised by Ianello (1971), and were accordingly made responsible for this transformation of the sedimentary rocks. Regional granitisation is, however, not possible without extensive intrusive magmatism and therefore Ianello's view does not carry much weight. This is confirmed by the granite contacts and the sedimentary nature of the Leeuwpoort wall rocks. Greisenisation only occurred on a small scale and only in localised areas such as the narrow zone on the edge of the Rooiberg Fragment. C Mine is the only mine where topaz has been noted as an accessory mineral in the mineral assemblage. Greisenisation can be defined as '*A process of hydrothermal alteration in which feldspar and muscovite are converted to an aggregate of quartz, topaz, tourmaline and lepidolite by the action of water vapour containing fluorine*' (Bates & Jackson 1987). Alteration in the Rooiberg quartzite was brought about by tin-bearing hydrothermal fluids, and although the host rocks are not proper greisens, the reactions were similar and an almost granitic type of meta-sediment was formed.

Three major alteration phases were recorded by Phillips (1982) in the wall rocks of the Leeuwpoort deposit (C Mine): a sericitic alteration type, a transitional chlorite alteration type and a feldspathic alteration type. Minor quartz on quartz overgrowths are evidence of the mobilisation of silica during sericitic alteration, whereby sericite and muscovite replace quartz so that the remaining quartz shows ragged outlines. Chloritic alteration goes a step further, when sericite is replaced by chlorite, and some secondary K-feldspars replace the micas. This seems to be a step between sericitic and feldspathic

alteration. Feldspathic alteration is characterised by alkali feldspars replacing earlier formed sericite as well as primary quartz and feldspars. Albite is only replaced after the replacement of orthoclase by secondary K-feldspar. This secondary K-feldspar was found to contain, apart from fine haematite dust, microcrystallites of rutile. This then accounts for the red-brown discolouration of the K-feldspars under the microscope (appendix C, plate 57).

Less common alteration types are tourmalinisation, carbonatisation, pyritisation and chloritisation. Tourmalinisation occurs locally, the tourmaline (schorl) replacing both feldspars and quartz. Tourmaline preferentially replaces K-feldspar in a quartz-orthoclase-albite rock. It is often accompanied by carbonatisation, with a tendency to form a quartz-tourmaline-carbonate rock. K-feldspars, sericite and chlorite are replaced during carbonatisation, while albite tends to resist replacement in comparison with orthoclase. The carbonate also seems to post-date the chloritisation of sericite. Pyritisation occurs through feldspar and quartz replacement, and pyrite grains often show inclusions of quartz and sericite where the grains were only partially replaced. The formation of chlorite lodes was either the last phase of wall rock alteration before open space filling or lode mineralisation, or it was a preliminary phase to mineralisation. Chlorite normally replaces sericite, as well as orthoclase and quartz.

Dinsdale (1981) studied the formation of pockets and zones of sedimentary alteration at Rooiberg. He concluded that the cassiterite mineralisation is related to complex fracture systems and he related the different pocket types to structural features in the Boschoffsberg Quartzite. He also studied fluid movement resulting in alteration of sedimentary minerals by introduced hydrothermal minerals.

Dinsdale (1981) recognised the following factors as indication of fluid movement in pockets:

a. intergranular replacement,
b. traces of replacement in all sedimentary grains, and
c. complete replacement.

Haloes of alteration zones were probably formed by diffusion of elements around the pockets. Movement of elements was apparently controlled by atomic weight.

The major types of reactions to have taken place seem to be ion exchange and hydrogen metasomatism. The latter played an important role in sericitisation and greisenisation. The wall rock alteration at Leeuwpoort can be typified as alkali-alumina metasomatism, characterised by earlier sericitisation and chloritisation with later feldspathisation, followed by greisenisation. The acidity of the environment probably changed during alteration, as chloritisation occurs under alkaline (high pH) conditions and greisenisation under acid (low pH) conditions. This type of wall rock alteration can be recognised in the NAD deposit, though chloritisation played a much smaller role, with more pronounced tourmalinisation and carbonatisation.

4.2. The Tin Zone Hypothesis.

Tin occurrences are located within the top zone of the Boschoffsberg Quartzite Member and in the shaly arkose of the Blaauwbank Shale Member. This favourable zone is approximately 300 m thick with a strike of about 20 km. It was found that, in the A Mine Complex, tin mineralisation was localised within steep fractures and was confined to their intersection with a favourable stratigraphic horizon. This concept lead to the postulation of the Tin Zone Hypothesis.

In figure 4.1 Rozendaal *et al* (1986) summarize the mineralogical characteristics of the 300 m thick favourable zone in the A Mine Complex.

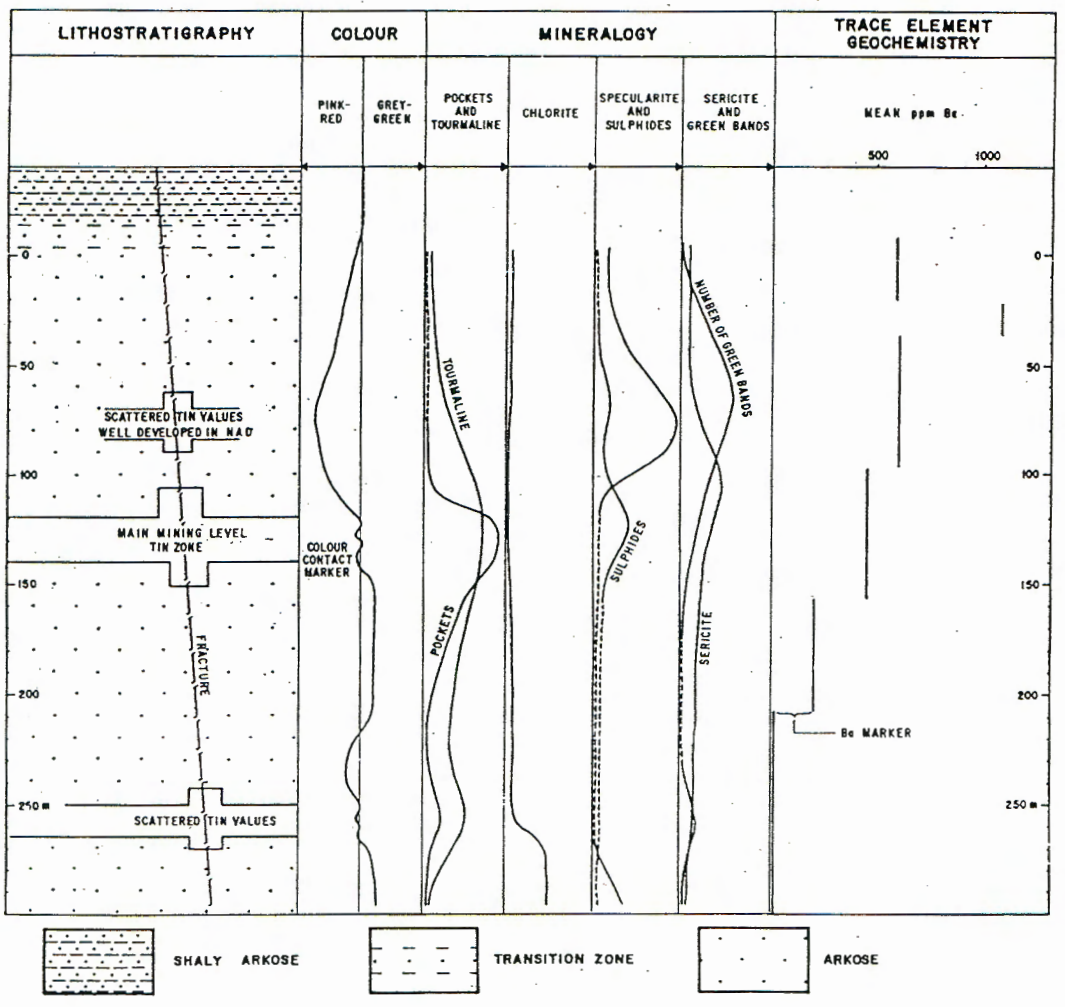

Figure 4.1. An idealised profile of the upper 250 m of the Boschoffsberg Quartzite Member in the A6 And A7 areas of A Mine (Rozendaal *et al* 1986).

Three conformable zones with anomalously high tin concentrations are present within the stratigraphy. The main producer is a 50 m thick zone located ± 120 m below the shaly arkose contact. Most of the mining was confined to this zone. The nature and origin of this so-called Tin Zone are still unknown.

The tin zone of the NAD deposit was contoured to depict changes in dip and strike for mining purposes (figure 1.3). The lowest pay values for all the surface AMS- and underground NAU-boreholes were used to determine the bottom of the geological tin zone.

The tin zone was probably chemically and physically controlled during the mineralising event. Fluid movement and wall rock alteration was chemically dependent on the availability of mineral parageneses that were susceptible to alteration and metasomatism. Investigation of tin-bearing fluids indicates that fluid acidity, oxygen fugacity and pH of the fluids controlled fluid composition, transport and precipitation. If there then was any agent present that would change these parameters, precipitation could take place.

The tin zone was also influenced by the reigning temperature and pressure controls of the fluids. Change in temperature will cause changes in the chemical controls, thereby initiating precipitation from the fluid. If temperature was the major controlling factor on transporting tin complexes, the tin zone would be similar to an isothermal surface (Bruce 1979). The form and position of the tin zone would then be a result of the isothermal surface, the regional geothermal gradient and the distance from the granitic source.

However, if pressure was the major controlling factor, an isobaric surface would be formed where the pressure components were the isostatic load pressure and directed pressure from the intruding granites (Bruce 1979). This would result in an isobaric surface parallel to surface topography at the time of mineralisation.

However, it is also possible that neither pressure nor temperature were the dominant factors, in which case the resultant tin zone would be a composite of isothermal surfaces and the topographic pressure surface. Under these circumstances the tin zone could be conformable over moderate distances with strike deviating significantly from that of the sediments.

It is concluded that the tin mineralisation was contained by various factors within a specific zone and was structurally controlled by fractures which introduced the hydrothermal fluids into the favourable zone.

4.3. Mineralogy and Petrography of the NAD Deposit.

As mentioned before, several lodes were sampled in the NAD deposit. The lodes are the AMS-lode, Bonus lode, B-lode, Cotton lode, C-lode, T-lode, Union lode and U-lode. The prominent lode minerals are cassiterite, tourmaline, carbonate (ankerite and siderite), pyrite and chalcopyrite. Although the mineralogy in each of these lodes is similar, small differences exist. The above minerals occur in varying proportions in the different lodes.

Pockets are abundant throughout the deposit, and may be identified as mature or immature pockets. Mature pockets are recognised when complete replacement of the host rock by ore lode minerals have occurred (appendix C, plate 8). Thus, nothing of the original host rock remains. Immature pockets are recognised when ore mineral replacement of the host rock have not been completed. Large areas within the pocket are still filled with host rock (appendix C, plates 1, 9 & 19).

4.3.1. Macroscopic Examination of the NAD Lodes.

The edge of the AMS-lode is not well defined and has a tendency to form pockets. Both ankerite and siderite occur. Tourmalinisation is evident in

plates 1 and 2 (appendix C). The sample in plate 1 is a pocket that apparently did not reach maturity. The colour zonation present indicates mineral zoning, with tourmaline-cassiterite deposited as a first phase around the core of the wall rock material, followed by carbonate and then by K-feldspar (orthoclase). The bleached haloes indicate the absence of K-feldspar and therefore relative enrichment of albitic plagioclase. Plate 2 shows extensive sericitisation in association with carbonate fracture filling. The AMS-lode is poor in sulphides compared with most of the other lodes. Cassiterite also seems finer grained and not easily recognisable underground. Mining of the AMS-lode was stopped because of metallurgical problems, connected with difficulties recovering fine-grained cassiterite.

The B-lode also displays hydraulic fracturing. The fracture edge and brecciated wall rock pieces served as crystallising surfaces (appendix C, plate 5). Minor fractures formed sub-parallel to the main fracture and were filled by carbonate. Both ankerite and siderite are present. Sericite and chlorite are also very abundant compared with the other lodes. Chalcopyrite is the major sulphide present and seems to be later than the tourmaline-cassiterite phase, but earlier than the carbonate phase. Plates 6 and 7 (appendix C) are typical of a green band in the wall rock. It is believed that these denser green bands were partly responsible for pocket formation, acting as a blanket for the mineralising fluids.

The Bonus lode is very rich in cassiterite and of a coarser grained texture. The host rock was hydraulically fractured, and filled by hydrothermal deposition, as can be seen in plate 3 (appendix C). This sample was taken on the edge of the fracture. The fracture surface, as well as the brecciated wall rock pieces within the lode, served as crystallising surfaces for the mineralising fluids. The dark mineralised areas have a distinct brown colour, and are indicative of the high cassiterite content. Both ankerite and siderite occur in the lode, but siderite seems to be the most abundant. Chalcopyrite is the most abundant sulphide, with only minor pyrite present. Plate 4 (appendix

C) shows a sample taken from the wall rock of the Bonus lode. Tourmaline filled the microfractures, accentuating the brecciated nature of the lode. Replacement-type mineralisation of the brecciated wall rock fragments is also evident.

The C-lode is very carbonate and sulphide rich, as is illustrated in plates 10 and 11 (appendix C). Pockets close to the lode also occur commonly. Plates 13 and 14 (appendix C) give proof of hydraulic fracturing. The fracture edge is smooth and served as a crystallisation surface for tourmaline and cassiterite. The lode is filled with brecciated fragments, which in turn also served as crystallisation surfaces within a carbonate mass. The dominant mineral in the C-lode is siderite. Chalcopyrite occurs as a later phase, but earlier than the carbonate phase. Some pyrite is present, mostly as pentagondodecahedra. Plate 12 (appendix C) shows mineralisation by metasomatic action which started along hairline fractures, but penetrated into the wall rock, as well as pocket formation on the lode.

The Cotton lode was mined out completely during earlier mining activities. Little evidence of the actual lode remains. Plate 8 (appendix C) shows a good example of a mature or complete pocket. Intimate tourmaline and cassiterite intergrowth is evident, later phase ankerite and free quartz are present. The sulphides present are well-crystallised pyrite (pentagondodecahedra and cubes) and some massive chalcopyrite. The red feldspar is orthoclase, which has been recrystallised during pocket formation. Plate 9 (appendix C) shows a partly formed or immature pocket in the red feldspathic wall rock.

The T-lode is very tourmaline-rich with mottled pyrite (appendix C, plate 15). Very little chalcopyrite is present. The carbonate is to be mostly ankerite. An intimate intergrowth of tourmaline and cassiterite occurs in a matrix of very fine-grained tourmaline and secondary quartz. The effect of the green band on the mineralising fluids can be seen in plate 16 (appendix C). Note the

difference in colour above and below the green band. Plate 17 (appendix C) is more typical of the T-lode. The intergrowth of quartz and tourmaline is here evident on larger scale.

The U-lode is also known as an undulating lode, as it has no constant strike and dip and varies in thickness. The wall rock is mostly dark red, and very rich in tourmaline. Both ankerite and siderite are present. Ankerite seems to be the most abundant. Tourmalinisation of the wall rock is metasomatic in origin, with movement of the mineralising fluids along hairline fractures. Pockets are often formed, though mostly only partly formed or immature. Plate 19 (appendix C) shows replacement mineralisation in the form of an immature pocket. The lode itself is filled with white carbonate, and this is the only area where ankerite is associated with fluorite. The lode was also hydraulically brecciated, with the breccia fragments serving as crystallisation surfaces (appendix C, plate 20).

Although the Union lode can be more than a meter wide, these areas were already mined out by the time sampling took place. This is also the only fracture along which extensive movement had occurred. The lode is very tourmaline-rich, with fewer sulphides present (appendix C, plate 18). The carbonate is mostly siderite. Hydraulic fracturing took place, as well as metasomatic replacement of the wall rock. The main type of mineralisation here seems to be replacement, rather than vein-filling as in the case of the B- and C-lodes.

4.3.2. Observations on the NAD Deposit.

Paragenetic tables convey graphically the relationship between various minerals in the wall rock and the ore lodes to one another. Tables 4.2 and 4.3 show the paragenesis of the host rock minerals and lode minerals respectively. The tables should be viewed in conjunction with the discussion on the microscopic examination of the host rock and the lodes respectively.

Table 4.2.
Summary of the paragenetic tables of the NAD host rock

LEGEND:

Replacement

- remnant - inclusion after partial replacement
- partial replacement
- complete replacement
- preferential replacement

Alteration

- alteration rim
- complete alteration
- partial alteration
- preferential alteration

Other

- veinlets
- inclusions
- paragenetic
- matrix
- recrystallized
- not present
- intergrowth

Plate 4.3.
Summary of the paragenetic tables of the NAD ore lodes

	QZ p	QZ s	K-SP	PLAG	CARB	TOU p	TOU s	MICA	CHL	CAS	RUT	PY	CHPY	ZIR
QZ p	★													
QZ s		★			❖ ⅄		❖ ⅄	❖ ⅄		❖		❖	❖	
K-SP		⅄	★		⅄		⅄	⅄		❖	⊙			
PLAG				★										
CARB		❖			★		❖ ⅄	⅄		❖		❖	❖	
TOU p						★								
TOU s		❖			❖		★	⅄		❖ ▩	⊙	❖	❖	
MICA		❖			⅄			★		❖		❖		
CHL									★					
CAS		⅄	⅄		⅄ ⇳		❖ ▩	⅄		★	⊙	❖	❖	
RUT											★			
PY		❖ ⅄			❖ ⅄		❖ ⅄	⅄		❖		★	❖ ▩	
CHPY		❖ ⅄			❖ ⅄		❖ ⅄	⅄		❖		❖ ▩	★	
ZIR														★

LEGEND:

Replacement

- ❄ remnant - inclusion after partial replacement
- ⅄ partial replacement
- ⊂ complete replacement
- ♓⅄ preferential replacement

Alteration

- ⊙ alteration rim
- ● complete alteration
- ◔ partial alteration
- ☯ preferential alteration

Other

- ⇔ veinlets
- ⊙ inclusions
- ❖ paragenetic
- ⅄ matrix
- ♌ recrystallized
- × not present
- ▩ intergrowth

The tables should be read in such a way that the symbols portray the influence of the X axis on the Y axis. Therefore, the minerals on the X axis replace, enclose and are the alteration products of the minerals on the Y axis.

Replacement is defined in the *"Glossary of Geology"* (Bates and Jackson 1987) as a *'change in composition of a mineral or mineral aggregate, presumably accomplished by diffusion of new material into old material without breakdown of the solid state'*. Replacement then generally occurs with introduction of new material from a fluid, replacing old material in another mineral. Quite often this replacement is not completed and remnants of the replaced mineral are included in the newly crystallised mineral as can be seen in plate 28 (appendix C) (quartz with remnants of feldspathic grains). This replacement can often be recognised by the original crystal form of the former mineral, so that the new mineral now is a pseudomorph of the original, as displayed by plates 47 and 27 (appendix C) (tourmaline needles replaced respectively by carbonate and quartz). Preferential replacement can occur as shown in plates 25 and 26 (appendix C), where only specific twin lamellae of an oligoclase grain has been replaced. This normally relates to the internal structure of a mineral, and twin planes are often susceptible to initial attack.

Recrystallisation is defined in the *"Glossary of Geology"* (Bates and Jackson 1987) as '*the formation, essentially in the solid state, of new crystalline mineral grains in a rock. The new grains are generally larger than the original grains and may have the same or a different mineralogical composition. ... The statement in thermodynamics is that solution of a mineral tends to occur most readily at points where external pressure is greatest, and that crystallisation occurs most readily at points where external pressure is least. This can be applied to recrystallisation in metamorphic rocks with attendant change in mineral shapes'.* Plate 21 (appendix C) shows the product of recrystallisation in the case of quartz.

Alteration is defined in the *"Glossary of Geology"* (Bates and Jackson 1987) as *'any change in the mineralogical composition of a rock brought about by physical or chemical means, especially by the action of hydrothermal solutions'.* Alteration often comprises sericitisation, chloritisation, and carbonatisation, called after the alteration product, and it takes place because of the introduction of new fluids into the system. The introduction of OH^- and CO_3^- ions cause chemical weathering, which is a form of alteration.

During a hydrothermal event the wall rock is often fractured and brecciated by increased hydraulic pressure. This fracturing also occurs on a microscopic scale, so that veinlets of a hydrothermal crystallite often cut through the original wall rock and minerals.

The mineral paragenesis in the NAD lode is cassiterite, tourmaline, carbonate pyrite and chalcopyrite. These minerals often surround cores of wall rock, or orthoclase, but generally occur within the main lode as fracture filling the fracture. Cassiterite and tourmaline apparently crystallised together, being intimately intergrown with one another. The carbonate crystallised later, together with the sulphides.

The wall rock paragenesis is quartz, orthoclase, oligoclase and sericite, with interstitial carbonate. The quartz is generally recrystallised, with sericite and carbonate replacing the feldspars.

4.3.3. Microscopic Examination of the NAD Deposit.

4.3.3.1. The Host Rock.

The host rock at the Rooiberg NAD-deposit is of sedimentary origin. Since the feldspar content of the rocks is generally higher than 50%, this rock cannot be classified as a quartzite. Haikney (1986) did some petrographic work on the deposits of A Mine Complex, and found the dominant minerals in the hanging wall of the host rock to be quartz (± 43.5%) and K-feldspar (±

33.5%) with the additional minerals ankerite (± 9%), plagioclase (± 6%) as well as tourmaline, sericite and chlorite. The original grain size varies between 0.5 mm - 0.75 mm. Ankerite forms anhedral masses, with bladed muscovite-sericite grains replacing feldspars. Cassiterite grains are generally 0.01 mm in diameter, with skeletal subhedral to anhedral tourmaline grains of ± 0.5 mm in diameter.

In hand specimen, the host rock is mostly of a dark red colour, and alteration on the bedding planes is evidence of the sedimentary origin of the host rock. The host rock within the Tin Zone is characterised by the dominant minerals K-feldspar (± 46%) and quartz (± 41%), with minor tourmaline (± 6.5%), plagioclase (± 6%) and accessory cassiterite (± 0.4%) and ankerite (± 0.2%). Tourmaline grains have an original size of ± 0.5 mm diameter and anhedral and irregular shapes with discrete grains and small aggregates of radiating crystals.

The above statements can be confirmed by petrographic studies conducted on the NAD-wall rock. The original grains are generally subrounded with some smaller rounded grains. The original wall rock is densely packed, with evidence of recrystallisation, especially in quartz. The interstitial matrix makes up only a small fraction of the bulk wall rock composition.

Quartz, orthoclase, plagioclase, muscovite-sericite, tourmaline and carbonate may be recognised by microscopic examination. Quartz displays undulatory extinction, indicating recrystallisation. The quartz also occurs interstitially, often replacing the feldspars and primary tourmaline. Fluid inclusions are present in the quartz grains, but can not be used for microthermometry studies (plate 58, appendix C) as they are too small.

The feldspars are generally orthoclase and plagioclase. Previous workers have identified microcline in some of the other tin deposits, but was not found in the NAD deposit. Orthoclase appears to be primary, and is much altered.

The orthoclase grains are mostly amorphous with red-brown discolouration and tiny rutile inclusions. The red-brown discolouration is probably the result of fine haematite dust included in the feldspar structure. Orthoclase is often replaced by interstitial quartz and carbonate. Sericitisation also occurs, often replacing complete grains and retaining the twin planes present in the original grain. Plates 56 and 57 (appendix C) are typical examples of K-feldspar microscopic morphology. There is a tendency for K-feldspars to be altered extensively. The main types of alteration are sericitisation as well as carbonatisation.

The anorthite content of the plagioclase varies from 15% to 23% and falls in the oligoclase range. Plagioclase is less altered and display no discolouration. It does, however, display preferential alteration or replacement where only specific twin lammellae have been replaced (plates 25 & 26, appendix C). Interstitial quartz and carbonate may partially replace plagioclase.

Previous workers mostly believed the carbonate to be ankerite, but recent microprobe work proved a substantial amount of siderite to be present. Microscopic distinction between siderite and ankerite is difficult and therefore the two carbonates were grouped together for petrographic purposes. The chemical differences will, however be discussed later. The carbonates mostly occur interstitially, replacing the feldspars and primary tourmaline. Small carbonate veinlets may be present in the host rock, often in association with secondary tourmaline.

Three major alteration phases affected the NAD-deposit, and can be recognised by microscope. Quartz in the wall rock seems to be generally recrystallised and it replaces other wall rock constituents. The recrystallised quartz grains are mostly anhedral and display undulatory extinction, such as in plates 21, 22, 23 and 24 (appendix C). Replacement occurs preferentially along unstable and often partly altered areas (appendix C, plates 25, 26 and

55) from where it extends to complete replacement. Recrystallised quartz is often pseudomorphous after the original mineral, as in tourmaline replacement (appendix C, plate 27) and quite often encloses remnants of the former mineral, which still exhibits the original grain morphology (appendix C, plates 28 and 29). Twinning characteristics are often retained in the secondary replacement material, as in the case of K-feldspar replacement by quartz. The Karlsbad twinning of the original orthoclase is still visible in plate 30 (appendix C).

Silicification was a major alteration event during the first phases of mineralisation in the NAD-deposit. The close association of quartz with tourmaline and cassiterite in the ore lodes (appendix C, plates 31 and 32) is evidence of this factor. As pointed out by Phillips (1982), the excess in silica indicates that earlier silicification than that associated with the mineralisation event, had also taken place.

Two further alteration events which can be associated with the mineralisation, are carbonatisation and sericitisation. The close association between carbonate and muscovite-sericite indicates that these alterations seem to have taken place simultaneously. Chlorite is mostly associated with primary tourmaline alteration, as well as areas where the so-called green-bands occur (appendix C, plates 33, 34 and 35). Sericite appears as a fine-grained alteration product of K-feldspar (appendix C, plates 30, 36 and 38), usually replacing complete grains. A coarser variety, apparently muscovite, occurs interstitially and often associates with carbonate (appendix C, plates 37, 39 and 40).

Carbonates in the wall rock occur interstitially, replacing altered wall rock constituents. Plate 41 (appendix C) is an example of inclusion by replacement, where a feldspar grain was enclosed by the interstitial growth of carbonate. The typical association of carbonate and muscovite-sericite (appendix C, plates 39, 42 and 43), results from carbonatisation after

alteration. It also seems that carbonatisation occurred after silicification in the wall rock. Plate 47 (appendix C) depicts carbonate replacement of euhedral tourmaline grains.

Two varieties of tourmaline occur in the wall rock. The first is primary and was deposited before the major mineralisation event. The second is associated with the mineralisation event, where it accompanies recrystallised quartz (appendix C, plates 31 and 32) and cassiterite. The primary tourmaline is often partially altered and replaced by chlorite and sericite (appendix C, plates 44, 45 and 46). Whole euhedral tourmaline grains were replaced by quartz, and the chloritisation event was associated with the carbonatisation event.

The ore minerals in the wall rock are mostly pyrite, chalcopyrite and cassiterite. These minerals occur in association with secondary tourmaline, muscovite-sericite and carbonate. The pyrites are mostly subhedral to euhedral grains, often including sericite (appendix C, plate 48), where different growth phases occurred. Chalcopyrite occurs as anhedral grains, and is often included as exsolution lamellae in pyrite (appendix C, plate 49). The cassiterite grains are subhedral with a darker to almost opaque colouring and are often associated with small grains of rutile.

Zircon occurs as an accessory mineral, and is part of the original sedimentary rock. The grains are well rounded and cracked, as displayed by plates 50 and 51 (appendix C). The zircons can be associated with any of the wall rock constituents.

4.3.3.2. The Ore Lodes.

The ore lodes of the NAD deposit vary somewhat macroscopically, but tend to be more uniform microscopically. The ore lode minerals are cassiterite, tourmaline, carbonate, pyrite, chalcopyrite and some free quartz. The cassiterite grains are usually anhedral to subhedral with some euhedral

crystals. The grains are mostly an orange-yellow colour with some darker patches. These darker patches may vary from orange to dark brown. Some colour variation occurs in the cassiterites, but there is very little conspicuous crystal zoning present. Cassiterite may also look opaque in transmitted light. Plates 52 and 53 (appendix C) are typical examples of the mode of cassiterite in the lode, and plate 54 (appendix C) is an example of the occurrence of interstitial cassiterite.

Brecciated fragments of wall rock in the ore lode served as crystallisation surfaces for the cassiterite. Complete wall rock fragments can be enclosed by lode crystallisation, but quite often only remnants of these fragments remain in the form of a small cluster of quartz and feldspar.

4.4. Geochemistry of the NAD Deposit.

Previous workers classified the host rock of the Rooiberg tin deposits as an arkose. Phillips (1982) refers to the host rock simply as a meta-arkose. This classification was underlined by the Pettijohn triangle (figure 4.2), used by Leube and Stumpfl (1963). Rozendaal *et al* (1986) employed the De la Roche (1966 in Rozendaal *et al* 1986) and Bard and Moine (1979 in Rozendaal *et al* 1986) diagrams to classify the host rock of the Rooiberg tin deposits. As illustrated by figures 4.3 and 4.4 the Boschoffsberg Quartzite Member rocks plot outside the defined fields for arkoses and greywackes. Figure 4.5 (Rozendaal *et al* 1986) attests to the sodic character of the Boschoffsberg Quartzite Member. The Rooiberg host rock seems to be aluminium-enriched sodic arkoses. However, none of the existing classification systems for sandstones correctly classify the NAD host rock and Boschoffsberg Quartzite Member. This is probably due to extensive alteration that took place during the mineralisation event by the introduction of hydrothermal or metasomatic fluids.

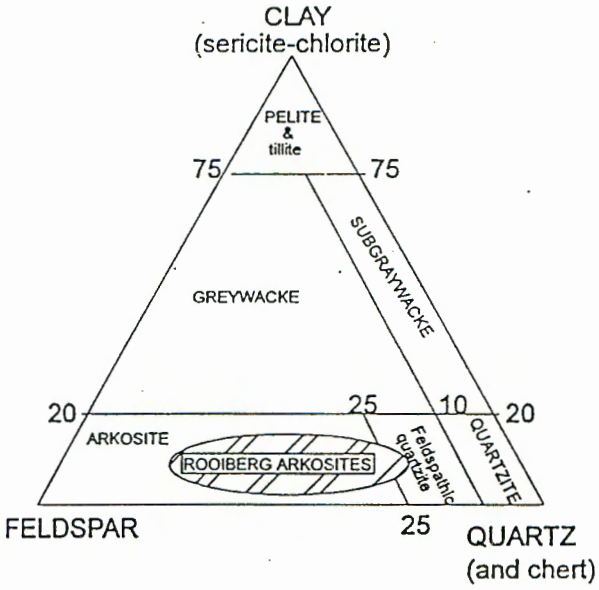

Figure 4.2. Position of the Rooiberg arkosites in the Pettijohn triangle (Leube and Stumpfl 1963).

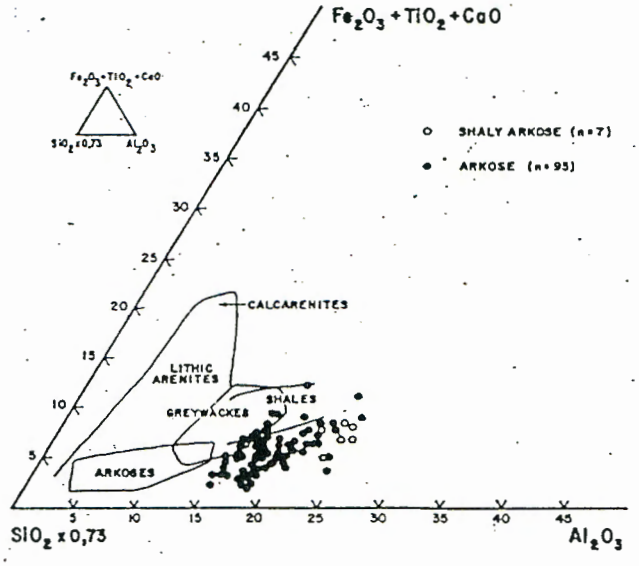

Figure 4.3. Ternary diagram illustrating the position of the Boschoffsberg Quartzite Member rocks to the fields for arkoses and greywackes (after De la Roche 1966 in Rozendaal *et al* 1986).

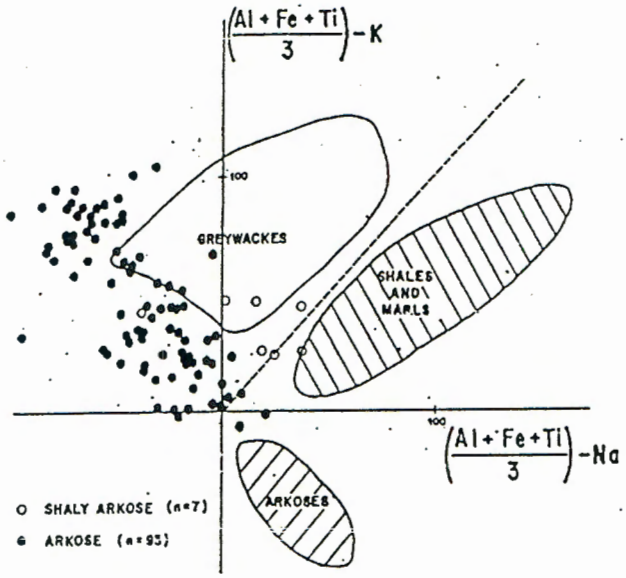

Figure 4.4. Diagram illustrating the position of the Boschoffsberg Quartzite Member rocks relative to typical greywackes and arkoses (after Bard and Moine 1979 in Rozendaal *et al* 1986).

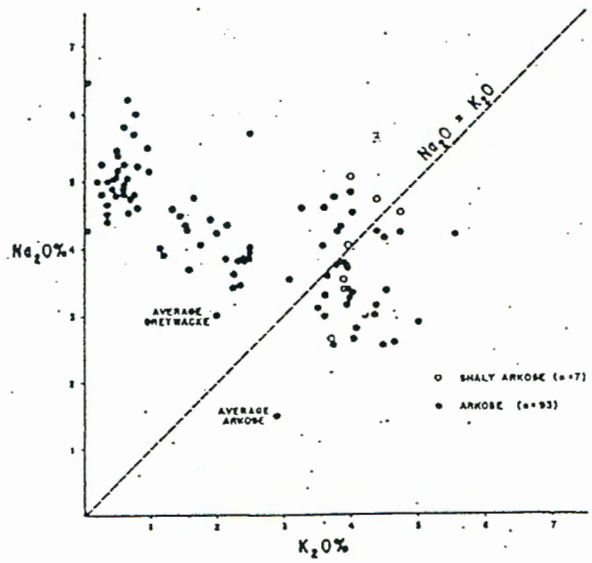

Figure 4.5. Diagram illustrating the sodic character of the upper Boschoffsberg Quartzite Member rocks (after Pettijohn 1975 in Rozendaal et al 1986).

The NAD quartzite is similar to the rest of the Boschoffsberg Quartzite Member as can be seen in figures 4.6 and 4.7. Figure 4.8 classifies the NAD host rock as a lith-arenite (Law *et al* 1990). However, as there are no lithic fragments present, this is not a correct classification. In comparison with the average shale, greywacke and arkose (Pettijohn 1975) the host rocks of the Rooiberg tin field show an unusually high sodium content. This indicates a predominance of sodic rather than potassic feldspar. In comparison with Strauss' (1947) unaltered quartzite, the NAD quartzite is somewhat depleted in some and enriched in other elements (table 4.4). From the geochemical data it seems that desilication has occurred. The relative increase of Al_2O_3, CaO, Na_2O and K_2O indicates feldspathisation and sericitisation of the quartzite. Potassic alteration seems prominent with the formation of both K-feldspar and muscovite-sericite. Plagioclase is generally albite rich, as indicated by its chemical analysis (table 4.5). Carbonatisation in the form of siderite, tourmalinisation and pyritisation may be responsible for the increase in FeO.

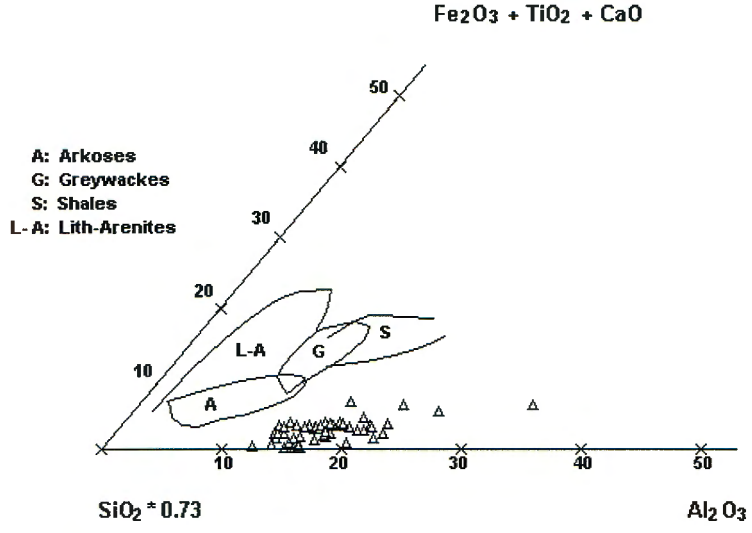

Figure 4.6. NAD whole rock chemistry in comparison to the geochemical fields for arkoses and greywackes (after Rozendaal *et al* 1986).

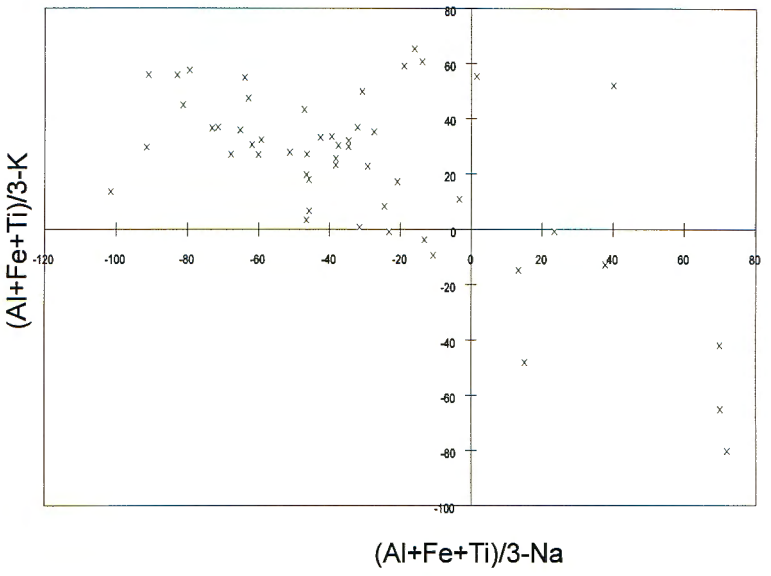

Figure 4.7. NAD whole rock chemistry showing a similar trend to that of figure 4.4 (after Rozendaal *et al* 1986).

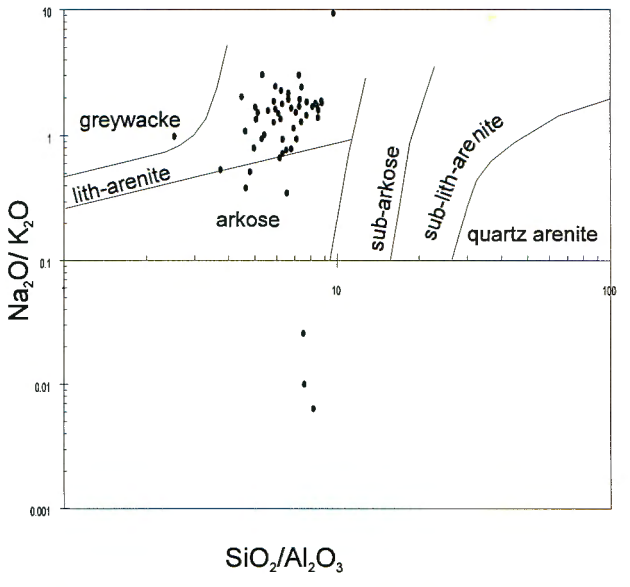

Figure 4.8. Geochemical classification scheme for sandstones (Law *et al* 1990).

Table 4.4

Geochemistry of the unaltered quartzite and average NAD host rock.

	Strauss' unaltered quartzite	Average: NAD Deposit
SiO2	89.01	73.32
TiO2		0.33
Al2O3	6.22	11.69
Fe2O3	0.56	0.50
FeO	0.07	1.35
MnO		0.05
MgO	0.50	0.77
CaO	0.39	1.04
Na2O	2.73	3.85
K2O	0.25	3.33
P2O5		0.06
H2O+	0.53	
H2O-		0.21
F		
CO2		
Total	100.26	99.11

(after Phillips 1982)

Table 4.5.

Plagioclase chemistry.

Sample	Na_2O	K_2O	SiO_2	Al_2O_3	FeO	MgO	CaO	Total
RB160-16	10.055	0.068	69.107	19.129	0	0	0.084	98.443
RB160-17	11.021	0	68.349	19.097	0	0	0.157	98.705
RB160-18	11.499	0.064	69.692	19.074	0	0	0	100.329
RB160-19	11.251	0.051	69.5	19.292	0	0	0.051	100.153
RB160-21	10.161	0.598	68.703	19.424	0	0	0.115	99
RB160-22	10.951	0.082	69.93	19.474	0	0	0.669	100.506
RB160-77	11.508	0.088	67.127	19.212	0	0	0	97.905
RB160-78	11.278	0.085	68.693	19.08	0	0	0.099	99.235
RB160-79	11.497	0.08	68.841	19.705	0	0	0	100.123
RB164-31	11.555	0.095	69.61	19.326	0	0	0	100.594
RB164-32	11.43	0.083	69.61	19.106	0	0	0	100.236
RB164-33	11	0.066	69.614	19.86	0	0	0	100.51
RB164-35	10.776	0.251	69.292	19.83	0	0	0.083	100.232
RB164-46	11.455	0.079	70.384	19.544	0	0	0	101.463
RB164-37	9.728	0.155	69.135	19.569	0	0	0.195	98.782
RB164-39	11.639	0.108	68.772	19.002	0	0	0.103	99.624
RB164-40	10.967	0.335	68.433	19.494	0	0.053	0	99.202
RB164-41	11.457	0.096	69.971	19.407	0	0	0.056	100.988
RB127-47	9.426	0.099	67.322	21.731	0.31	0	0.079	98.967
RB127-49	10.886	0.09	69.311	19.589	0	0	0.262	100.137
RB127-52	9.416	0.094	70.11	20.024	0	0	0.18	99.825
RB127-61	10.6	0.123	69.734	19.757	0	0	0.152	100.366
RB122-63	9.596	0.082	70.331	20.027	0	0	0	100.037
RB122-68	9.101	0.098	70.283	20.304	0	0	0.071	99.939

According to Strauss (1947) and Phillips (1982) the original wall rock was slightly feldspathic in nature and was then later feldspathised (desilicated) by the mineralising fluids in an open system. Phillips' silica versus alumina variogram shows a strong inverse ratio for the two elements (figure 4.9). Harker diagrams, however, often show strong inverse ratios that are not genetic and form part of the Chayes closure problem (Pearce 1968 & Nichols 1988). The use of Pearce element ratio (PER) diagrams overrides this closure problem. "Pearce element ratios are a method of testing hypotheses that involve material transfer in natural systems. In particular, Pearce element ratio diagrams are an effective means of portraying chemical variations within igneous rock suites and interpreting the causes of chemical diversity. Compared to oxide-oxide diagrams, Pearce element ratio diagrams are more discriminating. ... Using Pearce element ratio diagrams, the number of hypotheses that fail to be rejected is few" (Russel *et al* 1990). PER's may be a paradigm for testing hypotheses. It can, however, be used in any environment where chemical change or variation may be tested against an agent not participating in the various processes within the environment.

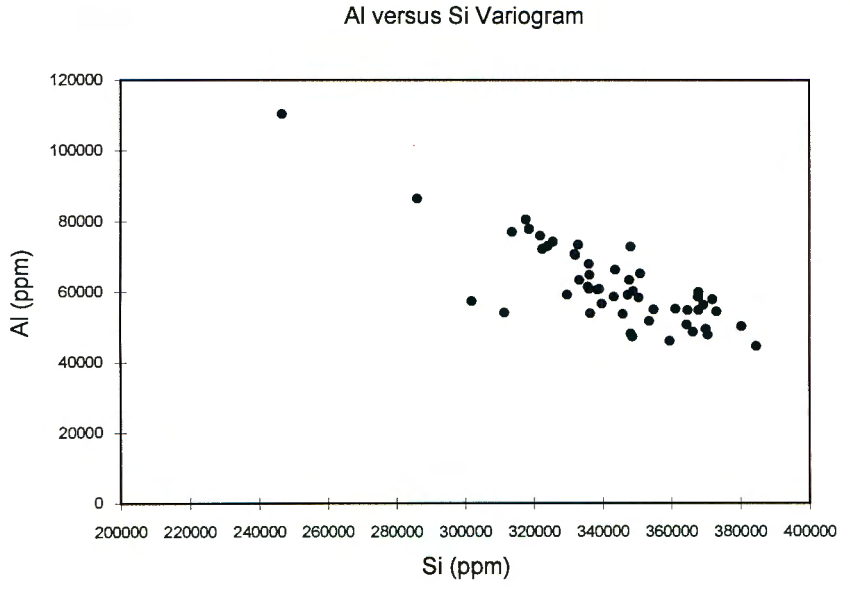

Figure 4.9. Phillips' Si versus Al variogram displaying an inverse ratio for the two elements (after Phillips 1982).

PER's were calculated with Ga as the common denominator. Ga often replaces Al in the geochemical environment, but since no alumina activity is present in the NAD deposit and the Ga values are relatively unchanging, it may be used to portray the alteration processes accompanying the mineralisation event. In comparison with the inverse Si-Al ratio of the Phillips (1982) variogram, the PER diagram shows a direct ratio for the same elements (figure 4.10). As the wall rock consists of almost 50% feldspar, it is apparent that Al should be in direct relationship with Si, confirming the validity of the PER diagram.

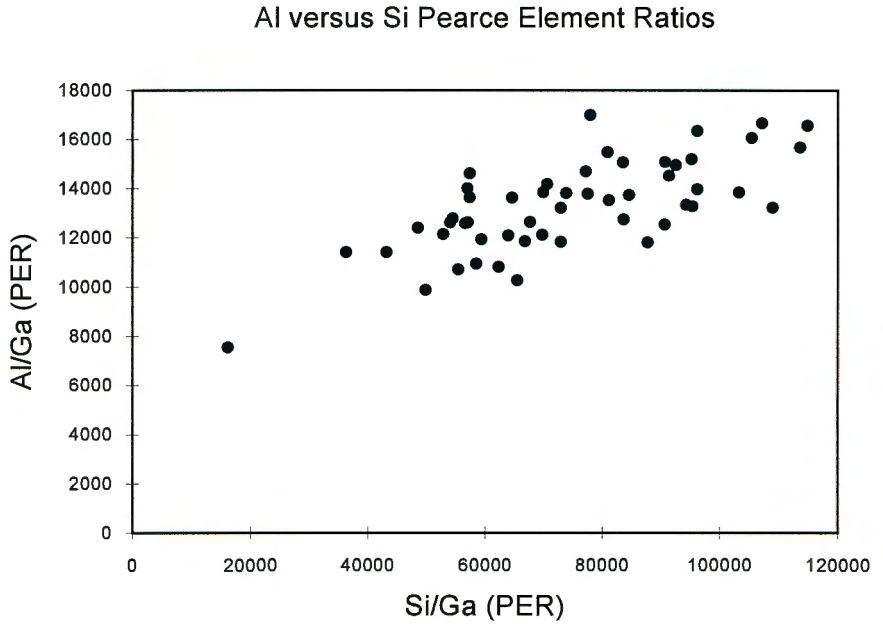

Figure 4.10. Al versus Si Pearce Element Ratio diagram showing that no real inverse ratio exist for the two elements.

The sodic character of the NAD host rock is illustrated by figure 4.11. Mark how the inverse ratio of Na and K stay inverse. This then would indicate that the Na and K have different origins in the host rock. From later statistical factor analysis that was conducted, it appears that Na was introduced by the mineralising fluids, while K was merely remobilised and originally came from the sedimentary host rock.

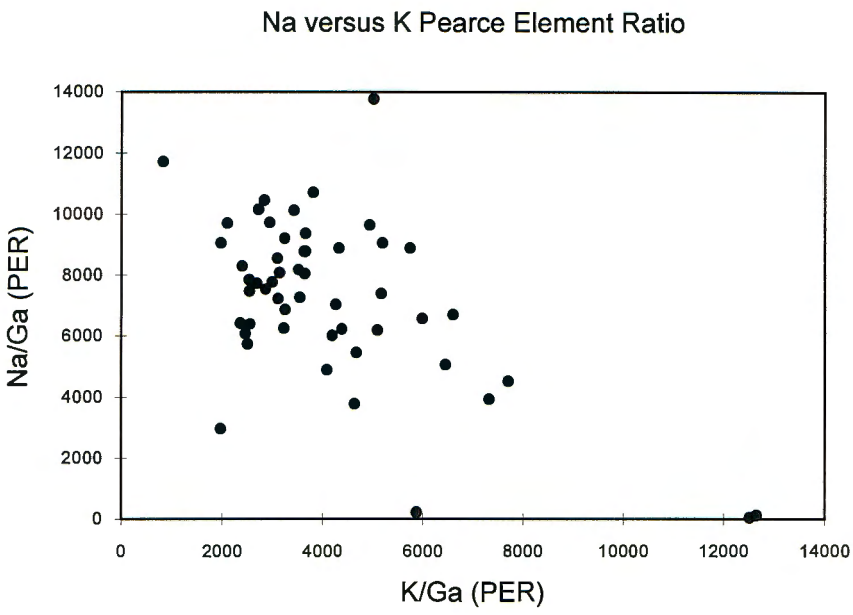

Figure 4.11. Na versus K Pearce Element Ratio diagram showing the inverse ratio of the two elements in the NAD deposit.

Haikney (1986) reported that the upper tin zone limit is defined by a sharp decrease in Ba:Sr, Ba, K_2O and K:Na values and ratios and a sharp increase in the Rb:Ba ratio with transition from the hanging wall to the tin zone. No definite markers were found to delineate the base of the tin zone.

Faure (1984 in Haikney 1986), however, found that Ba-values of 100 - 500 ppm indicate the tin zone, with values greater than 500 ppm being the hanging wall and values less than 100 ppm being the foot wall.

Vickers (1985 in Haikney 1986) found that the A Mine deposit is overlain by rocks with increased K_2O, Rb, Ba, Ba:Sr values and ratios and underlain by a layer of rocks with relatively increased SiO_2, CaO, Na_2O, Mn, Cu, Rb:Ba and K:Ba values and ratios. There is also a relative decrease in K:Rb ratios. Haikney produced a schematic diagram, indicating the geochemical variation across the tin zone (figure 4.12).

Ternary diagrams of certain trace elements may be used to classify the primary source of the host rock, or perhaps the source of the mineralising fluids in relation to a tectonic domain. Figure 4.13 depicts the relationship of La : Y : Nb (after Lécolle *et al* 1991) of the NAD whole rock chemistry. The whole rock chemistry data plots in the syn-orogenic domain, with a few points plotting towards Nb. Nb is associated with cassiterite and the mineralising fluids.

Scanning of zircons with the microprobe indicated that the zircons contain relatively high amounts of La, Ce and Y. The zircons are often cracked and well rounded, indicating a detrital origin and therefore implying that the ternary plot in figure 4.13 represents the source of the primary sediments of the NAD deposit. The spread of the points towards the right of the diagram (Nb) may

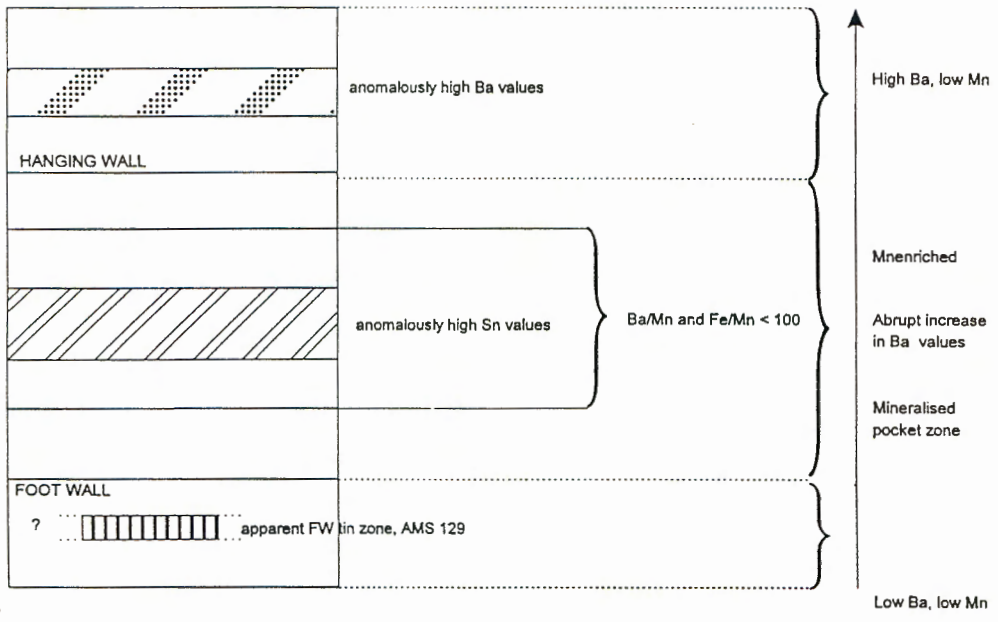

Figure 4.12. A schematic geological sequence of the Rooiberg tin deposit (after Haikney 1986).

be due more to the lack of La than a higher Nb content. These samples probably contain few zircons, explaining the low La values. The samples plotting in the non-orogenic and late to post orogenic domains all have relatively high Sn values (> 40 000 ppm), but are not exclusive to these domains.

It was found that some of the Archean granites from the Kaapvaal craton also plot in the syn-orogenic domain (pers. comm. D.K. Hallbauer), indicating that such rocks were the primary sources for the quartzites.

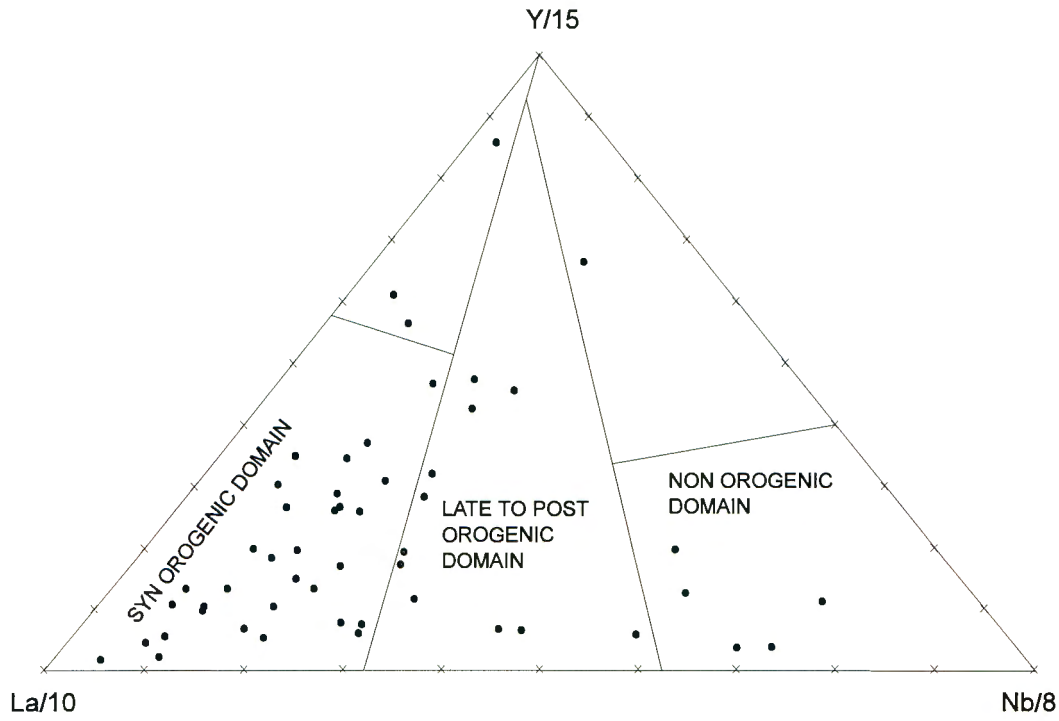

Figure 4.13. The relationship of La : Y : Nb is used to determine the tectonic domain of the source of the host rocks (after Lécolle *et al* 1991).

Further statistical analyses were conducted on the whole rock chemistry data, using the VAX BMDP factor analysis. At first the factor analysis was conducted on all the samples. The variation in the communalities obtained for the 7 factors (the communality of a variable is its squared multiple

correlation with the factors, ideally close to 1.0), is statistically unacceptable and this analysis could therefore not be used. Deviding the samples into low and high Sn-content (cut-off point at 100 ppm), two statistically acceptable analyses were obtained with average communality values of 0.8220 and 0.8735 respectively. These would then refer to the less and more mineralised parts of the wall rock.

The factors for the samples with high Sn content are listed in table 4.6. Factor 1 contains the heavy elements, indicating that it represents the heavy mineral concentrate found in the original sedimentary rock. These minerals were probably zircon containing the REE and elements such as Th, and rutile. No other accessory minerals have been identified, but there is a possibility of xenotime being present.

Factor 2 represents the feldspar factor, containing K-feldspar and albite. The negative ratio of Na implies that albitisation took place, and that the original feldspar was mainly orthoclase. Na and K have a true inverse ratio (figure 4.11) that may be explained by two different phases of feldspar formation. This implies that the K-feldspar is of primary origin with the later addition of albite. The plagioclases are all albite rich, containing up to 10 % Na_2O (table 4.5).

Factors 3, 4 and 5 represent the alteration phases during the mineralisation event. A ternary diagram is plotted from the squared factor loadings i.e. the variance explained by the elements of factors 3, 4 and 5, being representative of the alteration processes that took place. Figure 4.14 depicts the percentage of variance explained by the various elements in the rock. It must be kept in mind, though, that the three factors share various elements and will therefore not all plot as end-members to each of the factors. However, the closer an element plots to the corner points (factors), the higher the variance explained and its contribution to a specific mineral assemblage.

Table 4.6.

Sorted, rotated factor loadings for high tin values.

	Factor 1	Factor 2	Factor 3	Factor 4	Factor 5	Factor 6	Factor 7
Nd	0.945	0.000	0.000	0.000	0.000	0.000	0.000
La	0.942	0.000	0.000	0.000	0.000	0.000	0.000
Ce	0.932	0.000	0.000	0.000	0.000	0.000	0.000
Ti	0.868	0.000	0.000	0.273	0.000	0.000	0.000
Th	0.818	0.000	0.000	0.000	0.377	0.000	0.386
Zr	0.815	0.000	0.000	0.000	0.344	0.000	0.290
Y	0.643	-0.579	0.000	0.000	0.000	0.000	0.000
V	0.605	0.000	-0.259	0.522	0.264	0.000	0.000
Cr	0.577	0.000	0.435	0.266	0.000	-0.256	0.477
Pb	0.000	0.895	0.000	0.000	0.000	0.000	0.000
Na	0.000	-0.856	0.000	0.000	0.000	0.000	0.000
K	0.000	0.831	0.440	0.000	0.000	0.000	0.000
Ba	0.000	0.774	0.502	0.000	0.000	0.000	0.000
RSi	0.000	0.000	0.912	0.000	0.000	0.000	0.000
Al	0.000	0.360	0.831	0.000	0.000	0.000	0.000
Mo	0.000	0.490	0.703	0.000	0.000	0.000	0.000
Fe	0.000	0.000	0.000	0.897	0.000	0.000	0.000
Mg	0.000	0.000	0.000	0.801	0.000	0.511	0.000
Mn	0.000	-0.398	0.000	0.748	0.000	0.338	0.000
Sc	0.390	0.000	0.375	0.678	0.000	0.000	0.000
Ni	0.000	0.000	0.000	0.628	0.267	-0.446	0.266
Sn	-0.288	0.000	0.000	0.000	0.861	0.000	0.000
Rb	0.308	0.000	0.000	0.000	0.707	-0.310	0.000
Cu	0.000	-0.542	0.000	0.374	0.650	0.000	0.000
Nb	0.315	-0.397	0.000	0.000	0.620	-0.349	0.000
Ca	0.000	0.000	0.000	0.000	0.000	0.875	0.000
Sr	0.000	0.000	0.549	0.000	0.000	0.678	0.000
U	0.000	0.000	0.000	-0.283	0.000	0.000	0.806
P	0.437	0.000	0.000	0.000	-0.383	0.000	0.552
Zn	0.389	0.000	-0.268	0.294	0.422	0.000	-0.371
Factor Total	6.933	4.561	4.346	3.909	3.100	2.282	1.948

Elements explaining up to 70% variance in the alteration processes of the highly mineralised NAD host rock are:

Factor 3: Ba, Rsi, Al, Mo, K, Sr, Cr, (La, Ce, Nd)

Factor 4: Mn, Fe, Mg, Y, Ni, Sc

Factor 5: Th, Sn, Nb, Rb, P, Cu, Zr, (Na).

Factor 3 represents free quartz and some K-feldspar, as well as displaying the close association of Mo with the free quartz. This association may be explained by the presence of MoO_4^{2-} in the fluid inclusions of quartz. Such an association was confirmed for the Vladeasa Granite, Romania (pers. comm. D.K. Hallbauer). Approximately 20 ppm MoO_4^{2-} was found to be present in some inclusions. Free quartz was calculated by subtracting the equivalent of Al in feldspar from the total quartz (Si - 3Al = RSi). The association of free quartz with the K-feldspar implies that the Si is also from primary origin, that it was remobilised and then recrystallised. In the absence of abundant quartz veins and free quartz in the ore lodes, it may be concluded that very little Si was introduced by the mineralising fluids.

Factor 4 appears to represent a combination of ore lode minerals. A definite association is that of tourmaline and pyrite, and also the occurrence of siderite and ankerite. The heavy elements associated with this factor are mostly found in tourmaline and may also be present in pyrite.

Factor 5 is the mineralisation factor, containing Sn and Nb together with Rb and Na. The P and Th probably are because of a P-mineral that associates with the mineralisation factor. However, no such association was found microscopically.

Factor 6 represents the carbonate factor containing Ca, Sr and some Mg. The somewhat negative ratios of Ni, Rb and Nb indicate that the carbonates were deposited after cassiterite and tourmaline, as represented by the major

mineralisation phase. The carbonate phase is then a much later phase of the mineralisation event.

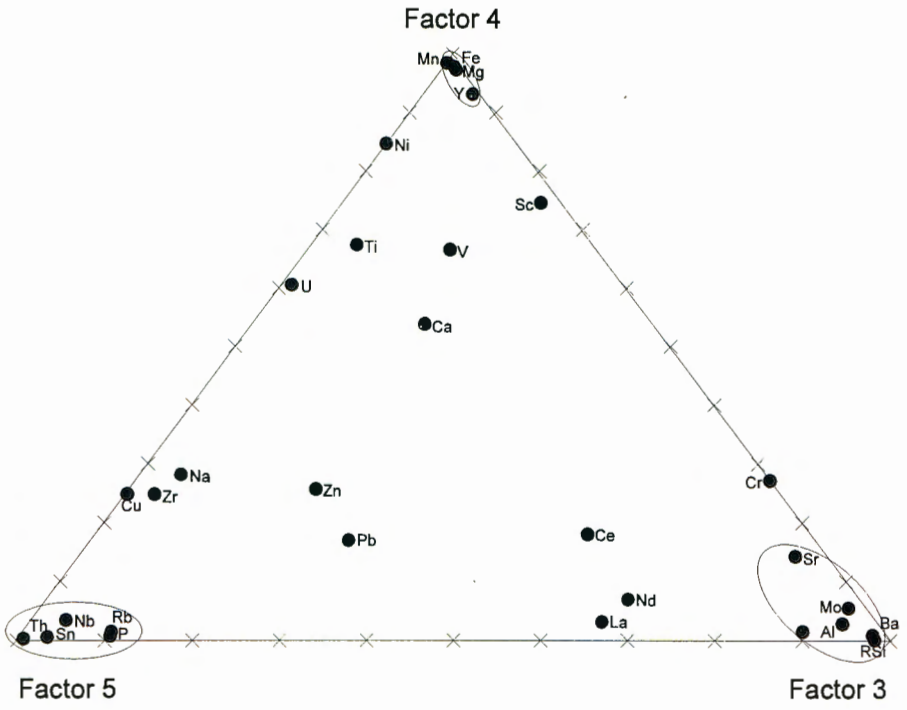

Figure 4.14. Percentage of variance explained by the various alteration processes present in the highly mineralised host rock.

The factors for the samples with low Sn content are listed in table 4.7. Factor 1 again contains the heavy mineral elements, and is indicative of the original sedimentary rock. The minerals represented by this factor appear to be zircon, rutile and possibly xenotime (P, as no apatite or other P-minerals were identified). Nb also appears in factor 1. This may be due to the low Sn content of these samples, which may suppress the inherent character of elements supposedly associated with cassiterite or the mineralisation event.

Factor 2 is the feldspar factor, containing K, Pb, Ba, Rb, Al and Na. Again the less mineralised nature of the samples (containing less Sn), gives less

pronounced differentiation between the elements. The inverse Na-K ratio is also evident, implying that K and Na do not have the same origin.

Table 4.7.

Sorted, rotated factor loadings for low tin values.

	Factor 1	Factor 2	Factor 3	Factor 4	Factor 5	Factor 6	Factor 7
Ti	0.911	0.000	0.000	0.000	0.000	0.000	0.000
Th	0.893	0.000	0.000	0.000	0.000	0.000	0.000
Zr	0.854	0.000	0.000	0.000	0.000	0.000	0.000
Nb	0.827	0.000	0.000	0.000	0.000	0.000	0.000
Ce	0.793	-0.346	0.000	0.000	0.000	0.000	0.000
La	0.735	-0.478	0.000	0.000	0.000	0.000	0.000
Nd	0.723	-0.436	0.000	0.000	0.000	0.000	0.000
V	0.689	0.000	-0.367	0.000	0.327	0.000	0.000
P	0.688	0.267	0.000	0.269	0.000	0.000	0.000
K	0.000	0.935	0.000	0.000	0.000	0.000	0.000
Pb	0.000	0.913	0.000	0.000	0.000	0.000	0.000
Ba	0.000	0.868	0.000	0.000	0.000	0.000	0.000
Rb	0.000	0.578	0.000	-0.286	-0.416	0.000	0.000
Al	-0.356	0.530	0.513	-0.256	-0.321	0.000	0.000
RSi	0.000	0.000	0.949	0.000	0.000	0.000	0.000
U	0.272	0.000	0.596	-0.458	0.000	0.000	0.000
Na	0.000	-0.334	0.586	-0.265	0.000	-0.309	-0.400
Mo	0.000	0.000	0.578	-0.385	0.000	0.000	0.348
Sc	0.000	0.000	0.000	0.796	0.000	0.000	0.262
Fe	0.303	0.000	0.000	0.723	0.351	0.000	0.000
Sn	0.000	0.000	0.263	-0.716	0.000	0.000	0.250
Ni	0.000	0.347	-0.359	0.693	0.000	0.000	0.000
Zn	0.000	0.263	0.000	0.592	0.000	0.481	0.000
Mg	0.000	0.000	0.000	0.000	0.935	0.000	0.000
Ca	0.000	0.000	0.000	0.000	0.910	0.000	0.000
Mn	0.000	0.000	0.000	0.000	0.783	0.477	0.000
Sr	0.000	0.000	0.000	0.000	0.709	-0.369	0.000
Cr	0.465	0.000	0.000	0.000	0.000	0.732	0.000
Y	0.358	0.000	0.000	0.000	0.000	0.000	0.814
Cu	0.000	-0.450	0.425	-0.482	0.000	0.000	0.255
Factor Total	6.741	4.491	3.911	3.692	3.522	1.720	1.404

Elements explaining up to 70% variance in the alteration processes of the less mineralised NAD host rock are:

Factor 3: Rsi, Nd, La, Na, Ti, Zr, Ce

Factor 4: Sc,Cr, Zn, Sn Fe, Ni, K

Factor 5: Mg, Ca, Mn, Th, Sr.

Factors 3, 4 and 5 again represent the alteration phases during the mineralisation event. A ternary diagram is plotted from the squared factor loadings. Figure 4.15 depicts the percentage of variance explained by the various elements in the rock.

Factor 3 represents free quartz, La, Ce, Nd, Zr, Ti and Na, and a weak association with Mo. The REE are probably from the zircons present in the various samples, while the Mo association may be explained by MoO_4^{2-} in quartz fluid inclusions. The association of Na with free quartz indicates that Na was introduced by the mineralising fluids. This is also based on the inverse ratio of K and Na, where K originates from the host rock, and Na from the mineralising fluids.

Factor 4 represents the mineralising factor with the presence of Sn and other heavy elements associated with pyrite and tourmaline formation. There is also a weak association with K, possibly because the lesser mineralised host rock is mostly feldspathic (orthoclase) and much sericitised. The occurrence of cassiterite ore is generally of disseminated type and therefore in close association with the host rock.

Factor 5 represents the carbonate factor with the presence of Ca, Mg, Mn, Sr and Th. This appears to be mostly ankerite, although it must be kept in mind that several elements are shared by the various factors (mineral processes) and that this factor then also represents siderite. The weak association with Pb and Rb indicates that this factor forms part of the mineralising event, though as a later phase as indicated by mineralogy and petrography.

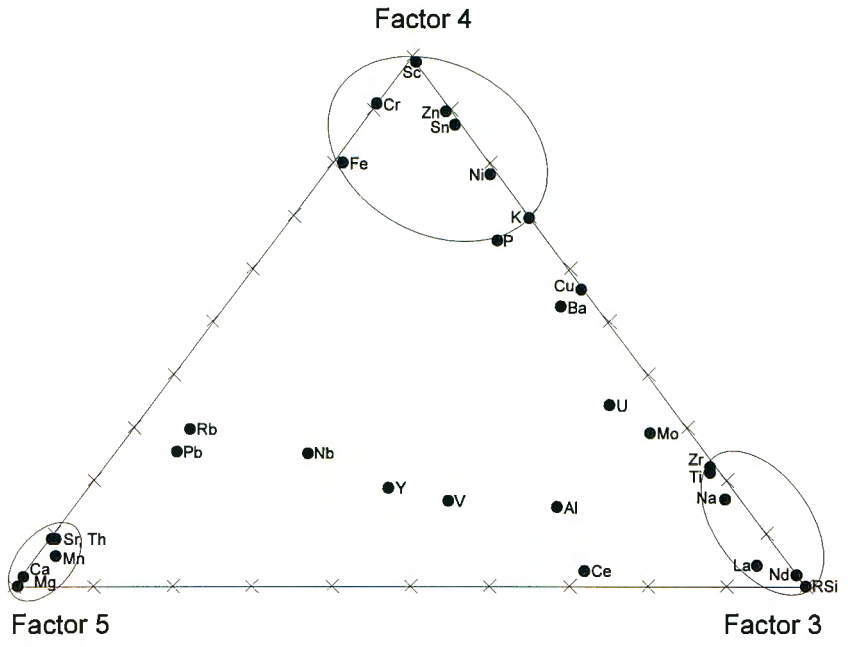

Figure 4.15. Percentage of variance explained by the various alteration processes present in the less mineralised host rock.

Implications of chemical processes that took place during mineralisation.

The inverse ratio of K vs Na: extensive sericitisation is indicative of K remobilisation, while the high Na_2O content of plagioclase indicates albitisation. No or very little K was introduced into the system by the mineralising fluids. Almost no free K-feldspar or newly crystallised orthoclase is associated with the ore lodes and replacement bodies. There are only more or less orthoclase rich host rocks and host rock fragments associated with the ore lodes and replacement bodies.

Very little free quartz was found in the form of veinlets in the host rock and in the ore lodes. It may be deduced that very little Si was introduced by the

mineralising fluids. Some quartz was newly crystallised, but it was mostly recrystallised from the host rock.

Differentiation on the basis of high and low Sn values shows the alteration processes associated with mineralisation more clearly. Although the chemical and mineralogical processes are less pronounced in the less mineralised samples, it may be deduced that the same processes were active during mineralisation in the highly and lesser mineralised areas of the NAD deposit. The major alteration processes are K-remobilisation (sericitisation), and carbonatisation, tourmalinisation and pyritisation in association with Sn-mineralisation.

Chapter 5 .

5. Mineral Chemistry.

5.1. Cassiterite chemistry.

Several cassiterite grains from different ore lodes in the NAD mine were analysed on the microprobe for Sn, Fe, W, Ti, Ta, Nb, Mn, and Ca. Both selected spot-analyses and line-analyses were conducted to pinpoint trace element variation in the grain structure. The NAD cassiterites contained no detectable Ca, as the values were consistently nil, with below detection values for Mn, Ta, and Nb. High values for Fe and W were found.

Cassiterite occurs petrographically as fine-grained masses often intergrown with tourmaline. Crystallisation seems to have taken place around feldspathic cores in the ore lode, with later crystallisation of carbonate as vein filler. The grains are generally subhedral with an orange-yellow colour in thin section. Typical colour-zonation is almost completely absent. Some colour zonation occurs, but seems to be mostly of the type where the core is darker brown-yellow and the rim more yellow. The darker brown patches occur commonly without specific boundary. Analysis lines were put across these colour variations to determine the relationship between colour and trace element content in the cassiterite grains.

Research conducted by Goncharev and Filatov (1971 in Mills 1985) indicates that "Ti may cause the SnO_2 lattice to contract isotropically, but does not alter the colour of the crystal. Fe appears to cause anisotropic lattice deformation and to colour the cassiterite brown". As an abundance of W was found in the darker brown patches, it can be assumed that the larger ion would act as in the case of Fe, and cause anisotropic lattice deformation. No W-minerals

were found, and it can be safely concluded that all the W was substituted for Sn in the cassiterite lattice.

Figures 5.1 and 5.2 display typical trace element variation in single cassiterite grains. It was found that W is mostly antipathetic to Fe, so that the two elements seldom occur together in high concentrations. The darker brown patches tend to have high W values, while high Fe values are not necessarily related to the darker areas. This observation is, however, in contrast to the work of several authors, who have found that Fe is responsible for typical colour zonation in cassiterites. Since the typical zonation of cassiterite is almost completely absent, it might be that the darker W-rich patches overshadow the general darker orange colour of the cassiterite caused by high Fe values. Higher Ti values evidently do not alter the crystal colour.

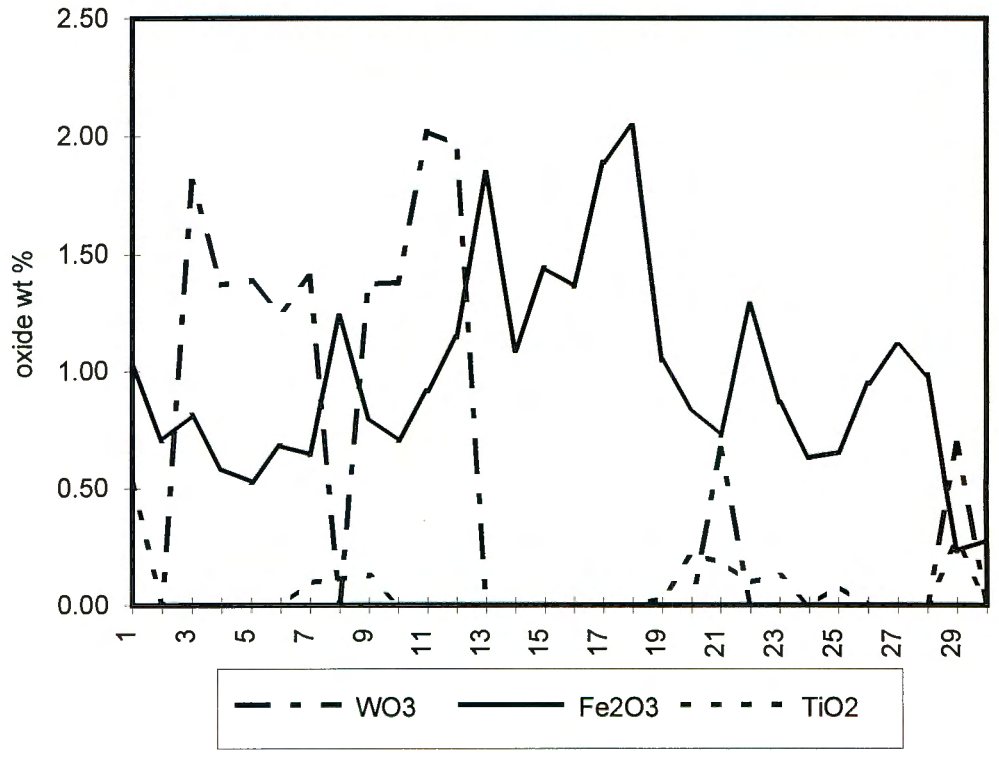

Figure 5.1. Trace element traverse from microprobe data on a single cassiterite grain, RB088.91(1).

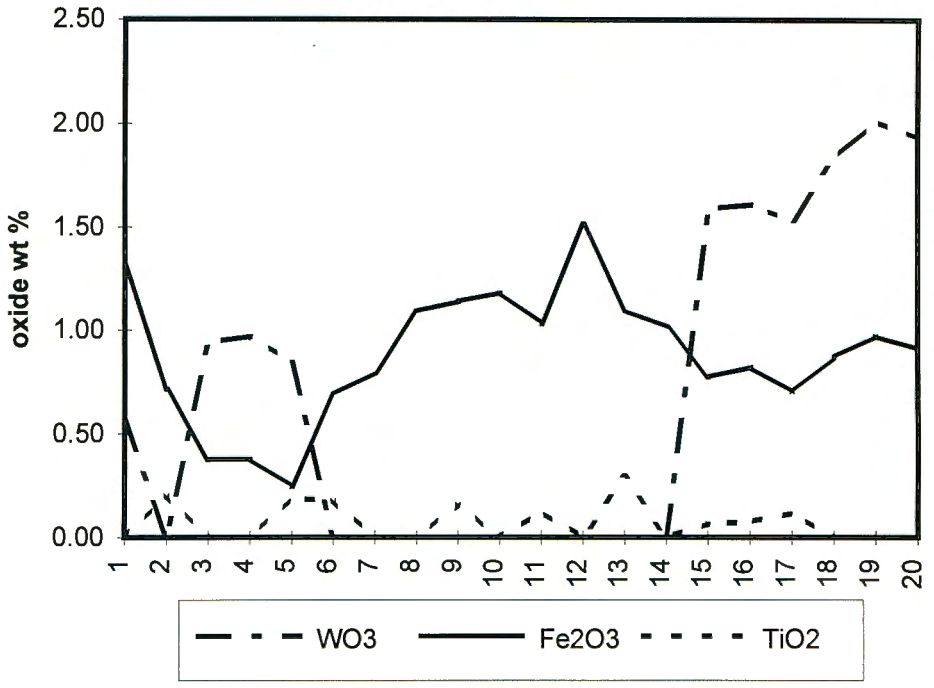

Figure 5.2. Trace element traverse from microprobe data on a single cassiterite grain, RB088.91(2).

The cassiterite is generally very fine-grained, with slight variation in grain size. It seems to have crystallised over a period, at first forming larger grains, and then forming finer grains as the temperature decreased. From mineral chemistry data, it appears that very little variation in fluid composition occurred during the crystallisation history of cassiterite.

Unfortunately no fluid inclusions were found in the cassiterite itself. Other inclusions are also rare, but intergrowths with tourmaline, rutile and the sulphides are common.

All the trace elements found in the NAD cassiterites by quantitative optical emmission spectrography are listed in table 5.1. The analyses were conducted on clean cassiterite samples. Although not as many elements

could be analysed than on the microprobe, the results are in accordance with the microprobe analyses.

Table 5.1.

Cassiterite trace element chemistry.

(ppm)	RB066.91	RB014.91	RB010.91	RB020.91	RB004.91	RB120.91
Cr	10.2	12.6	5.3	6.6	6.8	8.1
Cu	2.9	173.0	199.0	15.7	319.0	1315.0
Fe	4627.0	4874.0	4160.0	5000.0	4999.0	4562.0
Ga	3.4	7.2	<2.4	2.5	2.9	2.6
In	12.0	8.4	8.6	13.2	11.6	15.8
Mn	14.6	55.3	12.9	14.5	25.8	5.8
Nb	33.2	47.5	63.2	30.1	70.6	56.6
Ni	6.2	4.5	2.5	6.7	2.6	13.8
Pb	<2.4	5.0	<2.4	<2.4	25.0	36.5
Sb	74.8	-	44.2	80.3	37.9	50.0
Sc	25.1	12.2	31.4	23.2	8.4	39.4
V	137.0	124.0	234.0	291.0	233.0	323.0
Ti	1079.0	1296.0	1618.0	605.0	2406.0	1277.0
W	1894.0	521.0	1764.0	1152.0	709.0	1713.0
Y	-	49.1	22.8	25.8	21.5	19.6
Zr	20.1	106.0	14.2	9.2	21.1	10.9

(Optical emission spectrographic analysis conducted under supervision of U. Kempe and P. Biskop at the Bergakademie Freiberg, Germany)

5.2. Tourmaline Chemistry.

Tourmaline is present in the ore lode as one of the major ore lode minerals. From the mineral paragenesis it can be deduced that tourmaline crystallised before and simultaneously with cassiterite. The abundance of tourmaline in the lode suggests that the mineralising fluids were enriched in B.

The tourmaline is of the schorl variety (Henry & Guidotti 1985 in Henry & Dutrow 1992). The grains are subhedral to euhedral with a dark brown-green to blue-green colour in polarised light. Masses of very fine-grained tourmaline are associated with the ore lode minerals. Needle-like radiating clusters of tourmaline are also present. There is little chemical variation across the tourmaline grains and also among the different ore lodes, which indicate that the mineralising fluid composition was constant during tourmaline

crystallisation. The NAD tourmalines plot across several fields in the ternary plot of Henry and Guidotti (figure 5.3). The secondary tourmalines are, however, hydrothermal in origin and not associated with the original host rock, and can therefore not be used to classify the host rocks. The source of the mineralising fluids, being the Bushveld granites, will fall into category B (Li-poor granitoids, pegmatites and aplites).

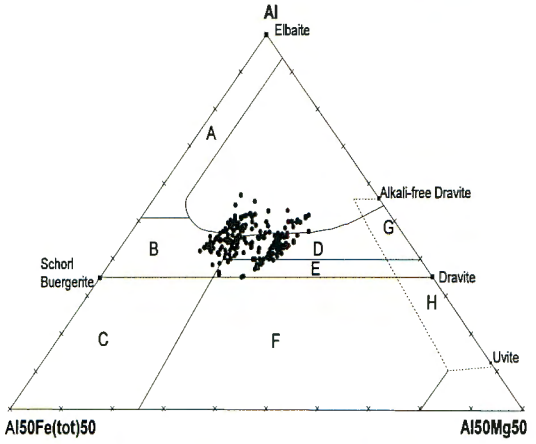

A	Li-rich granitoids, pegmatites and aplites
B	Li-poor granitoids, pegmatites and aplites
C	Hydrothermally altered granitic rocks
D	Metapelites and metpsammites (aluminous)
E	Metapelites and metpsammites (Al-poor)
F	Fe3+ -rich quartz-tourmaline rocks, calc-silicates and metapelites
G	Low Ca ultramafics
H	Metacarbonates and metapyroxenites

Figure 5.3. Al-Fe-Mg ternary diagram classifying the NAD tourmalines as schorl, crystallised from Li-poor granitoids and crystallised in metapelites and metapsammites (after Henry and Guidotti 1985 in Henry and Dutrow 1992).

Table 5.2 contains the optical emmission spectrography trace element analysis conducted on clean tourmaline samples under supervision of Prof. D. Wolf and Dr. U. Kempe.

Table 5.2.

Tourmaline trace element chemistry.

(ppm)	RB156.91	RB066.91	RB028.91	RB020.91	RB016.91	RB014.91	RB004.91
Ag	0.019	0.010	0.015	0.016	0.020	0.024	0.026
Ba	<80.0	<80.0	<80.0	114.0	87.5	<80.0	<80.0
Cu	>360.0	8.4	>360.0	>360.0	44.9	>360.0	350.0
Ga	61.6	85.4	75.9	45.2	141.0	168.0	109.0
Mn	277.0	<24.0	76.9	85.4	519.0	59.1	31.2
Pb	31.6	<6.4	8.5	12.5	11.6	186.0	79.6
V	161.0	356.0	242.0	280.0	298.0	220.0	193.0
Be	7.6	4.9	2.2	3.9	5.2	3.0	1.8
Co	8.7	25.2	15.6	5.8	7.8	12.1	10.0
Cr	264.0	193.0	85.0	236.0	203.0	105.0	105.0
Mo	3.2	2.9	2.2	2.2	3.4	2.5	1.8
Nb	17.2	9.2	<8.0	<8.0	37.0	<8.0	<8.0
Ni	102.0	149.0	116.0	105.0	117.0	114.0	99.0
Ti	6794.0	7226.0	5151.0	3794.0	4475.0	4663.0	3913.0
W	43.7	178.0	25.8	45.4	114.0	29.5	25.4
Y	237.0	9.7	8.0	19.4	25.2	16.6	14.4
Zr	813.0	200.0	122.0	156.0	156.0	197.0	89.5

(Optical emission spectrographic analysis conducted under supervision of U. Kempe and P. Biskop at the Bergakademie Freiberg, Germany)

Pirajno and Smithies (1992) have shown that the FeO/(FeO + MgO) ratio (Fe#) in tourmaline may be used to deduce the distance of an exogranitic ore body from the origin of the mineralising fluids. Tourmalines within endogranitic deposits have a Fe# number close to 1, while the Fe# number for progressively distal deposits systematically decreases. According to figure 5.4 three areas (A, B and C) relative to distance from the granitic source may be identified. Distance is relative and cannot be calculated accurately, because the wall rock probably influences tourmaline chemistry. The tourmaline chemistry and field evidence indicate that Fe# number greater than 0.8 are indicative of endogranitic to proximal deposits up to a few hundred metres from the granite contact. Values of 0.8 to 0.6 indicate proximal to intermediate deposits and values of less than 0.6 indicate

deposits at a distance of more than approximately 1 km from the source of the mineralising solutions (Pirajno and Smithies 1992). Applying this to the Rooiberg and Leeuwpoort tourmalines, Pirajno and Smithies found that the Leeuwpoort deposits are closer to the source of the mineralising hydrothermal fluids.

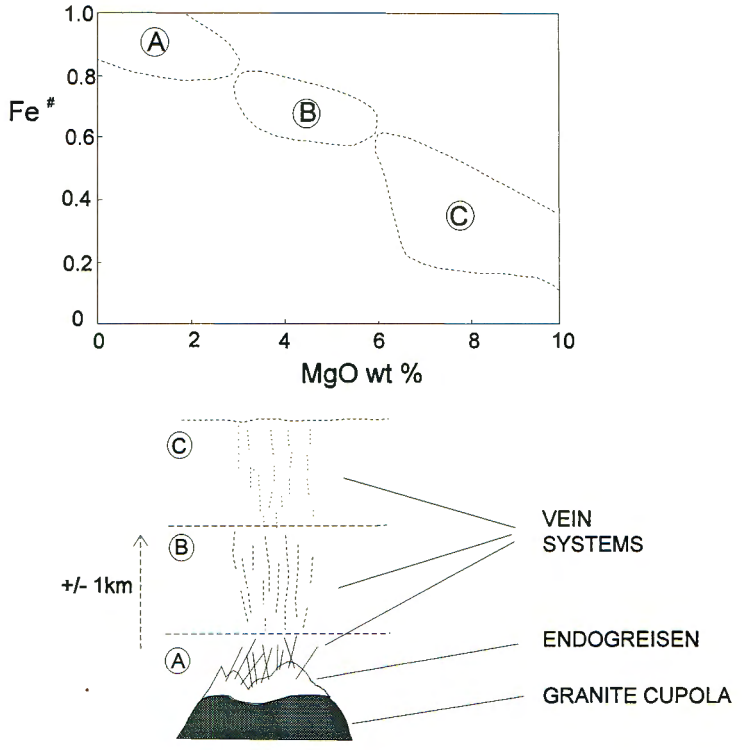

Figure 5.4. FeO/(FeO + MgO) diagram showing fields of endogranitic to proximal (A), proximal to intermediate (B) and distal (C) tourmalines and their respective position within an idealised granite-related Sn-W hydrothermal system.

The NAD tourmaline chemistry plots in areas B and C, which is intermediate to distal. Figures 5.5 and 5.5a to e display the combined plot for the different ore lodes, as well as the plots for the individual lodes respectively. The C-lode is the only lode to plot in only one field (B), and evidence is strongest from the tourmaline lode-plots for the furthest area (C) from the source rocks. Accepting Pirajno and Smithies' estimate, this would imply that the NAD deposit lies approximately 1 km or more from the granitic source of the hydrothermal mineralising fluids.

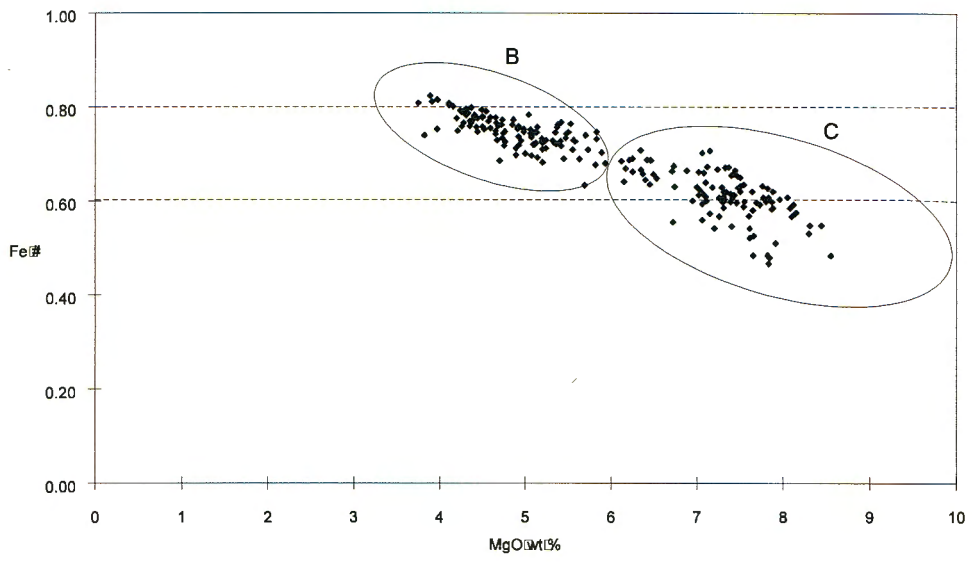

Figure 5.5. Compilation of tourmaline FeO/(FeO + MgO) ratios for the ore lodes of the NAD deposit (after Pirajno and Smithies 1992). Note that field linearity is less steep here than with the Pirajno and Smithies data. The field(s) defined by the NAD tourmalines do not correspond to the three clusters found by Pirajno and Smithies, but form a superimposed linear arrangement on two of the clusters (B and C).

Figure 5.5 a to e. The tourmaline chemistry plots for the individual ore lodes of the NAD deposit (after Pirajno and Smithies 1992), where

Fe # = FeO/(FeO + MgO).

Note that the tourmaline ratios correspond to the two fields B and C. The plots are not consistent with what Pirajno and Smithies have found, but a clear distinction may be made between proximal and distal. The NAD plots are mostly intermediate to distal, indicating that deposition took place at a considerable distance from the source rock.

a

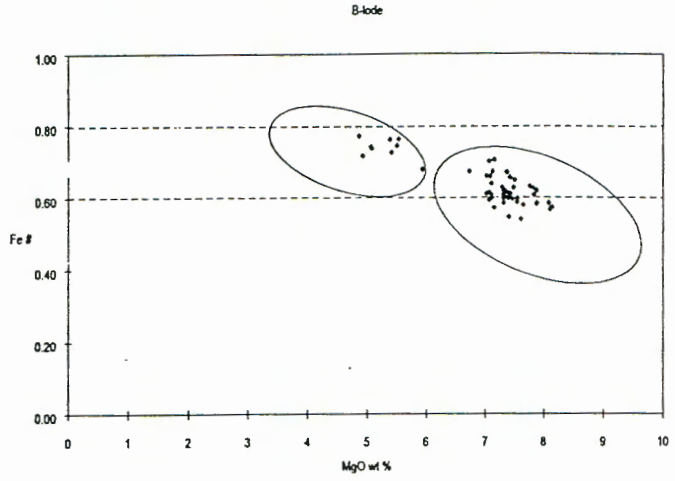

b

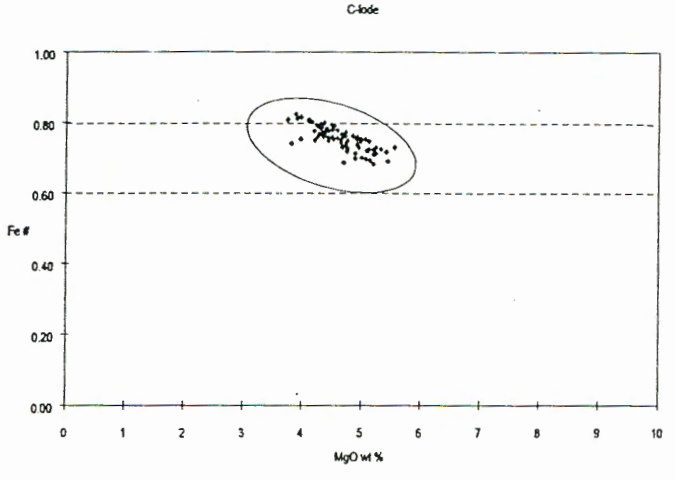

c

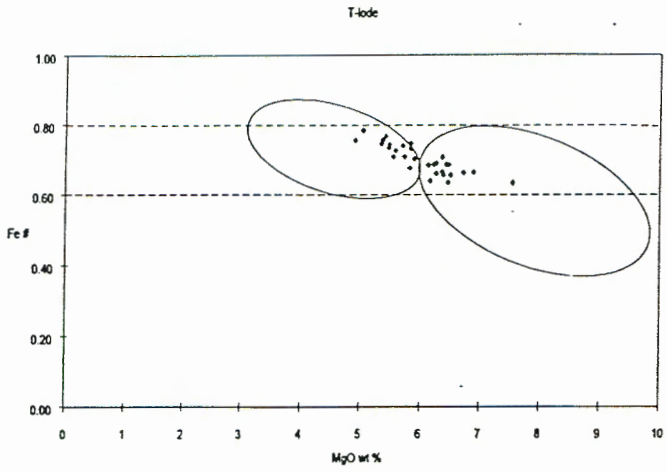

d

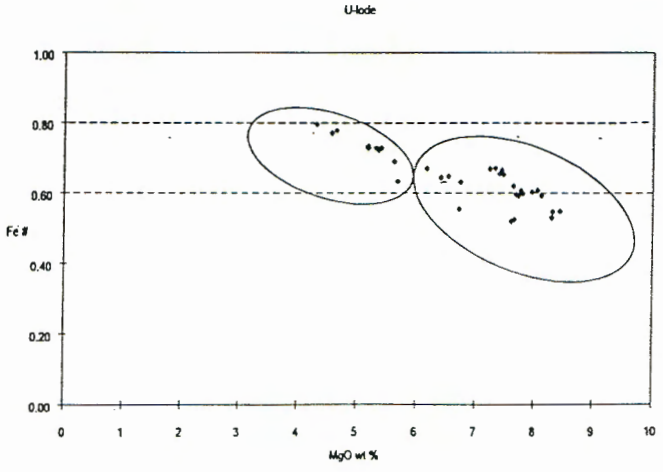

e

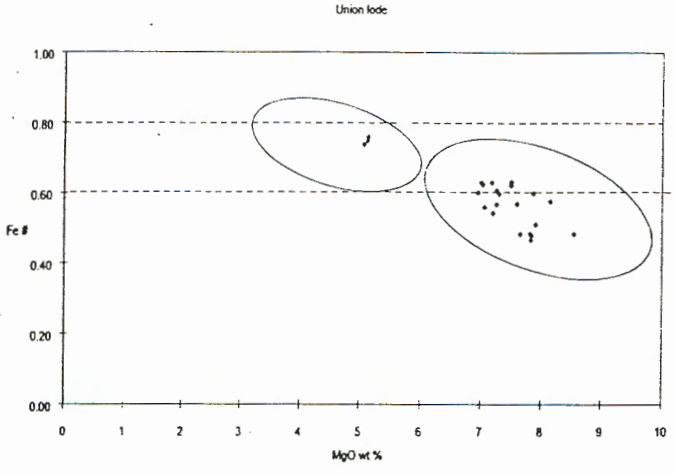

Figure 5.6 displays a small difference between the ore lodes on the basis of tourmaline mineral chemistry. It would seem that the C- and T-lodes are similar, as opposed to the B-, U- and Union lodes. This difference is also shown in figures 5.7 and 5.8. It would seem that Mg is responsible for the compositional differences between the lodes.

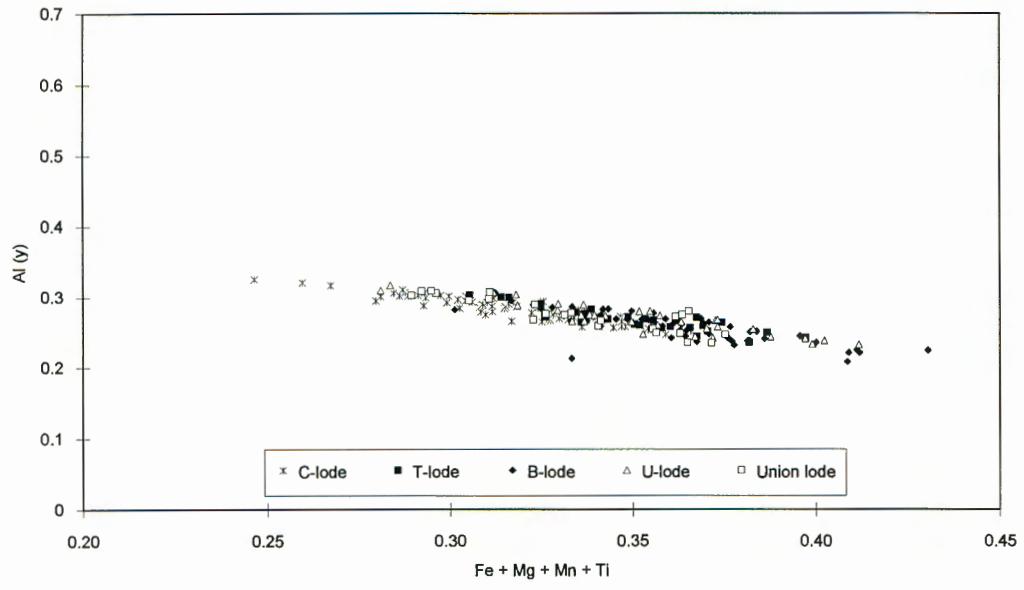

Figure 5.6. An Al versus Fe + Mg + Mn + Ti plot shows slight differences between the different ore lodes. The spread along the X axis indicates that Al do not differentiate between the different lodes, but that Fe, Mg, Mn & Ti may differentiate to some extent between the different ore lodes.

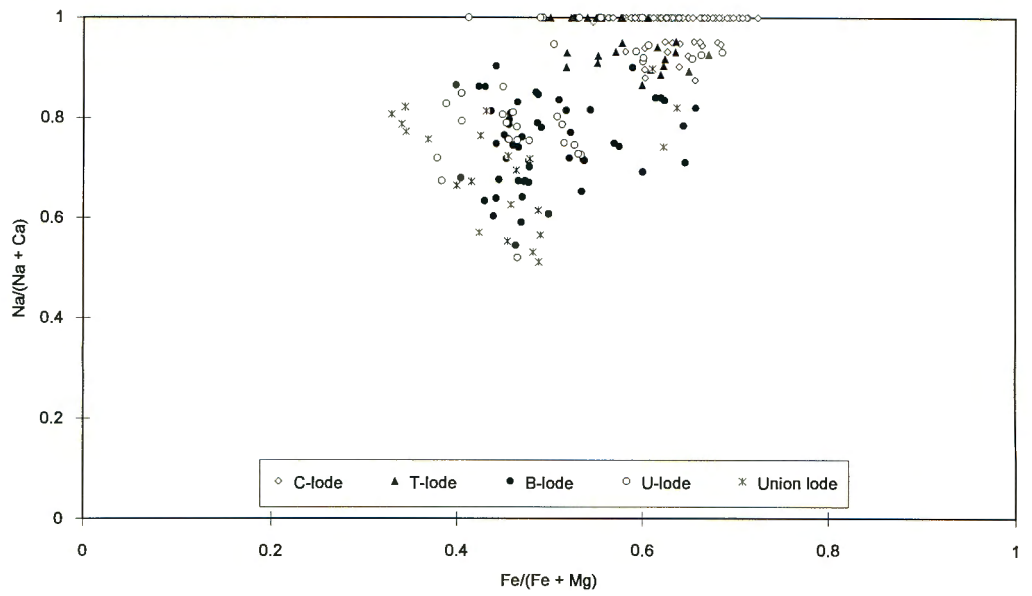

Figure 5.7. The Na and Fe ratios indicate no systematic variation in composition between the different ore lodes.

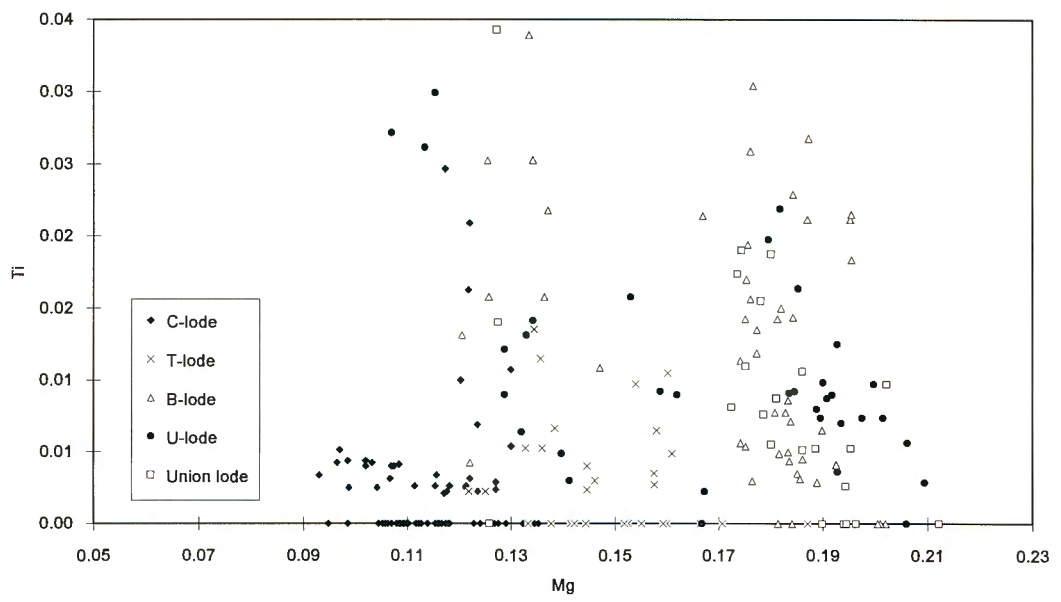

Figure 5.8. The Ti versus Mg plot shows that Mg has significant influence on chemical variation within the NAD tourmalines. It does, however, not differentiate significantly between the different ore lodes.

Slack *et al* (1993) found that the local clastic metasediments of the Broken Hill deposit provided most of the Fe, Mg and Na for the formation of tourmalinites. This may be approximated by the reaction:

$$23\ Mus + 9\ Chl + 21\ Alb + 63\ B(OH)3 + 23\ HCl$$
$$= 21\ Tur + 42\ Qtz + 141\ H2O + 23\ KCl,$$

where Mus = muscovite, Chl = Fe-Mg chlorite, Alb = albite, Tur = tourmaline and Qtz = quartz. This reaction would indicate low fluid/rock conditions in which tourmaline formation was controlled by the bulk composition of the sediment. In contrast there are high fluid/rock conditions, where tourmaline formation was controlled by the chemistry of the hydrothermal fluid. The latter conditions were operative during the mineralisation event in the NAD deposit. The brecciated ore lodes provide evidence of the high H_2O pressure that reigned in the mineralising fluid. Hydrothermal tin deposits are often associated with tourmaline, indicating that the fluids were B rich. The relatively constant composition of the tourmaline also indicates that it crystallised from a hydrothermal fluid, rather than crystallisation controlled by the bulk chemistry of the host rock. Sericitisation, chloritisation and albitisation occurred during the mineralisation event, and therefore refute the theory that the host rock chemistry controlled tourmaline formation.

5.3. Carbonate Chemistry.

Carbonate occurs as interstitial replacing material, as well as vein filling material in the ore lodes. Paragenetically it would seem that the carbonates formed part of the last hydrothermal depositional phase. The interstitial carbonates are usually associated with sericite-muscovite. The carbonates are therefore linked to the alteration processes in the host rock.

Previous workers grouped all carbonates as ankerite. Microprobe analyses were conducted on both the interstitial and lode carbonates. The carbonates contain very few impurities with regard to trace element content. As can be seen from figure 5.9, two definite populations of carbonate can be identified: ankerite and siderite. Interstitial carbonate is mostly siderite. Both carbonates occur in the ore lodes, but each seems to concentrate in a specific lode: Bonus, B- and C-lodes all contain mainly siderite, while the disseminated tin area, Cotton and U-lodes all contain mainly ankerite. It would seem that the carbonates crystallised during a late-phase and acted as a vein filler after deposition of cassiterite and tourmaline.

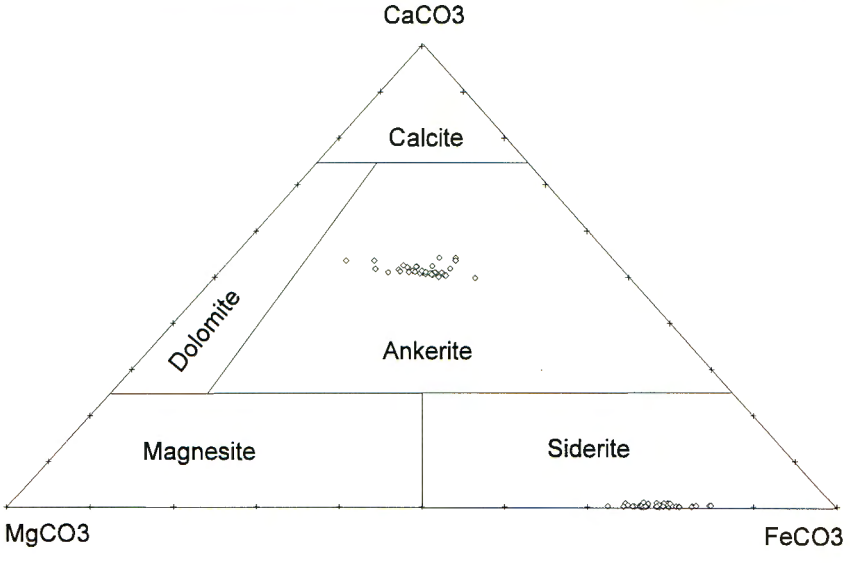

Figure 5.9. Classification of the carbonate in the NAD deposit.

Siderite has a very limited stability field, only occurring in environments with high P_{CO_2}, low dissolved sulphur and under reducing conditions (Nordstrom and Munoz 1986 in Laverne 1993). Depositing pyrite and siderite from solution is strongly Eh, pH, P_{S_2} and P_{CO_2} dependent. Figure 5.10a of the system Fe-O-H_2O-S-CO_2 at 25°C, shows that a slight variation in pH or Eh allows siderite to precipitate instead of pyrite, or conversely. Siderite and

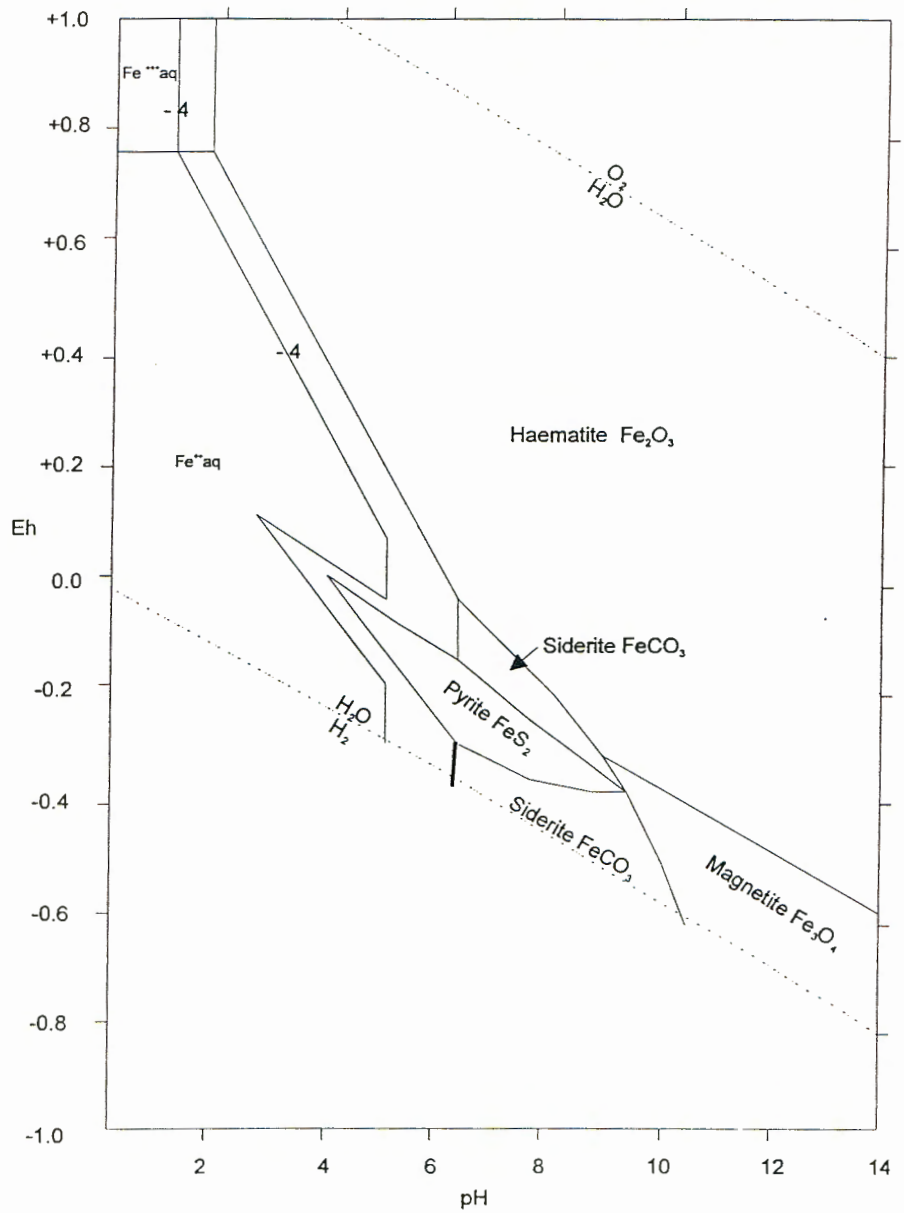

Figure 5.10 a. Stability relations of iron oxides, sulphides and carbonate in water at 25 °C abd 1 atmosphere total pressure. Total dissoveld sulfur = 10^{-6} mole. Total dissolved carbonate = 100 mole. Note elimination of FeS field by $FeCO_3$ under strongly reducing conditions, and remarkable stability of pyrite in presence of small amount dissolved sulfur (Garrels and Christ 1965).

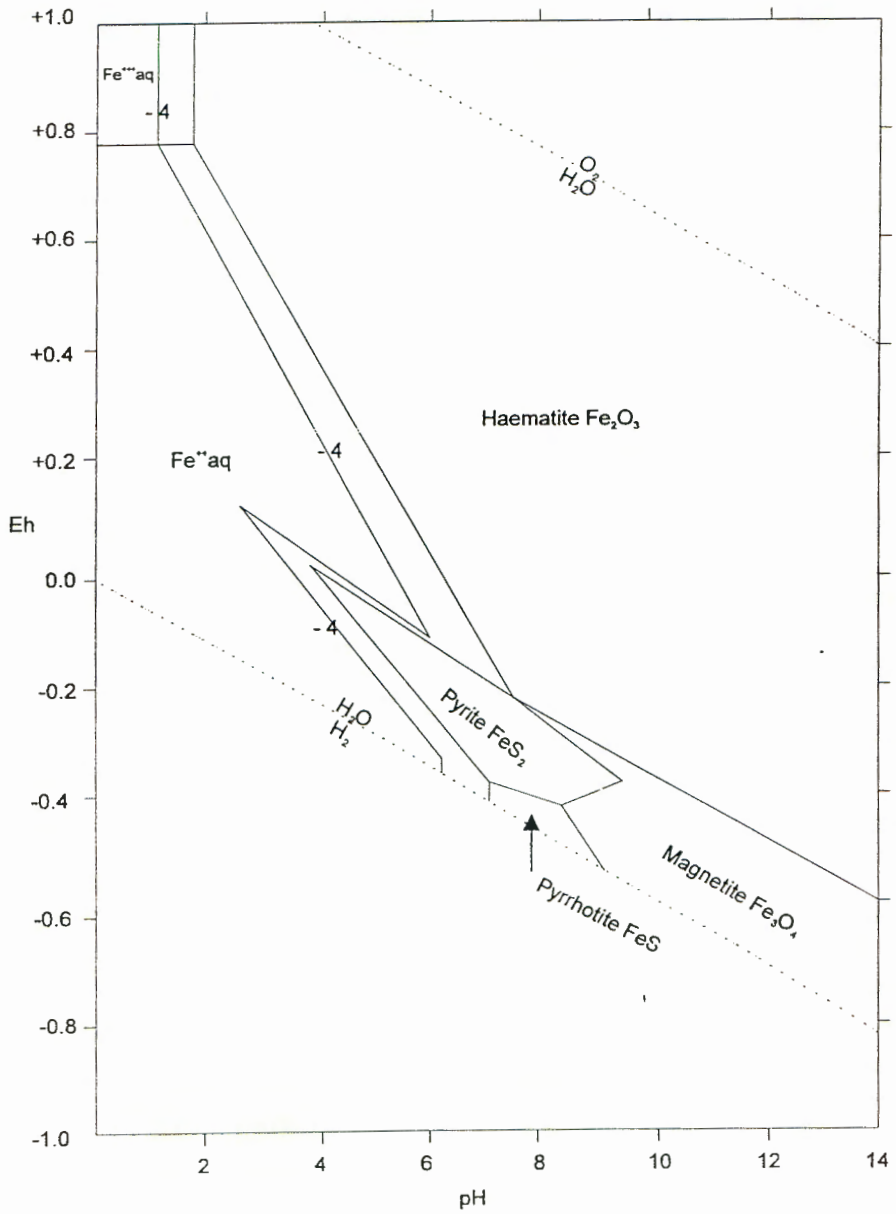

Figure 5.10 b. Stability relations of iron oxides and sulphides in water at 25°C and 1 atmosphere total pressure, when S = 10^{-6} mole. Note shrinkage af sulphide boundaries and appearance of FeS as a stable phase at intermediate pH under strongly reducing conditions, as well as marked increase in the area of "acid solubility" over a wide range of Eh
(Garrels and Christ 1965).

pyrite occurring together may be seen as the establishment of an equilibrium under evolving chemical conditions. Siderite is therefore indicative of strongly reducing conditions and the presence of CO_2 in more than atmospheric amounts. Fluctuations of pH without change in oxidation conditions can cause alternation of siderite and magnetite in a closed CO_2 system, but in an open system where P_{CO_2} is constant, the change from siderite to magnetite cannot take place without change in P_{CO_2}. Figure 5.10b shows the relationships in the system Fe-O-H_2O-S-CO_2 when $\sum CO_2 = 10^0$ and $\sum S = 10^{-6}$ moles (Garrels and Christ 1965). If siderite is to have an important field of stability, dissolved carbonate must be very high, and reduced sulphur extremely low. Under these conditions pyrite may also be present.

5.4. Sulphide Chemistry.

The sulphides pyrite and chalcopyrite belong to the ore lode mineral paragenesis. No other sulphides were identified in the NAD-mine. The pyrite grains often display microscopic exsolution lamellae of chalcopyrite. Pyrite and chalcopyrite are also often intergrown, so that clean pyrite or chalcopyrite grains were not easily found for spectrographic analysis. Table 5.3 contains the trace element content of the sulphides. This is applicable to both pyrite and chalcopyrite.

Table 5.3.

Sulphide trace element chemistry.

(ppm)	RB025.91 CHPY	RB028.91 PY	RB068.91 CHPY	RB038.91a PY	RB038.91b CHPY	RB067.91 CHPY
Ag	5	3	163	1	5	315
As	<240	972	<240	>12000	>12000	6643
Bi			-			34
Co	107	>1200	92.9	>1200	>1200	>1200
Mn	322	<240	309	-	279	268
Ni	196	>3600	505	>3600	>3600	>3600
Pb	6433	6353	108	272	325	657
Sn	>3600	19	669	>3600	>3600	>3600
Ti	-	44	-	56	117	298
Zn	82	95	109	118	153	<80

(ppm)	RB120.91 CHPY	RB148.91 PY	RB010.91 CHPY	RB014.91 CHPY	RB156.91 CHPY	RB004.91a PY	RB004.91b CHPY
Ag	195		13	3	206	3	6
As	359	>12000	-	336	508	555	840
Bi	-		-		-		
Co	126	>1200	45	884	1063	>1200	>1200
Mn	242	-	360	300	241	-	279
Ni	503	182	20	2668	>3600	>3600	>3600
Pb	498	50		73	205	6183	5587
Sn	994	9		>3600	1175	2903	1426
Ti	-	-	-	-	-	89	192
Zn	103	<80	130	129	136	108	192

(Analysis conducted under supervision of U. Kempe and P. Biskop at the Bergakademie Freiberg, Germany) Quantitative optical emission spectrography analysis of clean pyrite and chalcopyrite samples. The variation in the results indicate that pyrite-chalcopyrite mixtures were analysed.

Single pyrite grains were analysed on the microprobe, where the detection limits for the trace elements are unfortunately very high. Significant values for Co, Ni, As and Ag were found in both pyrite and chalcopyrite. In comparison with the pyrite chemistry of the C Mine, the NAD pyrites seem to differ. Figures 5.11 and 5.12 display normalised sulphide chemistry for the Leeuwpoort deposit (C Mine) and NAD-mine respectively. The raw data were normalised against the standard pyrite, as defined by Hallbauer (1991). In comparison with the Leeuwpoort deposit (C Mine) pyrites, the NAD pyrites are enriched in Ti, Mn, Pb, Ag and As and depleted in Ni and Co.

No direct relationship was found between Co and Ni content of the NAD pyrites. According to Hallbauer (pers. comm.) this is a phenomenon found for many pyrites. It is rare to find a correlation between Co and Ni in pyrites. It was generally found that the Co, Ni and As content do not indicate zonation in the pyrite grain (figure 5.13), but appear to be evenly distributed. Co and Ni concentrated in the residual fluid and were incorporated in the pyrite crystal structure, crystallising at a later stage. Pyrite crystallised after cassiterite and tourmaline, but at the same time as siderite.

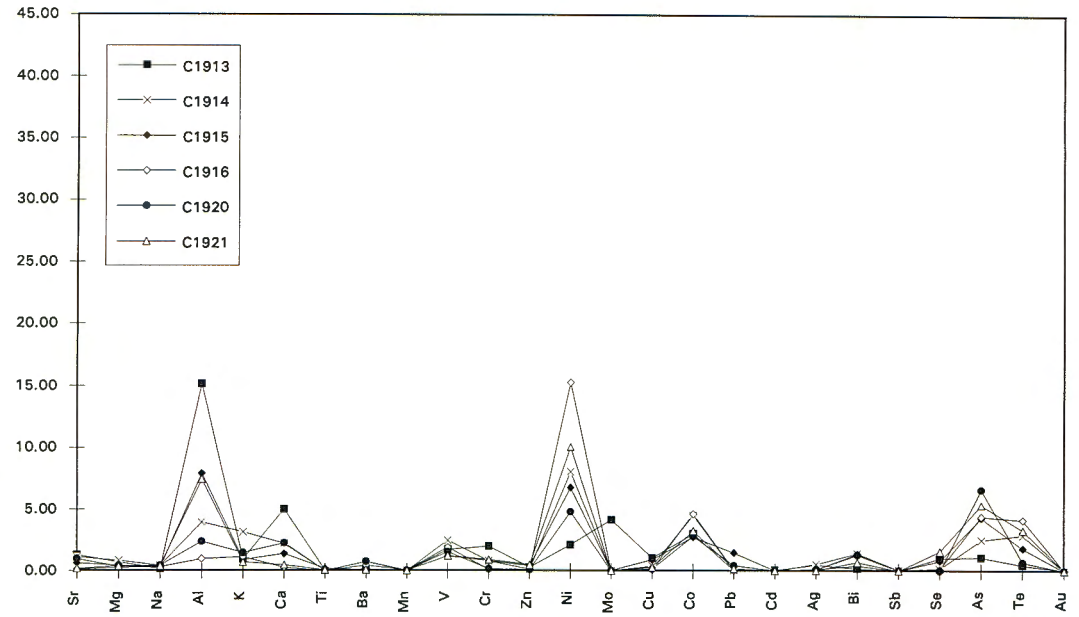

Figure 5.11. Leeuwpoort (C Mine) pyrites normalised to pyrite average (courtesy Hallbauer).

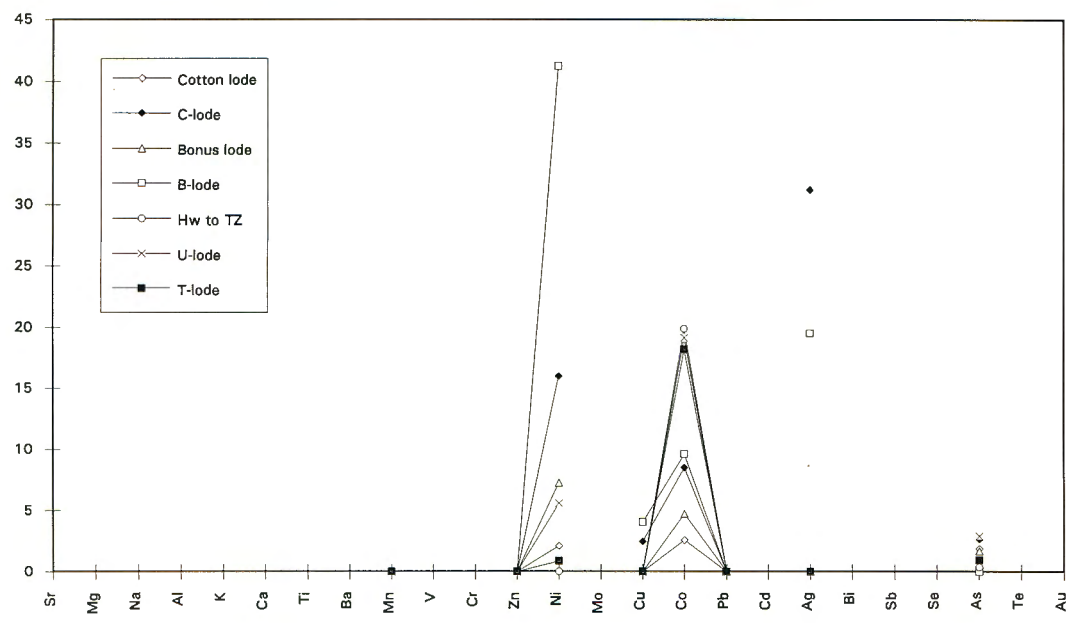

Figure 5.12. NAD pyrite chemistry normalised to pyrite standard.

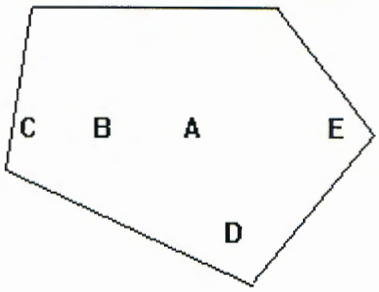

	Co	Ni	As
A	0.05	0.00	0.07
B	0.06	0.26	0.00
C	1.49	1.35	0.51
D	0.18	2.41	0.13
E	0.07	0.00	0.11

Figure 5.13. A typical example of chemical variation within a pyrite grain in the NAD deposit.

Chapter 6 .

6. The Chemical Nature of the Mineralising Fluids and Factors related to Ore Deposition.

The NAD deposit is an exogranitic hydrothermal tin deposit within the Transvaal sediments. It is commonly accepted that the mineralising fluids were derived from the Bushveld granite magmas. In chapter 5.2 tourmaline chemistry was applied to model the type of deposit associated with tourmaline. It was found that the NAD deposit was mineralised by boron-rich fluids, which caused hydraulic fracturing of the host rocks. Smith (1947 in Bruce 1979) concluded that mineralising fluids derived from deep-seated magmas by fractional crystallisation will be hot, aqueous and alkaline. "If cassiterite and tourmaline are found to have been deposited from the same solutions at the same time, then the solutions must have been alkaline, not acid". Tourmaline is intimately associated with cassiterite in the NAD deposit. This supports the inference that the solutions bearing the tin complexes were alkaline. Hallbauer (pers. comm.) found highly saline NaCl fluids in cassiterite as well as in coarse grained pyrite, from the Leeuwpoort deposit (C Mine), thus confirming Cl-complexes for the transport of tin.

The presence of tourmaline is indicative of boron-rich mineralising fluids. The general features for boron-rich tin environments are outlined in table 6.1 and figure 6.1 (Pollard *et al* 1987), in contrast to those of fluorine-rich environments. Some fluorite was found in the U-lode of the NAD deposit, but the mineral paragenesis is mainly one of tourmaline.

Mineralisation styles in boron-rich environments are dominated by brittle fracture, hydrothermal intrusive breccias, stockwork and vein deposits. The hydrothermal intrusive breccias may result from fluid overpressures in the magma. According to the tourmaline chemistry (chapter 5.2), these

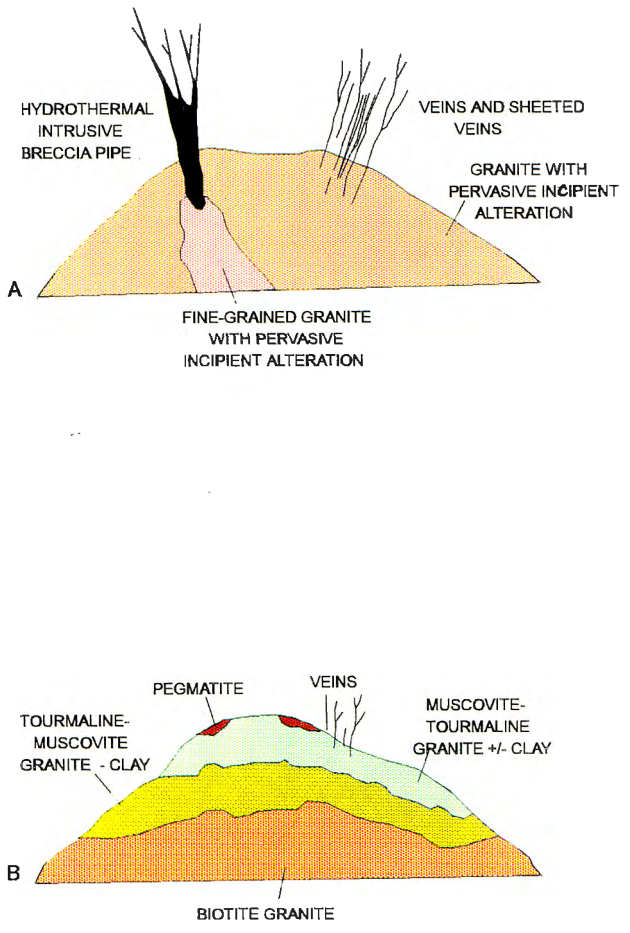

Figure 6.1. General features of boron-rich tin environments.
A breccia pipe and vein systems (common), and
B disseminated style (rare) (Pollard *et al* 1987)

overpressures during formation of the NAD deposit must have been extensive to have formed hydraulically brecciated fractures at such great distances from the granitic source.

Major alteration styles associated with boron-rich fracture-controlled mineralisation include tourmaline-, silica-, muscovite-, and chlorite-rich assemblages (Pollard *et al* 1987). Though very little chlorite is present in the NAD deposit, extensive sericitisation has occurred together with quartz recrystallisation and abundant occurrences of tourmaline.

Table 6.1.

The major features of F- and B-rich tin environments.

	Fluorine	**Boron**
Major granite type	peralkaline peraluminous	peraluminous
Tectonic setting	non orogenic post orogenic	post orogenic
Principle mineralisation styles in granitic host-rocks	disseminated (apogranite-massive greisen) stockwork / vein	breccia pipe stockwork / vein disseminated
Main alteration minerals in granitic host-rocks	feldspars muscovite topaz silica	tourmaline silica muscovite feldspars chlorite
Principle metals	Sn, W, Nb, Ta	Sn, W
Associated elements	Li, Be, (Zr, REE, Zn, As, Cu)	Cu, As, (Ta, Nb)
Examples	NE Tasmania (Australia) Nigeria Erzgebirge Mexico	Cooktown (Australia) SW Tasmania (Australia) Southern Bolivia SW Thailand

(after Pollard *et al* 1987)

Tin deposits are frequently associated with hydrothermal alteration involving alkali metasomatism (albitisation and K-feldspathisation) and / or a variety of other alteration types (greisenisation, tourmalinisation, chloritisation). The host rock of the NAD deposit was extensively altered by potassic remobilisation, and some tourmalinisation of the wall rock did occur. Several

stages of tourmaline crystallisation may be recognised and cassiterite may not be associated with all the stages (Charoy 1979, 1982 in Pollard *et al* 1987). This would explain the occurrence of barren tourmaline pockets in the hanging wall of the tin zone of the NAD deposit. Although the tourmaline chemistry varies little, the presence or absence of cassiterite may indicate different precipitation stages in the NAD deposit.

The water content of a magmatic phase is of great importance: limited experimental evidence shows that an isobaric increase of H_2O content in the residual melt shifts the minimum liquidus composition towards the Qz-Ab side in the normative Qz-Ab-Or diagram (Pichavant and Ramboz 1985 in Pollard *et al* 1987). This mechanism will produce residual melts enriched in normative albite. The presence of Cl and CO_2 in the melt may lower the H_2O activity, indirectly influencing phase relations in the melt. Though great quantities of carbonate are present in the NAD deposit, the plagioclase composition is albite-rich (oligoclase). It can be concluded that H_2O activity in the NAD deposit was not much reduced.

The higher H_2O content of the melt has important implications for the physical and mechanical processes of vapour phase exsolution (fracturing) during the magmatic stage. The boron-rich melt is high in silica and alkalis (mainly sodium) and low in aluminium. Boron partitions towards the vapour phase (Pichavant 1981 in Pollard *et al* 1987) causing boron to be progressively extracted from the crystallising magma. In the presence of boron, the silicate solute content of the hydrothermal phase in equilibrium with the magma, is significantly increased in comparison with pure H_2O systems (Pollard *et al* 1987).

The transport of tin in hydrothermal solutions is a function of a variety of parameters including temperature, pH, oxygen fugacity, bulk salinity and the nature and importance of complexing ligands. Precipitation of cassiterite will result from changes in these physico-chemical variables. Jackson and

Helgeson (1985) have calculated that fluoride complexing of Sn^{2+} is negligible compared with chloride complexing, even if fluorine-minerals are present in the paragenesis. Destruction of complexes and subsequent precipitation of cassiterite from NaCl solutions can be initiated by a drop in oxidation state, temperature, salinity and / or an increase in pH. It was calculated by Helgeson and Jackson (1985) that, in the absence of appreciable chloride and fluoride concentrations, $Sn(OH)^0_2$ and $Sn(OH)^0_4$ are the dominant tin species in H_2O up to 350°C at ~2<pH>7.5. The calculations also indicate that chloride complexes of Sn^{2+} predominate by several orders of magnitude over their fluoride and hydroxide counterparts in 1 - 3 molal (m) NaCl solutions, except in the presence of geologically unrealistic concentrations of fluoride or a pH greater than ~3.5 at 250°C or ~5.0 at 350°C. At higher pH values, most of the tin in solution is present as hydroxide complexes, even at concentrations of NaCl as high as 3 m.

Experimental studies, geologic-, mineralogic-, fluid inclusion- and isotope studies all indicate that saline fluids of magmatic origin were involved in the formation of most tin ores in alumino-silicate and carbonate rocks (Heinrich 1990). Transportation of the ore fluid from the magmatic source to the place of deposition should occur in an environment where complete chemical equilibration of the fluid with the quartzo-feldspathic wall rock is not possible. In this case high concentrations of Sn(II)-Cl complexes can be transported. Precipitation of cassiterite in economic concentrations requires oxidation and causes acidity which in turn must be balanced by reduction and acid-consuming reactions involving wall rock components and other fluid components.

During crystallisation in a hydrous magmatic body, Burnham (1979 in Heinrich 1990) has pointed out that crystallisation reactions of the type:

hydrous granitoid melt >>> granite + aqueous fluid(s)

involve a positive volume change up to several tens of percent (depending on H_2O content and emplacement depth) which leads to a fluid overpressure within the pluton. The carapace of the magmatic body and the intruded country rock will undergo hydraulic fracturing because of hydrostatic pressure build-up when the fluid pressure exceeds the lithostatic load pressure. The initial fracturing leads to fluid loss, decrease in fluid pressure, and a tendency for veins to collapse under lithostatic overpressure. Further hydrodynamic evolution depends on the rate of fluid flow from the pluton relative to the rate of magmatic fluid supply from the pluton into the vein, breccia or replacement body.

There is evidence that temperatures decrease with time during the evolution of tin deposits. This cooling might be caused by a general cooling of the deposit and the granitic source, as well as heat loss through conduction and convection of meteoric waters. The two most effective cooling mechanisms consistent with observations on tin-tungsten deposits are probably adiabatic expansion (reversible, or irreversible throttling, with or without vapour separation), and heat transfer between hot magmatic and cooler meteoric fluids, which may or may not include physical mixing.

Temperatures of 500 - 600°C at the beginning of the hydrothermal event provide one favourable condition for tin transport as Sn(II)-Cl complexes. Precipitation of cassiterite during cooling of the hydrothermal system is shown by fluid inclusion data and agrees with the decrease of cassiterite solubility with temperature. When no boiling occurs, a decrease in salinity is usually observed during the mineralising hydrothermal evolution (Dubessy *et al* 1987). The stannous chloride complex activity decreases and favours SnO_2 precipitation.

Taylor and Wall (1993) have shown that hundreds to tens of thousands of ppm tin can be transported in high-temperature, acidic, chloride-bearing fluids over a broad range of redox conditions, typically attending granitoid evolution.

The strong influence of oxygen fugacity on SnO_2 solubility over the range predicted for the crystallisation of most granitoids (QFM -1 and QFM +1.5), indicates that stannous species will dominate in natural magmatic hydrothermal fluids. Temperature and pressure appear to have little effect on the solubility of SnO_2 in the range 750°C to 500 °C, and from 2.0 to 1.0 kbars (Taylor and Wall 1993).

Aqueous tin concentrations will also be sensitive to alkali concentration and type. At any given fluid acidity, elevated alkali/acid and K/Na ratios will favour SnO_2 solubility. At fixed P, T, fO_2 $m_{HCl,aq}$ and $m_{Cl,aq}$, fluids exsolving from highly fractionated, K-feldspar rich granitoid will be capable of transporting more tin than fluids from a two feldspar granitoid. The lack of a strong temperature effect on SnO_2 solubility indicates that decreasing temperature, which is associated with increasing $m_{KCl,aq}/m_{HCl,aq}$ and $m_{NaCl,aq}/m_{HCl,aq}$ in the KSQ and ASQ rock-buffered systems, may be associated with increases in aqueous tin concentrations (Taylor and Wall 1993).

From geochemical studies of the NAD host rock, it is evident that the mineralising fluids contributed towards mineralisation through various factors. The factor analyses conducted on the geochemical data differentiated between 3 major chemical and mineralogical processes involved in mineralisation:

	High Sn	**Low Sn**
Factor 3	Quartz & K-feldspar	Quartz & Albite
Factor 4	Carbonate & Pyrite	Mineralisation (cassiterite, pyrite & chalcopyrite)
Factor 5	Mineralisation (cassiterite & tourmaline)	Carbonate

When comparing the two sets of factors, it may be noted that free quartz associates with K-feldspar which forms part of the original mineral assemblage of the host rock, but it also associates with albite which in turn

forms part of the mineralisation assemblage. This implies that at least some Si occurred in the mineralising fluid. The mineralisation factor associates not only with cassiterite and tourmaline, but also with the sulphides. Carbonate associates with pyrite which definitely forms part of the mineralisation assemblage, and it may be deduced that the carbonate also forms part of the mineralisation assemblage. It may therefore be concluded that there was one mineralising fluid present that crystallised into different mineralogical phases.

Proof that Sn(II)-Cl-complexes may be transported in the presence of HCO_3^- may be found in the experimental transport mechanisms defined in table 6.2 (after Taylor 1979). Heinrich (1990) discussed the thermodynamic data for the system Sn-W-Fe-Na-K-Al-Si-Cl-S-C-O-H, and found that this is a stable solution for the transportation of Sn. According to Pollard *et al* (1987) the components CO_2, Cl and to a lesser extent CH_4 and N_2 may also be present in both the F- and B-rich environments. Dubessy *et al* (1987) confirmed that Sn-W transporting and depositing fluids in the French South Massif Central have low salinity and contain H_2O, CO_2, CH_4 and N_2. These components are often found in fluid inclusions in Sn-W deposits (Heinrich 1990).

It may then be concluded that the NAD deposit was mineralised by one mineralising fluid, crystallising at different stages and according to the different chemical and physical constraints.

SnO_2 solubility in magmatic to hydrothermal fluids is controlled by fluid acidity, oxygen fugacity and alkali chloride concentration. Deposition of cassiterite is facilitated by decreases in fluid acidity and alkali chloride concentration and increases in oxygen fugacity. Fluid acidity exerts the strongest influence on cassiterite distribution in and around granitoid bodies.

Table 6.2.

Experimental Transport Systems for Sn.

Author	Experiment-Transport Mechanism	Comments
Barsukov and Kuril'chikova (1966) and Barsukov (1966)	Study of Sn solubility in Na and K solutions containing Cl, CO_2, B, H_4SiO_4 and F. Deposits of quartz-cassiterite and sulphide-cassiterite Sn transported as hydroxy-fluorostannate complexes of type $SnF_x(OH)_{6-x}$. In range 25 - 400 °C and pH 6.0 - 11.75.	Fluorine determinations in gas-liquid inclusions in vein quartz from both quartz-cassiterite and sulphide-cassiterite types indicate presence of sufficient fluorine.
Barsukov and Volosov (1968)	Experiments using fluids consistent with compositions of inclusions. Tin transport as $\{Sn(OH_xF_{6-x})]^{2-}$ complex at 300 °C, o.5 kbars, pH 7 - 10 in fluorine bearing Na-K-Cl solutions in presence of HCO_3^-, SiO_2 and BO_3^{3-}. Cassiterite precipitated by hydrolysis of complex in pH range 7 - 8.	1. Agrees with fluid inclusion evidence that cassiterite deposited at 250 - 380 °C and approximately 0.5 kbars. Composition of fluids 1 - 10 weight percent dissovled solids and of NaCl, Cl--HCO_3^- or Na+-K+-Ca+ types. Recalculated pH values 7 - 9.2 and fluorine contents up to 3.5 grams per liter. 2. Deposition of cassiterite dependent upon form in which fluorine is present. As SnO_2 precipitates by hydrolysis of hydroxy-flouro-stannate complex, fluorine is added to solution.
Barsukov and Sushchevskaya (1973)	Results from decripitation, homogenisation and analysis of aqeous inclusions from sulphide-cassiterite and quartz-cassiterite deposits. Tin deposited from Na-K-F-Cl-HCO_3 solutions which are originally alkaline but alkalinity falls during cassiterite deposition and fluorine concentration rises.	1. Quartz-cassiterite deposits produced mainly from Na-rich solutions. K content rises as solution reacts with granitoids. 2. Sulphide-cassiterite deposits mainly produced from solutions rich in K. 3. Data consistent with transport as hydroxy-flouro-stannate complexes and subsequent hydrolysis to give cassiterite.

(after Taylor 1979)

Chapter 7 .
7. Conclusions.

7.1. Discussion on the Formation of the NAD Deposit.

The sediments hosting the Rooiberg tin deposits originate from Archean type granites according to the La : Y: Nb ratios (figure 4.13) of the NAD host rock. These sediments have previously been classified as arkosites or arkoses. It is clear that, as none of the existing geochemical classification systems classify the host rock as an arkose or greywacke, these sediments have been altered to such an extent that the original sediment cannot be recognised geochemically. It would seem though, that the original sediments were slightly feldspathic in nature and then K was remobilised (sericitisation and some recrystallised orthoclase) during the mineralisation event.

With the intrusion of the Bushveld Igneous Complex into the Transvaal Supergroup, the sediments were structurally deformed. During this process the Rooiberg Fragment was detached to form a roof pendant. Tensile tectonism during the intrusion of the Bushveld Complex caused an extensive fracture system to evolve within the Rooiberg Fragment.

Residual fluids collected during the BIC intrusion were Sn-bearing and were transported by an extensive fracture system from the magma chamber(s). SnO_2 solubility in hydrothermal fluids is controlled by fluid acidity, oxygen fugacity and alkali-chloride concentration. Sn^{2+} is transported as chloride-complexes, starting at temperatures of 500ºC to 600ºC. The major features of boron-rich tin environments are applicable to the NAD deposit. The abundance of tourmaline confirms the boron-rich composition of the mineralising fluids, indicating the high H_2O content of the fluids. Boron tends to fractionate into the vapour phase, thereby extracting more boron from the

magma-origin, and also explaining the extensive hydraulic brecciation encountered in the NAD deposit.

Deposition of cassiterite is facilitated by decreases in fluid acidity and alkali-chloride content, and an increase in oxygen fugacity. Fluid inclusion studies on quartz from the Leeuwpoort area indicate low temperatures of formation (174°C to 220°C). The low Nb content of the cassiterites confirms this low temperature of formation and is consistent with the abundance of carbonates and sulphides in the ore lodes. NaCl-bearing saline inclusions in cassiterite from the Leeuwpoort deposit (C Mine) support a transport model of tin as chloride complexes.

The major reactions to have taken place during mineralisation have been ion exchange and hydrogen metasomatism Alteration may be typed as alkali-alumina metasomatism (remobilisation of K) and is characterised by sericitisation and feldspathisation. The introduction of B and CO_2 into the system caused extensive tourmalinisation and carbonatisation of the host rock. From statistical analyses conducted on the geochemical data of the NAD deposit, it is evident that there was one fluid present that was responsible for mineralisation of the NAD deposit. Mineralisation did, however occur in phases, explaining variation in the mineral paragenesis and abundances of cassiterite, tourmaline, pyrite, chalcopyrite, siderite or ankerite.

The close association of tourmaline and cassiterite indicates hot, aqueous and alkaline mineralisation fluids. Boron-rich fluids are generally enriched in silica and alkalis. Alkali metasomatism and tourmalinisation of the host rock therefore confirm the boron-alkali-enriched composition of the mineralising fluids.

Although it was aimed to test differences in alteration of the host rock perpendicular to the ore lodes, no global differences could chemically be detected. There are individual differences between the various samples, but

did not fit the hypothesis of two alteration groups: one close to the lode and another further from the lode.

It is evident from the discussion above that the NAD deposit was mineralised by hydrothermal fluids generated by a fractionated granitic magma. As dicussed in chapter 5.2, tourmaline chemistry indicates that the tin deposit is more than approximately 1 km from the fluid source (distance relative). The NAD deposit forms part of the A Mine Complex in the Rooiberg tin field, and mineralisation was structurally controlled within the tin zone at the top of the Boschoffsberg Quartzite Member and the shaly 'arkose' of the Blaauwbank Shale Member. It appears that the overlying shales confined the mineralising fluids, containing it in the quartzitic host rock.

Although there still is uncertainty as to the source of the mineralising fluids, the NAD deposit confirms a hydrothermal origin for the tin deposits.

7.2. Recommendations

NAD-Mine was closed on account of metallurgical problems and poor economic viability. Because of the fine-grained nature of the cassiterite, losses were experienced in the recovery plant. Although ore grade was relatively high, ore recovery was very low.

Should the metallurgical problems be solved and the tin price raised, the NAD tin deposit would be economically viable again.

Further studies can be recommended regarding the tin zone controls in the NAD deposit. Should these factors be known, viable predictions as to tin occurrences can be made in view of future exploration within the tin field. Fluid inclusion studies will be indicative of the reigning temperature conditions in the NAD deposit. The NAD deposit differs from the Leeuwpoort deposit,

where temperature of formation is known. The composition of the fluid inclusions will also give a better indication of the composition of the mineralising fluids in the NAD deposit.

Cathodoluminescence studies on cassiterite may give a better idea of the trace element distribution in the cassiterites and may be used to explain why the NAD cassiterites do not show typical colour zonation.

Isotope studies on boron in tourmaline and sulphur in pyrite could be indicative of the source of the mineralising fluids.

REFERENCES

Bates R.L. and Jackson J.A. 1987. *Glossary of Geology.* American Geological Institute, Alexandria.

Bruce J.T. 1979. "A" Mine Tin Zone Concept: A review of probable controls of mineralisation. *Internal report Rooiberg Tin Limited.*

Button A. 1976. Transvaal and Hammersley basins - review of basin development and mineral deposits. *Minerals Science and Engineering., 8*, 262 - 293.

Dinsdale J.L. 1982. *The development and control of pocket-mineralization in the Rooiberg quartzites.* M.Sc. thesis (unpubl.), University of Pretoria, 150pp.

Dubessy J., Ramboz C., Nguyen-Trung C., Cathelineau M., Charoy B., Cuney M., Leroy J., Poty B. and Weisbrod A. 1987. Physical and chemical controls (fO_2, T, pH) of the opposite behaviour of U and Sn-W as examplified by hydrothermal deposits in France and Great-Britain, and solubility data. *Bullitin Minéralogique 110*, 261 - 281.

Garrels R.M. and Christ C.L. 1965. *Solutions, Minerals, and Equilibria.* Harper & Row, New York.

Haikney S. 1986. *The mineralogy of the ore deposit at 'A' mine, Rooiberg.* Hons. Project, Rhodes University.

Hallbauer D.K. 1991. Mineralogical and geochemical 'fingerprinting' of hydrothermal pyrite - a possible exploration tool. *ICAM '91, Vol. I*

Hartzer F.J. 1989. Stratigraphy, structure and tectonic evolution of the Crocodile River Fragment. *Suid-Afrikaanse Tydskrif vir Geologie 92*, 110 - 124.

Heinrich C.A. 1990. The chemistry of hydrothermal tin (-tungsten) ore deposition. *Economic Geology 85*, 457 - 481.

Henry D.J. and Dutrow B.L. 1992. Tourmaline in a low grade clastic metasedimentary rock: an example of petrogenetic potential of tourmaline. *Contributions to Mineralogy and Petrology 112*, 203 - 218.

Ianello P. 1971. The Bushveld granites around Rooiberg, Transvaal, South Africa. *Geologisches. Rundschau* 60, 630 - 655.

Jackson K.J. and Helgeson H.C. 1985. Chemical and thermodynamical constraints on the hydrothermal transport and deposition of tin: I. Calculation of the solubility of cassiterite at high pressures and temperatures. *Geochimica et Cosmochimica Acta 49*, 1 - 22.

Labuschagne L.S. 1970. *The structure and mineralization of the ore bodies at Blaauwbank and Nieuwpoort, Rooiberg Tinfieds.* M.Sc. thesis (unpubl.) University of Pretoria, 77pp.

Laverne C. 1993. Occurrence of siderite and ankerite in young basalts from the Galápagos Spreading Center (DSDP Holes 506G and 507B). *Chemical Geology 106*, 27 - 46.

Law J.D.M., Bailey A.C., Cadle A.B., Phillips G.N. and Stanistreet I.G. 1990. Reconstructive approach to the classification of Witwatersrand 'quartzites'. *South African Journal of Geology 93*, 83 - 92.

Lécolle M., Derré C. and Nerci K. 1991.The Proterozoic sulphide alteration pipe of Sidi Flap and its host series. New data for the geotectonic evolution of the Pan-African Belt in the Eastern Anti-Atlas (Morocco). *Ore Geology Reviews 6*, 501 - 536.

Lenthall D.H. 1974. Tin production from the Bushveld Complex. *Information Circular Ecomomic Geology Research Unit, University of the Witwatersrand, Johannesburg 93*, 15pp.

Leube A. 1960. Structural control in the Rooiberg Tinfield. *Transactions geological Society of South Africa 63*, 265 - 282.

Leube A. and Stumpfl E.F. 1963. The Rooiberg and Leeuwpoort tin mines, Transvaal, South Africa. *Economic Geology 58*, 391 - 418, 527 - 557.

McCarthy T.S. and Fripp R.E. 1980. The crystallization history of a granitic magma as revealed by trace element abundances. *Journal of Geology 88*, 211 - 224.

McCarthy T.S. and Hasty R.A. 1976. Trace element distribution patterns and their relationship to the crystallization of granitic melts. *Geochimica et Cosmochimica Acta 40*, 1351 - 1358.

Mills A.B.W. 1985. A zoned cassiterite crystal from Leeuwpoort 'C' mine, Rooiberg, Transvaal. *Petros 12*, 58 - 62.

Nicholls J. 1988. The statistics of the Pearce element diagrams and the Chayes closure problem. *Contributions to Mineralogy and Petrology 99*, 36 - 43.

Norrish K. and Hutton J.T. 1969. An accurate X-ray spectrographic method for the analysis of a wide range of geological samples. *Geochimica et Cosmochimica Acta, Vol 33*, 431 - 453.

Ollila J.T. 1981. *Fluid inclusion and mineralogical study of the rocks and minerals associated with the Bushveld Complex.* Ph.D. thesis (unpubl.), Rand Afrikaans University, Johannesburg.

Pearce T.H. 1968. A contribution to the theory of variation diagrams. *Contributions to Mineralogy and Petrology 19*, 142 - 157.

Pettijohn F.J. 1975. *Sedimentary Rocks.* Harper and Row, New York, 628pp.

Phillips A.H. 1982. *The geology of the Leeuwpoort tin deposits and selected aspects of its environs.* M.Sc. thesis (unpubl.), University of the Witwatersrand, Johannesburg, 297pp.

Pirajno F. and Smithies R.H. 1992. The FeO/(FeO + MgO) ratio of tourmaline: a useful indicator of spatial variations in granite-related hydrothermal mineral deposits. *Journal of Geochemical Exploration, 42*, 371 - 381.

Pollard P.J., Pichavant M. and Charoy B. 1987. Contrasting evolution of fluorine- and boron-rich tin systems. *Mineralium Deposita, 22*, 315 - 321.

Roberts B.A. 1983. 'A' Mine complex. *Internal report Rooiberg Tin Limited.*

Rozendaal A, Toros M.S. and Anderson J.R. 1986. The Rooiberg tin deposits, West-central Transvaal. **In** Anhaeusser C.R. and Maske S (eds). *Mineral deposits of South Africa*, 1307 - 1327.

Russel J.K., Nicholls, J. Stanley C.R. and Pearce T.H. 1990. Pearce Element Ratios. A Paradigm for Testing Hypotheses. *EOS Jan 30.*

Schrön, W., Bauman, L. and Legler C. 1978. Zur Methodik und zu einigen Ergebnissen der s\Spurenelementbestimmung in Sulfiedmineralen aus Lagerstätten des Erzgebirges (DDR). *Zeitschrift für geolischer Wissenschaften - Berlin 6*, 767 - 778.

Schrön W., Kaiser, G. and Bombach G. 1983. Die emissionspektrographische Spurenelement-Bestimmung in geologischen Proben mit halbautomatischer Plattenauswertung. *Zeitschrift für angewandte Geologie, 29: 11*, 559 - 565.

Slack F. and Coad P.R. 1989. Multiple hydrothermal and metamorphic events in the Kidd Creek volcanogenic massive sulphide deposit, Timmins, Ontario: evidence from tourmalines and chlorites. *Canadian Journal of Earth Science, 26*, 694 - 715.

Slack F., Palmer M.R., Stevens B.P.J. and Barnes R.G. 1993. Origin and Significance of Tourmaline-Rich Rocks in the Broken-Hill District, Australia. *Economic Geology, 88*, 505 - 541.

Stear W.M. 1976. *The geology and ore-controls of the Northern Rooiberg Tinfield, Transvaal.* M.Sc. thesis (unpubl.), University of Stellenbosch, 89pp.

Stear W.M. 1977a. The stratigraphy and sedimentation of the Pretoria Group at Rooiberg, Transvaal. *Transactions geological Society of South Africa, 80*, 53 - 65.

Stear W.M. 1977b. The stratabound tin-deposits and structure of the Rooiberg Fragment. *Transactions geological Society of South Africa, 80*, 67 - 78.

Strauss C.A. 1947. Granitization and rheomorphism associated with the Bushveld Igneous Complex near the Leeuwpoort Tin Mine. *Transactions geological Society of South Africa, 50*, 161 - 170.

Swan R. 1985. Contouring of the tin zone. *Internal report Rooiberg Tin Limited.*

Taylor J.R. and Wall V.J. 1993. Cassiterite solubility, tin speciation and transport in a magmatic aqueous phase. *Economic Geology 88*, 437 - 460.

Taylor R.G. 1979. *Geology of tin deposits.* Elsevier, Amsterdam, 534pp.

Verwoerd W.J. 1962. Die geologiese struktuur van die Krokodilrivier-fragment. *Transactions geological Society of South Africa, 66*, 49 - 66.

Walraven F. 1976. Notes on the late-stage history of the Western Bushveld Complex. *Transactions geological Society of South Africa, 79*, 13 - 21.

Walraven F and Hattingh E. 1993. Geochronology of the Nebo Granite, Bushveld Complex. *South African Journal of Geology 96*, 31 - 41.

APPENDIX A.

Sample localities and Features

NUMBER	PEG NR	LEVEL	REMARKS
1	A9651	1580	Cotton lode x/c 0.9 grade, massif
2	A9651	1580	Cotton lode x/c Ankerite vein
3	A9651	1580	Cotton lode x/c Hydrothermally brecciated veins, not bedding parallel
4	A9651	1580	Cotton lode x/c Pocket type = sulphides
5	A9667	1480	Cotton lode x/c Ankerite vein
6	A9672	1480	C-lode, main raise Tourmaline pocket outside TZ
7		1480	C-lode, main raise
8	A9774	1480	C-lode, main raise
9	A9774	1480	C-lode, main raise
10	A9774	1480	C-lode, main raise Ankerite vein with cassiterite & sulphides
11	A9774	1480	C-lode, main raise Ankerite vein with cassiterite & sulphides
12	A9649	1580	C-lode, main raise Ankerite vein with cassiterite
13	A9649	1580	C-lode, main raise Ankerite
14	A9649	1580	C-lode, main raise Tourmaline
15	A9649	1580	C-lode, main raise Ankerite
16	A9814	1480	C-lode, main raise Pocket with ankerite
17	A9814	1480	C-lode, main raise Pocket with ankerite Photograph
18		1480	B-lode Ankerite vein with sulphides
19	A9690	1480	B-lode Ankerite vein with quartz and sulphides

NUMBER	PEG NR	LEVEL	REMARKS
21	A9833	1480	B-lode, shale Photograph
22	A9833	1480	B-lode, shale
23	A9744	1480	AMS-lode Ankerite vein plus wall rock
24	A9744	1480	AMS-lode Ankerite vein
25	A9744	1480	AMS-lode Ankerite vein
26	A9821	1480	AMS-lode Bulk mineralisation Stockwork from fracturing
28	A9821	1480	AMS-lode Bulk mineralisation Fissures, fractures, pockets
29		1480	AMS-lode, drive north
30		1480	AMS-lode, drive north
31	A9801	1480	Union lode Fracture mineralisation
32	A9770	1480	Union lode Ankerite vein with sulphides
33	A9771	1480	Union lode, drive north Tourmaline breccia
34	A9771	1480	Union lode, drive north Tourmaline breccia
35	A9812	1480	C-lode Ankerite vein with quartz
36	A9768	1380	Bonus lode Well mineralized, cassiterite
37	A9768	1380	Bonus lode Tourmaline stockwork breccia
38	A9768	1380	Bonus lode Well mineralized, cassiterite
39	A9661	1380	U-lode Tourmaline stockwork breccia
40	A9669	1380	U-lode Separated tourmaline, cassiterite
41	A9717	1380	U-lode, nr 2 main raise Clays on the weathered lode
42	A9717	1380	U-lode, nr 2 main raise Clays on the weathered lode

NUMBER	PEG NR	LEVEL	REMARKS
43	A9309		Flat lode, NAD incline shaft Brecciated vein Photograph
44	A9309		Flat lode, NAD incline shaft Red arkose
45	A9309		Flat lode, NAD incline shaft Brecciated vein
46	A9404		Cotton lode, NAD incline shaft Hanging wall with specularite Photograph
47	A9404		Cotton lode, NAD incline shaft Pocket = sulphides, no cassiterite Photograph
48			NAD incline shaft before crossing to new NAD mining area Hanging wall
49			Footwall to Tin Zone Bottom of NAD decline shaft
50			Footwall to Tin Zone Bottom of NAD decline shaft
51	A9741	1380	U-lode Green bar associated with U-lode
52	A9611	1380	U-lode White carbonate vein Photograph
53	A9611	1380	U-lode Pocket = no cassiterite
54	A9611	1380	U-lode white carbonate vein Picked up
55	A9644	1380	Crosscut south Tourmaline and sulphides, no cassiterite
56	A9644	1380	Crosscut south Disseminated ankerite
57	A9757	1380	Union lode
58	A9757	1380	Union lode - U-lode intersect

NUMBER	PEG NR	LEVEL	REMARKS
59	A9757	1380	Union lode - U-lode intersect Hostrock of ankerite veins Photograph
60	A9819	1480	AMS-lode
61		1480	AMS-lode Pocket
62	A9727	1480	T-lode Tourmaline sulphide veins, no cassiterite
63	A9727	1480	T-lode Red arcose Photograph
64	A9727	1480	T-lode Tourmaline and sulphide Picked up
65	A9768	1380	Bonus lode
66	A9768	1380	Bonus lode Picked up
67	A9768	1380	Bonus lode
68	A9745	1480	AMS-lode Ankerite-sulphide vein
69		1480	AMS-lode, drive north Black cassiterite bearing vein
70	A0001	1580	Union lode fw-close
71	A0001	1580	Union lode fw-far
72	A0001	1580	Union lode hw-close
73	A0001	1580	Union lode hw-far
74	A0001	1580	Union lode lode
75	A0002	1580	Union lode hw-far
76	A0002	1580	Unionlode hw-close
77	A0002	1580	Union lode fw-close
78	A0002	1580	Union lode fw-far
79	A0002	1580	Union lode lode

NUMBER	PEG NR	LEVEL	REMARKS
80	A0003	1580	Cotton lode hw-close
81	A0003	1580	Cotton lode hw-far
82	A0003	1580	Cotton lode lode
83	A0003	1580	Cotton lode fw-far
84	A0003	1580	Cotton lode fw-close
85	A0004	1580	Cotton lode fw-close
86	A0004	1580	Cotton lode fw-far
87	A0004	1580	Cotton lode hw-close
88	A0004	1580	Cotton lode hw-far
89	A0004	1580	Cotton lode lode
90	A0005	14/1580	Union lode fw-close
91	A0005	14/1580	Union lode fw-far
92	A0005	14/1580	Union lode hw-close
93	A0005	14/1580	Union lode hw-far
94	A0005	14/1580	Union lode lode
95	A9755	1480	AMS-lode hw-far
96	A9755	1480	AMS-lode hw-close
97	A9755	1480	AMS-lode fw-close
98	A9755	1480	AMS-lode fw-far
99	A9755	1480	AMS-lode lode
100	A0006	1480	Union lode fw-far
101	A0006	1480	Union lode hw-far
102	A0006	1480	Union lode hw-close

NUMBER	PEG NR	LEVEL	REMARKS
103	A0006	1480	Union lode fw-close
104	A0006	1480	Union lode lode
105	A0007	1480	AMS-lode hw-far
106			AMS-lode hw-close
107			AMS-lode lode
108			AMS-lode fw-close
109			AMS-lode fw-far
110	A9833	1480	B-lode fw
111	A9833	1480	B-lode lode
112	A9833	1480	B-lode hw
113	A0008	1480	B-lode hw
114	A0008	1480	B-lode lode
115	A0008	1480	B-lode fw
116	A9829	1480	B-lode fw
117	A9829	1480	B-lode hw
118	A0009	1480	B-lode hw
119	A0009	1480	B-lode fw
120	A0009	1480	B-lode lode
121	A9305	Decline	HW in Tin Zone
122	A9310	Decline	HW in Tin Zone
123	A9317	Decline	HW in Tin Zone
124	A9319	Decline	HW in Tin Zone
125	A9412	Decline	HW in Tin Zone
126	A9462	Decline	HW in Tin Zone
127	A9475	Decline	HW in Tin Zone
128	A9727	1380	T-lode lode

NUMBER	PEG NR	LEVEL	REMARKS
129	A9727	1380	T-lode hw
130	A9727	1380	T-lode fw
131	A0010	1380	Union lode fw-close
132	A0010	1380	Union lode hw-close
133	A0010	1380	Union lode fw-far
134	A0010	1380	Union lode hw-far
135	A0010	1380	Union lode lode
136	A0011	1380	Union lode fw-far
137	A0011	1380	Union lode hw-close
138	A0011	1380	Union lode hw-far
139	A0011	1380	Union lode fw-close
140	A0011	1380	Union lode (±A9827) lode
141	A9837	1380	AMS-lode hw-far
142	A9837	1380	AMS-lode hw-close
143	A9837	1380	AMS-lode fw-far
144	A9837	1380	AMS-lode fw-close
145	A9663	1380	U-lode hw-far
146	A9663	1380	U-lode hw-close
147	A9663	1380	U-lode fw-close
148	A9663	1380	U-lode lode
149	A9663	1380	U-lode fw-far
150	A9641	1380	U-lode hw-close
151	A9641	1380	U-lode fw-far

NUMBER	PEG NR	LEVEL	REMARKS
152	A9641	1380	U-lode fw-close
153	A9641	1380	U-lode lode
154	A9641	1380	U-lode hw-far
155	A0012	1480	C-lode fw-far
156	A0012	1480	C-lode lode
157	A0012	1480	C-lode hw-close
158	A0012	1480	C-lode fw-close
159	A0012	1480	C-lode hw-far
160	A9814	1480	C-lode fw-far
161	A9814	1480	C-lode lode
162	A9814	1480	C-lode hw-close
163	A9814	1480	C-lode hw-far
164	A9814	1480	C-lode fw-close
165	A9818	1480	Disseminated tin
166	A9818	1480	Disseminated tin
167	A9818	1480	Disseminated tin
168	A9821	1480	Disseminated tin Picked up
169	A9821	1480	Disseminated tin
170	A9835	1480	Disseminated tin Picked up
171	A9829		Quartz
172	A9862		Quartz, AMS-lode
173			Quartz, AMS-lode
174	0576/9675		Quartz, Bonus lode
175			Quartz Ancient workings close to A3 shaft

APPENDIX B.

Abbreviations used in the paragenetic tables:

QZ p	Primary quartz
QZ s	Secondary quartz (recrystallized or replacement type)
K-SP	K-feldspar
PLAG	Plagioclase
CARB	Carbonate
TOU p	Primary tourmaline
TOU s	Secondary tourmaline (associated with mineralising event)
MICA	Sheet silicates (Muscovite and Sericite)
CHL	Chlorite
CAS	Cassiterite
RUT	Rutile
PY	Pyrite
CHPY	Chalcopyrite
ZIR	Zircon

PARAGENETIC TABLE

SAMPLE ID: RB095-91

	QZ p	QZ s	K-SP	PLAG	CARB	TOU p	TOU s	MICA	CHL	CAS	RUT	PY	CHPY	ZIR
QZ p	★				⟲ ⅄				×				×	⊙ ❖
QZ s		★			⅄			⅄	×	❖			×	
K-SP		⟲	★		⟲ ⅄			☮ ⅄	×	❖	⊙		×	❖
PLAG		⟲		★	⟲ ⅄			☮ ⅄	×				×	
CARB					★			⅄ ❖	×	❖			×	
TOU p						★			×				×	
TOU s							★		×				×	
MICA								★	×	❖			×	
CHL	×	×	×	×	×	×	×	×	★				×	
CAS										★			×	
RUT											★		×	
PY												★	×	
CHPY	×	×	×	×	×	×	×	×	×	×	×	×	★	
ZIR														★

LEGEND:

Replacement

- ❄ remnant - inclusion after partial replacement
- ⟲ partial replacement
- ⊂ complete replacement
- ♓⟲ preferential replacement

Alteration

- ⭘ alteration rim
- ● complete alteration
- ☮ partial alteration
- ☯ preferential alteration

Other

- ⇔ veinlets
- ⊙ inclusions
- ❖ paragenetic
- ⅄ matrix
- ♌ recrystallized
- × not present

PARAGENETIC TABLE

SAMPLE ID: RB096-91

	QZ p	QZ s	K-SP	PLAG	CARB	TOU p	TOU s	MICA	CHL	CAS	RUT	PY	CHPY	ZIR
QZ p	★				⌀ ⅄	×		⅄	⇳				×	❖
QZ s		★				×							×	
K-SP		⌀	★		⌀ ⅄ ❄	×		☮ ⅄	⇳		⊙		×	❖
PLAG		⌀		★	⌀ ⅄ ❄	×		⅄	⇳				×	
CARB					★	×		⅄ ❖	●	❖	❖		×	
TOU p	×	×	×	×	×	★							×	
TOU s							★						×	
MICA								★		❖	❖ ⅄		×	❖
CHL									★				×	
CAS										★	❖		×	
RUT											★		×	
PY												★	×	
CHPY	×	×	×	×	×	×	×	×	×	×	×	×	★	
ZIR														★

LEGEND:

Replacement

- ❄ remnant - inclusion after partial replacement
- ⌀ partial replacement
- ⊂ complete replacement
- ⌀ preferential replacement

Alteration

- O alteration rim
- ● complete alteration
- ☮ partial alteration
- ☯ preferential alteration

Other

- ⇳ veinlets
- ⊙ inclusions
- ❖ paragenetic
- ⅄ matrix
- ♌ recrystallized
- × not present

PARAGENETIC TABLE

SAMPLE ID: RB097-91

	QZ p	QZ s	K-SP	PLAG	CARB	TOU p	TOU s	MICA	CHL	CAS	RUT	PY	CHPY	ZIR
QZ p	★				⊁ ⅄	×			×					⊙
QZ s		★				×			×					
K-SP		⊁	★		⊁ ⅄	×	❖	☮ ⅄	×		⊙			
PLAG		⊁		★	⊁ ⅄	×		☮ ⅄	×					
CARB					★	×		⅄	×	❖	❖			
TOU p	×	×	×	×	×	★			×					
TOU s							★		×					
MICA								★	×	❖	❖	❖		
CHL	×	×	×	×	×	×	×	×	★					
CAS										★				
RUT											★			
PY												★		
CHPY													★	
ZIR														★

LEGEND:

Replacement

- ❄ remnant - inclusion after partial replacement
- ⊁ partial replacement
- ⊂ complete replacement
- ♓⊁ preferential replacement

Alteration

- ⭘ alteration rim
- complete alteration
- ☮ partial alteration
- ☯ preferential alteration

Other

- ⇔ veinlets
- ⊙ inclusions
- ❖ paragenetic
- ⅄ matrix
- ♌ recrystallized
- × not present

PARAGENETIC TABLE

SAMPLE ID: RB099-91

	QZ p	QZ s	K-SP	PLAG	CARB	TOU p	TOU s	MICA	CHL	CAS	RUT	PY	CHPY	ZIR
QZ p	★					×			×			×	×	
QZ s		★				×	⅄		×	❖		×	×	
K-SP			★			×	⅄		×	❖		×	×	
PLAG				★		×	⅄		×			×	×	
CARB					★	×			×			×	×	
TOU p	×	×	×	×	×	★			×			×	×	
TOU s							★		×			×	×	
MICA								★	×			×	×	
CHL	×	×	×	×	×	×	×	×	★			×	×	
CAS					⇔		❖			★	❖ ⅄	×	×	
RUT											★	×	×	
PY	×	×	×	×	×	×	×	×	×	×	×	★	×	
CHPY	×	×	×	×	×	×	×	×	×	×	×	×	★	
ZIR														★

LEGEND:

Replacement

- ❄ remnant - inclusion after partial replacement
- ⌯ partial replacement
- ⊂ complete replacement
- ♓⌯ preferential replacement

Alteration

- ⓪ alteration rim
- complete alteration
- ☘ partial alteration
- ☯ preferential alteration

Other

- ⇔ veinlets
- ⊙ inclusions
- ❖ paragenetic
- ⅄ matrix
- ♌ recrystallized
- × not present

PARAGENETIC TABLE

SAMPLE ID: RB131-91

	QZ p	QZ s	K-SP	PLAG	CARB	TOU p	TOU s	MICA	CHL	CAS	RUT	PY	CHPY	ZIR
QZ p	★				⌀ ⅄		⌀ ⅄	❄	×	❖			×	❖
QZ s		★							×			❖	×	
K-SP		⌀ ⊂	★	○	⌀ ⅄		⌀		×		⊙		×	⊙
PLAG				★					×				×	
CARB					★		⅄		×	❖	❖		×	
TOU p		⌀				★		⌀ ☮	×				×	
TOU s							★		×				×	
MICA								★	×				×	
CHL	×	×	×	×	×	×	×	×	★				×	
CAS										★			×	
RUT											★		×	
PY												★	×	
CHPY	×	×	×	×	×	×	×	×	×	×	×	×	★	
ZIR														★

LEGEND:

Replacement

- ❄ remnant - inclusion after partial replacement
- ⌀ partial replacement
- ⊂ complete replacement
- ♓⌀ preferential replacement

Alteration

- ○ alteration rim
- complete alteration
- ☮ partial alteration
- ☯ preferential alteration

Other

- ⇔ veinlets
- ⊙ inclusions
- ❖ paragenetic
- ⅄ matrix
- ♌ recrystallized
- × not present

PARAGENETIC TABLE

SAMPLE ID: RB132-91

	QZ p	QZ s	K-SP	PLAG	CARB	TOU p	TOU s	MICA	CHL	CAS	RUT	PY	CHPY	ZIR
QZ p	★					×	×		×		⊙		×	
QZ s		★				×	×		×				×	❖
K-SP		⟲	★		⟲	×	×	☮ ⅄	×		⊙		×	❖
PLAG		⟲		★	⟲	×	×	☮ ⅄	×				×	
CARB					★	×	×	❖	×	❖	❖	❖	×	❖
TOU p	×	×	×	×	×	★	×		×				×	
TOU s	×	×	×	×	×	×	★		×				×	
MICA					❖			★	×	❖	❖	❖	×	❖
CHL	×	×	×	×	×	×	×	×	★				×	
CAS										★			×	
RUT											★		×	
PY												★	×	
CHPY	×	×	×	×	×	×	×	×	×	×	×	×	★	
ZIR														★

LEGEND:

Replacement

- ❄ remnant - inclusion after partial replacement
- ⟲ partial replacement
- ⊂ complete replacement
- ♓⟲ preferential replacement

Alteration

- ⭘ alteration rim
- ● complete alteration
- ☮ partial alteration
- ☯ preferential alteration

Other

- ⇔ veinlets
- ⊙ inclusions
- ❖ paragenetic
- ⅄ matrix
- ♌ recrystallized
- × not present

PARAGENETIC TABLE

SAMPLE ID: RB133-91

	QZ p	QZ s	K-SP	PLAG	CARB	TOU p	TOU s	MICA	CHL	CAS	RUT	PY	CHPY	ZIR
QZ p	★				⌯	×	×		×					
QZ s		★				×	×		×					❖
K-SP		⌯	★		⌯	×	×	☮ ⅄	×		⊙			
PLAG		⌯		★	⌯	×	×	⅄	×					
CARB					★	×	×	❖	×	❖	❖			❖
TOU p	×	×	×	×	×	★	×		×					
TOU s	×	×	×	×	×	×	★		×					
MICA					❖			★	×	❖	❖			❖
CHL	×	×	×	×	×	×	×	×	★					
CAS										★	❖			
RUT											★			
PY												★		
CHPY													★	
ZIR														★

LEGEND:

Replacement

- ❄ remnant - inclusion after partial replacement
- ⌯ partial replacement
- ⊂ complete replacement
- ♓⌯ preferential replacement

Alteration

- O alteration rim
- complete alteration
- ☮ partial alteration
- ☯ preferential alteration

Other

- ⇔ veinlets
- ⊙ inclusions
- ❖ paragenetic
- ⅄ matrix
- ♌ recrystallized
- × not present

PARAGENETIC TABLE

SAMPLE ID: RB134-91

	QZ p	QZ s	K-SP	PLAG	CARB	TOU p	TOU s	MICA	CHL	CAS	RUT	PY	CHPY	ZIR
QZ p	★				⊂ ⅄	×	⇳							×
QZ s		★				×		⅄						×
K-SP		⊂	★		⊂ ⅄	×	⇳	☮ ⅄	☮ ⅄		⊙			×
PLAG		⊂		★	⊂ ⅄	×	⇳	☮ ⅄ ☯	☮ ⅄					×
CARB					★	×	⇳ ❖	❖	❖	❖	❖			×
TOU p	×	×	×	×	×	★								×
TOU s							★							×
MICA								★	❖	❖	❖			×
CHL									★	❖	❖			×
CAS										★				×
RUT											★			×
PY												★		×
CHPY													★	×
ZIR	×	×	×	×	×	×	×	×	×	×	×	×	×	★

LEGEND:

Replacement

- ❄ remnant - inclusion after partial replacement
- ⊂ partial replacement
- ⊂ complete replacement
- ℋ ⊂ preferential replacement

Alteration

- ⊙ alteration rim
- ● complete alteration
- ☮ partial alteration
- ☯ preferential alteration

Other

- ⇳ veinlets
- ⊙ inclusions
- ❖ paragenetic
- ⅄ matrix
- ♌ recrystallized
- × not present

PARAGENETIC TABLE

SAMPLE ID: RB160-91

	QZ p	QZ s	K-SP	PLAG	CARB	TOU p	TOU s	MICA	CHL	CAS	RUT	PY	CHPY	ZIR
QZ p	★													
QZ s		★												
K-SP			★											
PLAG				★										
CARB					★			❖		❖	❖	❖		❖
TOU p						★								
TOU s							★							
MICA					❖			★		❖	❖	❖		❖
CHL									★					
CAS										★				
RUT											★			
PY												★		
CHPY													★	
ZIR														★

LEGEND:

Replacement

- remnant - inclusion after partial replacement
- partial replacement
- complete replacement
- preferential replacement

Alteration

- alteration rim
- complete alteration
- partial alteration
- preferential alteration

Other

- veinlets
- inclusions
- paragenetic
- matrix
- recrystallized
- not present

PARAGENETIC TABLE

SAMPLE ID: RB161-91

	QZ p	QZ s	K-SP	PLAG	CARB	TOU p	TOU s	MICA	CHL	CAS	RUT	PY	CHPY	ZIR
QZ p	★				⇳				×	⊂				×
QZ s		★							×			❖		×
K-SP		⊂	★		⇳				×		⊙			×
PLAG				★					×					×
CARB					★		❖		×			❖		×
TOU p						★			×					×
TOU s		❖					★		×	❖		❖		×
MICA								★	×			⊙		×
CHL	×	×	×	×	×	×	×	×	★					×
CAS							❖			★		❖		×
RUT											★			×
PY												★	❖	×
CHPY													★	×
ZIR	×	×	×	×	×	×	×	×	×	×	×	×	×	★

LEGEND:

Replacement

- ❄ remnant - inclusion after partial replacement
- ⇳ partial replacement
- ⊂ complete replacement
- ⋓ preferential replacement

Alteration

- ⊙ alteration rim
- ● complete alteration
- ◔ partial alteration
- ☯ preferential alteration

Other

- ⇔ veinlets
- ⊙ inclusions
- ❖ paragenetic
- ⅄ matrix
- ♌ recrystallized
- × not present

PARAGENETIC TABLE

SAMPLE ID: RB162-91

	QZ p	QZ s	K-SP	PLAG	CARB	TOU p	TOU s	MICA	CHL	CAS	RUT	PY	CHPY	ZIR
QZ p	★													
QZ s		★												
K-SP			★											
PLAG				★										
CARB					★									
TOU p						★								
TOU s							★							
MICA								★						
CHL									★					
CAS										★				
RUT											★			
PY												★		
CHPY													★	
ZIR														★

LEGEND:

Replacement

- remnant - inclusion after partial replacement
- partial replacement
- complete replacement
- preferential replacement

Alteration

- alteration rim
- complete alteration
- partial alteration
- preferential alteration

Other

- veinlets
- inclusions
- paragenetic
- matrix
- recrystallized
- not present

PARAGENETIC TABLE

SAMPLE ID: RB163-91

	QZ p	QZ s	K-SP	PLAG	CARB	TOU p	TOU s	MICA	CHL	CAS	RUT	PY	CHPY	ZIR
QZ p	★								×		×			×
QZ s		★							×		×			×
K-SP		⟲ ⅄	★		⟲ ⅄		⟲	⟲	×		×			×
PLAG		⟲ ⅄		★	⟲ ⅄		⟲	⟲ ⅄	×		×			×
CARB					★			❖	×	❖	×			×
TOU p		⟲				★			×		×			×
TOU s							★		×		×			×
MICA					❖			★	×		×	❖		×
CHL	×	×	×	×	×	×	×	×	★		×			×
CAS										★	×			×
RUT	×	×	×	×	×	×	×	×	×	×	★			×
PY												★		×
CHPY														×
ZIR	×	×	×	×	×	×	×	×	×	×	×	×	×	★

LEGEND:

Replacement

- ❄ remnant - inclusion after partial replacement
- ⟲ partial replacement
- ⊂ complete replacement
- ♓⟲ preferential replacement

Alteration

- ⭘ alteration rim
- complete alteration
- ☣ partial alteration
- ☯ preferential alteration

Other

- ⇔ veinlets
- ⊙ inclusions
- ❖ paragenetic
- ⅄ matrix
- ♌ recrystallized
- × not present

PARAGENETIC TABLE

SAMPLE ID: RB164-91

	QZ p	QZ s	K-SP	PLAG	CARB	TOU p	TOU s	MICA	CHL	CAS	RUT	PY	CHPY	ZIR
QZ p	★				⟲		×	⅄	×	×				×
QZ s		★					×		×	×				×
K-SP		⟲	★		⟲		×	⅄	×	×	⊙			×
PLAG		⟲		★	⟲		×	⅄	×	×				×
CARB					★		×	❖	×	×				×
TOU p		⟲			⟲	★	×		×	×				×
TOU s	×	×	×	×	×	×	★		×	×				×
MICA					❖			★	×	×				×
CHL	×	×	×	×	×	×	×	×	★	×				×
CAS	×	×	×	×	×	×	×	×	×	★				×
RUT											★			×
PY												★		×
CHPY													★	×
ZIR	×	×	×	×	×	×	×	×	×	×	×	×	×	★

LEGEND:

Replacement

- ❄ remnant - inclusion after partial replacement
- ⟲ partial replacement
- ⊂ complete replacement
- ♓⟲ preferential replacement

Alteration

- ⭘ alteration rim
- ● complete alteration
- ◔ partial alteration
- ☯ preferential alteration

Other

- ⇔ veinlets
- ⊙ inclusions
- ❖ paragenetic
- ⅄ matrix
- ♌ recrystallized
- × not present

APPENDIX C.
Colour Plates.

Table of abbreviations used.

	Description
A	Ankerite
C	Carbonatisation
Ca	Carbonate
Cs	Cassiterite
Chl	Chlorite
Chpy	Chalcopyrite
GB	Green Band
Ks	K-feldspar
Mus	Muscovite
P	Pocket
Pl	Plagioclase
Py	Pyrite
Qz	Quartz
RQ	Recrystallised Quartz
S	Sericitisation
Ser	Sericite
Su	Sulphide
T	Tourmalinisation
Tr	Tourmaline
WR	Wall Rock
Zr	Zircon

PLATE 1.

RB028.91 AMS-lode

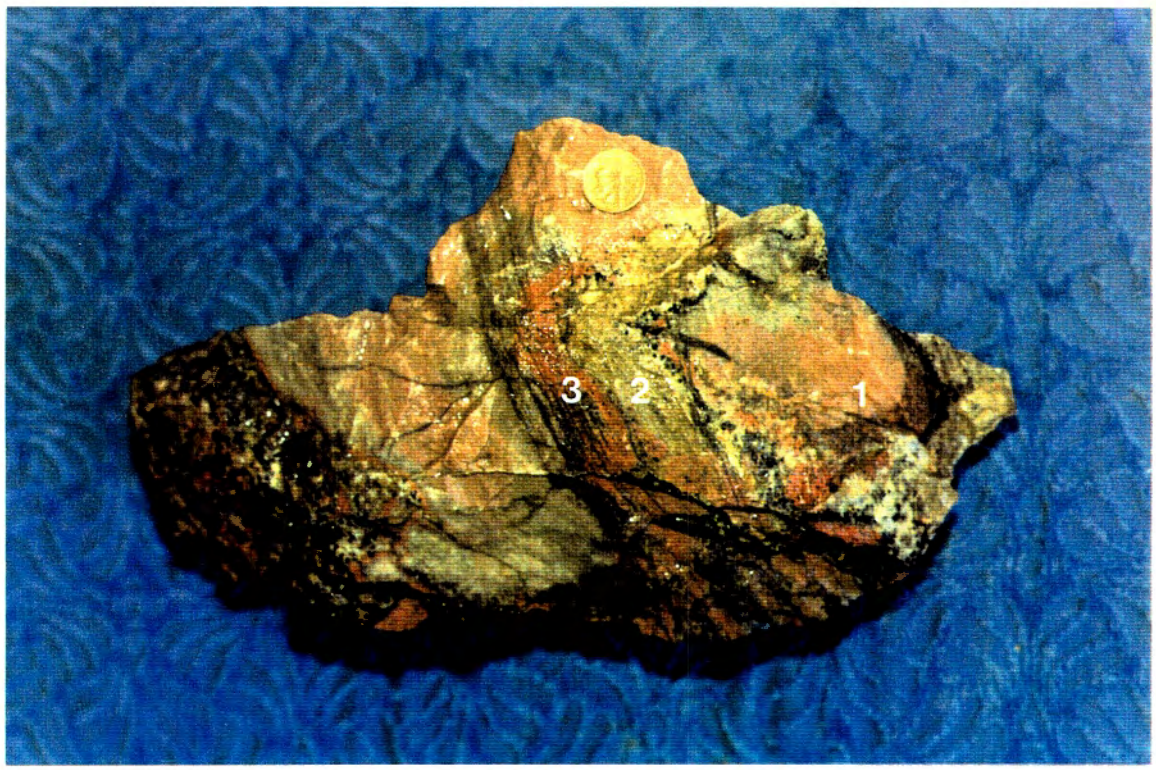

PLATE 1.
RB028.91 **AMS-lode**

Scale: The diameter of the coin (2c) is 22.4 mm.

A typical example of an immature pocket in the AMS-lode. Three different mineralogical phases related to the formation of a pocket may be recognised:

1. The pink original feldspathic host rock.
2. The bleached sericitic halo with the associated ore lode minerals tourmaline and cassiterite.
3. Red feldspathic halo, representing strong K-alteration and K-remobilisation.

PLATE 2.
RB027.91 AMS-lode

PLATE 3.
RB036.91 Bonus lode

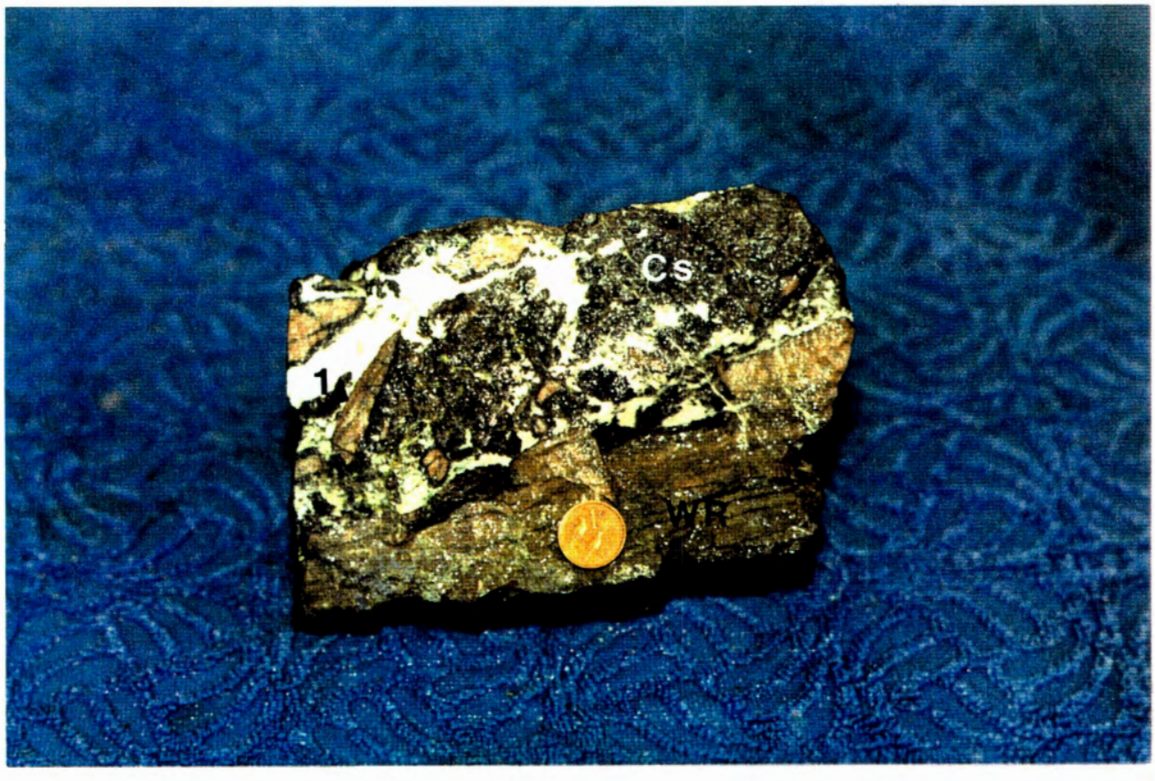

PLATE 2.
RB027.91 **AMS-lode**

Scale: The diameter of the coin (1c) is 19 mm.

An example of large scale sericitisation (S) and carbonate (Ca) vein filling between brecciated fragments.

PLATE 3.
RB036.91 **Bonus lode**

Scale: The diameter of the coin (1c) is 19 mm.

This sample was taken on the edge of the ore lode fracture of the Bonus lode. It is very rich in cassiterite (visible as a brown concentrate). It displays evidence for a hydraulic brecciated origin, with host rock fragments "floating" in a carbonate matrix. The ore lode minerals cassiterite and tourmaline concentrate on the crystallising surfaces of the breccia fragments and on the bottom of the main fracture surface.

PLATE 4.
RB037.91 Bonus lode

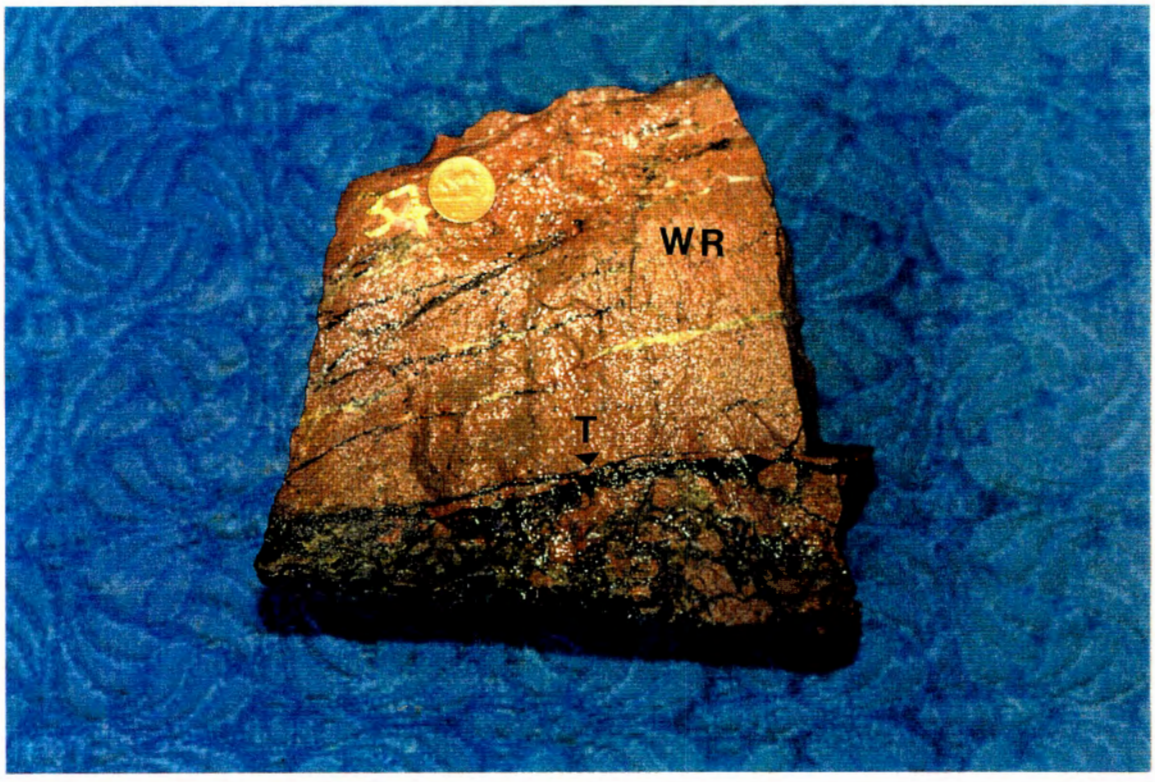

PLATE 5.
RB020.91 B-lode

PLATE 4.
RB037.91 **Bonus lode**

Scale: The diameter of the coin (2c) is 22.4 mm.

Tourmaline filled microfractures accentuating the brecciated nature of the lode. Replacement type mineralisation of the brecciated host rock fragments is evident.

PLATE 5.
RB020.91 **B-lode**

Scale: The diameter of the coin (1c) is 19 mm.

Hydraulically brecciated lode displaying the deposition sequence and the possible nature of the mineralising fluids: Tr - Cs - Ca - Ser. Minor fractures formed sub-parallel to the main fracture and were filled by carbonate (both siderite and ankerite being present). Abundant sericite and chlorite is present with chalcopyrite the predominant sulphide. Cassiterite and tourmaline crystallised around brecciated fragments and on the main fracture surface.

PLATE 6.
RB022.91 B-lode

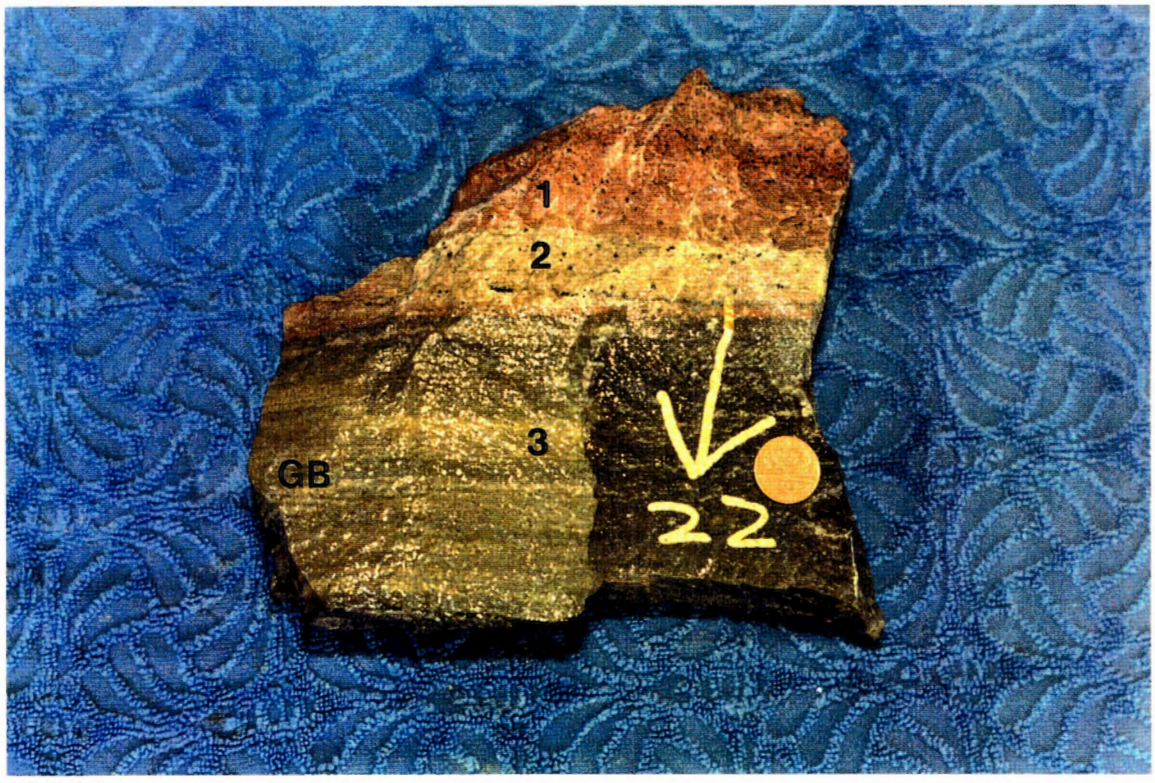

PLATE 7.
RB021.91 Cotton lode

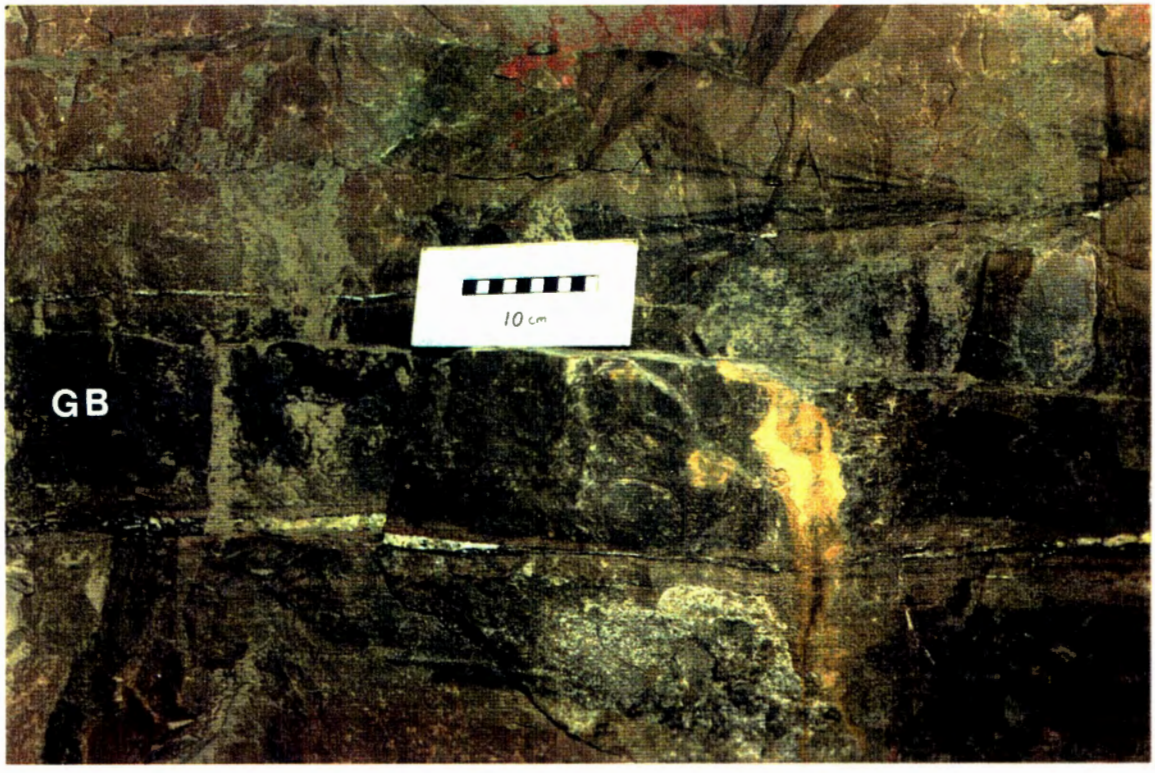

PLATE 6.

RB022.91 **B-lode**

Scale: The diameter of the coin (2c) is 22.4 mm.

Typical green band (GB) accompanied by colour zonation:

1. Feldspathic host rock.
2. White halo of muscovitic host rock.
3. Sericitic- and chloritic host rock forming the green band (GB).

PLATE 7.

RB021.91 **Cotton lode**

Green Band (GB) in the host rock.

PLATE 8.
RB004.91 Cotton Lode

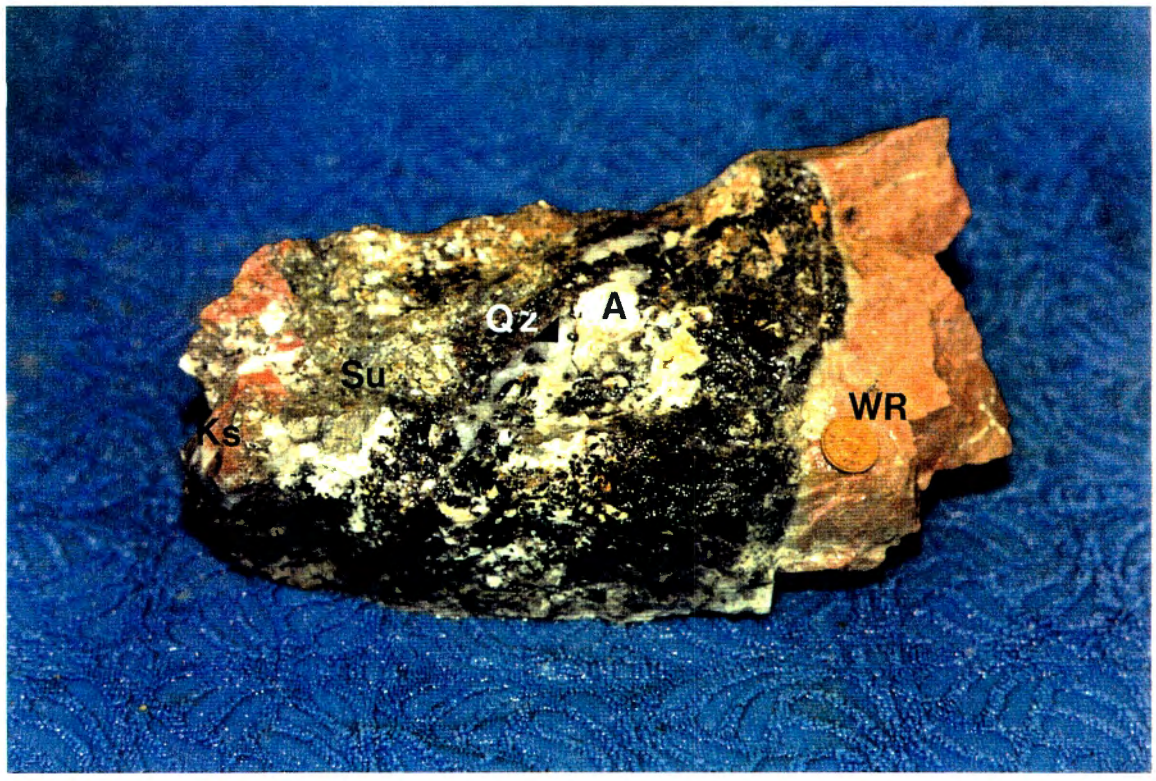

PLATE 9.
RB047.91 Cotton Lode

PLATE 8.
RB004.91 **Cotton Lode**

Scale: The diameter of the coin (1c) is 19 mm.

A mature pocket (P) displaying intimate intergrowth of tourmaline and cassiterite. Later phase ankerite and free quartz are also present. The sulphides are pyrite (mostly pentagondodecahedra and cubes) with subordinate massive chalcopyrite. Ks is orthoclase that recrystallised during pocket formation.

PLATE 9.
RB047.91 **Cotton Lode**

An example of a partly formed or immature pocket in the red feldspathic wall rock. It is a low grade pocket with cassiterite in association with tourmaline. It mainly consists of siderite and tourmaline needles in the carbonaceous matrix. Some free quartz occurs.

PLATE 10.
RB035.91 C-lode

PLATE 11.
RB010.91 C-lode

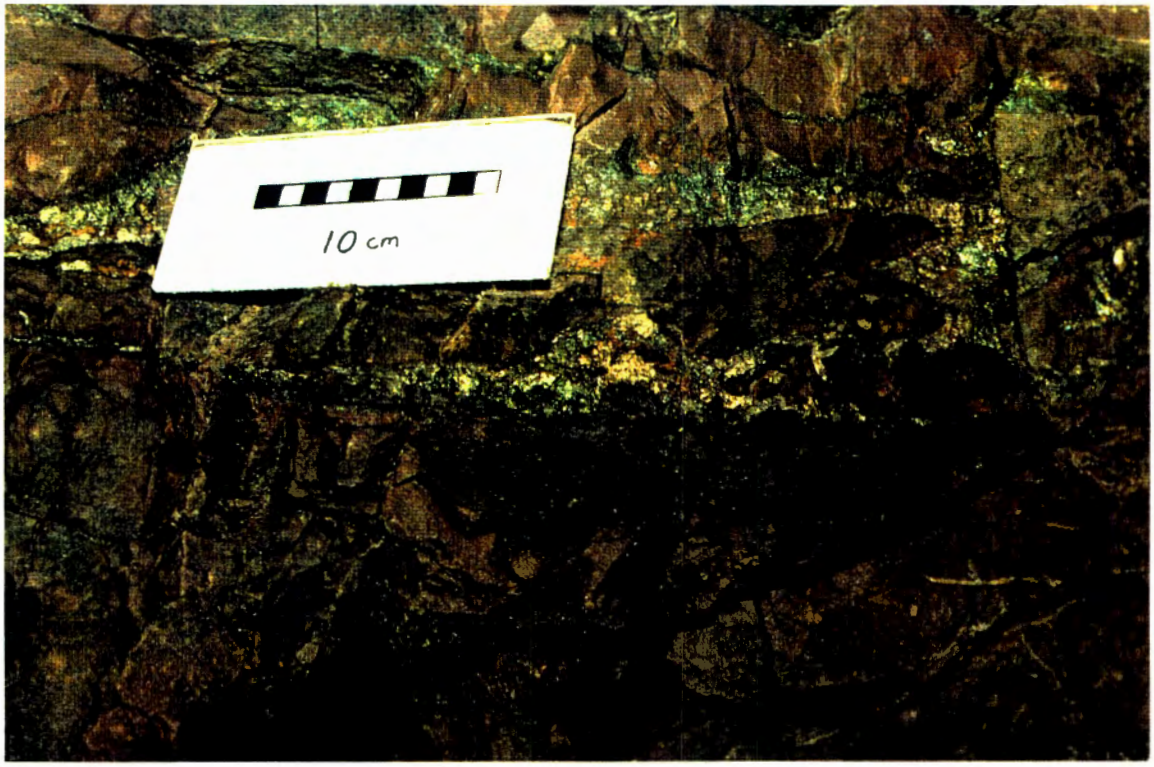

PLATE 10.
RB035.91 **C-lode**

Carbonate-rich brecciated ore lode. The fracture surface and brecciated fragments served as crystallising surfaces for tourmaline and cassiterite, while carbonate (predominantly siderite) acted as filler. Note how the rock fragments rest against each other, creating the impression that the fragments 'float' in the matrix.

PLATE 11.
RB010.91 **C-lode**

Sulphide-rich lode. The sulphides crystallised in the fractures after cassiterite and tourmaline deposition took place. The sulphides are predominantly chalcopyrite with subordinate pyrite.

PLATE 12.
RB017.91 C-lode

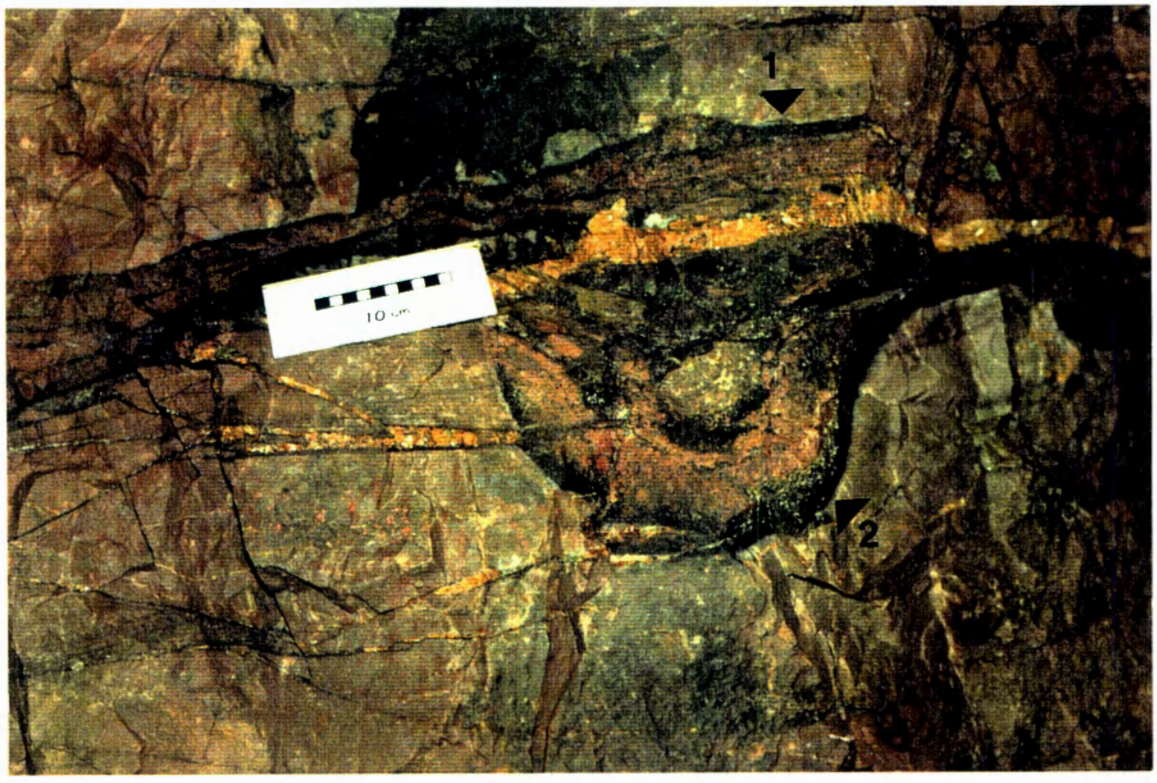

PLATE 13.
RB016.91 C-lode

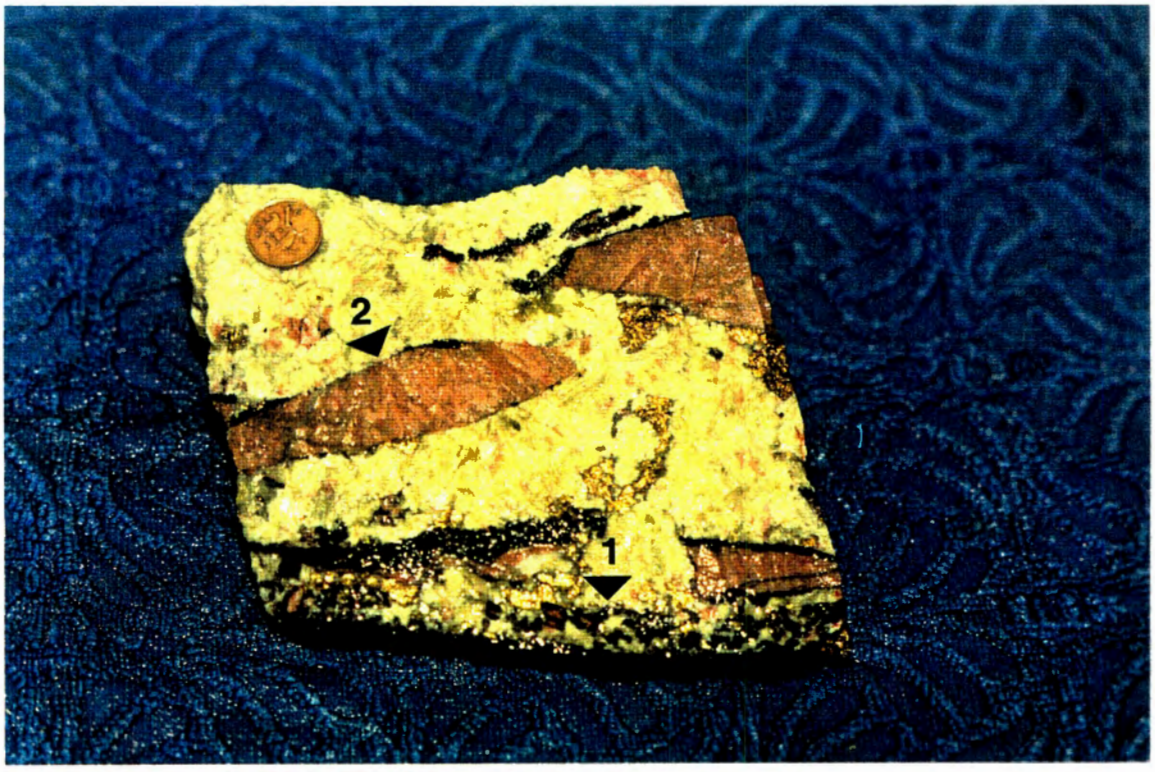

PLATE 12.
RB017.91 **C-lode**

A pocket formed from hairline fractures on a lode. Metasomatic action is evident at points 1 and 2. This pocket mainly consist of recrystallised orthoclase, tourmaline and cassiterite. The carbonate (siderite) is concentrated in crosscutting veinlets and in the major lode.

PLATE 13.
RB016.91 **C-lode**

Scale: The diameter of the coin (1c) is 19 mm.

This lode shows hydraulic fracturing in the NAD deposit, with brecciated fragments that served as crystallising surfaces. Note the close association of carbonate and chalcopyrite.

1. Small fragments serving as crystallising surfaces, but the fragments were almost completely replaced.
2. Larger fragment serving as a crystallising surface for cassiterite and tourmaline.

PLATE 14.
RB015.91 C-lode

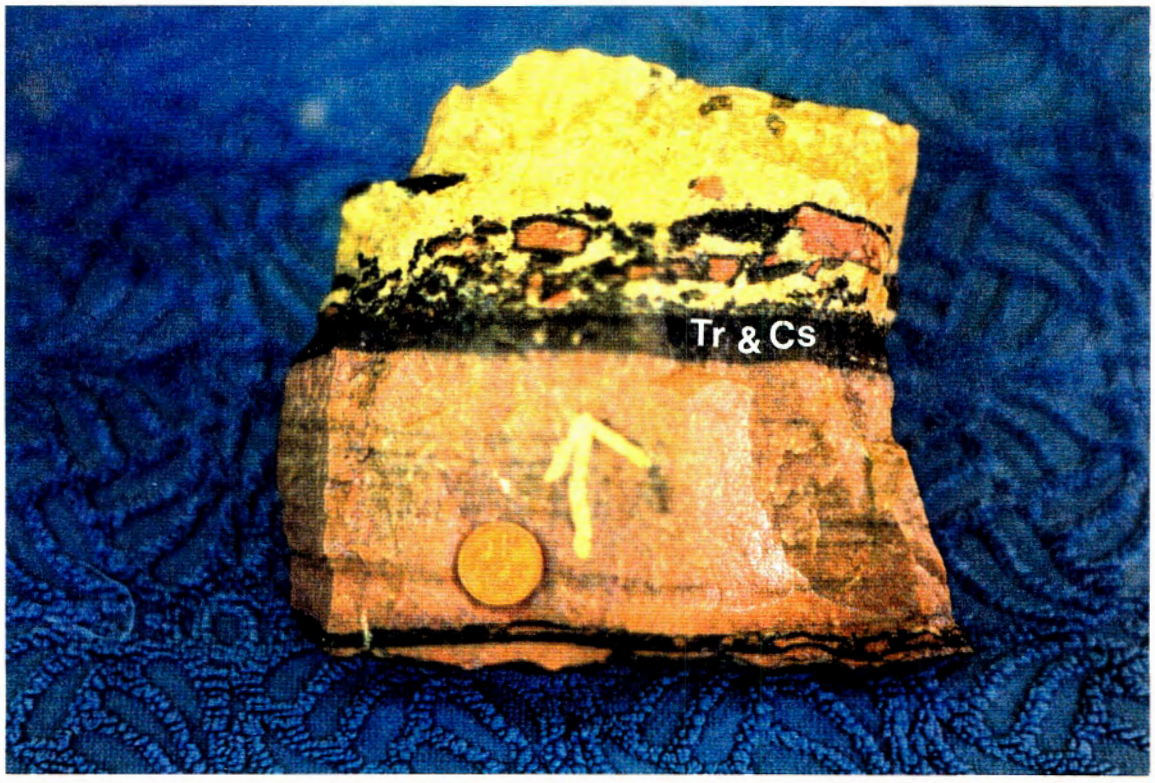

PLATE 15.
RB064.91 T-lode

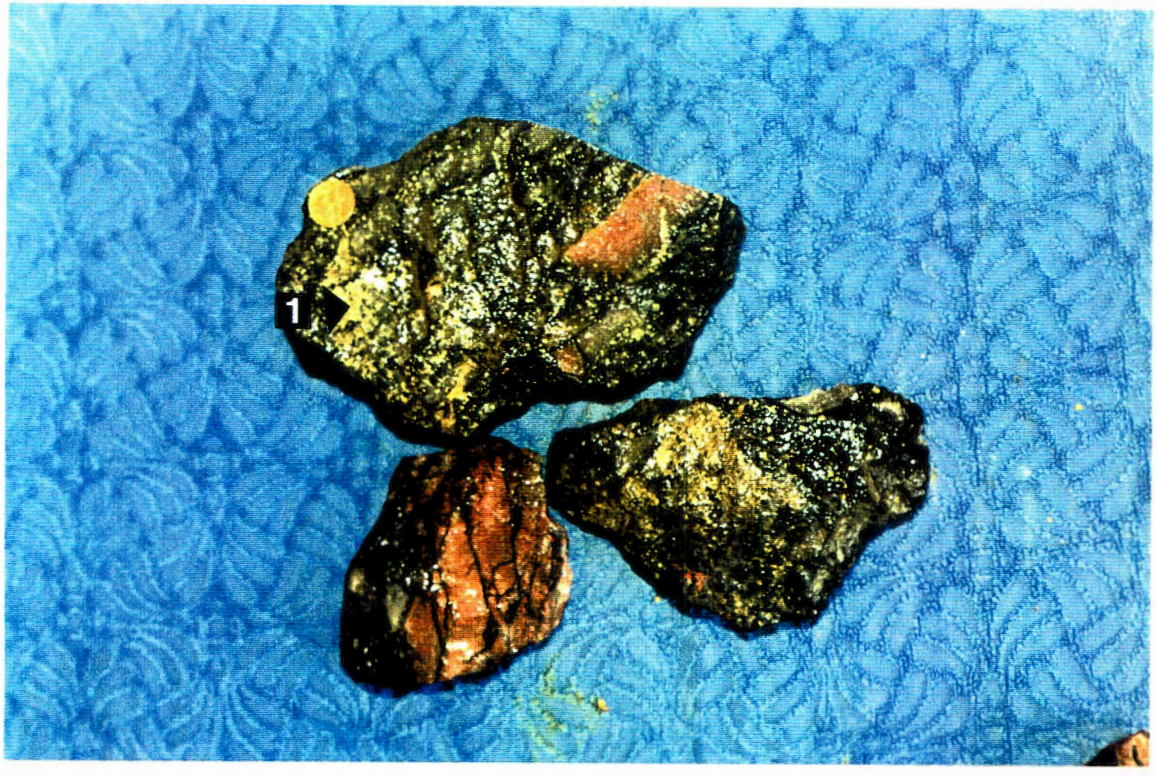

PLATE 14.
RB015.91 **C-lode**

Scale: The diameter of the coin (1c) is 19 mm.

Proof of hydraulic brecciation is evident from the rock fragments 'floating' in a carbonaceous matrix. Intimate tourmaline (Tr) and cassiterite (Cs) intergrowth can be seen on the crystallising surfaces.

PLATE 15.
RB064.91 **T-lode**

Scale: The diameter of the coin (1c) is 19 mm.

Very tourmaline rich lode associated mostly with pyrite. Very little chalcopyrite is present. An intimate intergrowth of tourmaline and cassiterite occurs within a matrix of very fine-grained tourmaline and secondary quartz.

Mottled pyrite associated with tourmaline and quartz.

PLATE 16.
RB040.91

PLATE 17.
RB063.91

T-lode

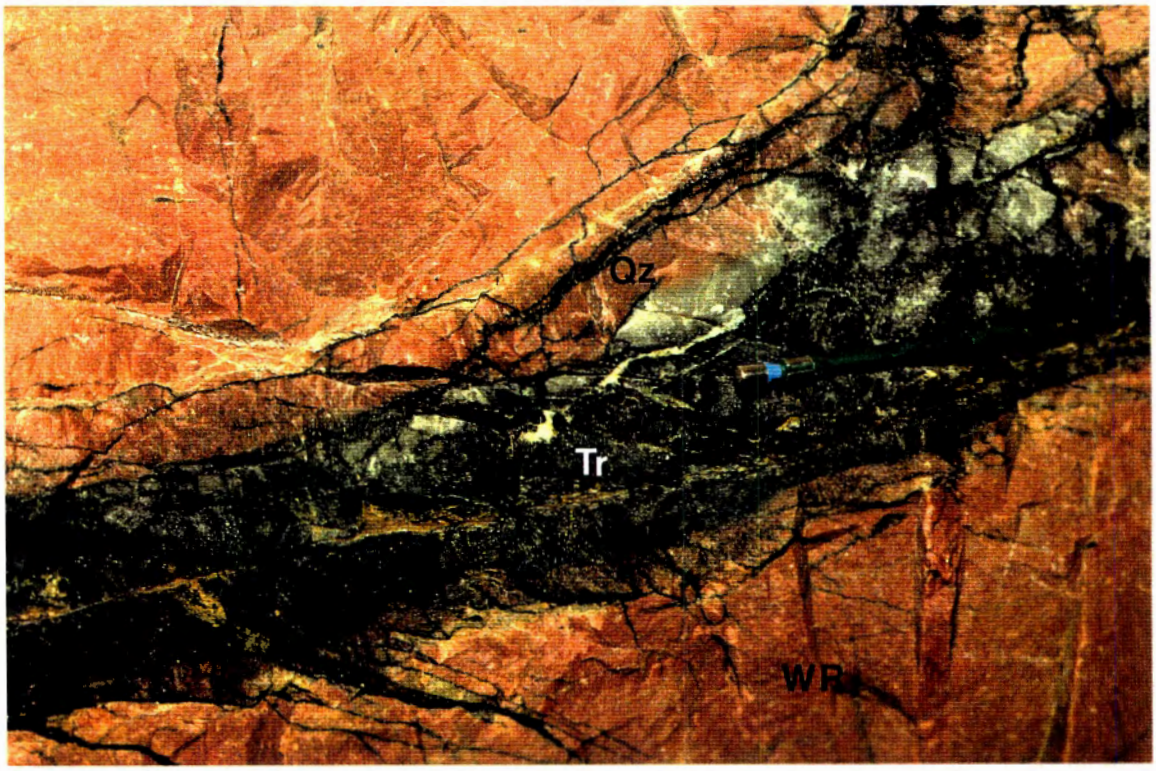

PLATE 16.
RB040.91 **T-lode**

Red feldspathic wall rock displaying a green band (GB) with a tourmaline-rich zone (*Tr*) underneath and pocket formation (P) below. It seems likely that the green band confined the mineralising fluids underneath it. (Red spots are splashes of paint.)

PLATE 17.
RB063.91 **T-lode**

A typical example of the T-lode: the red feldspathic wall rock (WR), and quartz-tourmaline (Qz-Tr) association in the lode.

PLATE 18.
RB034.91 Union lode

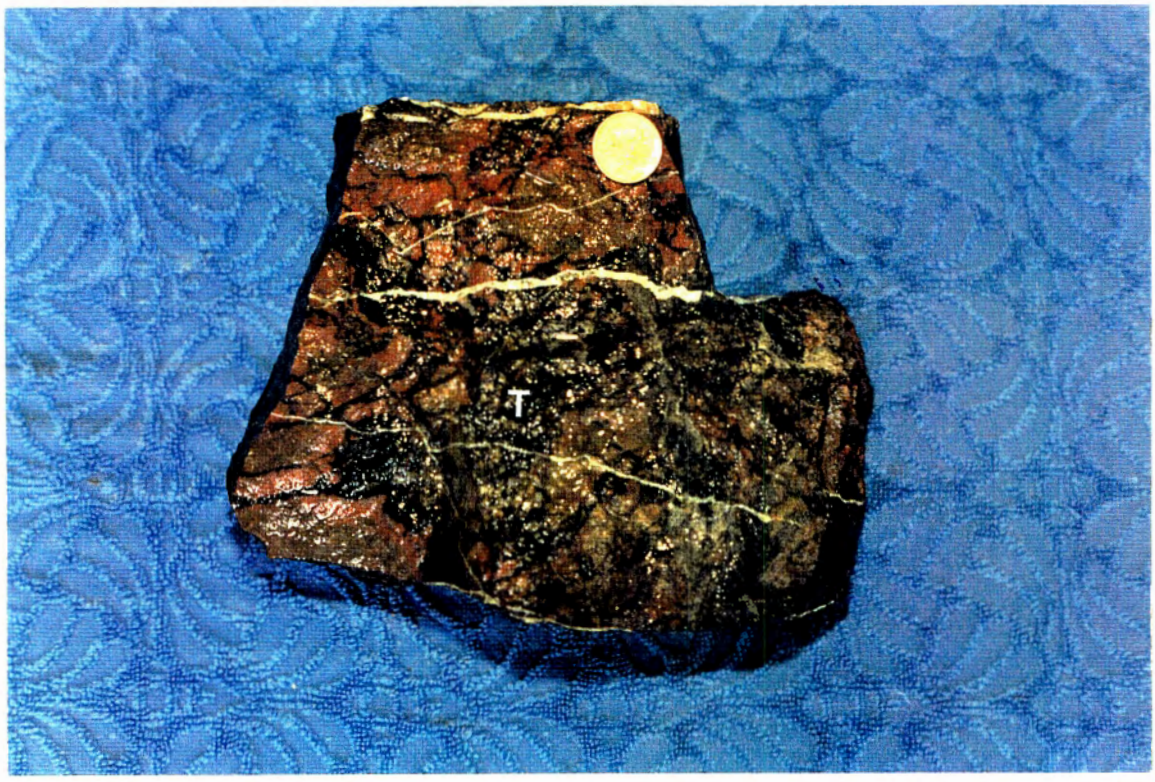

PLATE 19.
RB053.91 U-lode

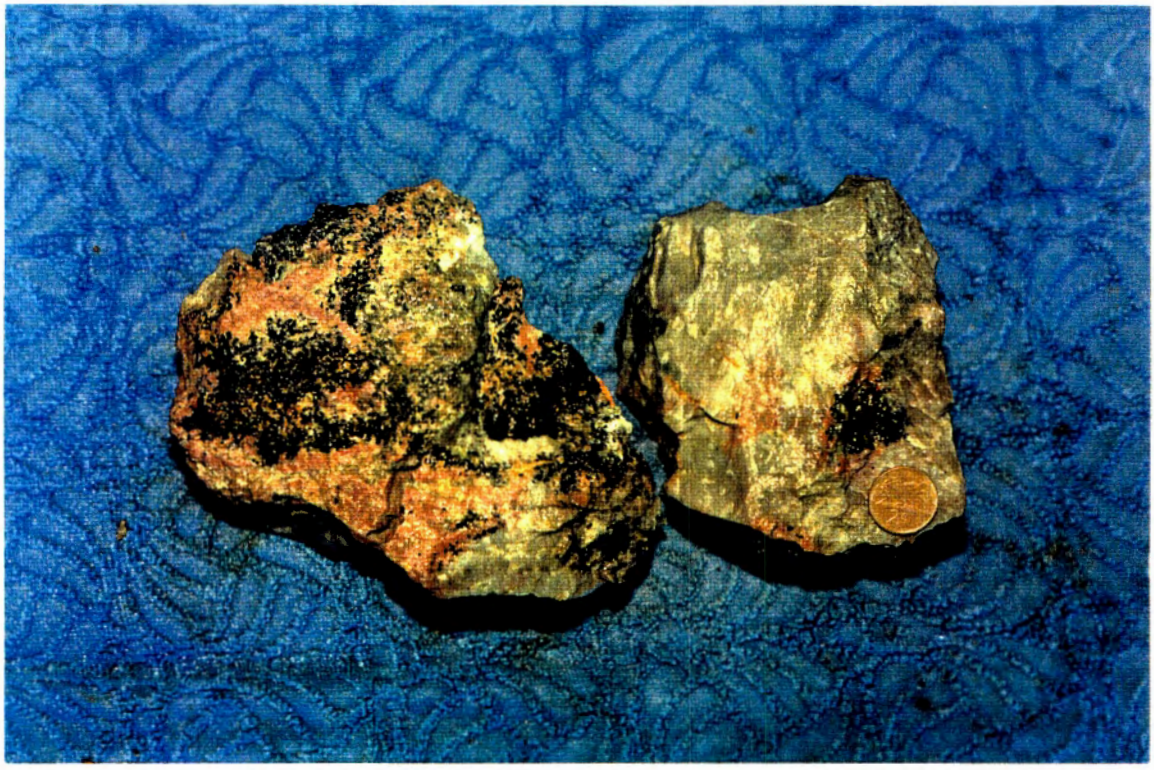

PLATE 18.
RB034.91 **Union lode**

Scale: The diameter of the coin (2c) is 22.4 mm.

Evidence of hydraulic brecciation as well as extreme metasomatic action in the form of tourmalinisation (T) are illustrated. Note the carbonate veinlets cutting through already tourmalinised rock, indicating that the carbonate was deposited during a later phase of mineralisation.

PLATE 19.
RB053.91 **U-lode**

Scale: The diameter of the coin (2c) is 22.4 mm.

An example of replacement mineralisation in the form of an immature pocket, displaying aggregates of tourmaline needles, the same colour and mineralogical zoning of a mature pocket (plate 8).

PLATE 20.
RB052.91 U-lode

PLATE 21.
RB168.91 Disseminated Tin

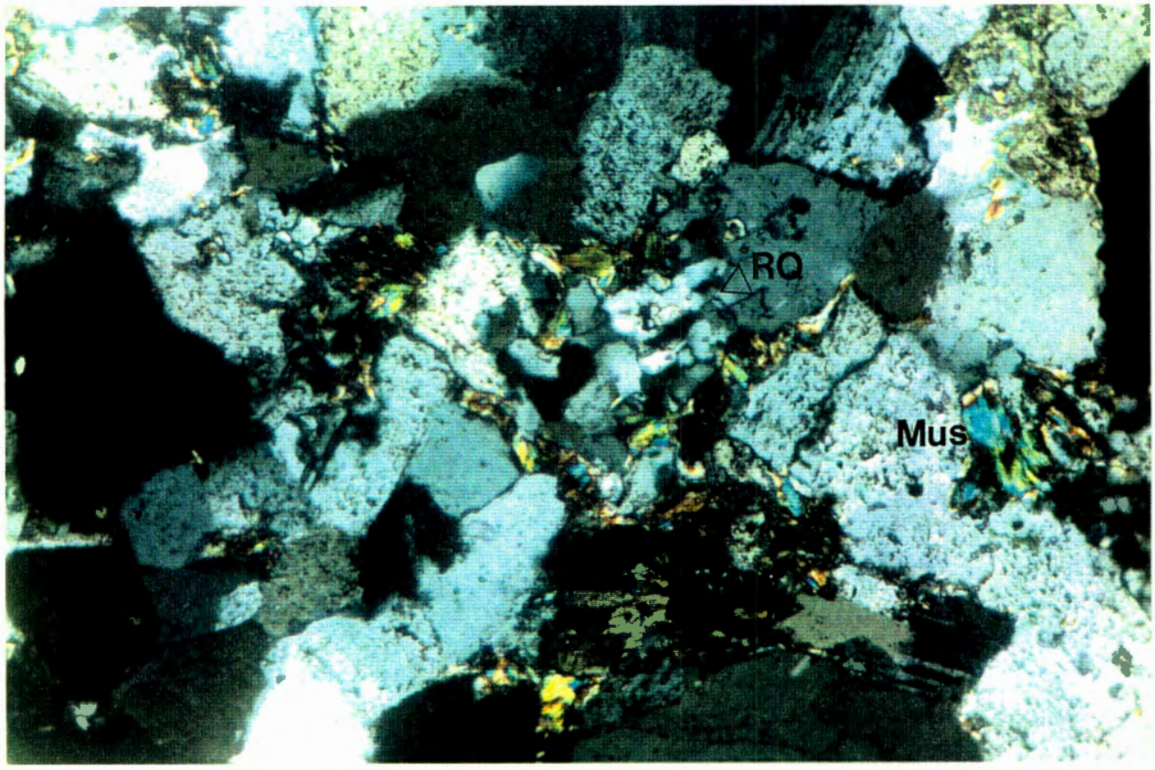

PLATE 20.
RB052.91 **U-lode**

Scale: The diameter of the coin (2c) is 22.4 mm.

Hydraulically brecciated lode. Some fluorite is present and is associated with ankerite. This is the only major occurrence of fluorite in the NAD deposit found by the writer. Although abundant tourmaline is present, very little cassiterite is present.

PLATE 21.
RB168.91 **Disseminated Tin**

Scale: width of photo equals 1 mm.

Recrystallised quartz shows undulatory extinction and replaces host rock material. Interstitial muscovite in the host rock forms part of the matrix of the sedimentary rock.

PLATE 22.
RB169.91 Disseminated Tin

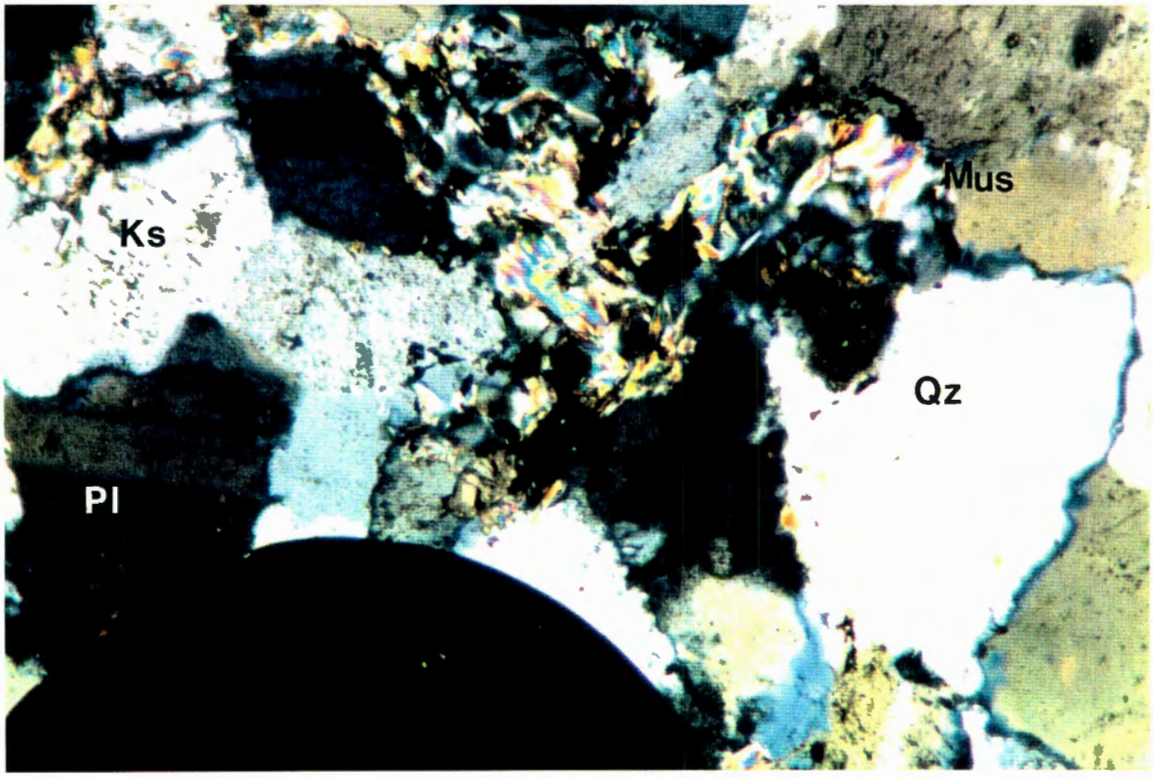

PLATE 23.
RB 163.91 C-lode

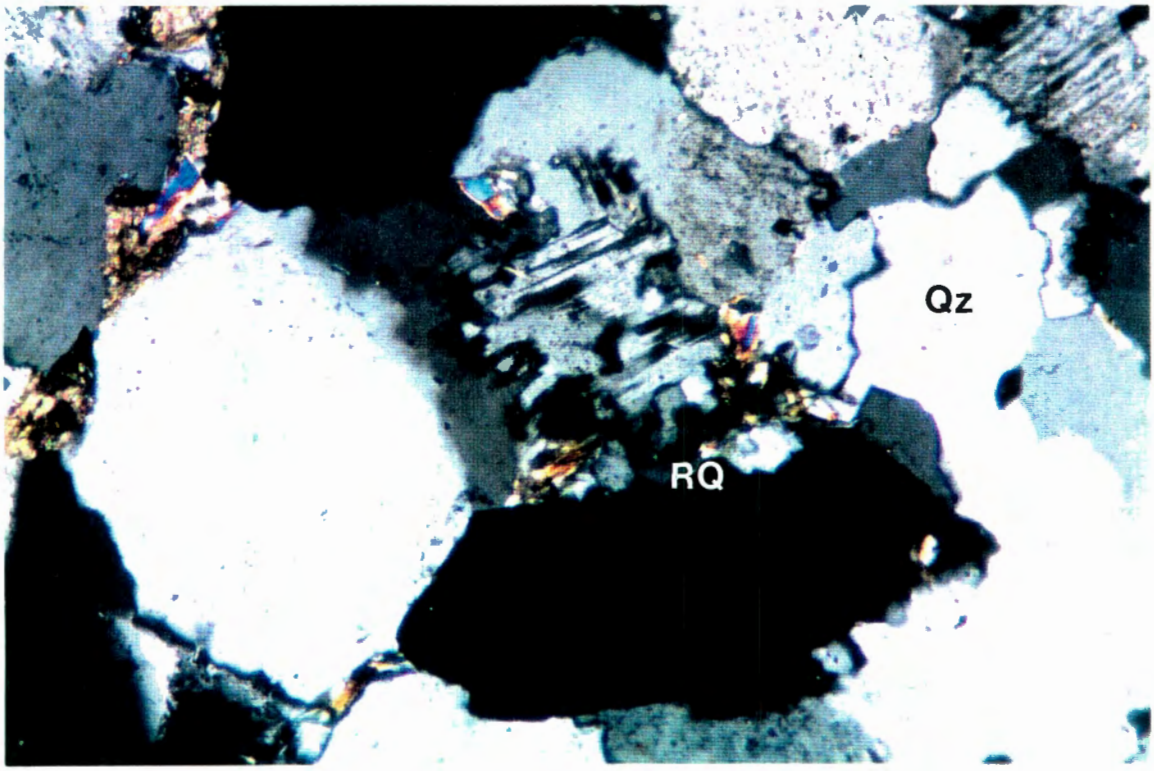

PLATE 22.
RB169.91 **Disseminated Tin**

Scale: width of photo equals 0.5 mm.

Recrystallised quartz replaces the feldspathic components of the host rock together with interstitial muscovite. Plagioclase resists replacement while orthoclase is most often replaced. Note the typical morphology of the K-feldspar.

PLATE 23.
RB 163.91 **C-lode**

Scale: width of photo equals 0.5 mm.

Massive silicification of the host rock by remobilisation and recrystallisation of quartz. Secondary quartz replaces feldspar. Some interstitial muscovite and carbonate is present.

PLATE 24.
RB163.91 C-lode

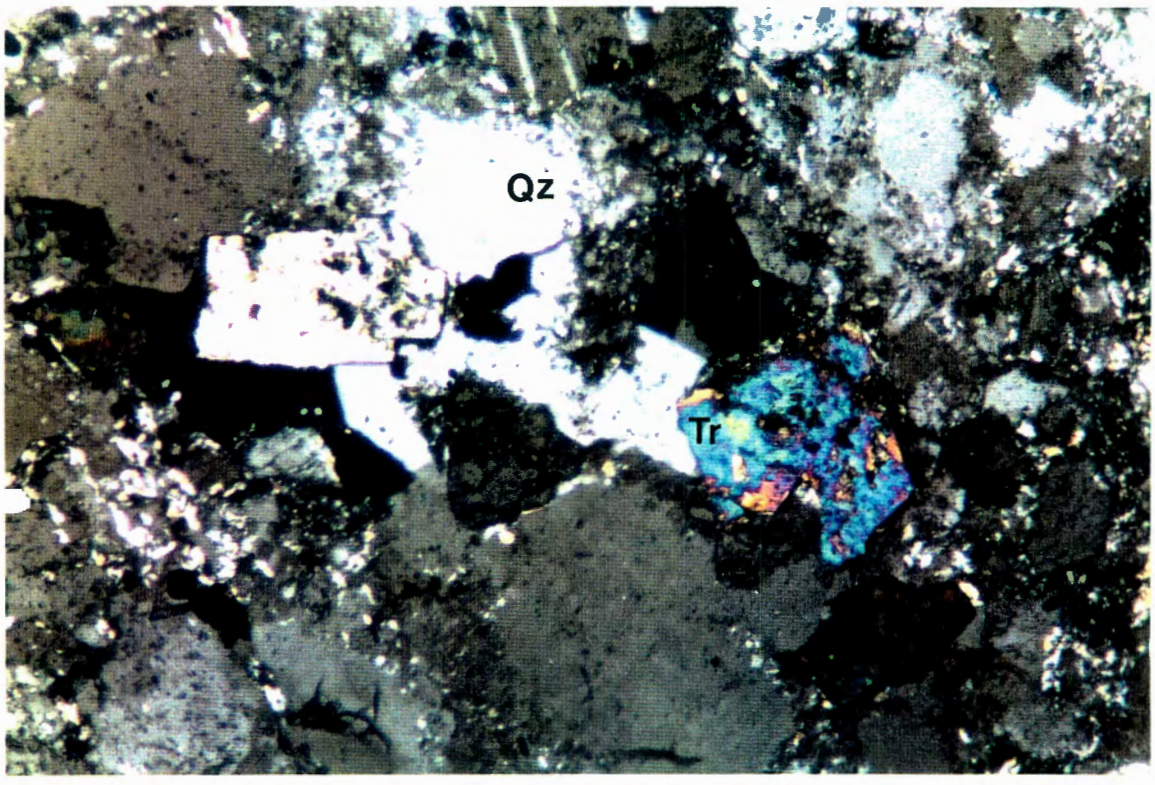

PLATE 25.
RB134.91 Union lode

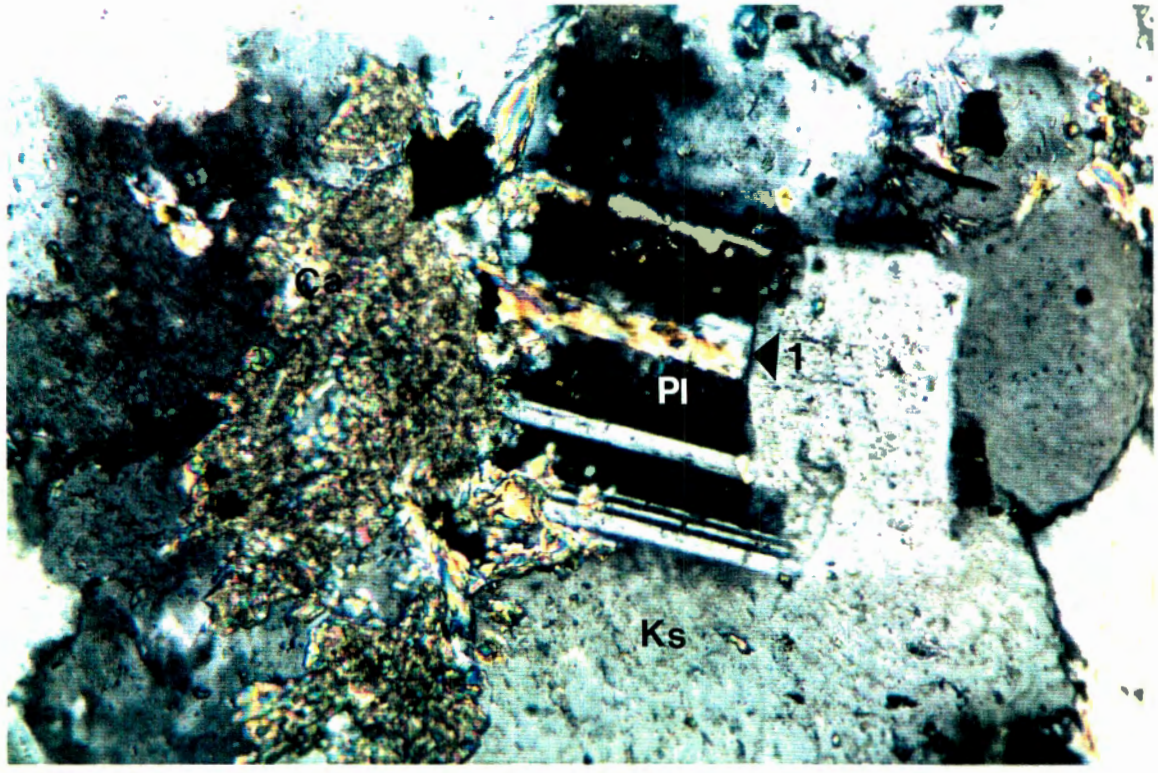

PLATE 24.
RB163.91 **C-lode**

Scale: width of photo equals 0.5 mm.

Quartz replaces the feldspars in the host rock. Note the remnants of feldspar within and between the quartz grains. The primary tourmaline is also being replaced.

PLATE 25.
RB134.91 **Union lode**

Scale: width of photo equals 0.5 mm.

Host rock consisting mainly of feldspars, partly replaced by interstitial carbonate and muscovite-sericite. Note the preferential replacement of polysynthetic twin lamellae of plagioclase (oligoclase) by muscovite.

PLATE 26.
RB134.91 Union lode

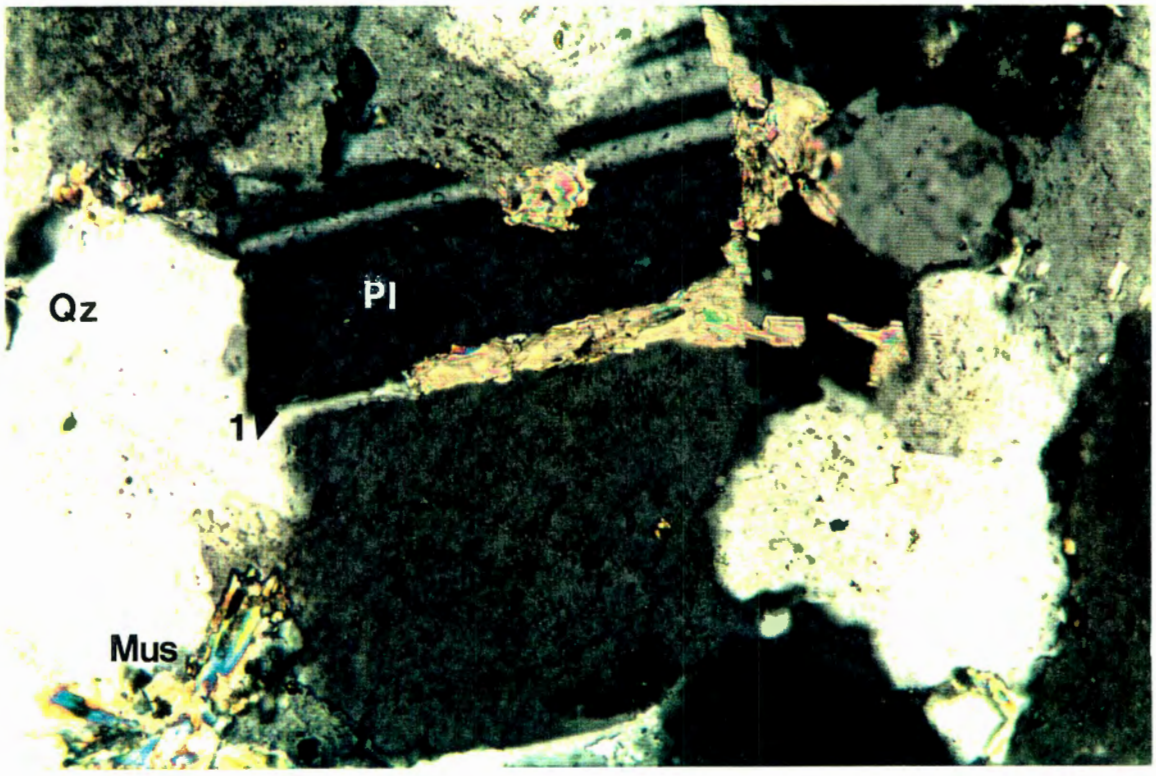

PLATE 27.
RB162.91 C-lode

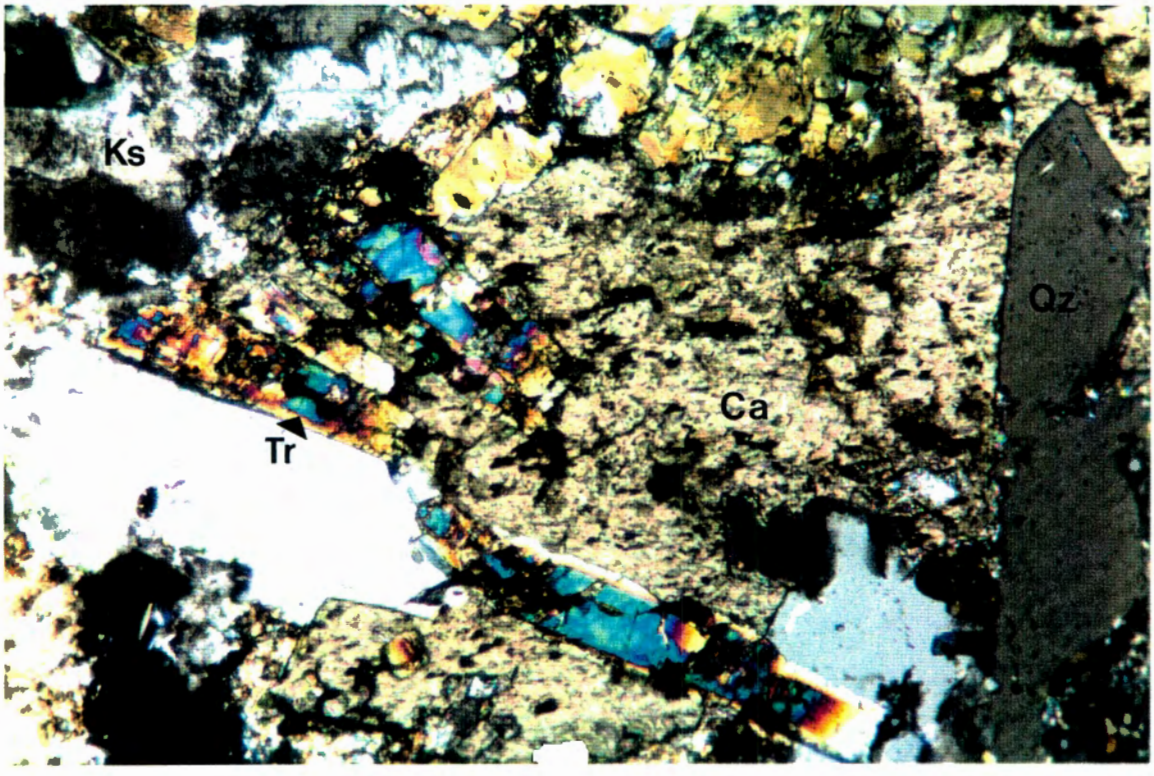

PLATE 26.
RB134.91 **Union lode**

Scale: width of photo equals 0.5 mm.

Host rock consisting mainly of feldspars, partly replaced by interstitial carbonate. Note the preferential replacement of polysynthetic twin lamellae of plagioclase (oligoclase) by carbonate. Note the presence of interstitial muscovite.

PLATE 27.
RB162.91 **C-lode**

Scale: width of photo equals 0.5 mm.

Extensive replacement by both carbonate and quartz occurred. Note how the quartz grains are pseudomorph after the tourmaline needles it replaced. Note the remnants of K-feldspar and its typical altered surface.

PLATE 28.
RB131.91 Union lode

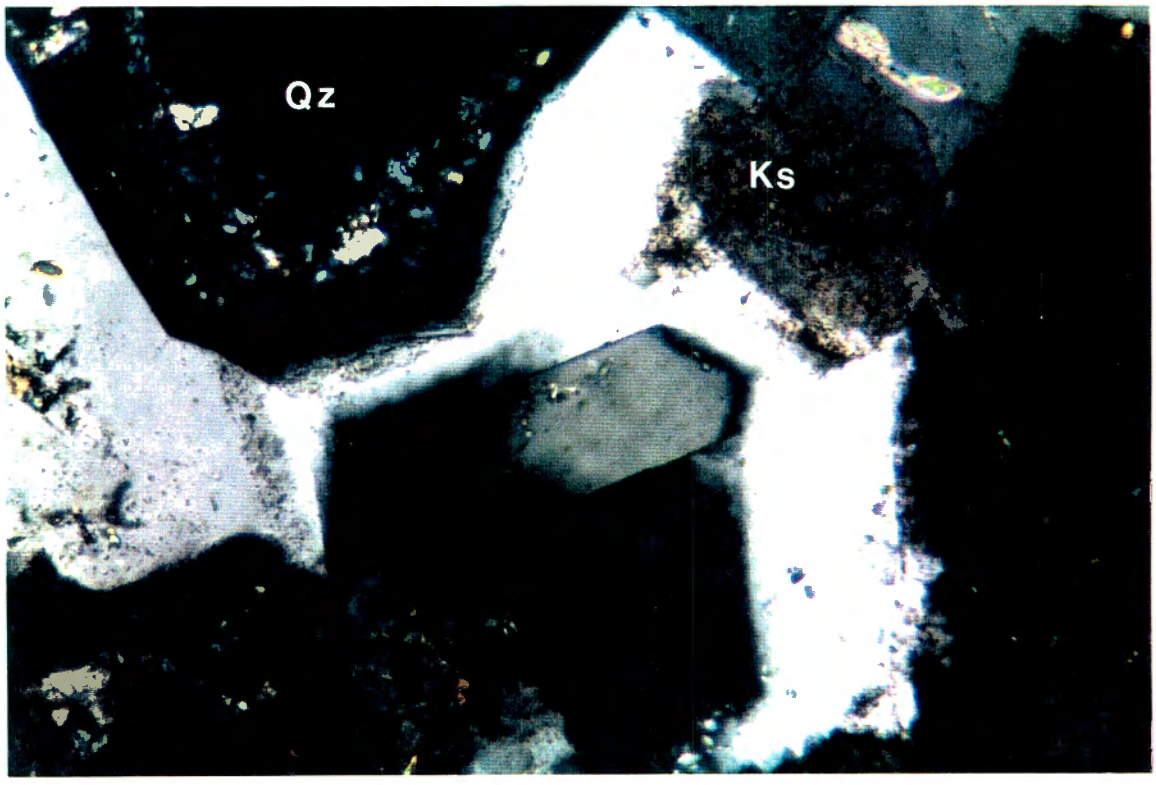

PLATE 29.
RB131.91 Union lode

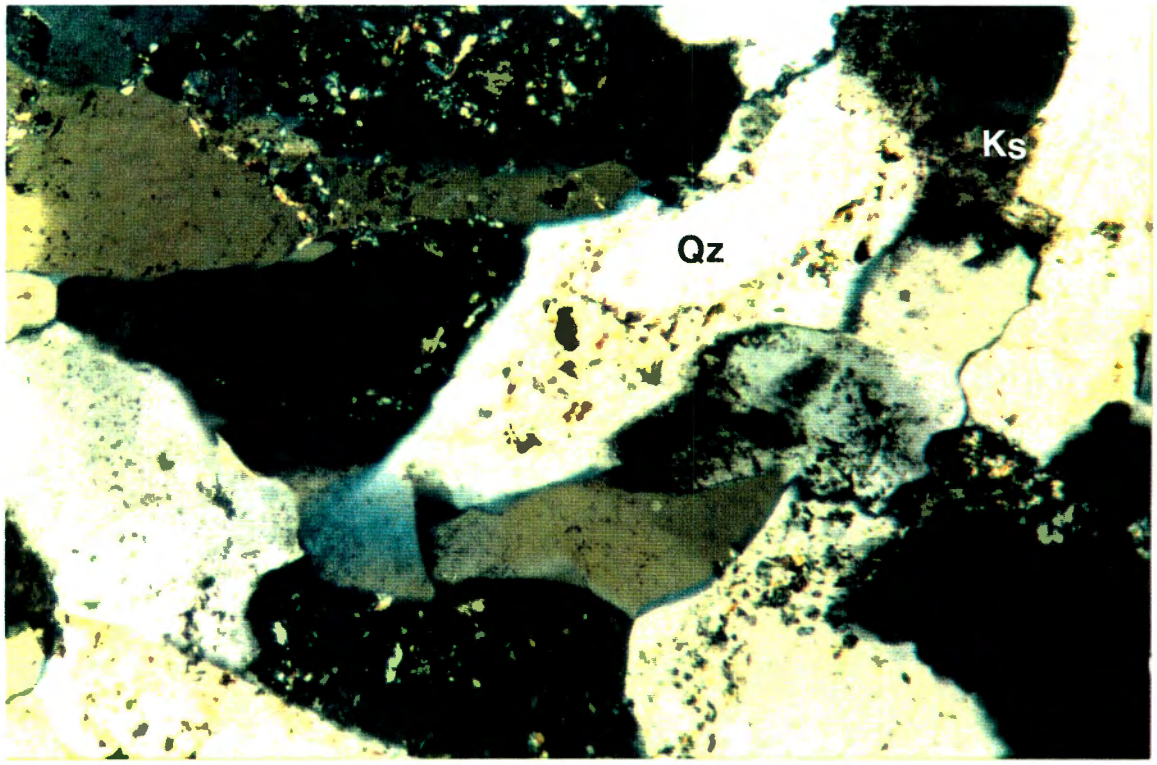

PLATE 28.
RB131.91 **Union lode**

Scale: width of photo equals 0.5 mm.

Quartz replacement of extensively altered host rock. Note the euhedral crystal morphology and the remnants of K-feldspar within the newly crystallised quartz grains.

PLATE 29.
RB131.91 **Union lode**

Scale: width of photo equals 0.5 mm.

Quartz replacement of extensively altered host rock. Note the inclusion of alteration products and remnants of K-feldspar within the newly crystallised quartz grains.

PLATE 30.
RB 147.91 U-lode

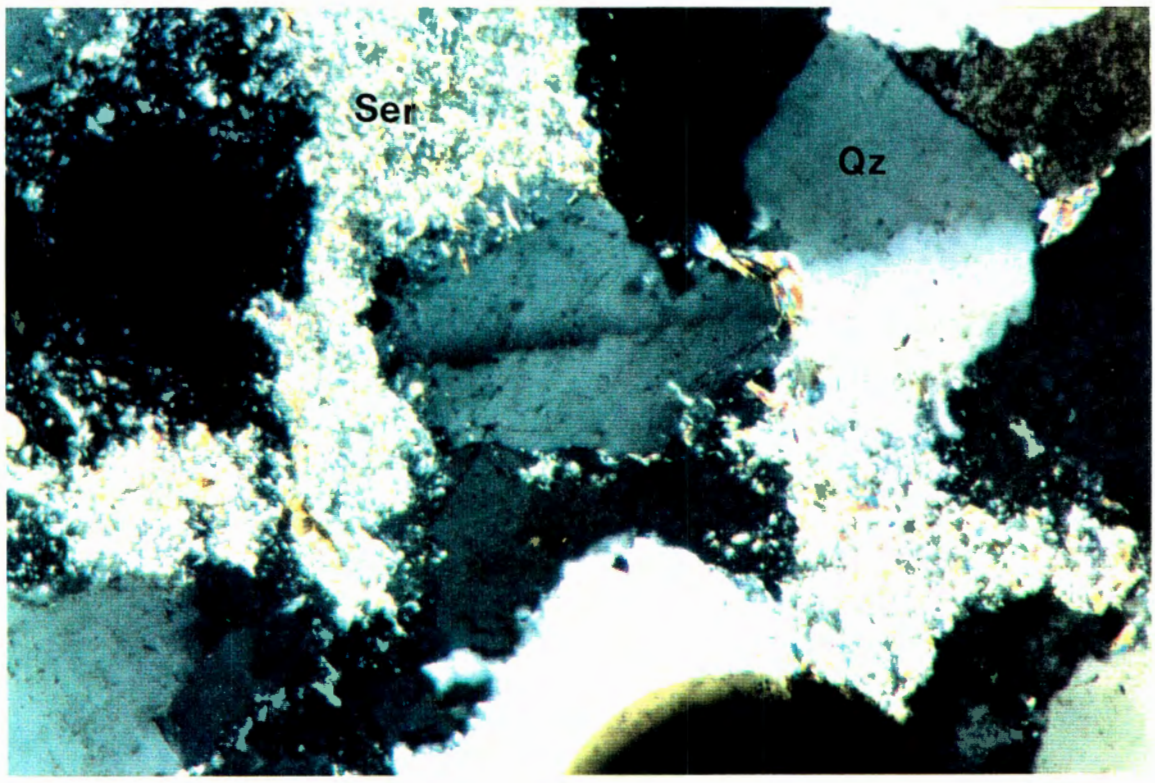

PLATE 31.
RB161.91 C-lode

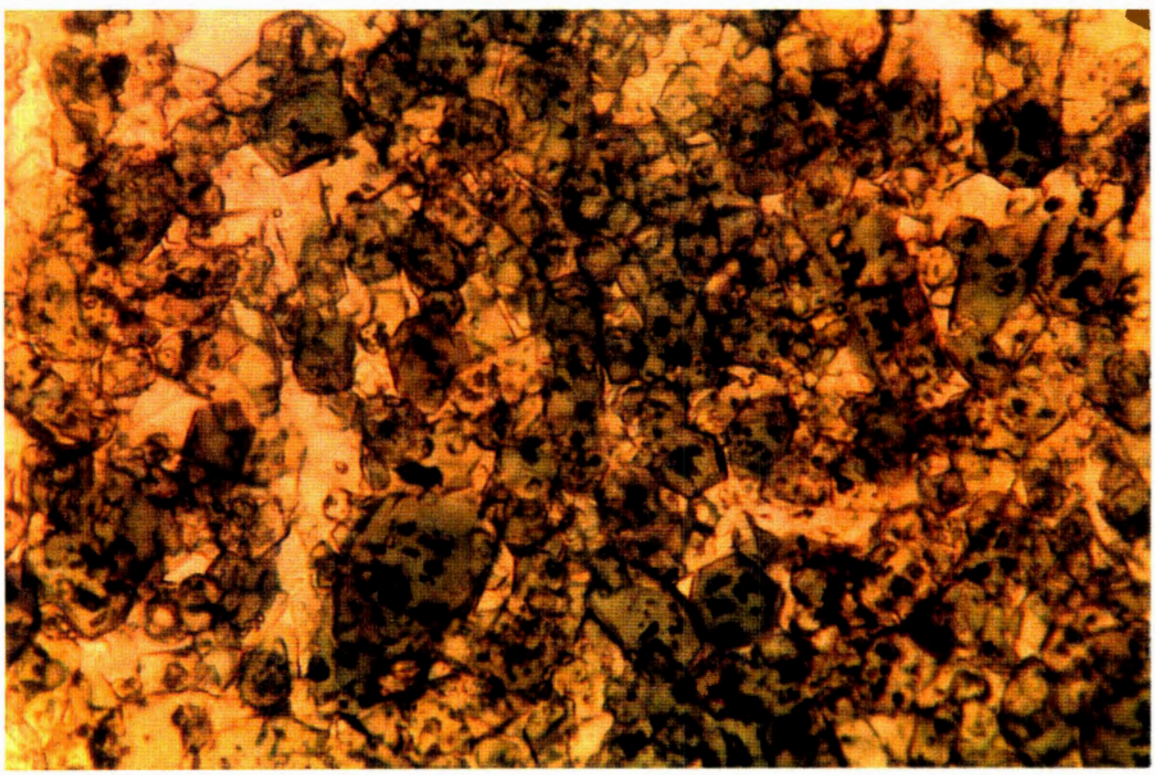

PLATE 30.
RB 147.91 **U-lode**

Scale: width of photo equals 0.5 mm.

Fine-grained, complete sericitic alteration of the feldspars combined with quartz replacing the K-feldspar and retaining the Karlsbad twins: thus, quartz pseudomorphous after K-feldspar

PLATE 31.
RB161.91 **C-lode**

Scale: width of photo equals 0.2 mm.

Secondary tourmaline-quartz association in the ore lodes. Note the fine-grained nature of the tourmaline.

PLATE 32.
RB099.91 AMS-lode

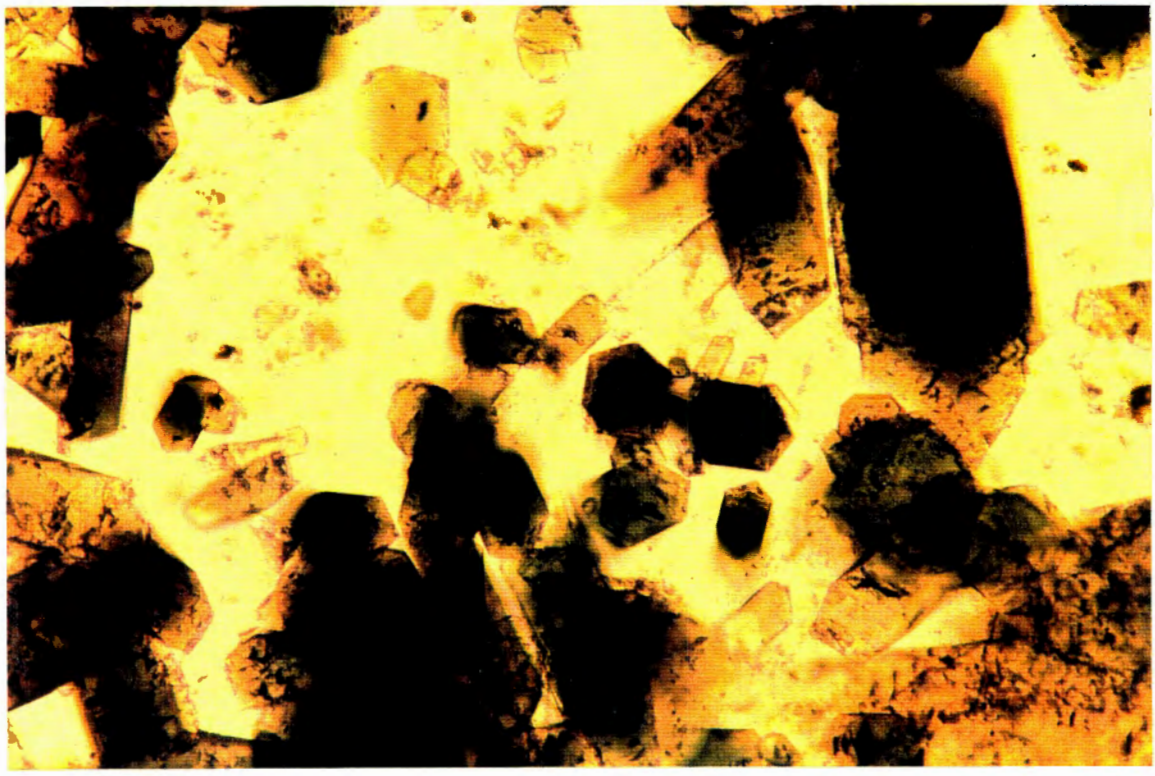

PLATE 33.
RB169.91 Disseminated Tin

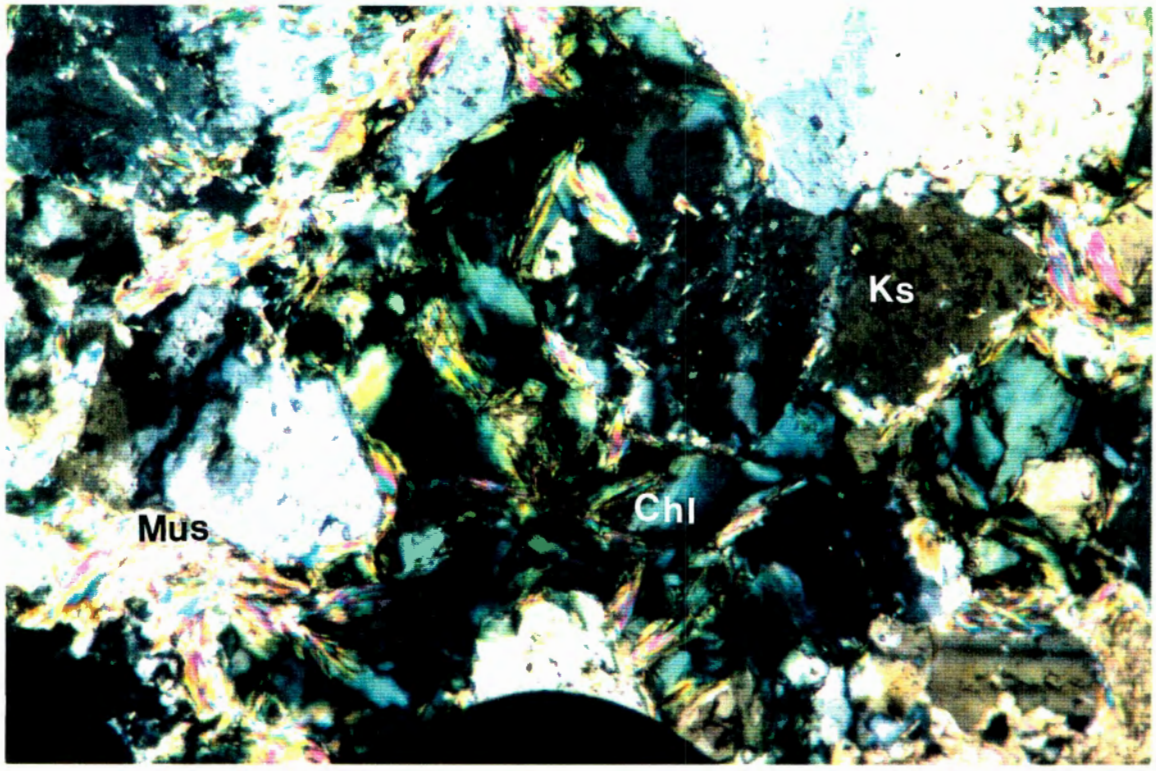

PLATE 32.
RB099.91 **AMS-lode**

Scale: width of photo equals 0.2 mm.

Secondary tourmaline-quartz association in the ore lodes. Note the fine-grained nature of the tourmaline and its euhedral morphology.

PLATE 33.
RB169.91 **Disseminated Tin**

Scale: width of photo equals 0.2 mm.

Chlorite is very rare in the NAD deposit, but occurs in the vicinity of green bands in association with muscovite-sericite.

PLATE 34.
RB169.91 Disseminated Tin

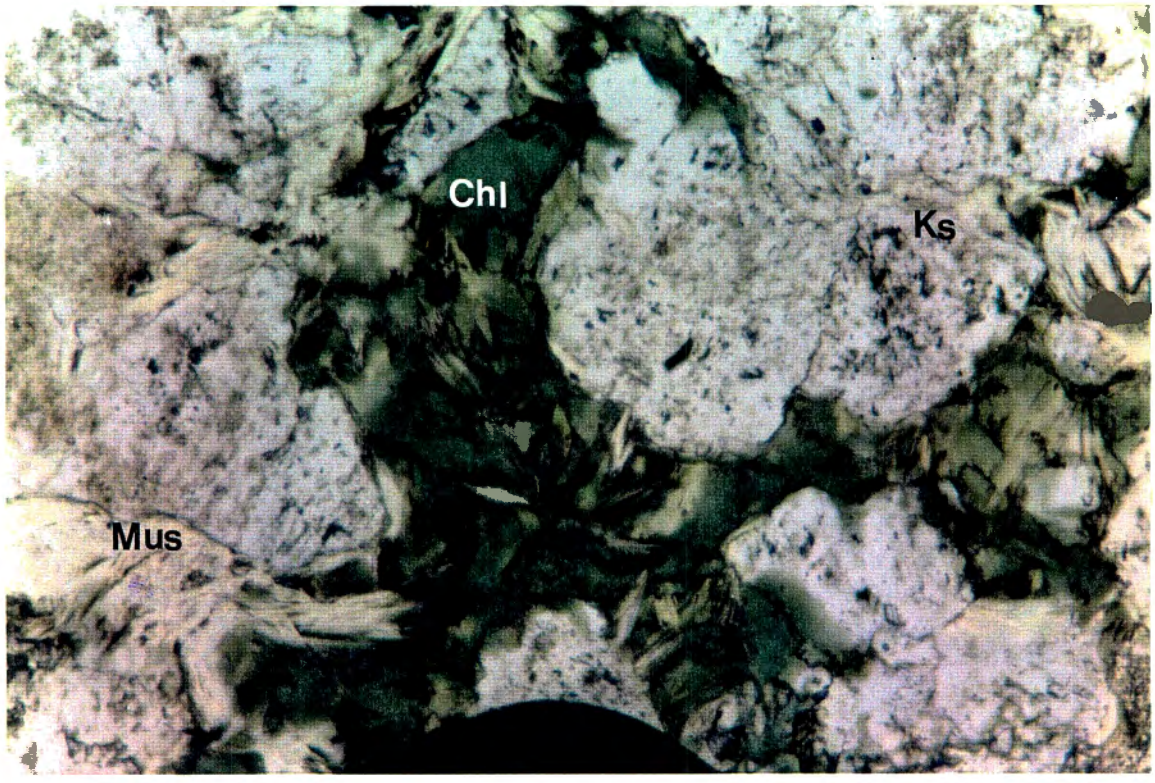

PLATE 35.
RB162.91 C-lode

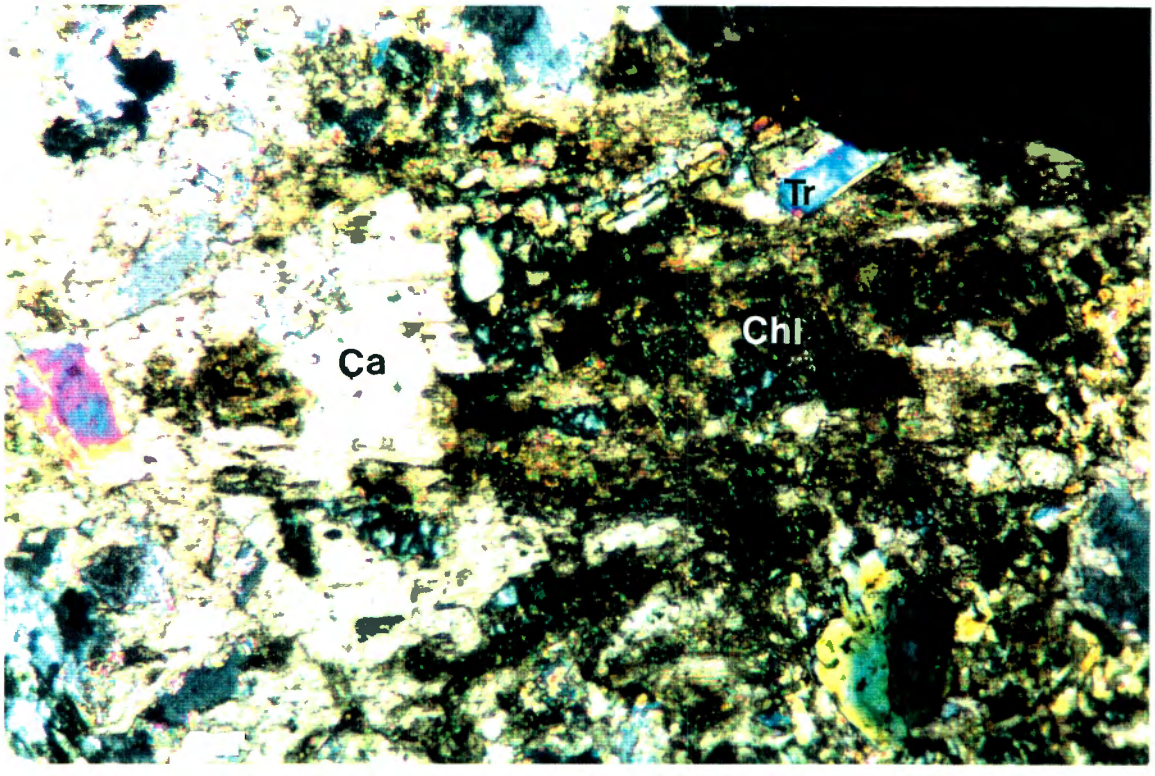

PLATE 34.
RB169.91 **Disseminated Tin**

Scale: width of photo equals 0.2 mm.

Note the interstitial nature of both muscovite-sericite and chlorite, replacing the host rock.

PLATE 35.
RB162.91 **C-lode**

Scale: width of photo equals 0.5 mm.

Chlorite (Chl) and carbonate (Ca) association replacing primary tourmaline (*Tr*).

PLATE 36.
RB147.91 U-lode

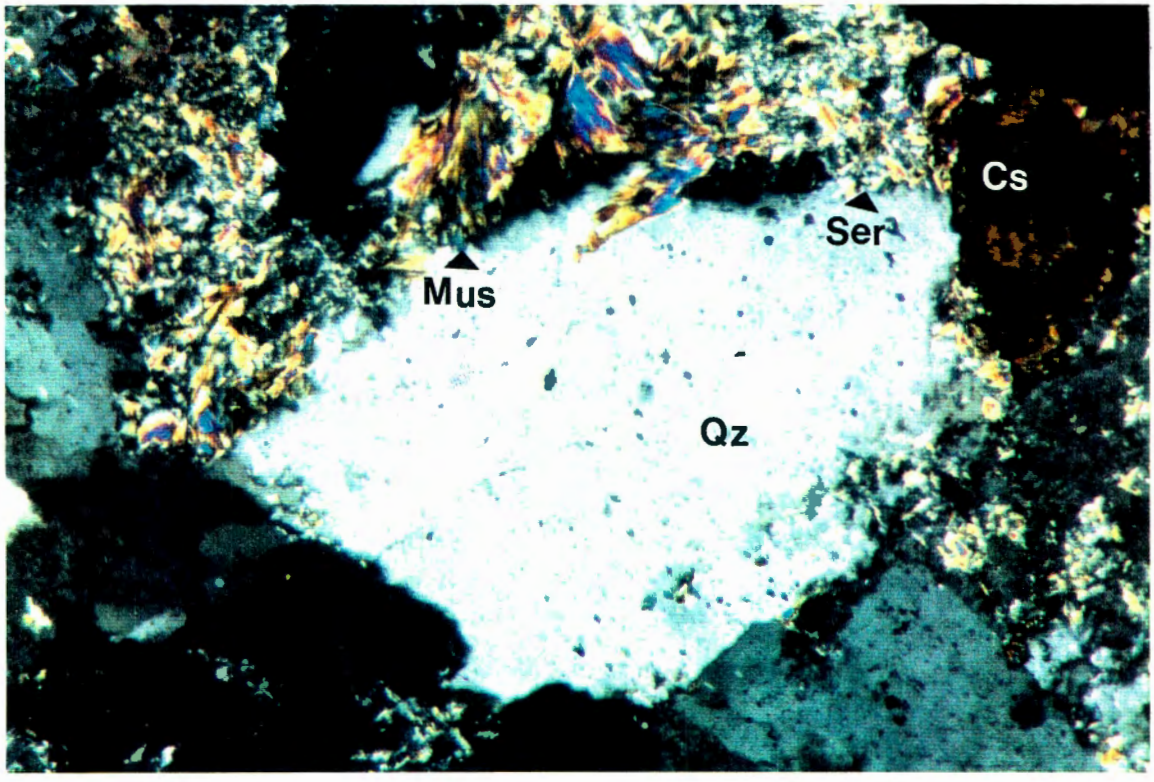

PLATE 37.
RB161.91 C-lode

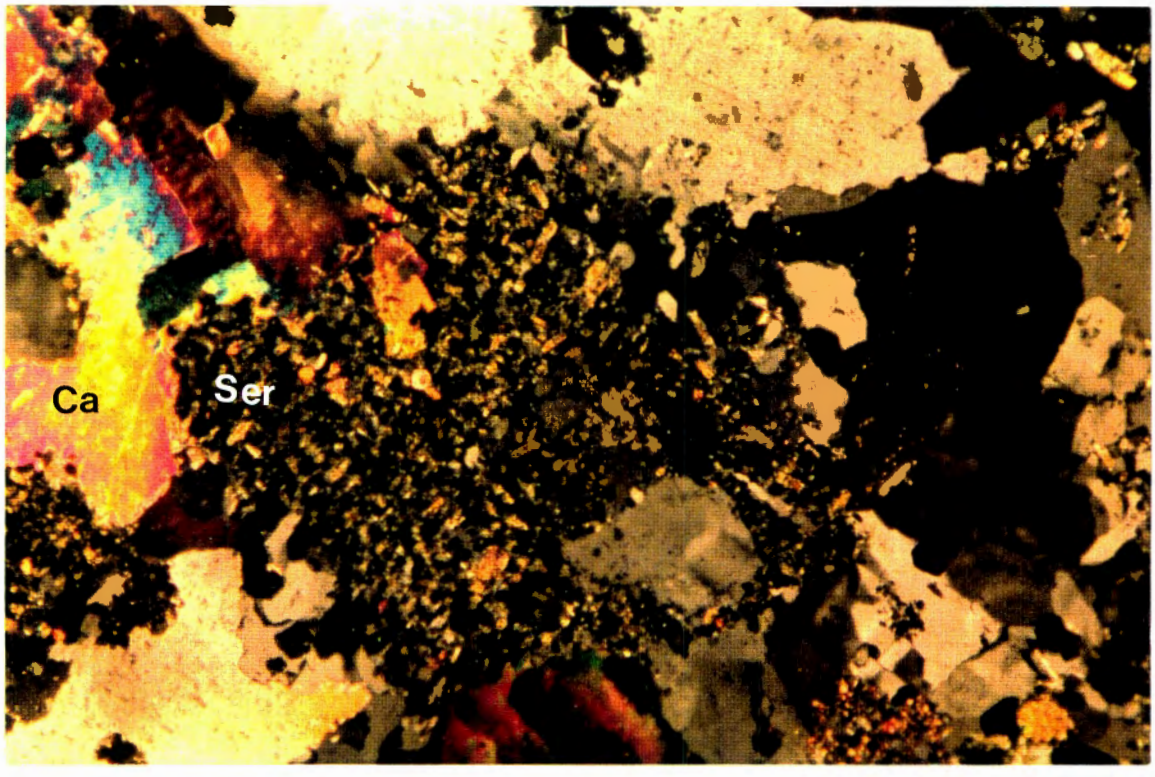

PLATE 36.
RB147.91 **U-lode**

Scale: width of photo equals 0.5 mm.

Note the fine- and coarser grained variety of muscovite-sericite, replacing feldspars. Cassiterite occurs interstitially in the host rock and associates with the matrix (muscovite-sericite-carbonate).

PLATE 37.
RB161.91 **C-lode**

Scale: width of photo equals 0.5 mm.

Association of fine-grained sericite (Ser) and carbonate (Ca) replacing the host rock.

PLATE38.
RB163.91

C-lode

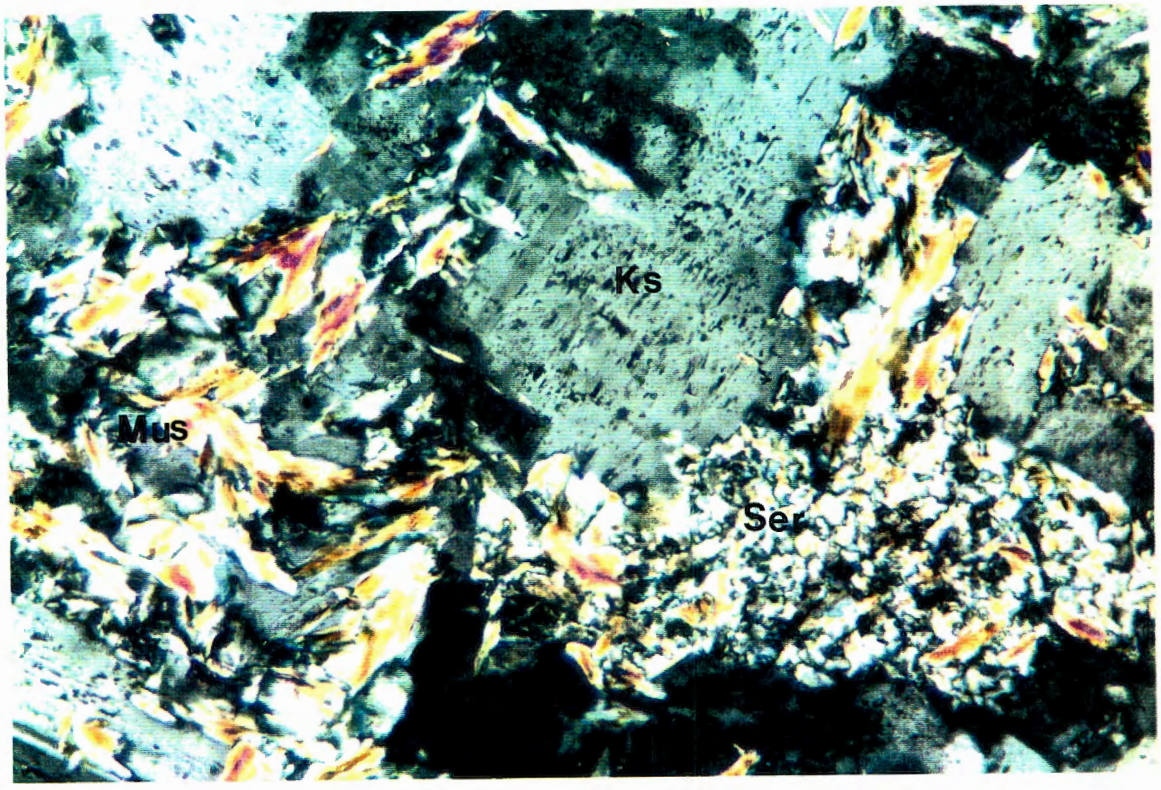

PLATE 39.
RB160.91

C-lode

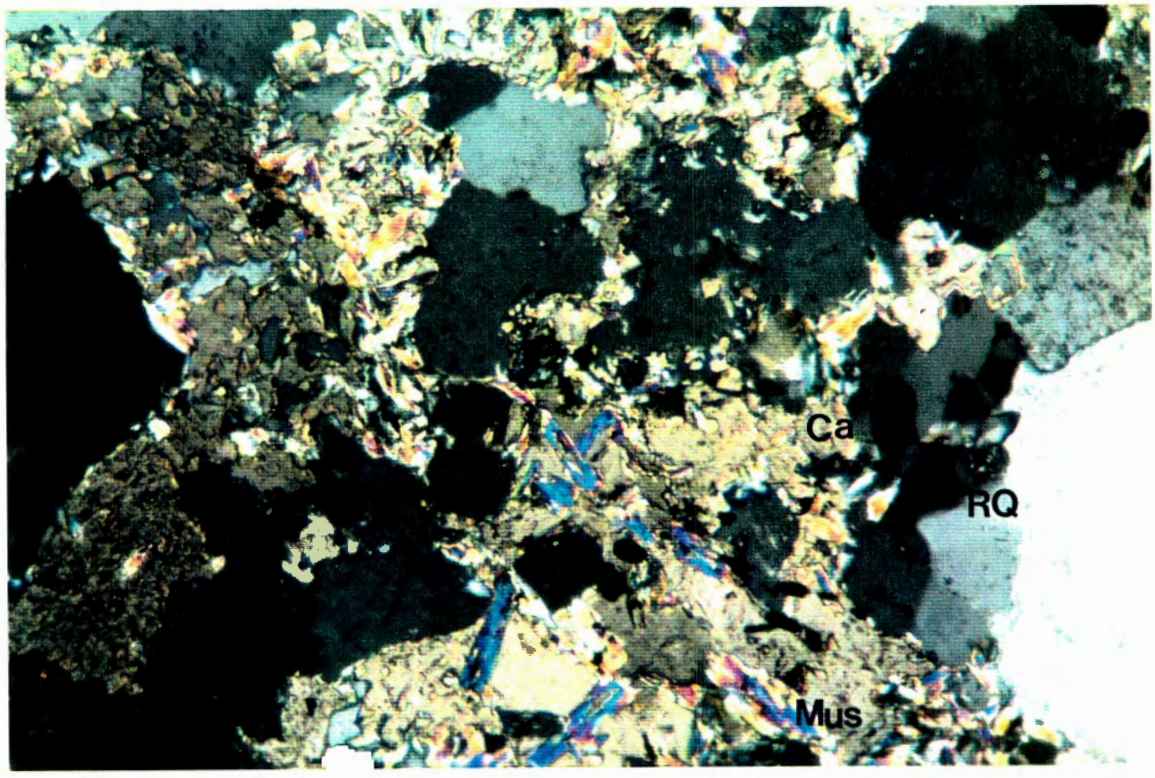

PLATE38.
RB163.91 **C-lode**

Scale: width of photo equals 0.5 mm.

K-feldspar replaced by both fine-grained and coarse-grained muscovite-sericite.

PLATE 39.
RB160.91 **C-lode**

Scale: width of photo equals 1 mm.

Almost complete replacement of the host rock by recrystallised quartz in association with carbonate and muscovite.

PLATE 40.
RB163.91 C-lode

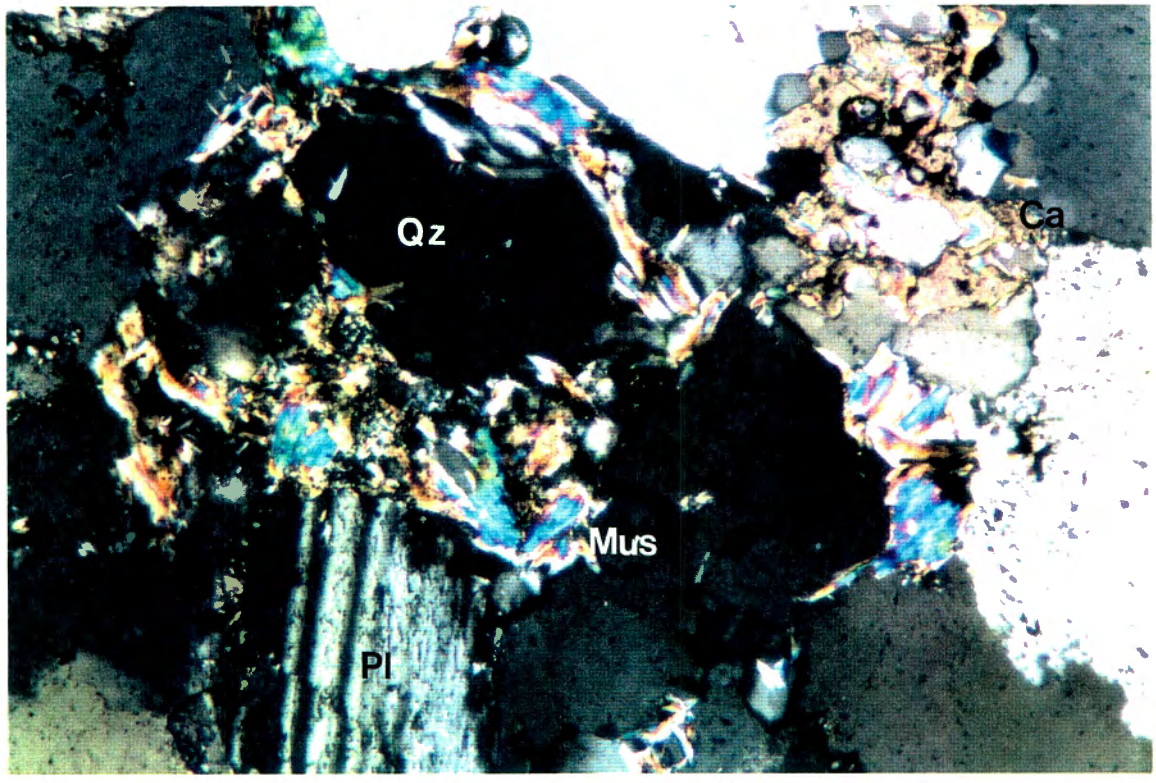

PLATE 41.
RB163.91 C-lode

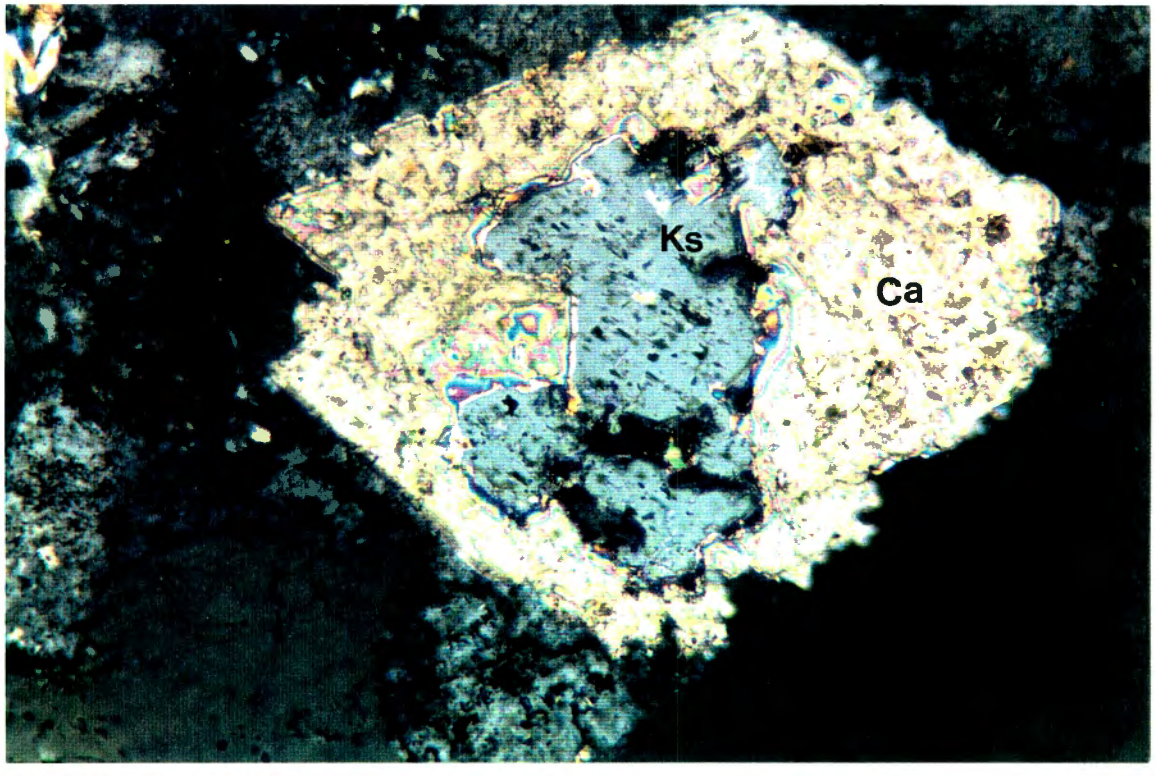

PLATE 40.
RB163.91 **C-lode**

Scale: width of photo equals 0.5 mm.

Replacement and alteration of the host rock. Note the large secondary quartz grains and the interstitial muscovite-sericite and carbonate.

PLATE 41.
RB163.91 **C-lode**

Scale: width of photo equals 0.2 mm.

Carbonate including K-feldspar by replacement.

PLATE 42.
RB122.91 Hanging Wall

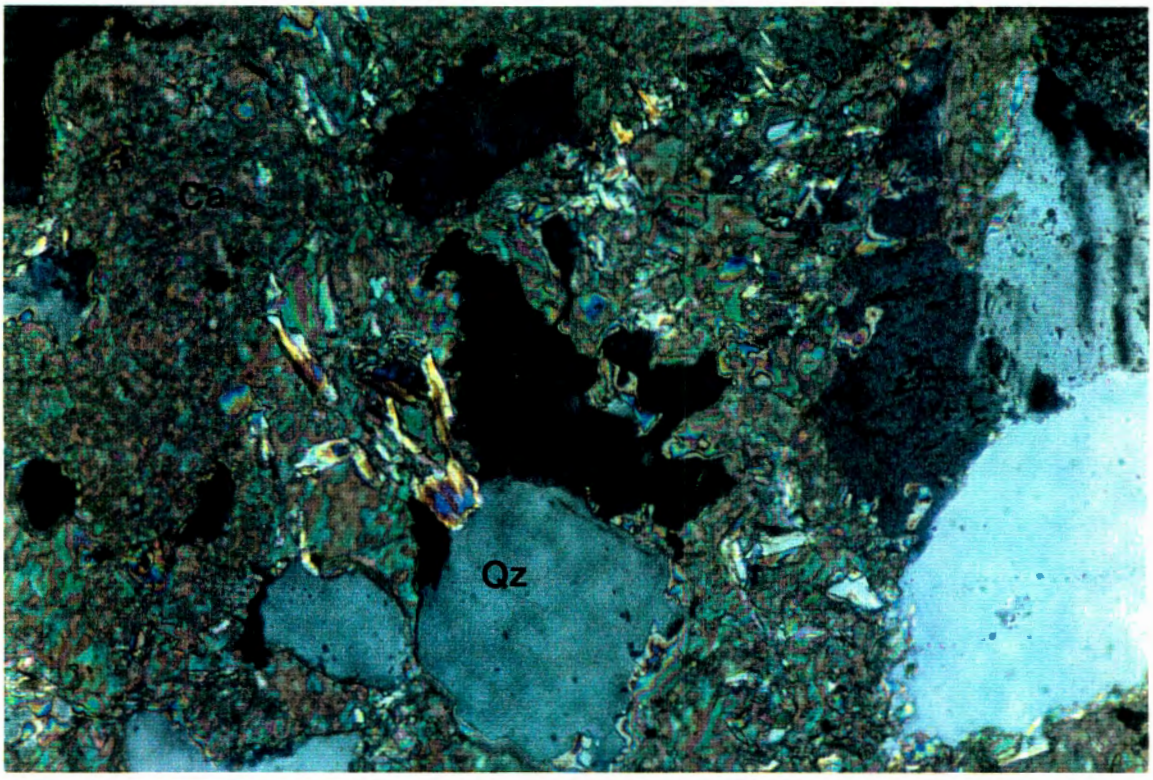

PLATE 43.
RB148.91 U-lode

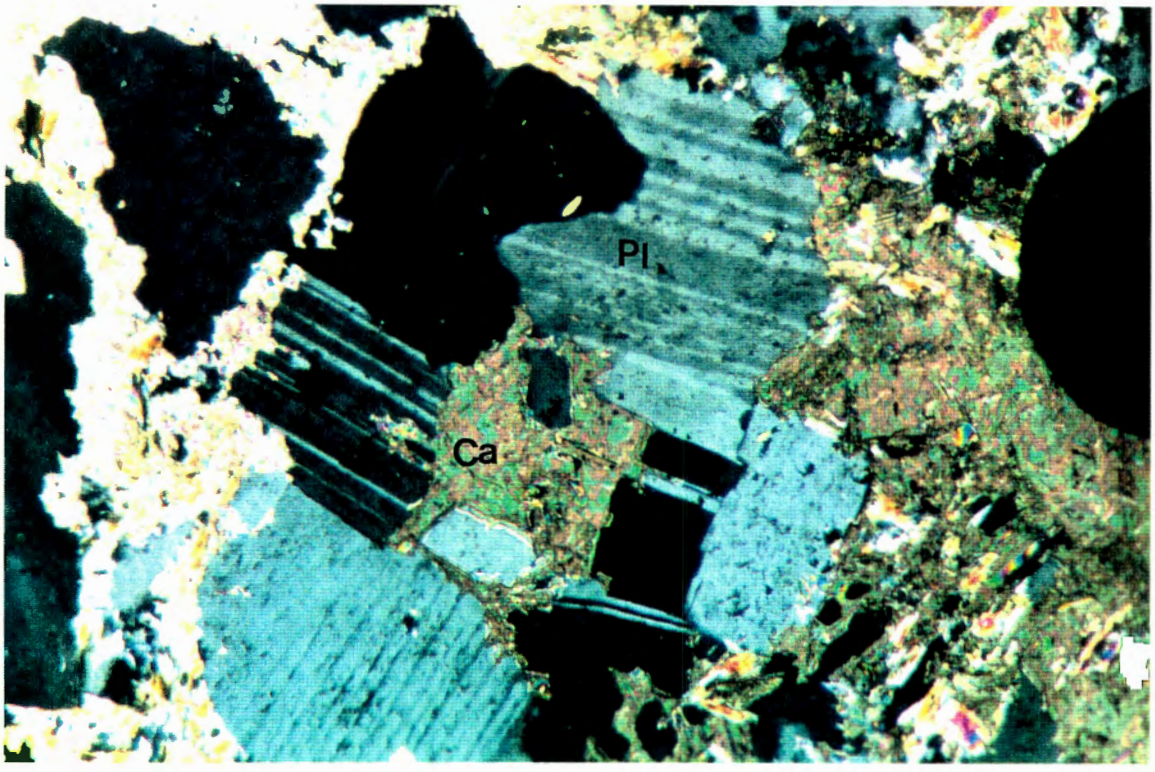

PLATE 42.
RB122.91 **Hanging Wall**

Scale: width of photo equals 1 mm.

Association of replacement (Qz) and alteration (Ca & Ser) products in the host rock. There is also some muscovite associated with the carbonate.

PLATE 43.
RB148.91 **U-lode**

Scale: width of photo equals 1 mm.

Association of plagioclase (Pl) and carbonate (Ca). The plagioclase appears to be more resistant towards replacement and alteration than K-feldspar.

PLATE 44.
RB169.91

Disseminated Tin

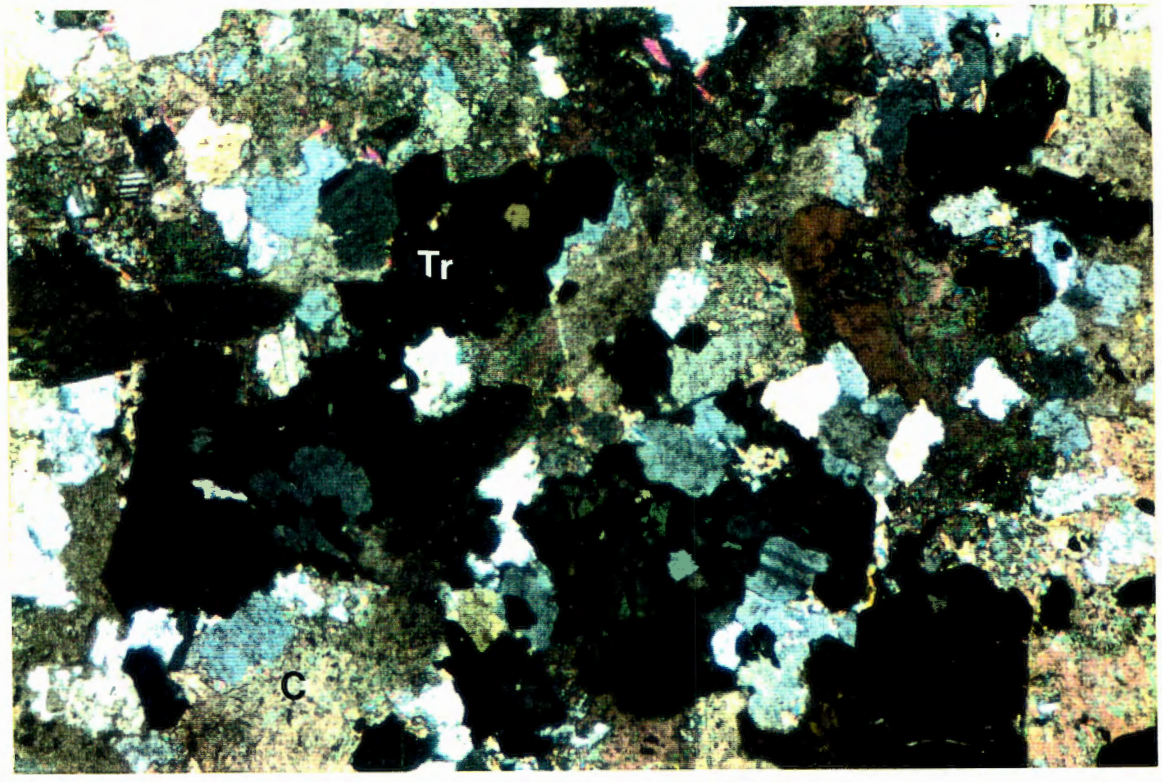

PLATE 45.
RB169.91

Disseminated Tin

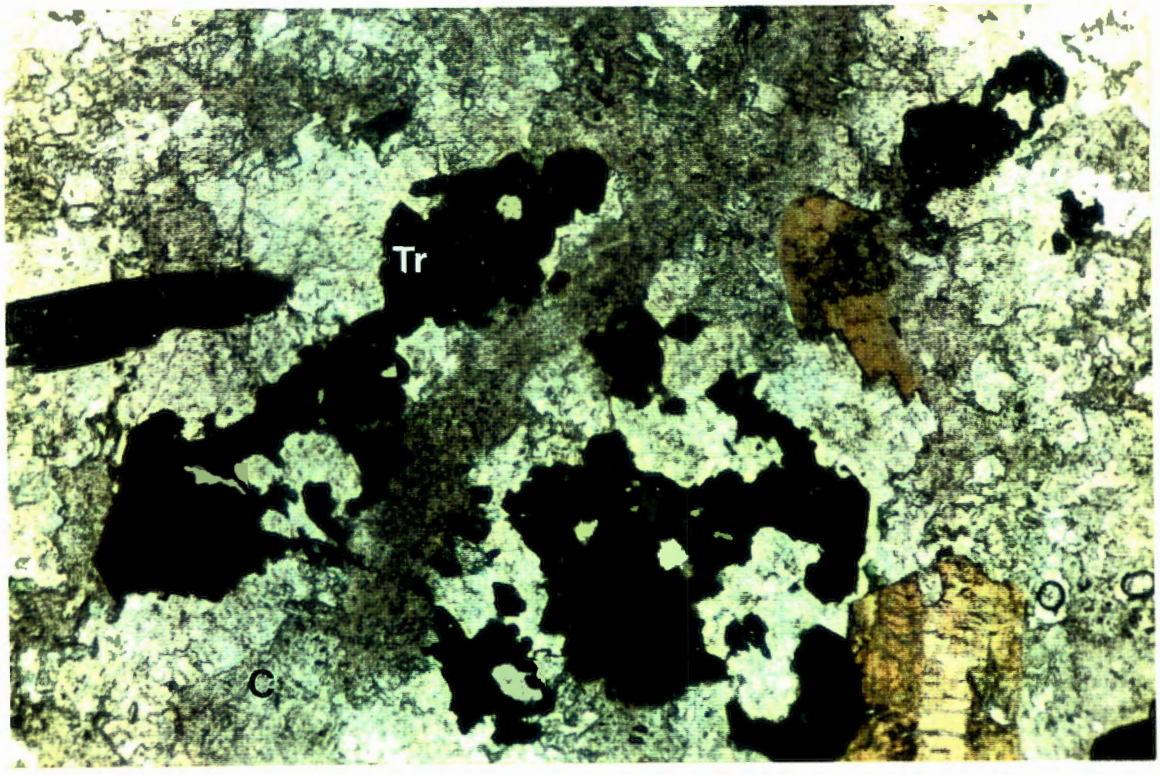

PLATE 44.
RB169.91 **Disseminated Tin**

Scale: width of photo equals 2 mm.

Primary tourmaline (Tr) partly replaced by interstitial carbonate (C) (crossed nichols).

PLATE 45.
RB169.91 **Disseminated Tin**

Scale: width of photo equals 2 mm.

Primary tourmaline (Tr) partly replaced by interstitial carbonate (C) (under polarised light).

PLATE 46.
RB146,91 U-lode

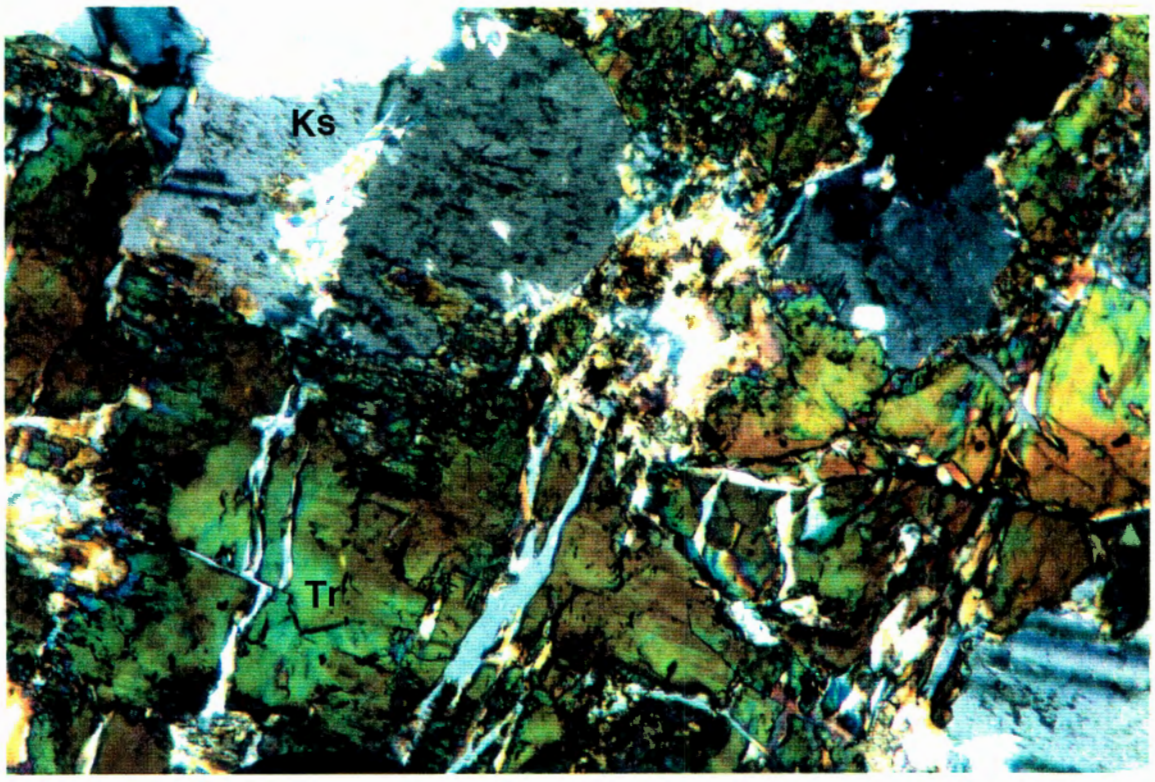

PLATE 47.
RB096.91 AMS-lode

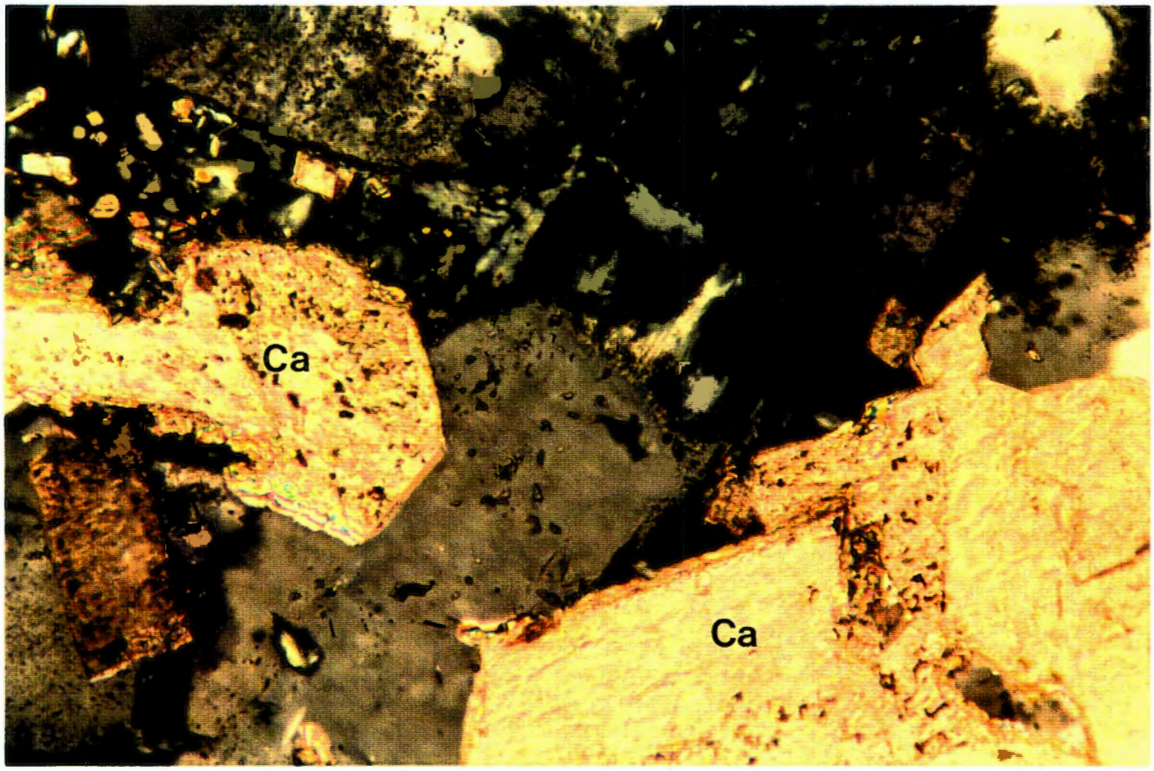

PLATE 46.
RB146,91 **U-lode**

Scale: width of photo equals 0.5 mm.

Sericitisation of K-feldspar. Note how the primary tourmaline is being replaced by secondary quartz along cracks.

PLATE 47.
RB096.91 **AMS-lode**

Scale: width of photo equals 0.5 mm.

Carbonate replaced primary euhedral tourmaline grains. Note the close association with secondary quartz.

PLATE 48.
RB161.91 C-lode

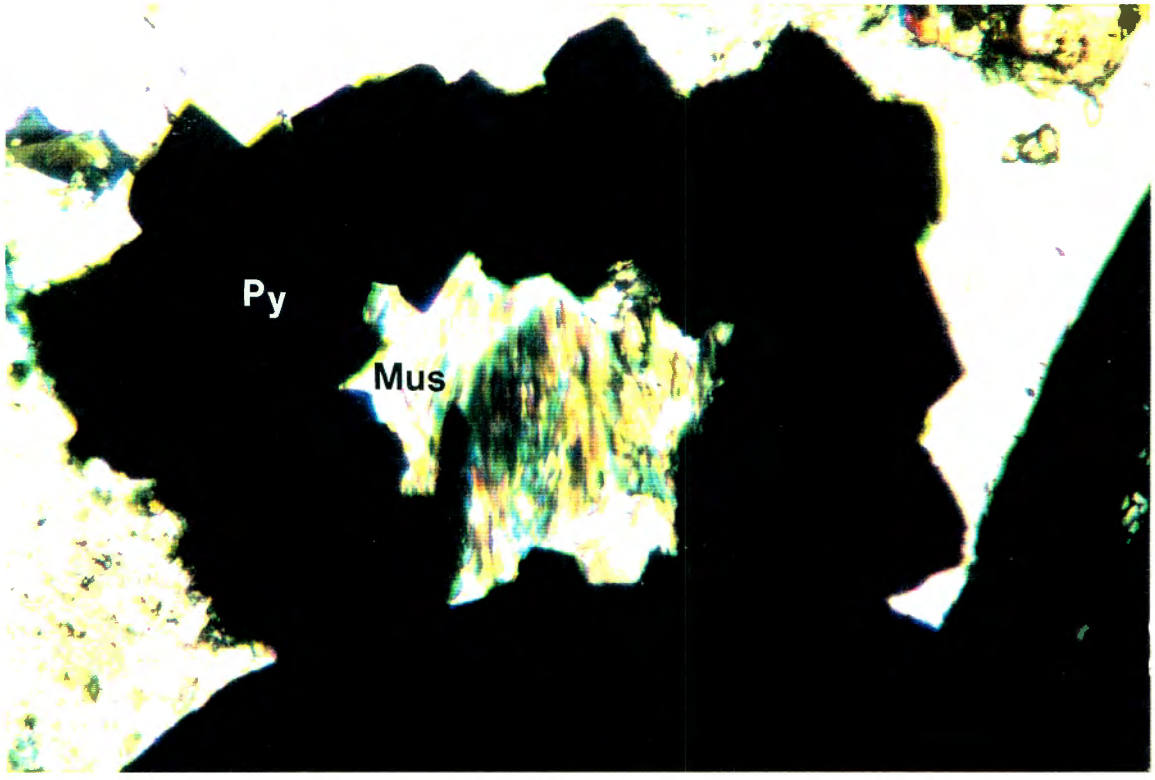

PLATE 49.
RB161.91 C-lode

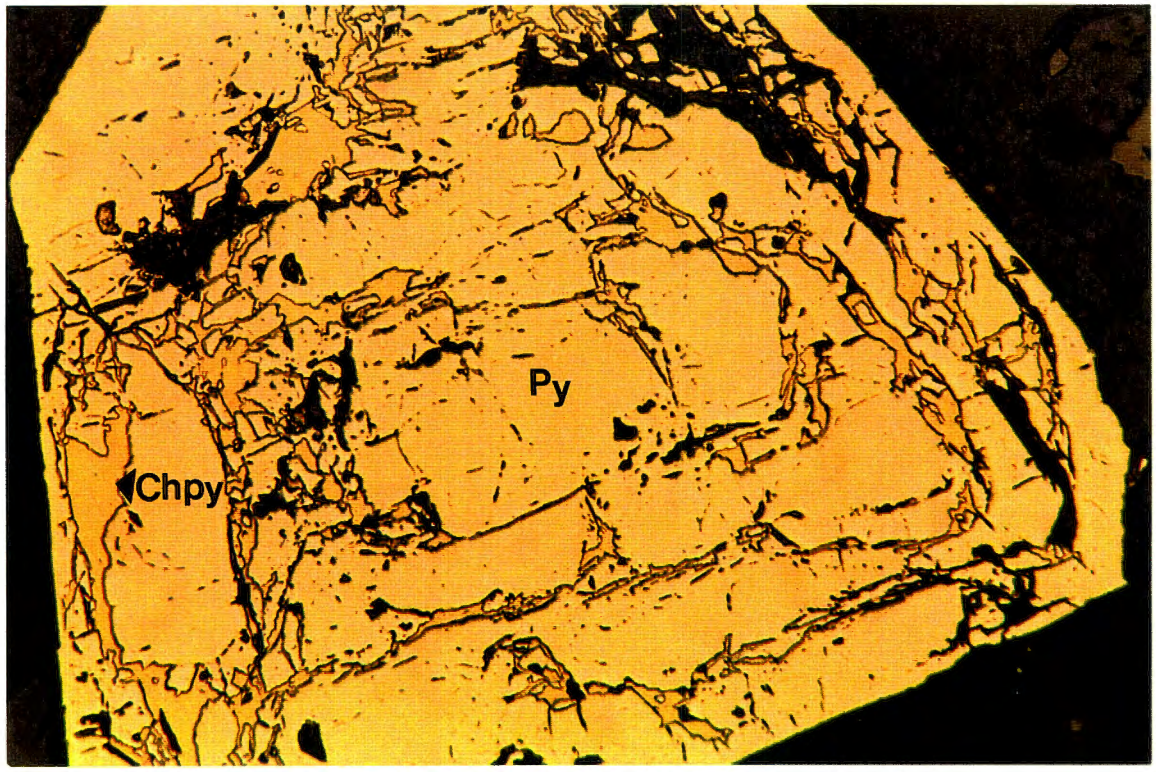

PLATE 48.
RB161.91 **C-lode**

Scale: width of photo equals 0.5 mm.

Later phase subhedral pyrite (Py) crystallised in circular formation and included muscovite (Mus).

PLATE 49.
RB161.91 **C-lode**

Scale: width of photo equals 0.5 mm.

An euheral pyrite grain displaying exsolution lamellae of chalcopyrite. The exsolution lamellae appear to be part of concentric growth zones within the pyrite crystal. There is also evidence for some muscovite in the pyrite grain.

PLATE 50.

RB170.91 Disseminated Tin

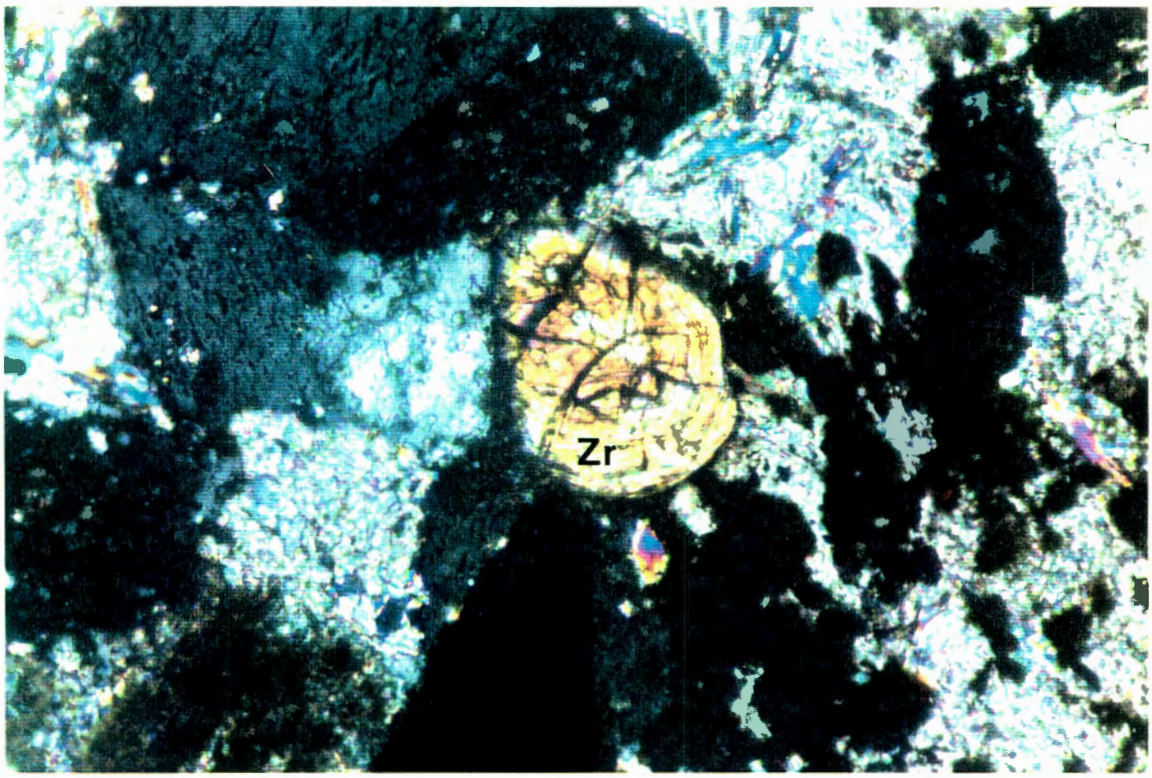

PLATE 51.

RB096.91 AMS-lode

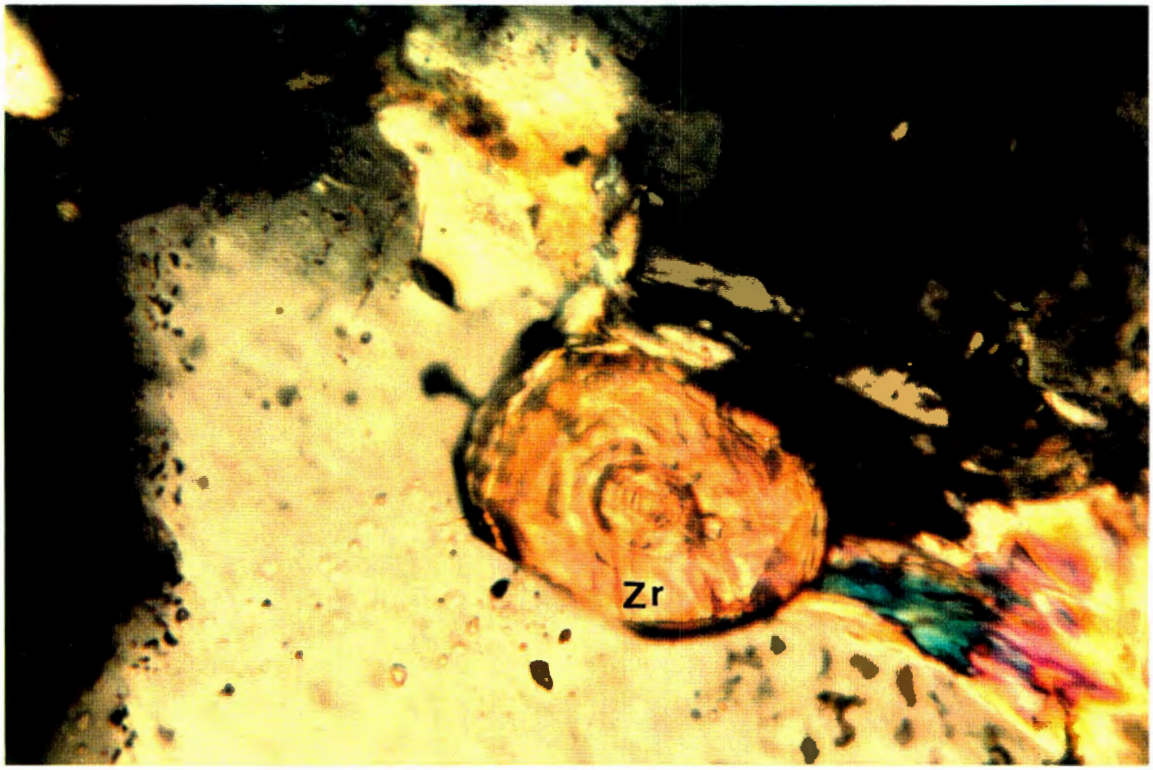

PLATE 50.
RB170.91 **Disseminated Tin**

Scale: width of photo equals 0.5 mm.

A cracked primary zircon (Zr) in the feldspathic host rock.

PLATE 51.
RB096.91 **AMS-lode**

Scale: width of photo equals 0.2 mm.

Subrounded primary zircon (Zr) partly included in secondary quartz within the host rock.

PLATE 52.
RB161.91 C-lode

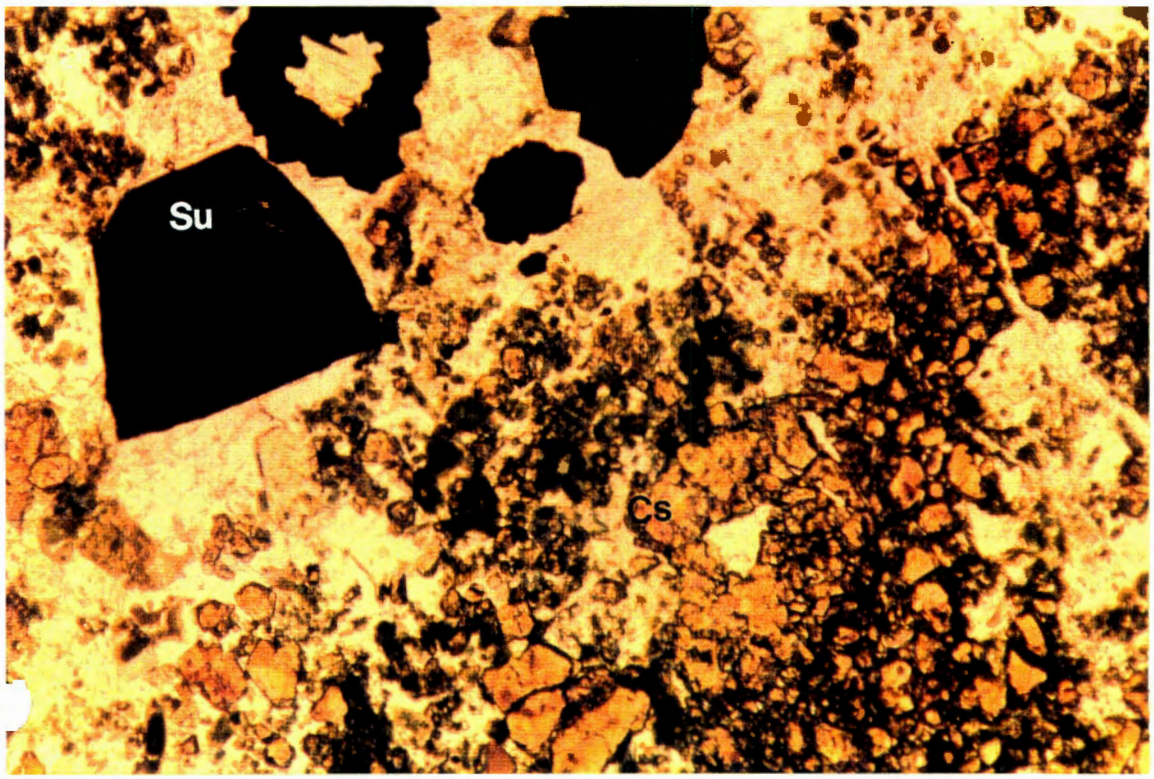

PLATE 53.
RB099.91 AMS-lode

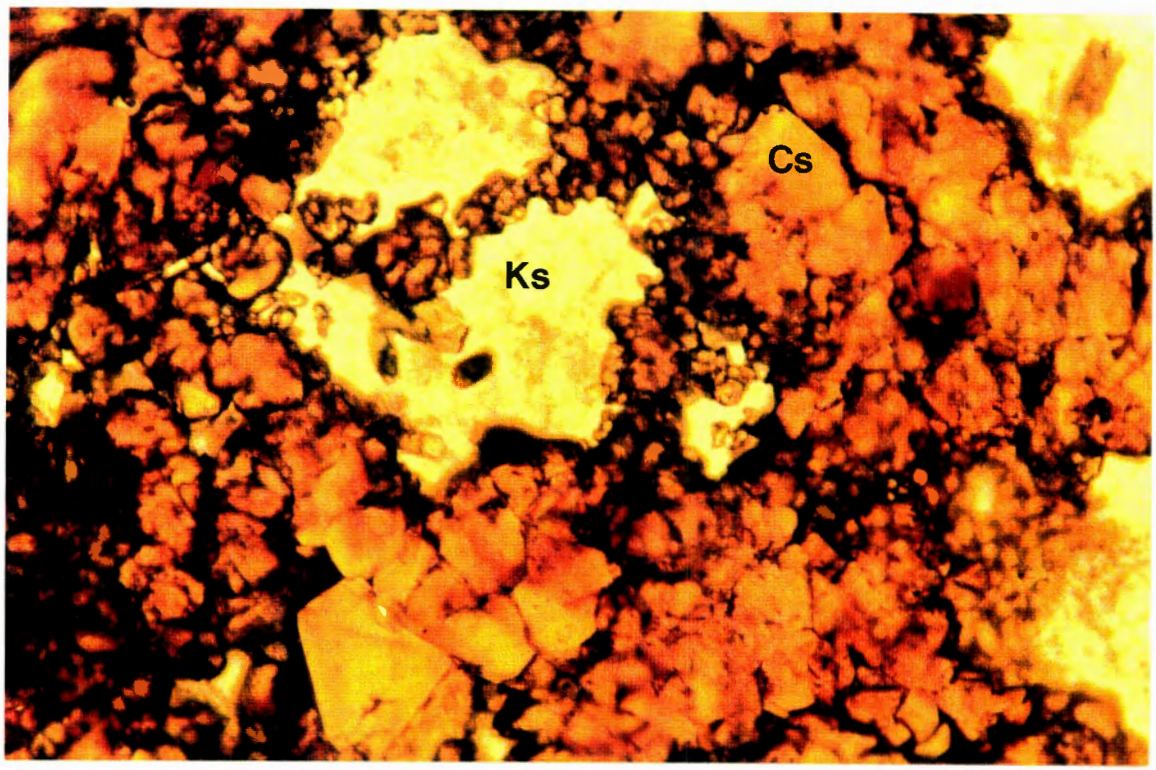

PLATE 52.
RB161.91 **C-lode**

Scale: width of photo equals 2 mm.

The sulphide grains are the same as in plates 48 and 49. Pyrite displaying Exsolution lamellae of chalcopyrite is associated with cassiterite. Note the irregular, fine-grained nature of the cassiterite.

PLATE 53.
RB099.91 **AMS-lode**

Scale: width of photo equals 0.5 mm.

Remnants of K-feldspar are included within the cassiterite mass. Note the irregular fine-grained morphology of the cassiterite. Also note the almost complete absence of the typical cassiterite colour zoning.

PLATE 54.
RB163.91 C-lode

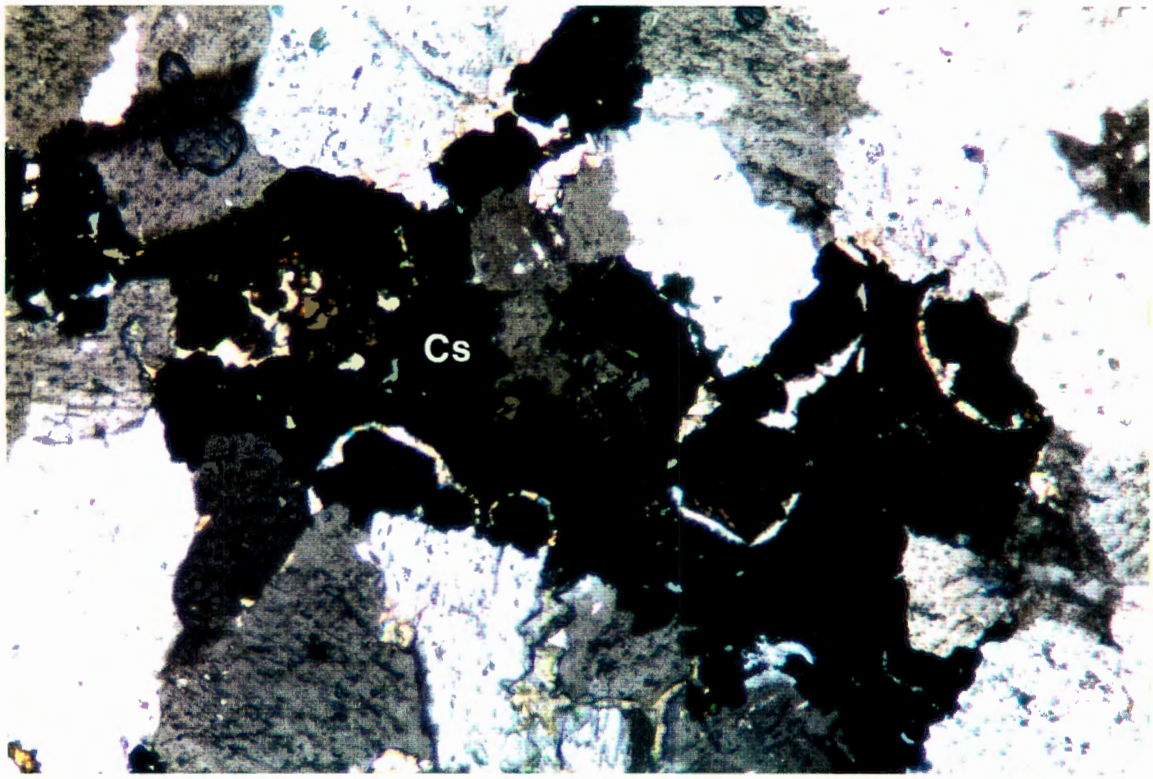

PLATE 55.
RB131.91 Union lode

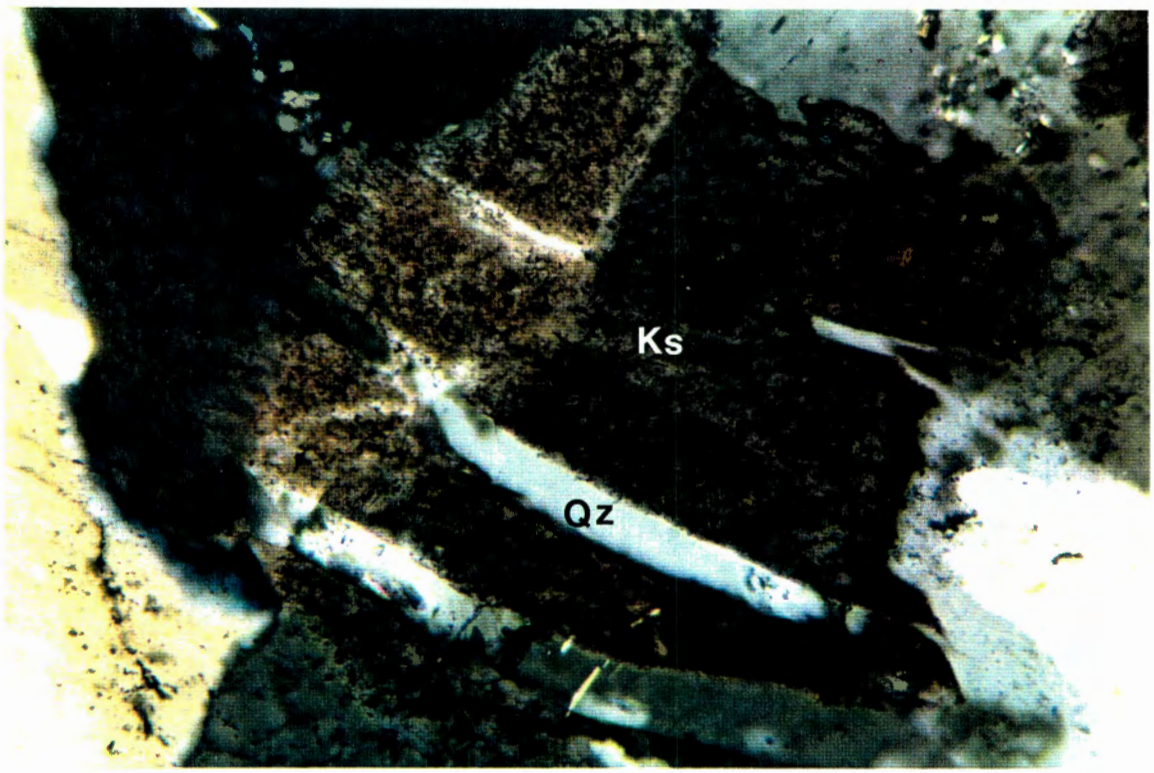

PLATE 54.
RB163.91 **C-lode**

Scale: width of photo equals 0.5 mm.

Occurrence of interstitial cassiterite in the feldspathic host rock.

PLATE 55.
RB131.91 **Union lode**

Scale: width of photo equals 0.2 mm.

Reddish-brown K-feldspar grain displaying cracks filled with secondary quartz.

PLATE 56.
RB149.91 U-lode

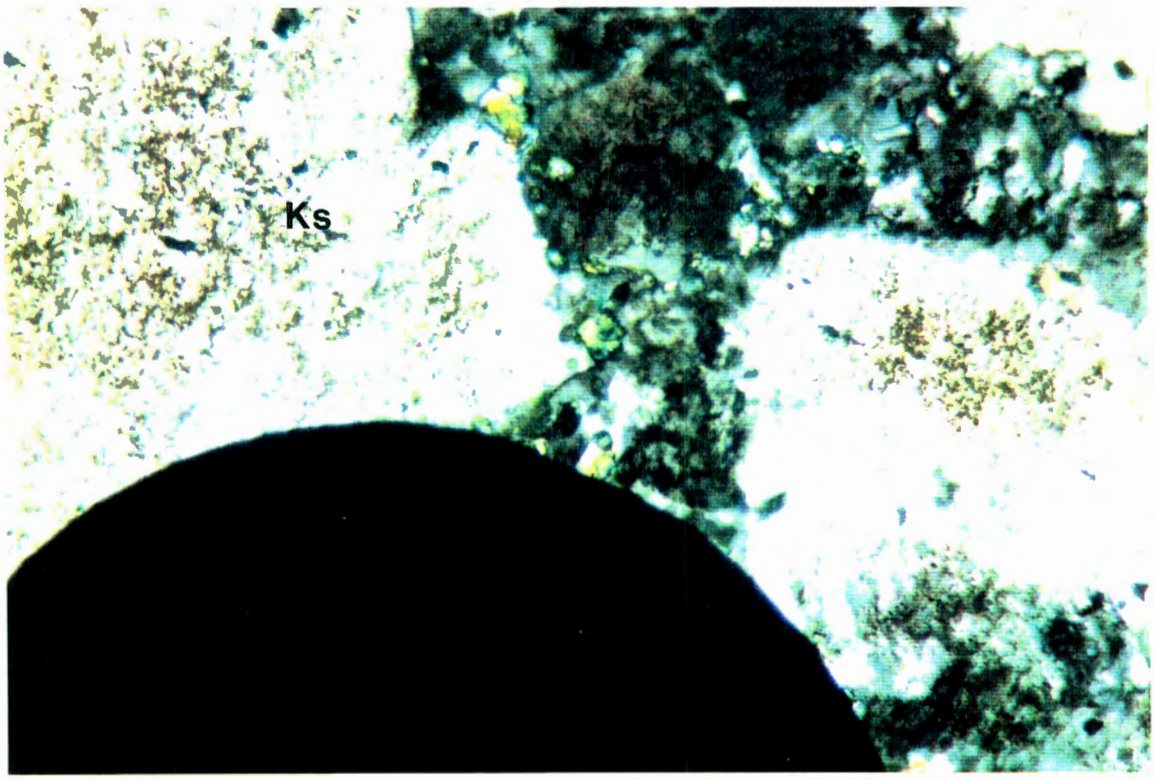

PLATE 57.
RB146.91 U-lode

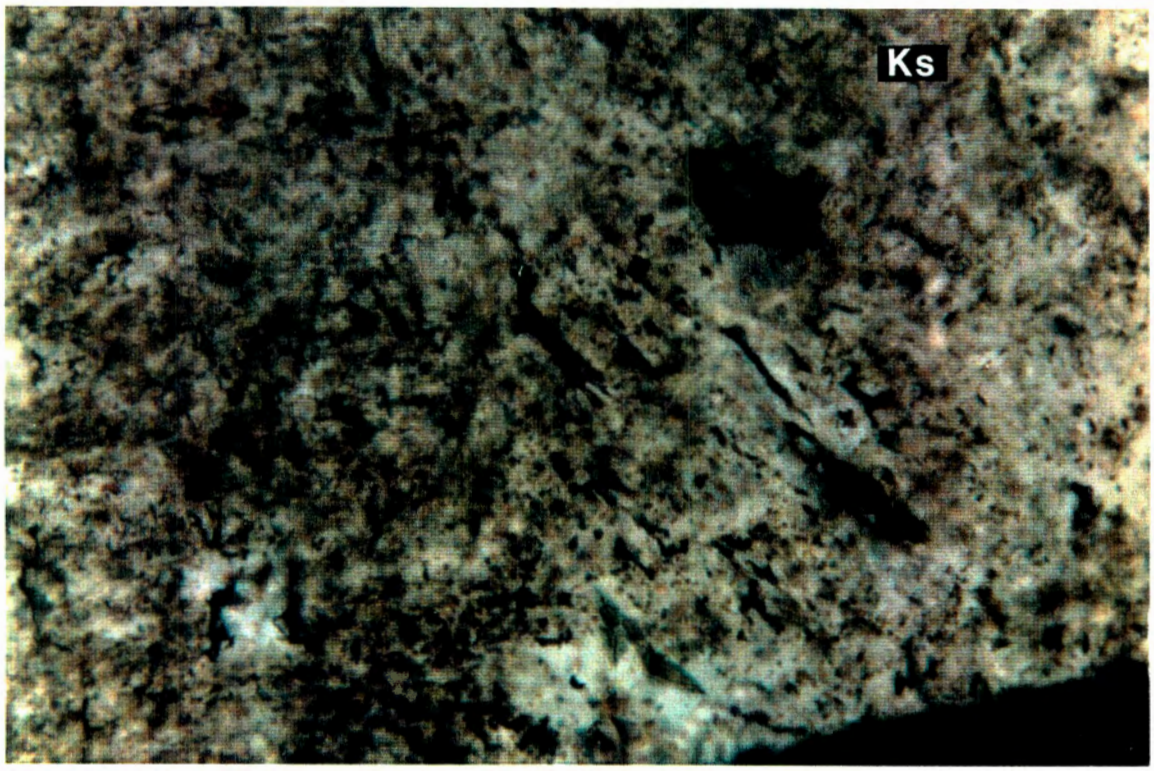

PLATE 56.
RB149,91 **U-lode**

Scale: width of photo equals 0.2 mm.

Typical K-feldspar morphology of the NAD deposit. Note the "rough" centre part of the grains and the smooth edges. The edges are often albite, though not always.

PLATE 57.
RB146.91 **U-lode**

Scale: width of photo equals 0.2 mm.

Typical K-feldspar surface morphology. Note the haematite dust (brown colouring) and small rutile inclusions (reddish inclusions).

PLATE 58.

RB160.91 C-lode

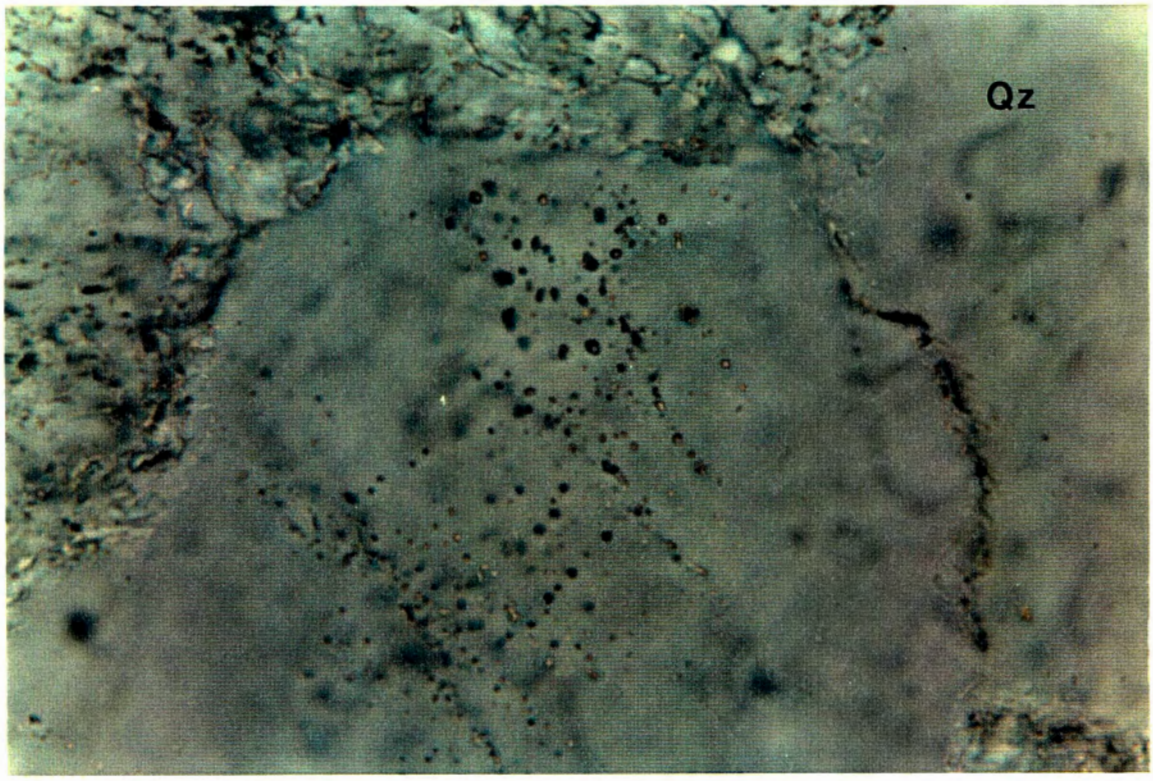

PLATE 58.

RB160.91 **C-lode**

Scale: width of photo equals 0.2 mm.

Fluid inclusions in quartz. Note the orange colour of the inclusions. The inclusions are, however, too small for fluid inclusion studies (50x enlargement on the microscope).

APPENDIX D.

D.1. Major Element Whole Rock Chemistry.

D.2. Trace Element Whole Rock Chemistry.

D.3. Single Grain Mineral Chemistry.
- D.3.1. Cassiterite Chemistry (SX50 and Camebax Data).
- D.3.2. Tourmaline Chemistry.
- D.3.3. Carbonate Chemistry.
- D.3.4. Sulphide Chemistry.

APPENDIX D.1.
MAJOR ELEMENT WHOLE ROCK CHEMISTRY (wt %).

Sample	LODE	Si02	TiO2	Al2O3	FeO	Fe2O3	Fe2O3 T	MnO	MGO	CAO	K2O	Na2O	P205	H2O-	LOI	TOTAL
RB095-91	ams	71.93	0.14	12.25	0.99	0.18	1.28	0.05	0.96	1.96	2.59	4.83	0.03	0.20	3.47	99.56
RB096-91	ams	71.30	0.15	11.97	1.22	0.20	1.55	0.06	1.06	2.21	2.17	5.34	0.04	0.18	3.87	99.77
RB098-91	ams	77.96	0.11	9.60	1.13	0.14	1.39	0.05	0.90	1.36	1.99	3.38	0.03	0.18	2.80	99.63
RB105-91	ams	69.35	0.61	13.81	1.35	0.38	1.88	0.07	0.88	1.19	3.64	6.15	0.06	0.26	2.90	100.65
RB108-91	ams	79.02	0.29	10.65	0.57	0.27	0.90	0.00	0.41	0.22	1.92	4.66	0.05	0.28	1.03	99.37
RB141-91	ams	79.29	0.18	9.05	1.35	0.26	1.76	0.05	0.79	1.23	1.90	3.60	0.04	0.25	2.42	100.41
RB142-91	ams	79.18	0.13	9.35	0.81	0.02	0.92	0.03	0.55	1.02	1.86	3.22	0.03	0.21	1.89	98.31
RB144-91	ams	78.37	0.11	9.21	0.90	0.09	1.09	0.04	0.77	1.44	2.20	3.06	0.01	0.14	2.59	98.94
RB110-91	b	74.44	0.13	12.00	1.71	0.32	2.22	0.06	0.73	0.88	3.26	4.42	0.04	0.17	2.73	100.91
RB112-91	b	72.73	0.84	10.69	3.65	0.67	4.72	0.04	1.02	0.41	2.33	3.84	0.07	0.25	2.92	99.47
RB113-91	b	82.30	0.12	8.47	1.31	0.00	1.43	0.04	0.45	0.32	0.49	4.57	0.03	0.38	1.60	100.08
RB114-91	b	52.78	1.47	20.85	2.79	1.07	4.17	0.10	1.95	1.47	5.04	4.99	0.24	0.34	5.46	98.53
RB115-91	b	79.58	0.12	10.95	0.54	0.06	0.66	0.01	0.25	0.08	1.56	4.70	0.01	0.17	0.82	98.85
RB118-91	b	71.97	0.31	10.18	2.12	0.26	2.61	0.10	1.02	1.69	2.44	3.74	0.04	0.18	3.96	98.01
RB119-91	b	74.99	0.72	11.05	0.81	0.28	1.18	0.04	0.75	1.22	3.44	2.71	0.08	0.21	2.46	98.76
RB037-91	bonus	68.87	0.39	14.35	1.89	0.46	2.56	0.07	0.77	0.31	6.11	3.15	0.05	0.29	2.40	99.11
RB155-91	c	79.84	0.09	10.30	0.72	0.08	0.88	0.02	0.23	0.12	2.26	4.18	0.02	0.14	0.95	98.94
RB157-91	c	75.11	0.76	12.31	0.54	0.26	0.86	0.02	0.54	0.53	2.66	4.00	0.08	0.22	1.32	98.35
RB158-91	c	78.71	0.10	11.34	0.32	0.00	0.31	0.00	0.18	0.11	3.33	3.81	0.02	0.17	0.59	98.69
RB159-91	c	69.01	0.26	13.66	1.22	0.29	1.64	0.06	1.04	1.82	3.54	4.77	0.06	0.20	3.43	99.37
RB160-91	c	66.63	0.80	10.23	5.40	0.66	6.66	0.22	1.68	0.89	3.35	2.57	0.11	0.19	6.03	98.76
RB163-91	c	71.06	0.25	13.34	0.81	0.17	1.07	0.04	0.79	1.53	1.92	5.81	0.05	0.18	2.74	98.69
RB164-91	c	76.92	0.19	8.74	1.08	0.13	1.33	0.06	1.03	2.06	1.81	3.29	0.03	0.15	3.46	98.95
RB081-91	cotton	74.51	0.18	13.77	0.27	0.34	0.64	0.00	0.20	0.12	4.30	4.38	0.06	0.28	0.75	99.17
RB084-91	cotton	71.90	0.50	12.85	0.81	0.26	1.16	0.03	0.73	1.40	3.19	5.04	0.07	0.24	2.58	99.61
RB086-91	cotton	75.96	0.32	10.40	0.90	0.30	1.30	0.04	0.74	1.57	2.20	4.29	0.03	0.20	2.74	99.70
RB165-91	diss	71.91	0.20	11.52	1.58	0.31	2.06	0.08	0.99	1.88	2.11	4.80	0.04	0.24	3.81	99.46
RB166-91	diss	70.56	0.33	11.20	3.69	0.92	5.02	0.12	0.88	0.15	2.23	3.99	0.03	0.16	3.87	98.17
RB167-91	diss	64.59	0.77	10.86	3.42	1.48	5.28	0.12	1.31	1.96	2.50	4.06	0.05	0.25	5.49	96.86
RB168-91	diss	81.38	0.12	9.52	0.36	0.07	0.46	0.01	0.24	0.40	2.03	3.24	0.03	0.22	0.95	98.57
RB169-91	diss	74.32	0.27	11.20	0.90	0.22	1.22	0.05	0.72	1.59	2.21	4.81	0.04	0.20	2.80	99.34
RB170-91	diss	73.99	0.40	10.17	3.15	0.68	4.18	0.07	0.68	0.23	2.38	4.06	0.07	0.20	3.11	99.20
RB049-91	fw	67.13	0.31	14.56	2.21	1.60	4.05	0.03	0.69	0.56	4.62	5.02	0.08	0.24	2.51	99.57
RB050-91	fw	67.97	0.55	15.22	0.68	3.35	4.10	0.00	0.35	0.55	3.12	6.35	0.12	0.21	1.15	99.62
RB048-91	hw	73.44	0.27	11.07	1.53	0.44	2.14	0.06	0.84	1.56	2.19	4.23	0.09	0.20	3.10	99.03
RB121-91	hw	71.02	0.35	13.40	0.50	2.65	3.20	0.03	0.39	0.10	4.12	3.89	0.05	0.58	2.23	99.31
RB122-91	hw	61.19	0.32	16.35	1.71	1.29	3.19	0.09	1.53	1.97	6.13	3.29	0.10	0.24	4.24	98.45

Sample	LODE	Si02	TiO2	Al2O3	FeO	Fe2O3	Fe2O3 T	MnO	MGO	CAO	K2O	Na2O	P205	H2O-	LOI	TOTAL
RB123-91	hw	71.84	0.12	11.64	1.08	0.33	1.53	0.05	1.00	1.89	4.59	3.06	0.05	0.17	3.37	99.20
RB124-91	hw	74.65	0.38	11.40	1.89	0.55	2.65	0.06	0.59	0.08	5.13	1.80	0.05	0.17	2.22	98.98
RB125-91	hw	72.54	0.30	11.50	1.62	0.66	2.46	0.06	0.63	0.75	4.62	3.33	0.06	0.18	2.65	98.89
RB126-91	hw	73.58	0.37	12.55	1.58	0.81	2.56	0.06	0.83	1.43	3.13	4.00	0.06	0.18	0.17	98.74
RB127-91	hw	74.60	0.26	8.95	1.98	0.40	2.60	0.07	0.87	1.44	3.11	5.62	0.06	0.14	3.47	100.97
RB129-91	t	72.43	0.21	11.47	0.95	0.38	1.43	0.04	0.96	1.93	3.67	3.43	0.14	0.22	3.37	99.20
RB130-91	t	77.28	0.08	10.45	1.58	0.28	2.03	0.04	0.60	0.19	3.13	4.04	0.04	0.19	1.86	99.76
RB145-91	u	78.72	0.21	10.37	0.36	0.14	0.54	0.00	0.38	0.27	7.20	0.00	0.04	0.15	1.05	98.91
RB146-91	u	74.50	0.13	9.10	1.13	0.21	1.46	0.05	1.31	2.20	6.43	0.04	0.03	0.13	3.98	99.23
RB147-91	u	78.03	0.30	10.38	0.45	0.28	0.78	0.03	0.77	0.64	5.48	0.14	0.04	0.19	2.03	98.77
RB149-91	u	71.24	0.58	13.88	0.63	0.32	1.02	0.02	0.63	1.00	3.29	5.03	0.08	0.10	2.08	98.88
RB150-91	u	78.69	0.17	11.08	0.18	0.12	0.32	0.00	0.19	0.11	3.51	3.31	0.04	0.11	0.73	98.25
RB151-91	u	75.66	0.17	9.78	0.95	0.26	1.31	0.05	0.90	1.89	2.58	3.75	0.03	0.08	3.26	99.35
RB152-91	u	69.67	0.41	14.04	0.72	0.46	1.26	0.03	0.76	1.29	4.85	3.88	0.11	0.13	2.53	98.88
RB154-91	u	68.17	0.35	14.72	0.50	0.48	1.03	0.01	0.57	0.73	7.18	2.77	0.09	0.28	1.77	97.64

APPENDIX D.2.
TRACE ELEMENT WHOLE ROCK CHEMISTRY (ppm).

SAMPLE	LODE	Sc	V	Cr	Ni	Cu	Zn	Ga	Rb	Sr	Y	Zr	Nb	Mo	Sn	Ba	La	Ce	Nd	Pb	Th	U
RB095-91	ams	3	18	29	10	2	1	12	159	27	3	55	0	1	22	183	3	8	3	1	3	1
RB096-91	ams	3	21	28	10	7	1	12	149	26	8	58	1	1	45	133	3	11	5	1	2	1
RB098-91	ams	2	14	19	14	26	1	9	121	23	2	65	0	1	48	150	3	8	3	1	3	1
RB105-91	ams	3	58	78	12	28	2	15	229	35	7	311	6	3	35	386	22	40	17	3	16	3
RB108-91	ams	2	16	38	6	39	1	10	138	8	6	148	2	1	64	109	5	21	9	2	6	1
RB141-91	ams	3	28	29	8	14	1	10	113	20	4	90	1	1	10	113	6	20	9	1	4	2
RB142-91	ams	3	17	23	9	34	1	10	110	21	4	67	1	8	24	126	3	12	5	1	2	1
RB144-91	ams	3	16	20	9	14	1	10	114	20	38	66	1	9	19	136	3	12	11	1	3	1
RB110-91	b	3	27	24	12	8	1	11	159	21	2	90	1	2	16	345	3	10	4	2	4	1
RB112-91	b	6	90	84	27	587	19	14	122	29	12	474	7	2	991	387	35	65	25	5	22	3
RB113-91	b	2	10	21	7	23	1	9	53	15	2	72	1	1	19	18	10	18	6	1	4	1
RB115-91	b	2	10	29	7	71	1	11	100	15	1	44	1	2	33	119	3	7	3	1	1	1
RB114-91	b	7	167	75	35	26	18	38	543	31	20	449	18	0	2589	253	203	322	128	9	34	8
RB118-91	b	2	21	41	9	322	1	10	128	29	6	140	9	2	5385	163	6	24	10	5	8	1
RB119-91	b	4	45	80	16	121	1	12	193	25	18	308	7	2	175	238	43	76	29	4	24	5
RB037-91	bonus	4	37	64	15	2	1	14	284	22	7	82	5	1	146	604	13	28	10	5	5	1
RB155-91	c	2	7	16	5	2	1	9	105	12	1	44	1	1	18	189	3	3	3	1	1	1
RB157-91	c	2	40	87	16	219	1	16	191	23	69	360	13	0	2961	150	37	71	30	11	24	5
RB158-91	c	2	11	20	8	21	1	9	155	15	9	59	0	1	26	347	3	10	3	5	2	1
RB159-91	c	6	37	50	14	8	1	15	208	29	7	85	2	2	42	335	27	53	16	3	3	1
RB160-91	c	8	47	89	16	11	2	11	178	21	30	380	9	4	118	265	70	114	45	4	22	2
RB163-91	c	2	27	48	14	49	1	14	137	23	1	70	2	2	43	108	41	67	27	1	5	2
RB164-91	c	3	15	28	9	36	1	9	103	34	7	71	2	3	26	107	9	19	6	1	3	1
RB081-91	cotton	2	11	37	14	2	1	11	197	17	8	87	2	1	80	357	3	10	5	8	4	1
RB084-91	cotton	3	52	72	9	2	1	13	170	29	11	186	5	1	40	297	24	45	18	13	13	3
RB086-91	cotton	3	39	36	5	22	7	10	112	30	8	149	4	1	1315	269	29	53	20	5	10	2
RB165-91	diss	4	29	37	9	44	1	13	130	32	6	53	2	1	191	135	3	10	4	1	1	1
RB166-91	diss	3	46	48	26	1084	3	14	138	15	4	127	13	1	7064	125	3	14	4	8	5	1
RB167-91	diss	5	95	82	36	4103	7	15	163	27	11	366	28	1	14712	182	17	44	18	15	27	5
RB168-91	diss	2	15	22	8	26	1	8	104	17	3	74	1	1	32	145	3	8	3	3	4	2
RB169-91	diss	2	21	40	9	18	1	11	124	34	13	129	3	1	134	137	6	22	9	6	8	3
RB170-91	diss	4	48	55	18	11	1	12	141	17	16	102	5	1	22	190	17	32	14	1	7	1
RB049-91	fw	8	44	69	47	2	12	16	177	35	5	109	2	1	2	598	5	16	6	3	6	1
RB050-91	fw	8	49	10	21	2	1	18	150	48	18	224	7	1	4	330	26	49	20	3	11	1
RB048-91	hw	3	33	53	18	2	5	13	130	35	15	105	3	1	5	265	24	43	20	2	7	1
RB121-91	hw	7	48	63	31	2	9	15	221	26	3	158	4	0	34	427	22	39	17	4	8	1
RB122-91	hw	2	60	71	33	2	6	20	304	45	2	112	3	0	39	579	6	25	8	2	6	1

SAMPLE	LODE	Sc	V	Cr	Ni	Cu	Zn	Ga	Rb	Sr	Y	Zr	Nb	Mo	Sn	Ba	La	Ce	Nd	Pb	Th	U
RB123-91	hw	4	22	14	14	2	1	10	215	41	1	75	0	0	10	357	4	11	4	1	3	1
RB124-91	hw	3	40	42	20	2	3	10	242	19	29	175	5	1	50	573	4	13	6	5	6	1
RB125-91	hw	4	35	48	22	2	3	11	209	23	1	116	3	1	4	520	4	18	6	1	6	1
RB126-91	hw	6	38	50	26	2	4	14	160	31	4	197	3	0	2	244	46	82	33	1	9	1
RB127-91	hw	2	22	37	12	2	2	9	144	32	1	130	3	1	38	238	8	23	6	2	9	1
RB129-91	t	2	18	39	11	2	3	12	205	31	1	101	2	1	321	318	3	15	5	1	5	2
RB130-91	t	2	11	18	10	2	3	9	141	16	1	50	0	1	2	350	3	12	6	1	1	1
RB145-91	u	2	18	34	11	2	2	9	331	12	1	97	2	4	93	581	8	17	7	7	5	1
RB146-91	u	3	14	19	12	2	1	8	293	26	1	68	1	3	353	548	4	8	4	1	2	1
RB147-91	u	2	25	42	13	4	1	14	334	9	1	122	8	3	5277	381	4	5	4	3	7	5
RB149-91	u	3	35	89	18	2	1	16	238	21	2	255	5	3	192	214	57	102	36	2	12	4
RB150-91	u	2	12	28	9	7	1	10	162	12	1	84	6	3	4099	285	3	6	3	4	4	3
RB151-91	u	3	18	28	12	2	1	10	134	23	2	79	1	2	10	208	3	10	3	1	4	2
RB152-91	u	5	59	83	20	39	1	14	255	23	5	138	3	2	157	497	11	25	11	5	9	10
RB154-91	u	2	33	74	16	18	1	14	351	20	1	160	4	3	9659	770	4	16	4	7	11	7

APPENDIX D.3.1.
SINGLE GRAIN MINERAL CHEMISTRY.
CASSITERITE CHEMISTRY (wt %) - SX 50 DATA

Sample numbering as follows: RB = Project reference, followed by sample number after the . follows the grain number / the point number of the analyses

SAMPLE	LODE	WO3	TiO2	Fe2O3	Nb2O5	SnO2	Total
RB009.1/1	c	0	0.364	0.67	0	98.70	99.73
RB009.1/2	c	0	0.135	0.49	0	99.20	99.83
RB009.1/3	c	0	0.282	0.34	0	99.52	100.14
RB009.1/4	c	0	0.377	0.62	0	98.85	99.85
RB009.1/5	c	0	1.366	1.05	0	96.51	98.93
RB009.1/6	c	0	0.621	0.76	0	99.16	100.54
RB009.2/1	c	0	0	0.92	0	99.68	100.60
RB009.2/2	c	0	0.472	0.45	0	98.61	99.53
RB009.2/3	c	0	0.277	0.79	0	98.48	99.54
RB009.2/4	c	0	0.177	0.90	0	98.92	100.00
RB009.2/5	c	0	0.115	0.87	0	98.82	99.81
RB009.2/6	c	0	0.198	2.53	0	96.97	99.70
RB009.2/7	c	0	0.46	0.46	0	99.47	100.39
RB009.2/8	c	0	0.417	1.01	0	98.74	100.16
RB009.2/9	c	0	0.11	0.49	0	99.54	100.14
RB009.2/10	c	0	0.289	0.58	0	99.26	100.12
RB009.2/11	c	0	0	1.42	0	98.37	99.80
RB009.2/12	c	0	0.193	0.48	0	99.81	100.48
RB009.2/13	c	0	0.123	0.24	0	100.32	100.68
RB009.2/14	c	0	0.692	0.77	0	98.23	99.69
RB009.2/15	c	0	0.61	0.83	0	98.45	99.90
RB009.2/16	c	0	0.422	0.34	0	99.49	100.25
RB009.2/17	c	0	0.098	0.95	0	98.51	99.57
RB009.2/18	c	0	0.464	0.55	0	98.85	99.86
RB009.2/19	c	0	0.289	1.20	0	97.89	99.38
RB009.2/20	c	0	0.352	0.40	0	98.86	99.61
RB009.2/21	c	0	0.13	0.78	0	99.24	100.16
RB009.2/22	c	0	0.532	0.76	0	98.69	99.98
RB009.2/23	c	1.155	0.138	0.37	0	98.15	99.81
RB036.2/1	bonus	0	0.804	1.32	0	98.64	100.77
RB036.3/2	bonus	0	0.162	2.07	0	97.88	100.11
RB036.3/3	bonus	0	0	1.88	0	96.69	98.57
RB036.3/4	bonus	0	0	2.21	0	96.94	99.15
RB036.3/5	bonus	1.61	0.335	0.56	0	97.53	100.04
RB036.3/6	bonus	0	0.454	0.16	0	99.42	100.04
RB036.3/7	bonus	0	0.404	1.39	0	97.99	99.78
RB036.3/8	bonus	0	0.609	0.85	0	98.50	99.96
RB036.3/9	bonus	0	0.168	1.55	0	98.07	99.79
RB036.3/10	bonus	0	0.077	1.18	0	97.90	99.16
RB036.3/11	bonus	0	0	2.06	0	98.09	100.16
RB036.3/12	bonus	0	0	0.20	0	99.93	100.14
RB036.3/13	bonus	0	0	1.57	0	98.84	100.41
SAMPLE	**LODE**	**WO3**	**TiO2**	**Fe2O3**	**Nb2O5**	**SnO2**	**Total**
RB036.3/14	bonus	0	0.906	0.38	0	98.22	99.50
RB020.1/1	b	0	0.265	0.51	0	99.37	100.14

RB020.1/2	b	0	0.098	0.57	0	99.66	100.32
RB020.1/3	b	0	0	2.11	0	97.25	99.36
RB020.1/4	b	0	0.15	1.53	0	98.44	100.12
RB020.1/5	b	0	0.834	0.47	0	99.27	100.58
RB020.1/6	b	1.426	0.2	0.85	0	0.98	3.45
RB020.1/7	b	0	0	1.99	0	97.22	99.22
RB020.1/8	b	0	0	1.77	0	97.89	99.66
RB020.1/9	b	0	0.272	0.67	0	98.62	99.56
RB020.1/10	b	0	0.407	0.41	0	99.31	100.12
RB020.1/11	b	0	0.269	0.62	0	99.26	100.15
RB020.1/12	b	0	0.44	0.75	0	98.64	99.82
RB020.1/13	b	0.443	0.425	0.07	0	99.85	100.79
RB020.1/14	b	0	0	1.33	0	98.27	99.60
RB020.1/15	b	0	0.349	0.47	0	99.45	100.27
RB020.1/16	b	0	0.314	1.06	0	98.51	99.88
RB067.1/1	bonus	1.18	0.317	0.36	0	95.71	97.57
RB067.1/2	bonus	0	0.842	0.81	0	96.84	98.49
RB067.1/3	bonus	0	0.239	0.47	0	97.76	98.47
RB067.1/4	bonus	0	0.412	0.98	0	96.47	97.85
RB067.1/5	bonus	0	0.505	0.43	0	96.36	97.29
RB156.1/1	c	0	0.342	0.74	0	99.45	100.53
RB156.1/2	c	0	0	0.12	0	100.48	100.60
RB156.1/3	c	0	0.784	0.88	0	98.76	100.42
RB156.1/4	c	0	1.276	0.63	0	98.27	100.18
RB156.1/5	c	0	0.297	1.43	0	98.27	99.99
RB088.1/1	cotton	0	0.524	1.03	0	99.23	100.78
RB088.1/2	cotton	0	0	0.71	0	99.82	100.52
RB088.1/3	cotton	1.811	0.003	0.82	0	97.62	100.25
RB088.1/4	cotton	1.37	0	0.59	0	98.44	100.39
RB088.1/5	cotton	1.387	0	0.53	0	97.88	99.79
RB088.1/6	cotton	1.252	0	0.68	0	98.19	100.12
RB088.1/7	cotton	1.406	0.097	0.65	0	98.46	100.61
RB088.1/8	cotton	0	0.112	1.24	0	99.31	100.66
RB088.1/9	cotton	1.373	0.128	0.80	0	98.40	100.70
RB088.1/10	cotton	1.38	0	0.71	0	98.18	100.26
RB088.1/11	cotton	2.02	0	0.92	0	97.13	100.07
RB088.1/12	cotton	1.966	0	1.15	0	96.66	99.77
RB088.1/13	cotton	0	0	1.85	0	98.58	100.43
RB088.1/14	cotton	0	0	1.09	0	98.76	99.85
RB088.1/15	cotton	0	0	1.45	0	98.60	100.05
RB088.1/16	cotton	0	0	1.36	0	99.54	100.90
RB088.1/17	cotton	0	0	1.89	0	98.58	100.47
RB088.1/18	cotton	0	0	2.04	0	98.46	100.50
RB088.1/19	cotton	0	0.028	1.05	0	98.43	99.51
RB088.1/20	cotton	0	0.215	0.85	0	98.60	99.66
RB088.1/21	cotton	0.672	0.185	0.73	0	99.46	101.04
RB088.1/22	cotton	0	0.098	1.29	0	98.47	99.86
RB088.1/23	cotton	0	0.127	0.87	0	99.46	100.46
SAMPLE	**LODE**	**WO3**	**TiO2**	**Fe2O3**	**Nb2O5**	**SnO2**	**Total**
RB088.1/24	cotton	0	0	0.63	0	98.99	99.62
RB088.1/25	cotton	0	0.08	0.66	0	99.23	99.96
RB088.1/26	cotton	0	0	0.95	0	99.07	100.02
RB088.1/27	cotton	0	0	1.12	0	99.03	100.15

RB088.1/28	cotton	0	0	0.99	0	98.73	99.72
RB088.1/29	cotton	0.695	0.28	0.23	0	98.75	99.96
RB088.1/30	cotton	0	0	0.28	0	98.98	99.26
RB088.2/1	cotton	0.567	0	1.32	0	96.83	98.72
RB088.2/2	cotton	0	0.203	0.72	0	97.90	98.82
RB088.2/3	cotton	0.941	0	0.38	0	98.15	99.46
RB088.2/4	cotton	0.97	0	0.38	0	98.28	99.62
RB088.2/5	cotton	0.846	0.19	0.25	0	98.49	99.77
RB088.2/6	cotton	0	0.177	0.69	0	98.57	99.44
RB088.2/7	cotton	0	0	0.80	0	98.70	99.50
RB088.2/8	cotton	0	0	1.09	0	98.32	99.41
RB088.2/9	cotton	0	0.158	1.14	0	97.22	98.51
RB088.2/10	cotton	0	0	1.18	0	98.16	99.34
RB088.2/11	cotton	0	0.123	1.03	0	98.76	99.91
RB088.2/12	cotton	0	0	1.52	0	97.90	99.41
RB088.2/13	cotton	0	0.295	1.10	0	98.30	99.69
RB088.2/14	cotton	0	0	1.02	0	98.72	99.74
RB088.2/15	cotton	1.59	0.065	0.78	0	96.99	99.42
RB088.2/16	cotton	1.61	0.075	0.82	0	97.35	99.86
RB088.2/17	cotton	1.531	0.117	0.70	0	97.74	100.09
RB088.2/18	cotton	1.836	0	0.87	0	97.32	100.03
RB088.2/19	cotton	2.013	0	0.97	0	97.49	100.48
RB088.2/20	cotton	1.932	0	0.91	0	96.47	99.32
RB111.1/1	b	0.421	0.59	0.32	0	98.35	99.68
RB111.1/2	b	0	0.804	1.36	0	97.36	99.52
RB111.1/3	b	0	0.642	1.14	0	97.74	99.52
RB111.1/4	b	0	0.909	0.66	0	99.17	100.73
RB111.1/5	b	0	0.118	1.35	0	98.75	100.22
RB111.1/6	b	0	0.547	0.74	0	98.27	99.56
RB111.1/7	b	0	0.345	0.67	0	98.71	99.72
RB111.1/8	b	0	0.29	0.88	0	98.84	100.01
RB111.1/9	b	0	0.097	0.83	0	99.09	100.02
RB111.1/10	b	0	0	0.86	0	98.47	99.33
RB111.2/1	b	0	0.597	1.47	0	97.63	99.70
RB111.2/2	b	0	0.749	0.49	0	98.81	100.05
RB111.2/3	b	0	0.427	0.76	0	98.70	99.88
RB111.2/4	b	1.463	0.294	0.63	0	97.74	100.13
RB111.2/5	b	1.218	0.365	0.44	0	97.37	99.40
RB111.2/6	b	1.019	0.33	0.26	0	97.52	99.13
RB111.2/7	b	1.686	0.168	0.66	0	97.18	99.70
RB111.2/8	b	1.498	0.26	0.57	0	97.55	99.87
RB111.2/9	b	0.457	0.193	0.34	0	98.27	99.25
RB111.2/10	b	0	0.474	0.88	0	98.50	99.85
RB111.2/11	b	0	0.294	0.83	0	98.09	99.22
RB111.2/12	b	0	0.454	0.71	0	99.19	100.36
RB111.2/13	b	0	0.412	0.63	0	98.76	99.80
SAMPLE	**LODE**	**WO3**	**TiO2**	**Fe2O3**	**Nb2O5**	**SnO2**	**Total**
RB111.2/14	b	0	0.22	0.78	0	98.97	99.97
RB111.2/15	b	0	0.172	0.70	0	98.39	99.26
RB111.2/16	b	0	0.359	0.58	0	98.77	99.71
RB111.2/17	b	0	0.085	0.91	0	98.46	99.45
RB111.2/18	b	0	0.112	0.69	0	98.65	99.44
RB111.2/19	b	0.474	0.292	0.18	0	99.17	100.12

RB111.2/20	b	0.482	0.46	0.09	0	98.89	99.93
RB111.3/1	b	0	0.639	0.84	0	97.76	99.24
RB111.3/2	b	1.319	0.55	0.29	0	97.80	99.96
RB111.3/3	b	0.706	1.453	0.73	0	97.46	100.35
RB111.3/4	b	0.653	1.256	0.17	0	98.38	100.46
RB111.3/5	b	1.057	0.882	0.26	0	98.94	101.14
RB111.3/6	b	0.8	0.39	0.31	0	99.65	101.15
RB111.3/7	b	0.897	0.435	0.33	0	97.86	99.52
RB111.3/8	b	1.532	0.504	0.55	0	98.03	100.62
RB111.3/9	b	1.025	0.774	0.43	0	99.02	101.25
RB111.3/10	b	0	0.976	0.50	0	99.38	100.86
RB111.3/11	b	0	0.659	1.16	0	99.03	100.85
RB111.3/12	b	0	0.646	0.83	0	98.68	100.16
RB111.3/13	b	0	0.967	0.84	0	98.26	100.06
RB111.3/14	b	0	0.43	1.36	0	98.20	100.00
RB111.3/15	b	0	0.946	0.57	0	98.99	100.50
RB111.3/16	b	1.05	0.906	0.19	0	98.43	100.58
RB111.3/17	b	0.69	0.519	0.26	0	98.58	100.05
RB111.3/18	b	0.725	0.991	0.36	0	98.09	100.17
RB111.3/19	b	1.789	0.677	0.85	0	97.03	100.34
RB111.3/20	b	0	0.424	1.27	0	98.16	99.86
RB111.4/21	b	0.004	1.181	0.60	0	98.19	99.97
RB111.4/22	b	0	0.766	1.28	0	97.63	99.68
RB111.4/23	b	0	0.681	0.99	0	98.18	99.85
RB111.4/24	b	0	0.384	1.33	0	98.57	100.29
RB111.4/25	b	0	0.732	0.65	0	98.52	99.90
RB111.4/26	b	0	0.814	0.41	0	99.31	100.54
RB111.4/27	b	0	0.747	0.26	0	99.12	100.13
RB111.4/28	b	0	0.734	0.60	0	98.64	99.97
RB111.4/29	b	0	0.602	0.62	0	98.84	100.06
RB111.4/30	b	0	0.811	0.26	0	99.63	100.70
RB111.5/1	b	0	0.319	0.07	0	99.91	100.30
RB111.5/2	b	1.211	0.939	0.24	0	98.32	100.71
RB111.5/3	b	0	0.941	0.48	0	99.19	100.62
RB111.5/4	b	0	0.879	0.70	0	98.72	100.30
RB111.5/5	b	0	0.794	0.81	0	98.45	100.05
RB111.5/6	b	0	0.861	0.82	0	99.04	100.72
RB111.5/7	b	0.435	1.086	0.28	0	98.53	100.34
RB111.5/8	b	0	1.233	0.49	0	98.73	100.45
RB111.5/9	b	0	1.002	0.54	0	97.91	99.45
RB111.5/10	b	0	0.826	0.26	0	99.20	100.28
RB111.6/1	b	0	0.609	0.31	0	99.16	100.08
RB111.6/2	b	0	0.972	0.20	0	98.94	100.12
RB111.6/3	b	0	0.781	0.84	0	97.89	99.51
SAMPLE	**LODE**	**WO3**	**TiO2**	**Fe2O3**	**Nb2O5**	**SnO2**	**Total**
RB111.6/4	b	0	0.731	0.63	0	98.25	99.61
RB111.6/5	b	0	0.627	0.88	0	97.64	99.14
RB111.6/6	b	0	0.662	0.68	0	98.15	99.49
RB111.6/7	b	0	0.957	1.03	0	97.76	99.74
RB111.6/8	b	0.589	0.826	0.15	0	98.87	100.43
RB111.6/9	b	0.967	0.989	0.43	0	97.87	100.25
RB111.6/10	b	0	0.465	1.39	0	97.87	99.72
RB111.7/1	b	0	0.15	0.10	0	100.22	100.47

RB111.7/2	b	0.004	0.812	1.59	0	97.50	99.91
RB111.7/3	b	0	0.767	1.20	0	97.62	99.58
RB111.7/4	b	0	0.721	0.67	0	98.07	99.46
RB111.7/5	b	0	0.462	0.83	0	98.13	99.42
RB111.7/6	b	0	1.054	0.81	0	98.01	99.87
RB111.7/7	b	1.243	0.562	0.40	0	97.47	99.67
RB111.7/8	b	0.82	1.149	0.48	0	96.99	99.44
RB111.7/9	b	5.709	2.514	3.79	0	98.32	110.34
RB111.7/10	b	1.235	0.791	0.34	0	96.36	98.73
RB111.8/1	b	0	0.632	1.28	0	98.25	100.17
RB111.8/2	b	0	0.672	1.19	0	97.44	99.31
RB111.8/3	b	0	0.492	1.33	0	97.84	99.66
RB111.8/4	b	0	1.184	1.22	0	97.87	100.27
RB111.8/5	b	1.72	1.006	0.71	0	95.73	99.17
RB111.8/6	b	0.696	0.555	0.40	0	98.16	99.81
RB111.8/7	b	0.691	0.524	0.45	0	98.05	99.72
RB111.8/8	b	0	0.907	1.37	0	97.01	99.28
RB111.8/9	b	0	0.544	1.60	0	97.71	99.85
RB111.8/10	b	0	0.827	1.59	0	97.62	100.03
RB111.8/11	b	0	1.121	1.18	0	97.46	99.76
RB111.8/12	b	0	0.944	1.44	0	97.53	99.91
RB111.8/13	b	0	0.525	1.57	0	97.35	99.45
RB111.8/14	b	0	0.917	1.57	0	96.91	99.40
RB111.8/15	b	4.435	1.735	1.62	0	93.03	100.82
RB111.8/16	b	0.81	0.737	0.60	0	96.11	98.26
RB111.8/17	b	0	0.612	0.77	0	98.48	99.86
RB111.8/19	b	0	1.293	0.36	0	98.14	99.80
RB111.8/20	b	0	0.362	0.37	0	98.71	99.44
RB111.8/21	b	0	0.262	0.10	0	99.59	99.95
RB111.8/22	b	0	0.956	0.97	0	97.23	99.16
RB111.8/23	b	0	0.776	0.91	0	97.95	99.63
RB111.8/24	b	0	0.482	1.15	0	98.45	100.08
RB111.8/25	b	0	0.465	1.03	0	98.29	99.79
RB111.8/26	b	0	0.39	1.16	0	97.68	99.23
RB111.8/27	b	0	0.769	1.52	0	98.03	100.31
RB111.8/28	b	0	0.636	1.47	0	97.32	99.42
RB111.8/29	b	0	0.17	1.90	0	97.43	99.50
RB111.8/30	b	0	0.5	1.47	0	98.15	100.12
RB155.5/1	c	0	0.183	2.26	0	97.41	99.85
RB155.5/2	c	0	0.08	3.02	0	97.11	100.20
RB155.5/3	c	0	0.201	2.86	0	96.08	99.14
RB155.5/4	c	0	0	1.04	0	98.67	99.71
SAMPLE	**LODE**	**WO3**	**TiO2**	**Fe2O3**	**Nb2O5**	**SnO2**	**Total**
RB155.5/5	c	0	0.34	2.01	0	96.82	99.17
RB155.5/6	c	0.408	0	1.64	0	97.57	99.62
RB155.5/7	c	0	0	2.82	0	96.35	99.17
RB155.5/8	c	0	1.027	1.92	0	97.40	100.35
RB155.5/9	c	0	0	2.54	0	97.87	100.41
RB155.5/10	c	0	0.128	2.14	0	98.13	100.39
RB155.5/11	c	0	0	2.69	0	97.16	99.84
RB155.5/12	c	0	0	2.54	0	96.99	99.53
RB155.5/13	c	0	0	1.98	0	97.98	99.96
RB155.5/14	c	0	0	2.27	0	97.63	99.90

RB155.5/15	c	0	0	2.71	0	97.62	100.33
RB155.5/16	c	0	0	2.01	0	96.83	98.84
RB155.5/17	c	0	0.575	1.41	0	97.57	99.56
RB155.5/18	c	0	0.065	1.68	0	98.13	99.87
RB155.5/19	c	0	0	2.80	0	96.89	99.69
RB155.5/20	c	0	0	2.32	0	97.23	99.54
RB155.5/21	c	0	0	1.06	0	98.48	99.54
RB155.5/22	c	0.441	0	2.29	0	97.48	100.21
RB155.5/23	c	0	0.099	1.58	0	97.89	99.56
RB155.5/24	c	0	0	1.67	0	97.93	99.60
RB155.5/25	c	0	0	1.76	0	98.12	99.88
RB155.5/26	c	0	0	1.33	0	98.11	99.44
RB155.1/1	c	0	0.267	1.14	0	99.49	100.90
RB155.1/2	c	0	0	1.34	0	99.04	100.38
RB155.1/3	c	0	0.706	1.12	0	98.87	100.69
RB155.1/4	c	0	0.29	1.40	0	98.78	100.46
RB155.1/5	c	0	0.317	1.38	0	98.12	99.81
RB155.1/6	c	0	1.311	0.89	0	97.75	99.95
RB155.1/7	c	0	0	1.67	0	98.59	100.26
RB155.1/8	c	0	0.209	0.44	0	99.46	100.11
RB155.1/9	c	0	0	0.79	0	99.05	99.83
RB155.1/10	c	0	0	1.66	0	98.04	99.70
RB155.1/11	c	0	0	1.37	0	98.84	100.21
RB155.1/12	c	0	0	1.61	0	97.98	99.58
RB155.1/13	c	0	0	1.67	0	98.51	100.18
RB155.1/14	c	0	0	1.62	0	97.84	99.46
RB155.1/15	c	0	0	1.71	0	97.48	99.20
RB155.1/16	c	0	0	1.53	0	98.81	100.34
RB155.1/17	c	0	0	1.41	0	98.98	100.39
RB155.1/18	c	0	0.2	0.95	0	98.26	99.41
RB155.1/19	c	0	0	1.10	0	98.53	99.63
RB155.1/20	c	0	0	1.29	0	98.53	99.83
RB155.2/1	c	0	0.275	1.00	0	98.54	99.82
RB155.2/2	c	0	0.462	1.11	0	98.50	100.06
RB155.2/3	c	0	0	1.74	0	98.60	100.34
RB155.2/4	c	0	1.311	0.79	0	97.58	99.68
RB155.2/5	c	0	0.095	1.22	0	98.66	99.97
RB155.2/6	c	0	0	1.57	0	98.11	99.68
RB155.2/7	c	0	0	1.51	0	97.85	99.37
RB155.2/8	c	0	0	1.99	0	97.64	99.62
SAMPLE	**LODE**	**WO3**	**TiO2**	**Fe2O3**	**Nb2O5**	**SnO2**	**Total**
RB155.2/9	c	0	0	2.12	0	97.95	100.07
RB155.2/10	c	0	0.002	2.17	0	97.97	100.14
RB155.2/11	c	0	0	2.00	0	97.40	99.40
RB155.2/12	c	0	0	1.02	0	98.90	99.92
RB155.2/13	c	0	0	1.38	0	98.61	99.99
RB155.2/14	c	0	0.162	0.30	0	99.44	99.90
RB155.2/15	c	0	0	1.14	0	98.91	100.05
RB155.2/16	c	0	0	1.49	0	98.23	99.72
RB155.2/17	c	0	0	1.91	0	97.95	99.86
RB155.2/18	c	0	0	1.72	0	97.91	99.63
RB155.2/19	c	0	0	1.88	0	98.01	99.89
RB155.3/1	c	0	0.102	1.07	0	98.56	99.73

RB155.3/2	c	0	1.036	0.44	0.39	97.25	99.12
RB155.3/3	c	0	0.884	0.26	0.59	98.27	100.00
RB155.3/4	c	0	0.085	1.58	0	98.68	100.35
RB155.3/5	c	0.641	1.503	0.20	0	98.20	100.55
RB155.3/6	c	0	1.751	0.12	0.36	97.23	99.46
RB155.3/7	c	0	0.489	0.45	0	98.56	99.50
RB155.3/8	c	0	0.065	1.37	0	98.90	100.33
RB155.3/9	c	0	0.118	1.14	0	98.52	99.79
RB155.3/10	c	0	0	1.41	0	98.05	99.47
RB155.3/11	c	0	0	1.41	0	98.90	100.31
RB155.3/12	c	0	0.078	1.40	0	97.80	99.27
RB155.3/13	c	0	0.132	0.55	0	99.39	100.07
RB155.3/14	c	0	0	1.33	0	98.38	99.72
RB155.3/15	c	0	0	1.51	0	98.92	100.43
RB155.3/16	c	0	0	1.43	0	98.55	99.98
RB155.3/17	c	0	0	1.44	0	98.10	99.54
RB155.3/18	c	0	0	1.75	0	98.48	100.22
RB155.3/19	c	0	0.07	0.79	0	99.54	100.40
RB155.4/1	c	0	0.762	0.42	0	97.93	99.11
RB155.4/2	c	0	0	1.60	0	98.33	99.93
RB155.4/3	c	0	0.073	1.47	0	98.44	99.98
RB155.4/4	c	1.126	1.331	0.77	0	97.35	100.58
RB155.4/5	c	0	0	2.00	0	98.08	100.08
RB155.4/6	c	0	0.207	2.18	0	97.68	100.07
RB155.4/7	c	0	0.153	1.87	0	98.37	100.39
RB155.4/8	c	0	0.093	1.49	0	98.66	100.24
RB155.4/9	c	0	0	1.67	0	98.02	99.68
RB155.4/10	c	0	0	1.62	0	98.73	100.35
RB155.4/11	c	0	0	2.00	0	97.61	99.61
RB155.4/12	c	0	0	2.12	0	98.15	100.26
RB155.4/13	c	0	0	1.67	0	98.31	99.97
RB155.4/14	c	0	0	2.25	0	97.07	99.32
RB155.4/15	c	0	0	1.91	0	97.76	99.67
RB155.4/16	c	0	0	2.20	0	98.27	100.46
RB155.4/17	c	0	0.077	1.39	0	99.24	100.70
RB155.4/18	c	0	0	2.06	0	97.69	99.75
RB155.4/19	c	0.972	0	1.46	0	97.56	99.99
RB155.4/20	c	0	0	1.95	0	97.59	99.54
SAMPLE	**LODE**	**WO3**	**TiO2**	**Fe2O3**	**Nb2O5**	**SnO2**	**Total**
RB016.11/1	c	0	0.157	1.99	0	97.70	99.84
RB016.11/2	c	0	0.361	1.71	0	98.44	100.51
RB016.11/3	c	0	0.799	2.43	0	97.21	100.43
RB016.11/4	c	1.042	0	1.40	0	97.44	99.88
RB016.11/5	c	0	0.081	0.12	0	98.55	98.75
RB016.11/6	c	0	0.796	2.02	0	96.81	99.63
RB016.11/7	c	0	0	2.97	0	96.49	99.46
RB016.11/8	c	0	0.071	2.28	0	98.17	100.53
RB016.11/9	c	0	0.289	1.85	0	97.71	99.84
RB016.11/10	c	0.425	0.267	0.71	0	98.97	100.37
RB016.11/11	c	0	0.289	0.92	0	98.60	99.81
RB016.11/12	c	0	0.888	2.42	0	96.53	99.83
RB016.11/13	c	0	0.127	0.34	0	98.86	99.33
RB016.11/14	c	0	0	2.53	0	97.56	100.09

RB016.11/15	c	0	0	2.97	0	97.22	100.19
RB016.11/16	c	0	0.426	0.88	0	98.76	100.06
RB016.1/1	c	0	0.274	0.80	0	99.24	100.32
RB016.1/2	c	0	0	0.35	0	99.55	99.89
RB016.1/3	c	0	0	0.76	0	99.22	99.98
RB016.1/4	c	0	0	0.36	0	98.99	99.36
RB016.1/5	c	0	0.193	0.80	0	98.84	99.84
RB016.1/6	c	0	0	0.62	0	100.02	100.64
RB016.1/7	c	0	0	0.55	0	98.80	99.34
RB016.1/8	c	0	0.123	0.68	0	98.42	99.22
RB016.1/9	c	0	0	1.43	0	98.00	99.42
RB016.1/10	c	0	0	1.59	0	98.00	99.59
RB016.2/1	c	0	0	2.77	0	97.23	100.01
RB016.2/2	c	0	0	2.69	0	97.12	99.80
RB016.2/3	c	0	0.168	2.21	0	97.58	99.96
RB016.2/4	c	0	0	1.76	0	97.76	99.52
RB016.2/5	c	0	0.224	1.06	0	98.25	99.53
RB016.2/6	c	0	0	1.04	0	98.29	99.33
RB016.2/7	c	0	0.08	1.14	0	99.06	100.28
RB016.2/8	c	0	0.05	1.05	0	99.63	100.73
RB016.2/9	c	0	0.155	1.14	0	98.56	99.85
RB016.2/10	c	0	0	0.83	0	99.43	100.26
RB016.3/1	c	1.058	0.003	0.70	0	98.90	100.66
RB016.3/2	c	0	0	2.58	0	96.89	99.47
RB016.3/3	c	0	0	2.32	0	96.85	99.16
RB016.3/4	c	0	0.093	1.11	0	98.61	99.81
RB016.3/5	c	0.434	0.26	0.98	0	97.55	99.22
RB016.3/6	c	0	0.1	0.97	0	98.34	99.41
RB016.3/7	c	0	0.245	0.47	0	98.86	99.57
RB016.3/8	c	0	0	1.27	0	98.64	99.92
RB016.3/9	c	0	0.372	0.87	0	98.10	99.34
RB016.3/10	c	0	0	0.62	0	98.01	98.63
RB016.4/1	c	0	0.214	1.41	0	97.94	99.55
RB016.4/2	c	0	0.264	0.35	0	98.39	99.00
RB016.4/3	c	0	0	1.25	0	97.35	98.60
RB016.4/4	c	0	0.244	0.96	0	98.08	99.29
SAMPLE	**LODE**	**WO3**	**TiO2**	**Fe2O3**	**Nb2O5**	**SnO2**	**Total**
RB016.4/5	c	0	0.257	0.17	0	98.96	99.38
RB016.4/6	c	0	0.115	0.33	0.24	98.65	99.33
RB016.4/7	c	0	0.127	0.27	0	98.97	99.37
RB016.4/8	c	0.001	0.239	0.25	0	98.18	98.68
RB016.4/9	c	0	0	0.28	0	99.01	99.29
RB016.4/10	c	0	0	0.35	0	98.98	99.33
RB016.5/1	c	0	0	2.23	0	96.46	98.69
RB016.5/2	c	0	0.624	0.18	0	98.44	99.25
RB016.5/3	c	0	0	1.42	0	98.12	99.54
RB016.5/4	c	0	0.102	0.78	0	98.11	98.99
RB016.5/5	c	0	0	0.91	0	98.84	99.75
RB016.6/1	c	0	0	1.67	0	97.67	99.34
RB016.6/2	c	0	0	1.26	0	96.96	98.21
RB016.6/3	c	1.961	0	1.31	0	95.35	98.62
RB016.6/4	c	1.638	0.117	0.74	0	97.02	99.51
RB016.6/5	c	2.394	0	1.08	0	96.12	99.60

RB016.6/6	c	0	0	1.43	0	97.26	98.69
RB016.6/7	c	0	0	1.90	0	96.73	98.64
RB016.6/8	c	0	0.302	0.91	0	97.85	99.07
RB016.6/9	c	0	0	1.46	0	97.18	98.64
RB016.6/10	c	0	0	1.47	0	97.17	98.64
RB016.7/1	c	0	0	2.09	0	96.83	98.92
RB016.7/2	c	0	0	1.87	0	97.11	98.98
RB016.7/3	c	0	0	1.49	0	97.51	99.00
RB016.7/4	c	0	0	1.80	0	97.11	98.91
RB016.7/5	c	0	0.379	0.92	0	97.85	99.14
RB016.7/6	c	0	0	1.65	0	97.11	98.76
RB016.7/7	c	0	0.31	0.84	0	97.71	98.87
RB016.7/8	c	0	0	1.35	0	97.72	99.08
RB016.7/9	c	0	0	1.46	0	97.60	99.06
RB016.7/10	c	0	0.235	1.12	0	97.91	99.26
RB016.7/11	c	0	0.674	0.82	0	96.90	98.39
RB016.7/12	c	0	0.14	0.68	0	97.97	98.80
RB016.7/13	c	0	0.127	1.61	0	98.34	100.08
RB016.7/14	c	0.004	0.125	1.09	0	97.77	98.98
RB016.8/1	c	0	0	2.54	0	96.76	99.30
RB016.8/2	c	0	0.177	1.15	0	97.84	99.17
RB016.8/3	c	0	0	2.28	0	96.86	99.14
RB016.8/4	c	0	0	1.67	0	97.65	99.31
RB016.8/5	c	0	0.203	1.20	0	98.06	99.47
RB016.8/6	c	0	0.002	1.77	0	97.65	99.42
RB016.8/7	c	0	0.255	1.34	0	98.01	99.61
RB016.8/8	c	0	0.065	1.48	0	97.86	99.40
RB016.8/9	c	0	0	0.99	0	97.49	98.48
RB016.8/10	c	0	0	1.65	0	97.58	99.23
RB016.8/11	c	0	0.237	1.03	0	97.44	98.70
RB016.8/12	c	0	0.329	1.10	0	98.25	99.67
RB016.8/13	c	0	0.741	0.65	0	97.80	99.19
RB016.8/14	c	0	0.514	0.48	0	98.53	99.53
RB016.8/15	c	0	0.27	0.13	0	98.92	99.32
SAMPLE	**LODE**	**WO3**	**TiO2**	**Fe2O3**	**Nb2O5**	**SnO2**	**Total**
RB016.9/1	c	0	0	3.78	0	95.42	99.21
RB016.9/2	c	0	0	3.46	0	94.97	98.43
RB016.9/3	c	0	0	2.93	0	96.32	99.25
RB016.9/4	c	0	0.142	0.02	0	99.40	99.56
RB016.9/5	c	0	0	2.46	0	95.97	98.43
RB016.9/6	c	0	0.002	2.53	0	96.80	99.33
RB016.9/7	c	0	0	2.18	0	96.92	99.10
RB016.9/8	c	0	0	1.95	0	97.13	99.08
RB016.9/9	c	0	0	1.75	0	97.66	99.41
RB016.9/10	c	0	0.002	1.92	0	97.34	99.27
RB016.9/11	c	0	0	1.39	0	97.08	98.48
RB016.9/12	c	0	0	1.88	0	96.86	98.74
RB016.9/13	c	0	0	1.73	0	97.13	98.86
RB016.9/14	c	0	0	1.44	0	97.60	99.04
RB016.10/1	c	0	0	2.58	0	97.34	99.93
RB016.10/2	c	0	0	2.33	0	96.92	99.24
RB016.10/3	c	0	0	2.33	0	96.87	99.19
RB016.10/4	c	0	0.118	0.12	0	99.53	99.77

RB016.10/5	c	0	0.002	1.54	0	98.10	99.64
RB016.10/6	c	0	0	1.84	0	97.80	99.64
RB016.10/7	c	0	0	2.16	0	97.24	99.40
RB016.10/8	c	0	0.003	1.82	0	97.09	98.92
RB016.10/9	c	0	0.085	0.87	0	98.74	99.69
RB016.10/10	c	0	0	1.57	0	97.53	99.10
RB016.10/11	c	0	0	1.73	0	97.92	99.64
RB016.10/12	c	0	0	1.31	0	98.32	99.63
RB016.10/13	c	0	0	1.34	0	98.21	99.55
RB016.10/14	c	0	0	0.60	0	99.14	99.74
RB016.10/15	c	0	0	1.95	0	97.39	99.34

APPENDIX D.3.1.
CASSITERITE CHEMISTRY (wt %) - CAMEBAX DATA.

Sample numbering as follows: RB = Project reference, followed by sample number after the / follows the point number of the analyses

SAMPLE	LODE	WO3	TiO2	FeO	SnO2
RB016/1	c	0.62	0	2.92	97.22
RB016/2	c	0	0.05	3.03	97.93
RB016/3	c	0	0	3.3	97.17
RB016/4	c	0.19	0.09	3.06	97.27
RB016/5	c	0	0	3.25	98.27
RB016/6	c	0	0.05	3.4	97.75
RB016/7	c	0	0	1.72	99.17
RB016/8	c	0	0	1.36	100.45
RB016/9	c	0	0	1.42	99.96
RB016/10	c	0	0	0.78	100.79
RB016/11	c	0	0.23	0.52	101.04
RB016/12	c	0	0.04	0.27	101.81
RB016/13	c	0	0.06	0.65	101.25
RB016/14	c	0	0.05	2.93	97.53
RB016/15	c	0	0	3.18	97.68
RB016/16	c	0.96	0.05	2.63	97.22
RB016/17	c	0.63	0	2.8	97.57
RB016/18	c	1.52	0	0.78	99.2
RB088/1	cotton	1.86	0.49	1.25	98.3
RB088/2	cotton	0	0.51	1.99	98.21
RB088/3	cotton	1.69	0.21	1.03	97.69
RB088/4	cotton	0	0.11	1.7	99.23
RB088/5	cotton	0	0.07	1.3	99.87
RB088/6	cotton	0.88	0	0.84	99.82
RB088/7	cotton	1.46	0.65	0.83	98.31
RB088/8	cotton	0	0	1.04	100.52
RB088/9	cotton	1.52	0.24	0.61	99.06
RB088/10	cotton	0	0.11	1.44	99.66
RB161/1	c	1.52	0.24	0.61	99.06
RB161/2	c	0	0.11	1.44	99.66
RB161/3	c	1.33	0.13	0.45	99.88
RB161/4	c	0	0.14	0.81	100.26
RB161/5	c	1.59	0.05	0.63	99.17
RB161/6	c	0	0.05	0.56	100.95
RB161/7	c	0.37	0.15	0.55	100.2
RB161/8	c	0.37	0.1	0.66	99.87
RB161/9	c	0	0.12	0.92	99.51
RB161/10	c	1.46	0.1	0.61	99.08
RB161/11	c	1.3	0.09	0.45	99.95
RB161/12	c	0	0.07	0.86	100.35
RB099/1	ams	0	0.17	1.1	100
RB099/2	ams	0	0.38	1.1	100.29
RB099/3	ams	0	0.39	1.09	99.83

SAMPLE	LODE	WO3	TiO2	FeO	SnO2
RB099/4	ams	0	0.15	0.85	97.05
RB099/5	ams	0	0.19	0.94	100.43
RB099/6	ams	0	0.2	1.1	99.57
RB099/7	ams	0	0.1	1.41	97.35
RB099/8	ams	0	0.1	1.38	97.84
RB099/9	ams	0	0.21	1.9	97.51
RB099/10	ams	0	0.13	1.3	99.56
RB099/11	ams	0	0.22	1.66	99.57
RB099/12	ams	0	0.17	1.58	99.64
RB099/13	ams	0	0.16	1.18	99.81
RB099/14	ams	0	0.13	0.87	100.11
RB099/15	ams	0	0.04	0.94	100.17
RB120/1	b	0	0.44	1.18	99.35
RB120/2	b	0	0.46	1.09	99.55
RB120/3	b	0	0.19	0.86	100.08
RB120/4	b	1.35	0.06	0.75	99.29
RB120/5	b	0	0.49	0.5	99.85
RB120/6	b	0	0.48	1.7	98.63
RB120/7	b	0	0.49	1.69	99.45
RB120/8	b	0	0.64	1.5	100.34
RB120/9	b	0	0.68	1.25	99.07
RB120/10	b	0.92	0.18	0.41	100.61
RB120/11	b	0.76	0.05	0.38	100.69
RB120/12	b	0.7	0.07	0.32	98.71
RB120/13	b	0	0.04	0.3	101.64
RB037/1	bonus	0	0	0.52	101.77
RB037/2	bonus	1.76	0	0.92	99.12
RB037/3	bonus	2.05	0.04	1.06	98.75
RB037/4	bonus	0	0.33	0.7	100.47
RB037/5	bonus	0.79	0.07	0.68	100.19

APPENDIX D.3.2.
TOURMALINE CHEMISTRY (wt %).

Sample numbering as follows: RB = Project reference, followed by sample number
after the . follows the grain number / the point number of the analyses

SAMPLE	LODE	FeO	Na2O	K2O	SiO2	MnO	CaO	NiO	Al2O3	TiO2	Cr2O3	MgO	Total
RB016.1/1	c	11.162	2.52	0	36.25	0	0.02	0	31.16	0	0	5.2	86.312
RB016.1/2	c	13.3	2.85	0	36.19	0	0	0	29.1	0	0	4.95	86.39
RB016.1/3	c	10.89	2.14	0	36.19	0	0	0	33.19	0	0	3.82	86.23
RB016.1/4	c	11.55	2.37	0	36.49	0	0	0	30.75	0	0	5.14	86.3
RB016.1/5	c	13.05	2.67	0.1	36.07	0	0	0	29.77	0	0	4.73	86.39
RB016.1/6	c	14.36	2.93	0	36.24	0	0	0	28.44	0	0	4.37	86.34
RB016.1/7	c	15.97	2.8	0	35.46	0	0	0	27.57	0	0	4.5	86.3
RB016.2/1	c	15.98	2.67	0	36.42	0	0	0	28.02	0	0	4.26	87.35
RB016.2/2	c	13.15	2.5	0	35.75	0	0	0	30.51	0	0	4.44	86.35
RB016.2/3	c	12.08	2.35	0	36.04	0	0	0	30.8	0	0	4.75	86.02
RB016.2/4	c	12.14	2.61	0	36.18	0	0	0	30.72	0	0	5.45	87.1
RB016.2/5	c	14.07	2.71	0	36.01	0	0	0	30.15	0	0	4.28	87.22
RB016.2/6	c	12.12	2.47	0	35.35	0	0	0	32.29	0	0	3.97	86.2
RB016.2/7	c	13.1	2.76	0	35.62	0	0	0	29.36	0	0	5.09	85.93
RB016.2/8	c	14.17	3.09	0	35.49	0	0	0	29.52	0	0	4.5	86.77
RB016.2/9	c	13.59	2.77	0	35.9	0	0	0	29.2	0	0	5.2	86.66
RB016.2/10	c	13.79	2.77	0	35.03	0	0	0	30.08	0	0	4.52	86.19
RB016.2/11	c	14.7	3.11	0	35.05	0	0.14	0	28.75	0.55	0	4.98	87.28
RB016.3/1	c	15.8	3.2	0	35.14	0	0.17	0	27.75	0	0	4.5	86.56
RB016.3/2	c	15.92	3.12	0	35.1	0	0	0	27.67	0	0	4.41	86.22
RB016.3/3	c	13.77	3.01	0	35.91	0	0	0	30.74	0	0	4.35	87.78
RB016.3/4	c	13.41	2.82	0	35.96	0	0	0	30.26	0	0.17	4.65	87.27
RB016.4/1	c	13.93	2.88	0	35.6	0	0	0	30.36	0.21	0	4.65	87.63
RB016.4/2	c	12.98	2.62	0	35.63	0	0	0	29.54	0.43	0	5.24	86.44
RB016.4/3	c	16.66	2.89	0	35.17	0	0	0	27.34	0.25	0	4.3	86.61
RB016.4/4	c	13.79	2.87	0	35.72	0	0	0	29.77	0.25	0	4.92	87.32
RB016.4/5	c	17.2	2.99	0	35.54	0	0.14	0	26.73	0	0	4.54	87.14
RB016.4/6	c	15.54	2.93	0	35.74	0	0	0	27.72	0.8	0	4.85	87.58
RB016.4/7	c	16.08	2.91	0	35.67	0	0	0	27.72	0	0	4.59	86.97
RB016.4/8	c	14.19	3.04	0	35.84	0	0	0	29.73	0	0	4.59	87.39
RB016.4/9	c	15.59	2.65	0	35.75	0	0	0	28.96	0	0	4.31	87.26
RB156.1/1	c	13.84	2.81	0	35.17	0	0	0	28.95	0	0	4.43	85.2

SAMPLE	LODE	FeO	Na2O	K2O	SiO2	MnO	CaO	NiO	Al2O3	TiO2	Cr2O3	MgO	Total
RB156.1/2	c	12.58	2.59	0	35.38	0	0.17	0	30.05	0	0	4.21	84.98
RB156.1/3	c	14.58	2.77	0	35.11	0	0	0	28.04	0.2	0	4.2	84.9
RB156.1/4	c	11.27	2.55	0	34.11	0	0	0	30.69	0.21	0	4.89	83.72
RB156.1/5	c	15.83	2.92	0	34.19	0	0	0	27.09	0.27	0	3.75	84.05
RB156.1/6	c	13.77	2.87	0	34.09	0	0	0	28.49	0.18	0	4.74	84.14
RB156.1/7	c	18.15	3.03	0	33.82	0	0	0	25.79	0.34	0	3.89	85.02
RB156.1/8	c	17.6	3.08	0	34.88	0	0	0	26.32	0.35	0	3.97	86.2
RB156.1/9	c	15.2	2.97	0	34.86	0	0.14	0	27.95	0.18	0	4.98	86.28
RB156.1/10	c	16.01	2.93	0	34.2	0	0	0	28.31	0.32	0	4.33	86.1
RB156.1/11	c	12.09	2.92	0	34.56	0	0.19	0	31.33	0.2	0	4.89	86.18
RB156.1/12	c	16.08	2.97	0	34.4	0	0.38	0	25.62	1.97	0	4.73	86.15
RB156.1/13	c	17.49	3.11	0	34.79	0	0	0	26.16	0.2	0	3.98	85.73
RB156.2/1	c	15.34	3.06	0	35.35	0	0	0	27.61	0	0	5.06	86.42
RB156.2/2	c	15.55	3.01	0	34.98	0	0	0	27.18	0.32	0	4.31	85.35
RB156.2/3	c	17.28	3.14	0	34.94	0	0	0	26.33	0.35	0	4.11	86.15
RB156.2/4	c	16.2	3.09	0	35.55	0	0	0	27.65	0	0	4.24	86.73
RB156.2/5	c	14.62	3.16	0	35.15	0	0	0	29.27	0	0	4.35	86.55
RB156.2/6	c	15.13	3.02	0	35.3	0	0	0	27.48	0.17	0	4.72	85.82
RB156.2/7	c	17.31	3.16	0	35.14	0	0.16	0	26.81	0.21	0	4.49	87.28
RB156.2/8	c	14.81	3.1	0	35.36	0	0.14	0	28.91	0	0	4.38	86.7
RB156.2/9	c	14.12	2.89	0	35.44	0	0.3	0	28.54	0.86	0	5.24	87.39
RB156.3/1	c	15.13	3.2	0	35.37	0	0	0	27.74	0.23	0	5.12	86.79
RB156.3/2	c	16.76	3.3	0	34.59	0	0	0	26.33	0.34	0	4.16	85.48
RB156.3/3	c	17.36	3.05	0	35.5	0	0	0	26.04	0.33	0	4.37	86.65
RB156.3/4	c	16.81	3.03	0	34.78	0	0	0	26.24	0.41	0	3.91	85.18
RB156.3/5	c	15.02	3.07	0	35.34	0	0	0	27.16	1.3	0.32	4.91	87.12
RB156.3/6	c	14.15	2.91	0	35.29	0	0	0	29.2	0	0.19	4.76	86.5
RB156.3/7	c	13.43	2.6	0	36.02	0	0	0	29.35	0	0	4.26	85.66
RB156.4/1	c	11.62	2.96	0	35.84	0	0	0	31.27	0	0	5.07	86.76
RB156.4/2	c	14.04	2.87	0	35.46	0	0	0	28.75	0	0	5.33	86.45
RB156.4/3	c	11.7	2.68	0	35.95	0	0	0	31.67	0	0	5	87
RB156.4/4	c	12.59	2.76	0.09	35.95	0	0.16	0	30.84	0	0	4.67	87.06
RB156.4/5	c	15.33	3.23	0	35.34	0	0.24	0	27.33	0.27	0	4.66	86.4
RB156.4/6	c	16.87	3.09	0	34.79	0	0	0	27.46	0.32	0	4.11	86.64
RB156.4/7	c	12.69	2.72	0	35.71	0	0	0	30.83	0.21	0	4.76	86.92
RB156.4/8	c	12.55	2.6	0	35.63	0	0	0	31.16	0	0	4.76	86.7
RB156.4/9	c	13.4	2.91	0	35.2	0	0	0	29.62	0.19	0	5.12	86.44
RB156.4/10	c	15.65	2.9	0	35.41	0	0	0	27.46	0	0	4.4	85.82
RB156.4/11	c	13.72	2.99	0	35.95	0	0	0	29.92	0	0	5.42	88
RB156.4/12	c	15.01	3.09	0	35.11	0	0.38	0	27.01	0	0	5.56	86.16
RB156.4/13	c	13.17	2.68	0	35.35	0	0	0	29.83	0	0	5.11	86.14

SAMPLE	LODE	FeO	Na2O	K2O	SiO2	MnO	CaO	NiO	Al2O3	TiO2	Cr2O3	MgO	Total
RB156.4/14	c	12.71	2.81	0	34.55	0	0	0	29.87	0	0	5.2	85.14
RB156.4/15	c	10.26	2.37	0	35.74	0	0	0	32.67	0	0	4.7	85.74
RB156.4/16	c	14.81	2.87	0	35.25	0	0.14	0	28.31	0	0	4.68	86.06
RB156.4/17	c	15.44	3.03	0	34.45	0	0.14	0	27	0	0	4.44	84.5
RB156.4/18	c	15.52	2.78	0.09	34.87	0	0.27	0	25.16	1.67	0	4.92	85.28
RB128.1/1	t	13.62	2.82	0	35.25	0	0.21	0	27.41	0.78	0	6.21	86.3
RB128.1/2	t	17.22	2.83	0	35.92	0	0.23	0	25.44	0.19	0	5.83	87.66
RB128.1/3	t	12.41	2.94	0	36.05	0	0.29	0	28.81	0.39	0.63	6.49	88.01
RB128.1/4	t	12.21	3.24	0	36.37	0	0.22	0	28.34	0.52	0	6.37	87.27
RB128.1/5	t	14.13	3	0	36.18	0	0.27	0	27.62	0.84	0	6.46	88.5
RB128.1/6	t	17.91	2.78	0	35.35	0	0.3	0	24.71	1.08	0	5.42	87.55
RB128.1/7	t	16.25	2.87	0	35.5	0	0.16	0	24.9	0	0	5.7	85.38
RB128.1/8	t	12.62	3.04	0	35.76	0	0	0	28.18	0.28	0	6.35	86.23
RB128.2/1	t	15.94	3.06	0	35.76	0	0	0	25.64	0.32	0	5.83	86.55
RB128.2/2	t	15.14	2.88	0	35.88	0	0.3	0	26.15	0.92	0	5.47	86.74
RB128.2/3	t	14.86	2.72	0	35.44	0	0.38	0	26.5	0.53	0	5.58	86.01
RB128.2/4	t	15.71	3.11	0	35.81	0	0.3	0	26.18	0.42	0	5.35	86.88
RB128.2/5	t	16.7	3.32	0	35.55	0	0.15	0	26.16	0	0	5.37	87.25
RB128.2/6	t	13.94	2.59	0	35.52	0	0.17	0	27.4	0.24	0	5.89	85.75
RB128.2/7	t	15.87	2.76	0	35.58	0	0.32	0	27.14	0.42	0	5.48	87.57
RB128.2/8	t	18.29	2.89	0	35.39	0	0.21	0	24.03	0.18	0	5.04	86.03
RB128.3/1	t	13.52	2.93	0	35.93	0	0.14	0	27.7	0	0	5.55	85.77
RB128.3/2	t	11.21	2.74	0	35.49	0	0	0	30.55	0	0	6.45	86.44
RB128.3/3	t	12.2	2.69	0	36.4	0	0	0	29.58	0	0	6.25	87.12
RB128.3/4	t	13.97	2.91	0	35.97	0	0	0	28.04	0	0	5.73	86.62
RB128.3/5	t	15.22	2.86	0	35.4	0	0.19	0	26.95	0.18	0	4.91	85.71
RB128.3/6	t	12.18	2.84	0	35.99	0	0	0	30.61	0	0	5.82	87.44
RB128.3/7	t	13.22	2.77	0	35.2	0	0	0	26.67	0	0	6.71	84.57
RB128.3/8	t	10.97	2.65	0	35.46	0	0	0	30.88	0	0	6.15	86.11
RB128.4/1	t	13.62	2.8	0	35.09	0	0	0	26.3	0	0	6.88	84.69
RB128.4/2	t	13.09	2.87	0	35.62	0	0	0	26.47	0	0	7.54	85.59
RB128.4/3	t	13.32	2.93	0	35.29	0	0	0	27.25	0	0	6.12	84.91
RB128.4/4	t	13.91	2.92	0	35.17	0	0	0	27.7	0	0	6.25	85.95
RB128.4/5	t	14.11	3.03	0	35.89	0	0	0	27.23	0	0	6.42	86.68
RB128.4/6	t	15.38	3.04	0	35.56	0	0	0	26.91	0.22	0	6.35	87.46
RB114.1/1	b	10.32	2.75	0	35.29	0	0.76	0	27.08	1.14	0	7.06	84.4
RB114.1/2	b	13.89	2.83	0	35.41	0	0.5	0	25.61	0.36	0	7.5	86.1
RB114.1/3	b	10.67	2.44	0	36.33	0	0.52	0	29.09	0.24	0	7.11	86.4
RB114.1/4	b	11.79	2.23	0	35.75	0	0.98	0	27.33	0.4	0	7.39	85.87
RB114.1/5	b	15.05	2.33	0	35.23	0	1.12	0	24.01	0.62	0	7.37	85.73
RB114.1/6	b	10.98	2.17	0	35.72	0	1.29	0	26.85	1.69	0	7.87	86.57

SAMPLE	LODE	FeO	Na2O	K2O	SiO2	MnO	CaO	NiO	Al2O3	TiO2	Cr2O3	MgO	Total
RB114.1/7	b	11.01	2.43	0	35.46	0	0.86	0	28.78	0.28	0	7.46	86.28
RB114.1/8	b	10.95	2.9	0	35.87	0	0.42	0	27.25	0	0	8.14	85.53
RB114.1/9	b	10.6	2.85	0	34.79	0	0.41	0	27.36	0	0	8.1	84.11
RB114.1/10	b	8.93	2.35	0	34.85	0	1	0	31.23	0.35	0	7.4	86.11
RB114.1/11	b	10.92	2.6	0	34.67	0	0.6	0	29.18	0	0	7.31	85.28
RB114.1/12	b	11.7	2.03	0	34.59	0	1.27	0	27.14	1.15	0	7.43	85.31
RB114.1/13	b	12.58	2.33	0	34.9	0	1.36	0	24.2	2.07	0	7.1	84.54
RB114.1/14	b	16.62	2.58	0.09	34.68	0	0.78	0	22.54	0.43	0	7.06	84.78
RB114.1/15	b	10.77	2.36	0	35.07	0	1.02	0	26.38	1.69	0.17	7.54	85
RB114.1/16	b	13.32	2.52	0	34.46	0	0.64	0	25.55	0.33	0	7.76	84.58
RB114.1/17	b	11.4	1.97	0	34.99	0	1.49	0	28.53	0.57	0	7.41	86.36
RB114.1/18	b	10.32	2.53	0	35.57	0	0.77	0	28.8	0	0	7.31	85.3
RB114.1/19	b	13.12	2.91	0	34.72	0	0.46	0	26.31	0	0	7.82	85.34
RB114.1/20	b	11.32	2.45	0	34.47	0	1.07	0	26.88	1.36	0.16	7.07	84.78
RB114.1/21	b	11.88	2.39	0	34.84	0	1.06	0	26.69	1.14	0.27	7.31	85.58
RB114.1/22	b	14.18	2.49	0	35.09	0	0.51	0	24.25	0	0	7.42	83.94
RB114.1/23	b	11.12	2.37	0	35.75	0	1.21	0	27.45	1.47	0	7.88	87.25
RB114.2/1	b	10.56	2.51	0	35.17	0	0.52	0	28.86	0.52	0	7.65	85.79
RB114.2/2	b	11.39	2.89	0	35.4	0	0.28	0	27.38	0	0	8.08	85.42
RB114.2/3	b	13.72	2.24	0	34.9	0	0.79	0	24.55	1.55	0	7.08	84.83
RB114.2/4	b	16.57	2.57	0	34.67	0	0.51	0	24.93	1.05	0	4.86	85.16
RB114.2/5	b	17.21	2.43	0.17	34.33	0	0.76	0	22.9	1.08	0	7.15	86.03
RB114.2/6	b	13.91	2.6	0	35.03	0	0.94	0	24.29	1.71	0	6.73	85.21
RB114.2/7	b	12.56	2.62	0	35.36	0	0.26	0	28.77	0.34	0.65	4.92	85.48
RB114.2/8	b	17.33	2.26	0	34.38	0	0.56	0	21.21	2.71	0	5.38	83.83
RB114.2/9	b	11.26	2.57	0	35.03	0	0.63	0	25.24	2.14	0	7.55	84.42
RB114.2/10	b	11.75	2.32	0	34.99	0	1.17	0	26.94	1.83	0	7.43	86.43
RB114.2/11	b	14.45	2.49	0.1	34.62	0.49	1	0	24.14	2.02	1.86	5.41	86.58
RB114.2/12	b	12.59	2.16	0	47.69	0	0.44	0	21.72	0.87	0	5.93	91.4
RB114.2/13	b	16.2	2.57	0	35.41	0	0.46	0	23.64	1.26	0	5.5	85.04
RB114.2/14	b	14.34	2.67	0	35.58	0	0.46	0	26.38	1.26	0	5.07	85.76
RB114.2/15	b	14.67	2.56	0	35.35	0	0.44	0	25.89	2.02	0.43	5.06	86.42
RB114.2/16	b	12.35	2.93	0	35.35	0	0.48	0	24.67	0.62	0	7.29	83.69
RB114.2/17	b	14.66	2.32	0	35.11	0	0.83	0	22.94	2.43	0	7.12	85.41
RB114.2/18	b	11.94	2.47	0	35.44	0	0.89	0	26.66	1.2	0	7.34	85.94
RB114.2/19	b	11.04	2.38	0	35.74	0	1.04	0	27.39	1.25	0	7.1	85.94
RB114.2/20	b	8.98	2.7	0	36.27	0	0.38	0	30.1	0.23	0	7.61	86.27
RB114.2/21	b	11.12	2.49	0	36.25	0	0.77	0	27.97	0.39	0	7.32	86.31
RB114.2/22	b	12.64	2.5	0	36.2	0	0.6	0	25.73	0.25	0	7.48	85.4
RB114.2/23	b	13.68	2.53	0	25.54	0	0.68	0	24.7	0.91	0	7.02	75.06
RB114.2/24	b	12.12	2.84	0	35.45	0	0.52	0	25.78	0	0	7.83	84.54

SAMPLE	LODE	FeO	Na2O	K2O	SiO2	MnO	CaO	NiO	Al2O3	TiO2	Cr2O3	MgO	Total
RB114.2/25	b	10.98	2.63	0	35.5	0.77	0.76	0	28.26	0.69	0	7.39	86.98
RB114.2/26	b	17.96	2.39	0	34.83	0	0.88	0	22.53	1.74	0	5.53	85.86
RB114.2/27	b	12.84	2.5	0.43	35.78	0	0.96	0	24.98	1.72	0	7.88	87.09
RB114.2/28	b	9.59	2.09	0	35.99	0	1.09	0	29.43	0.95	0	7.15	86.29
RB114.2/29	b	11.36	2.59	0	35.41	0	0.82	0	27.86	0	0	7.31	85.35
RB114.2/30	b	11.08	2.44	0	35.15	0	0.69	0	28.58	0.45	0	7.02	85.41
RB147.1/1	u	14.74	2.72	0	33.93	0	0.84	0	23.78	0.74	0	7.44	84.19
RB147.1/2	u	14.94	2.41	0.1	34.39	0	0.82	0	23.74	1.75	0	7.33	85.48
RB147.1/3	u	12.46	2.12	0	34.98	0	1.77	0	25.95	0.78	0	8.05	86.11
RB147.1/4	u	11.99	2.66	0	35.55	0	0.67	0	27	0.29	0	7.77	85.93
RB147.1/5	u	14.01	2.66	0	34.94	0	0.8	0	24.83	0.73	0	7.4	85.37
RB147.1/6	u	11.34	2.71	0	35.7	0	0.65	0	27.92	0.7	0	7.69	86.71
RB147.1/7	u	12.02	2.66	0	34.79	0	0.78	0	27.22	1	0	7.77	86.24
RB147.1/8	u	11.21	2.77	0	35.07	0	0.6	0	26.54	0.72	0	7.73	84.64
RB147.1/9	u	11.59	2.8	0	35.02	0	0.14	0	28.73	0.74	0.28	6.4	85.7
RB147.1/10	u	12.01	2.97	0	33.74	0	0.66	0	28.05	0.72	0.5	6.53	85.18
RB147.1/11	u	10.05	2.74	0	35.87	0	0.44	0	28.51	0.45	0	8.31	86.37
RB147.1/12	u	12.09	2.8	0	35.52	0	0.59	0	27.33	0.59	0	7.96	86.88
RB147.1/13	u	12.45	2.72	0	35.53	0	0.8	0.84	26.04	0.59	0	7.64	86.61
RB147.1/14	u	10.23	2.89	0	35.48	0	0.68	0	28.54	0.23	0	8.44	86.49
RB147.1/15	u	8.26	2.47	0	35.86	0	0.87	0	31.3	0.64	0	7.61	87.01
RB147.1/16	u	8.48	2.47	0	35.48	0	1.08	0	30.95	0.79	0	7.66	86.91
RB147.1/17	u	16.28	2.91	0.1	35.11	0	0.21	0	24.71	2.39	0	4.65	86.36
RB147.2/1	u	14.23	3.24	0	35.36	0	0.17	0	27.96	0.72	0	5.19	86.87
RB147.2/2	u	14.58	2.58	0	34.98	0	0.87	0	24.32	1.58	0	7.24	86.15
RB147.2/3	u	11.81	2.9	0	35.4	0	0.42	0	26.3	0.59	0	8.12	85.54
RB147.2/4	u	14.04	2.85	0	34.75	0	0.7	0	24.6	1.31	0	7.47	85.72
RB147.2/5	u	11.63	2.75	0	35.81	0	0.8	0	27.9	0.56	0	7.8	87.25
RB147.2/6	u	9.38	2.93	0	35.75	0	0.55	0	29.49	0	0	8.3	86.4
RB147.2/7	u	9.82	2.85	0	35.51	0	0	0	31.58	0.24	0.62	5.69	86.31
RB147.3/1	u	15.32	2.73	0.1	24.84	0	0.22	0	25.23	2.09	0	4.57	75.1
RB147.3/2	u	13.89	2.94	0	35.2	0	0.19	0	27.98	1.05	0.19	5.36	86.8
RB147.3/3	u	8.39	2.78	0	36.19	0	0	0	32.32	0	0.24	6.72	86.64
RB147.3/4	u	13.83	2.98	0.09	35.63	0	0	0	27.09	0.97	0	5.19	85.78
RB147.3/5	u	16.73	2.98	0.09	34.99	0	0.2	0	24.88	2.17	0	4.31	86.35
RB147.3/6	u	12.47	3.09	0	36.34	0	0	0	27.9	1.26	0	6.17	87.23
RB147.3/7	u	12.49	3.12	0	35.62	0	0	0	29.39	0.39	0	5.63	86.64
RB147.3/8	u	14.46	3.13	0	35.23	0	0.27	0	27.01	1.13	0	5.41	86.64
RB147.3/9	u	11.5	3	0	35.37	0	0	0	29.61	0.18	0	6.74	86.4
RB147.3/10	u	14.25	3.2	0	35.01	0	0.25	0	27.11	0.51	0	5.32	85.65
RB131.1/1	union	11.02	3.05	0	34.66	0	0.63	0.59	28.53	0.78	0	8.15	87.41

SAMPLE	LODE	FeO	Na2O	K2O	SiO2	MnO	CaO	NiO	Al2O3	TiO2	Cr2O3	MgO	Total
RB131.1/2	union	6.84	2.27	0	35.76	0	0.49	0	31.45	0.21	0	7.83	84.85
RB131.1/3	union	10.82	2.01	0	34.75	0	1.47	0	26.45	0.7	0	7.3	83.5
RB131.1/4	union	7.33	2.21	0	35.34	0	0.59	0	31.17	0	0	7.82	84.46
RB131.1/5	union	7.15	2.29	0	36.12	0	0.45	0	30.87	0	0	7.65	84.53
RB131.1/6	union	11.64	1.93	0	35.31	0	1.54	0	26	1.52	0.22	7.03	85.19
RB131.1/7	union	9.51	2.03	0	35.5	0	1.38	0	27.99	1.5	0	7.26	85.17
RB131.1/8	union	8.23	2.27	0	36.17	0	0.66	0	31.29	0	0	7.91	86.53
RB131.1/9	union	7.2	2.13	0	36.41	0	0.52	0	31.52	0	0	7.84	85.62
RB131.2/1	union	10.01	2.44	0	35.23	0	0.68	0	28.3	0.42	0	7.6	84.68
RB131.2/2	union	12.16	2.21	0	35.22	0	1.25	0	25.34	1.24	0	7.18	84.6
RB131.2/3	union	12.83	2.07	0	25.78	0	1.44	0	25.18	0.85	0	7.5	75.65
RB131.2/4	union	12.25	2.14	0.21	36.12	0	0.76	0	27.75	0.41	0	7.5	87.14
RB131.2/5	union	14.15	2.83	0	35.41	0	0.29	0	27.31	0	0	5.07	85.06
RB131.3/1	union	16.05	2.68	0	33.13	0	0.53	0	24.03	1.12	0	5.14	82.68
RB131.3/2	union	11.71	2.49	0	35.11	0	0.86	0	28.01	0.42	0	7.87	86.47
RB131.3/3	union	7.98	2.76	0	35.67	0	0.54	0	29.48	0	0	8.55	84.98
RB131.3/4	union	11.88	1.91	0	34.89	0	1.65	0	25.43	1.39	0.25	7	84.4
RB131.3/5	union	10.46	2.32	0	35.88	0	1.25	0	28.14	0.65	0	6.95	85.65
RB131.3/6	union	8.94	2.25	0	36.14	0	0.99	0	30.33	0.88	0	7.06	86.59
RB131.3/7	union	8.53	2.24	0	35.89	0	1.02	0	30.11	0.61	0	7.2	85.6
RB131.3/8	union	15.09	2.29	0.11	35.35	0	0.72	0	23.95	2.74	0	5.13	85.38
RB131.3/9	union	11.18	2.07	0	35.49	0	0.82	0	27.2	0.44	0	7.26	84.46

APPENIX D.3.3.
CARBONATE CHEMISTRY (wt %).

Sample numbering as follows: RB = Project reference, followed by the year.

SAMPLE	LODE	CaCO3	MgCO3	FeCO3	MnCO3	TOTAL
RB118.91	b	0.26	14.7	77.45	4.44	96.85
RB118.91	b	0.19	20.14	74.02	2.83	97.18
RB118.91	b	0.82	24.31	68.85	3.32	97.3
RB118.91	b	0.43	21.38	75.34	3.11	100.26
RB118.91	b	0.23	22.58	73.58	1.74	98.13
RB118.91	b	0.84	19.2	73.05	3.49	96.58
RB118.91	b	0	23.02	72.98	2.11	98.11
RB118.91	b	0.23	22.13	73.92	1.55	97.83
RB118.91	b	0.47	23.08	72.95	2.49	98.99
RB118.91	b	0.49	19.55	71.42	2.83	94.29
RB118.91	b	0.17	23.97	74.61	2.96	101.71
RB088.91	cotton	48.54	22.21	21.65	2.97	95.37
RB088.91	cotton	48.3	20.83	22.72	2.76	94.61
RB088.91	cotton	52.85	23.6	24.53	2.74	103.72
RB088.91	cotton	50.1	23.86	21.38	2.79	98.13
RB088.91	cotton	52.27	23.36	23.7	2.96	102.29
RB088.91	cotton	47.8	22.11	22.08	2.59	94.58
RB088.91	cotton	49.67	23.67	21.49	3.08	97.91
RB088.91	cotton	49.36	21.49	24.39	2.46	97.7
RB020.91	b	0.17	22.54	73.32	2.45	98.48
RB020.91	b	0	19.19	73.02	2.86	95.07
RB020.91	b	1.01	22.09	70.89	3.34	97.33
RB020.91	b	0.24	18.64	72.9	3.25	95.03
RB020.91	b	0.12	18.64	75.31	2.93	97
RB020.91	b	51.95	28.93	20.05	0.7	101.63
RB020.91	b	0.14	23.83	71.5	3.07	98.54
RB020.91	b	0.2	24.68	73.48	2.73	101.09
RB085.91	cotton	53.52	18.51	24.54	2.14	98.71
RB085.91	cotton	51.1	19.53	21.53	2.01	94.17
RB085.91	cotton	50.6	17.9	23.28	2.39	94.17
RB085.91	cotton	54.77	21.71	24.33	4.63	105.44
RB066.91	bonus	0.14	21.82	77.82	2.12	101.9
RB066.91	bonus	0.2	21.72	75.93	3.22	101.07
RB066.91	bonus	0.74	21.53	71.31	3.14	96.72
RB066.91	bonus	0.17	16.43	75.57	2.99	95.16
RB066.91	bonus	0.13	21.87	76.43	2.58	101.01
RB066.91	bonus	0.64	19.18	72.89	3.02	95.73
RB066.91	bonus	0.18	22.58	74.24	2.06	99.06
RB161.91	c	50.74	24.99	20.33	2.57	98.63
RB161.91	c	48.9	23.76	20.77	2.65	96.08
RB161.91	c	50.62	24.89	20.54	2.82	98.87
RB161.91	c	49.48	23.3	20.92	2.51	96.21
RB161.91	c	48.96	22.88	20.92	2.92	95.68
RB161.91	c	50.45	23.36	22.21	3.16	99.18

Sample		CaCO3	MgCO3	FeCO3	MnCO3	TOTAL
RB115.91	b	0	16.77	76.85	2.74	96.09
RB115.91	b	0.2	22.84	71.94	2.97	97.95
RB115.91	b	0.86	20.36	71.64	3.34	96.2
RB115.91	b	0.85	19.81	73.59	3.37	97.62
RB115.91	b	0.78	19.4	75.44	3.26	98.88
RB169.91	diss	50.34	21.8	24.52	3.19	99.85
RB169.91	diss	52.99	22.69	21.84	3.5	101.02
RB169.91	diss	52.08	24.23	19.6	3.54	99.45
RB016.91	c	0	24.2	77.83	2.32	104.35
RB016.91	c	0	21.14	75.45	2.51	99.1
RB016.91	c	0.16	20.73	76.48	2.36	99.73
RB016.91	c	0.55	21.17	75.75	2.97	100.44
RB016.91	c	0.47	24.43	70.75	2.56	98.21
RB016.91	c	0.23	26.49	68.06	1.94	96.72
RB016.91	c	0.12	25.28	71.42	2.03	98.85
RB089.91	cotton	51.74	27.86	14.19	2.62	96.41
RB089.91	cotton	52.68	31.66	10.41	3.36	98.11
RB089.91	cotton	46.85	17.46	27.96	1.71	93.98
RB089.91	cotton	48.59	22.16	25.09	1.06	97.17
RB052.91	u	52.97	27.63	117.56	4.32	102.48
RB052.91	u	53.32	26.27	18.63	4.37	102.59
RB052.91	u	50.58	24.79	17.02	4.42	96.81
RB052.91	u	51.26	25.23	17.1	3.86	97.45
RB052.91	u	51.49	24.08	19.01	3.78	98.36
RB052.91	u	47.11	24.75	16.47	3.52	91.85
RB120.91	b	0.15	21.63	69.94	2.81	94.53
RB120.91	b	0.17	18.26	74.95	3.44	96.882
RB120.91	b	0.31	14.27	77.36	3.57	95.51
RB120.91	b	0	18.16	74.91	3	96.07
RB120.91	b	0.26	16.38	78.1	2.97	97.71
RB037.91	bonus	0.13	20.55	71.56	3.1	95.34
RB147.91	u	49.88	23.11	24.33	1.15	98.47
RB147.91	u	50.54	28.91	17.42	0.61	97.48
RB147.91	u	51.28	26.05	22.26	0.68	100.27

APPENDIX D.3.4.
SULPHIDE CHEMISTRY (wt %).

Sample numbering as follows: RB = Project reference, followed by the year

SLIDE NR	LODE	POINT	DESCR.	S	Fe	Cu	Co	Ni	Zn	Mn	As	Pb	Ag	TOTAL
RB088.91	cotton	PY 1		51.32	47.53	0	0.08	0	0	0	0	0	0	99.04
RB088.91	cotton	PY 2	EDGE	51.04	47.46	0	0.16	0	0	0	0.44	0	0	99.16
RB088.91	cotton	PY 2	MID	51.87	47.74	0	0.07	0.06	0	0	0.12	0	0	99.9
RB088.91	cotton	PY 3	EDGE	52.14	47.41	0	0.1	0	0	0	0.14	0	0	99.86
RB088.91	cotton	PY 3	MID	51.33	47.58	0	0.07	0	0	0	0	0	0	99.1
RB088.91	cotton	PY 3	EDGE	51.31	47.25	0	0.24	0	0	0	0.5	0	0	99.34
RB088.91	cotton	PY 4	MID	51.37	47.5	0	0.07	0	0	0	0	0	0	99.04
RB088.91	cotton	PY 4	EDGE	50.69	46.16	0	0.32	1	0	0	0.25	0	0	98.47
RB088.91	cotton	PY 5	MID	50.89	47.33	0	0.11	0	0	0	0.4	0	0	98.81
RB088.91	cotton	PY 5	EDGE	50.99	46.14	0	0.25	1.02	0	0	0.16	0	0	98.62
RB088.91	cotton	PY 6	MID	51.51	47.3	0	0.15	0	0	0	0.15	0	0	99.28
RB016.91	c	PY 1		51.98	43.51	0.23	0.15	4.35	0	0	0	0	0	100.3
RB016.91	c	PY 2	IN CHPY	52.28	44.85	0.24	0.25	2.74	0	0	0.11	0	0	100.5
RB016.91	c	PY 4		52.21	47.03	0.12	0.1	0.21	0	0	0.07	0	0	99.86
RB016.91	c	PY 5		51.68	45.7	1.6	0.35	1.24	0	0	0.08	0	0.09	100.79
RB016.91	c	PY 6		52.22	44.15	0.07	2.61	0.81	0	0	0.13	0	0	100.04
RB161.91	c	PY 1	MID	48.59	43.96	0	0.23	2.57	0	0	3.8	0	0.06	99.25
RB161.91	c	PY 1	MID	50.03	44.37	0	0.15	0.55	0	0	0	0	0.27	96.03
RB161.91	c	PY 3		52.2	46.71	0	0.09	0.2	0	0	0.19	0	0.07	99.51
RB161.91	c	PY 4	INCL LIGH	44.04	40.45	0	0.08	0.18	0	0	0.19	0	16.97	101.95
RB161.91	c	PY 5	INCL LIGH	52.89	47.08	0	0.45	0.27	0	0	0.09	0	0.16	100.95
RB161.91	c	PY 6	INCL LIGH	52.56	47.06	0	0.14	0.32	0	0	0.41	0	0.07	100.57
RB161.91	c	PY 6		52.84	47.18	0	0.1	0.12	0	0	0.18	0	0	100.47
RB161.91	c	PY 7		52.91	46.71	0	0.24	0	0	0	0.12	0	0	100.06
RB161.91	c	PY 8		52.85	46.95	0	0.06	0.04	0	0	0.13	0	0	100.14
RB161.91	c	PY 9 A	MID	52.72	46.76	0	0.05	0	0	0	0.07	0	0	99.65
RB161.91	c	PY 9 B		52.79	46.54	0	0.06	0.26	0	0	0	0	0	99.74
RB161.91	c	PY 9 C		52.3	44.55	0	1.49	1.35	0	0	0.51	0	0	100.22
RB161.91	c	PY 9 D		52.92	44.97	0	0.18	2.41	0	0	0.13	0	0	100.65
RB161.91	c	PY 9 E		52.81	47.13	0	0.07	0	0	0	0.11	0	0	100.18
RB161.91	c	PY 10	ASS MUSC	53.08	47.13	0	0.07	0.48	0	0	0	0	0.06	100.9
RB161.91	c	PY 12		52.92	47.02	0.2	0.19	0	0	0	0.07	0	0	100.48
RB085.91	cotton	PY 1	INCL LIGH	52.35	47.42	0	0.07	0.09	0	0	0.16	0	0	100.18
RB085.91	cotton	PY 2		52.04	46.85	0	0.07	0.16	0	0	0.16	0	0	99.32

SLIDE NR	LODE	POINT	DESCR.	S	Fe	Cu	Co	Ni	Zn	Mn	As	Pb	Ag	TOTAL
RB085.91	cotton	PY 3		52.62	47.41	0	0.08	0.05	0	0	0.19	0	0	100.42
RB085.91	cotton	PY 4	LIGHT STR	52.44	47.45	0	0.07	0	0	0	0.12	0	0	100.11
RB085.91	cotton	PY 5		52.51	47.21	0	0.08	0	0	0	0.19	0	0	100.04
RB085.91	cotton	PY 6		52.27	47.07	0	0.07	0	0	0	0.09	0	0	99.55
RB085.91	cotton	PY 8		52.56	46.94	0	0.07	0	0	0	0.13	0	0	99.77
RB085.91	cotton	PY 9	INCL LIGH	52.63	47.83	0	0.07	0	0	0	0.13	0	0	100.84
RB066.91	bonus	PY 1	EDGE	52	47.25	0	0.08	0.25	0	0	0.62	0	0	100.24
RB066.91	bonus	PY 1	MID	52.36	47.49	0	0.06	0.16	0	0	0.1	0	0	100.26
RB066.91	bonus	PY 2		51.67	46.83	0	0.07	0.69	0	0	0.4	0	0	99.7
RB066.91	bonus	PY 3		52.52	47.07	0	0.09	0.39	0	0	0.07	0	0	100.22
RB066.91	bonus	PY 4		52.29	46.55	0	0.07	1.04	0	0	0.07	0	0	100.07
RB066.91	bonus	PY 5	MID	52.09	45.78	0	0.06	1.95	0	0	0	0	0	100
RB066.91	bonus	PY 5	EDGE	52.2	45.97	0	0.33	1.51	0	0	0.31	0	0	100.38
RB066.91	bonus	PY 6		51.36	47.25	0	0.07	0.44	0	0	0.41	0	0	99.57
RB066.91	bonus	PY 7		51.81	47.75	0	0.06	0.18	0	0	0.33	0	0	100.2
RB037.91	bonus	PY 1	MID	52.09	46.96	0	0.29	0.17	0	0	0.1	0	0	99.66
RB037.91	bonus	PY 1	EDGE	51.83	46.65	0	0.84	0.04	0	0	0.09	0	0	99.56
RB037.91	bonus	PY 2		52.01	47.46	0	0.12	0	0	0	0.08	0	0	99.71
RB037.91	bonus	PY 3		52.22	47.46	0	0.13	0	0	0	0.11	0	0	99.99
RB037.91	bonus	PY 4		51.72	46.71	0	0.43	0.38	0	0	0.27	0	0	99.57
RB037.91	bonus	PY 5	ASS CASS	52.24	47.74	0	0.13	0	0	0	0.07	0	0	100.21
RB037.91	bonus	PY 6	EDGE	51.92	47.22	0	0.26	0	0	0	0.19	0	0	99.77
RB037.91	bonus	PY 6	MID	51.95	47.45	0	0.15	0	0	0	0.28	0	0	99.88
RB037.91	bonus	PY 7		51.66	46.46	0	0.28	0.65	0	0	0.08	0	0	99.18
RB037.91	bonus	PY 8		52.03	47.45	0	0.1	0	0	0	0	0	0	99.7
RB037.91	bonus	PY 9		51.98	47.27	0	0.17	0	0	0	0.28	0	0	99.76
RB115.91	b	CHPY 1		51.43	45.92	0.12	0.26	1.07	0	0	0	0	0	98.92
RB115.91	b	PY 2		51.69	44.71	0	0.69	2.4	0	0	0	0	0	99.62
RB115.91	b	PY 3		51.08	44.3	0.62	0.32	2.65	0	0	0	0	0	99.12
RB115.91	b	PY		50.98	44.26	0	0.18	2.74	0	0	0	0	0.22	98.5
RB115.91	b	PY 4		51.2	43.69	0.91	0.6	2.87	0	0	0	0	0	99.42
RB115.91	b	PY 5		50.8	44.12	0	1.13	2.23	0	0	0	0	0	98.42
RB115.91	b	PY 5		51.55	45.908	0	0.124	1.345	0	0	0	0	0	99.147
RB115.91	b	PY 6		51.328	46.043	0.082	0.09	1.36	0	0	0	0	0	98.998
RB115.91	b	PY 7		51.366	44.194	0	0.051	3.319	0	0	0	0	0	98.997
RB127.91	HW to TZ	PY 1	EDGE	52.381	47.027	0	0.757	0	0	0	0.073	0	0	100.257
RB127.91	HW to TZ	PY 1	MID	51.797	46.745	0	0.686	0	0	0	0.071	0	0	99.364
RB127.91	HW to TZ	PY 2		52.249	47.018	0	0.84	0	0	0	0	0	0	100.229
RB127.91	HW to TZ	PY 3		52.106	46.925	0	0.621	0	0	0	0	0	0	99.762
RB127.91	HW to TZ	PY 4		52.064	47.067	0	0.589	0	0	0	0	0	0	99.814
RB127.91	HW to TZ	PY 5		52.158	47.166	0	0.406	0	0	0	0	0	0	99.857

SLIDE NR	LODE	POINT	DESCR.	S	Fe	Cu	Co	Ni	Zn	Mn	As	Pb	Ag	TOTAL
RB127.91	HW to TZ	PY 6		51.84	46.969	0	0.457	0	0	0	0.073	0	0	99.375
RB127.91	HW to TZ	PY 7	MID	52.378	46.227	0	1.966	0	0	0	0.077	0	0	100.69
RB127.91	HW to TZ	PY 8		52.14	47.036	0	0.778	0	0	0	0.104	0	0	100.125
RB148.91	u	PY 1		51.344	46.16	0	0.774	0.056	0	0	0.294	0	0	98.657
RB148.91	u	PY 3		51.452	45.653	0	0.621	0.726	0	0	0.23	0	0	98.765
RB148.91	u	PY 4		51.559	47.252	0	0.106	0	0	0	0	0	0	99.031
RB148.91	u	PY 5		51.691	45.193	0	1.539	0.428	0	0	0.814	0	0	99.705
RB089.91	cotton	PY 1		52.162	47.515	0	0.058	0.083	0	0	0.071	0	0	99.923
RB089.91	cotton	PY 2		51.071	47.089	0	0.076	0.153	0	0	0.162	0	0	983591
RB089.91	cotton	PY 3		51.541	47.166	0	0.07	0.224	0	0	0	0	0	99.087
RB089.91	cotton	PY 4		52.273	47.389	0	0.068	0	0	0	0.114	0	0	99.938
RB089.91	cotton	PY 6		52.406	47.631	0	0.064	0.047	0	0	0.086	0	0	100.294
RB089.91	cotton	PY 7		52.384	47.526	0	0.068	0.081	0	0	0.182	0	0	100.283
RB089.91	cotton	PY 8		50.601	46.879	0	0.084	0	0	0	1.622	0	0	99.207
RB128.91	t	PY 1		51.669	46.606	0	0.511	0.036	0	0	0.099	0	0	98.963
RB128.91	t	PY 2		52.004	46.901	0	0.614	0.039	0	0	0.218	0	0	99.838
RB128.91	t	PY 3		52.268	47.311	0	0.432	0.13	0	0	0	0	0	100.204
RB128.91	t	PY 4		52.204	46.752	0	1.027	0	0	0	0	0	0	100.13
RB128.91	t	PY 4	REPEAT	51.752	46.784	0	0.552	0.038	0	0	0.105	0	0	99.282
RB128.91	t	PY 5		52.329	47.096	0	0.121	0	0	0	0.087	0	0	99.731
RB128.91	t	PY 6		52.551	46.072	0	1.769	0	0	0	0.083	0	0	100.513
RB128.91	t	PY 6 B		52.089	46.776	0	0.559	0.09	0	0	0	0	0	99.628
RB128.91	t	PY 7 A		51.798	46.409	0	0.587	0.122	0	0	0.243	0	0	99.263
RB128.91	t	PY 7 B		51.963	46.696	0	0.344	0	0	0	0.156	0	0	99.177
RB128.91	t	PY 7 C		51.79	46.19	0	1.001	0.062	0	0	0.236	0	0	99.407
RB128.91	t	PY 7 D		52.006	46.286	0	1.473	0	0	0	0.141	0	0	100.019
RB128.91	t	PY 7 E		51.942	46.247	0	0.894	0	0	0	0.149	0	0	99.367
RB128.91	t	PY 8		51.624	46.795	0	0.216	0.14	0	0	0	0	0	98.863
RB020.91	b	CHPY 2		33.862	31.355	34.405	0	0	0	0	0	0	0	99.804
RB020.91	b	CHPY 3		33.939	31.354	34.517	0.044	0	0	0	0.094	0	0	100.142
RB020.91	b	CHPY 4		33.799	31.072	34.675	0.035	0	0	0	0.082	0	0	99.666
RB020.91	b	CHPY 5		33.882	31.559	34.383	0.049	0	0	0	0	0	0	99.983
RB016.91	c	CHPY 1		34.07	31.26	34.85	0.04	0	0	0	0	0	0	100.28
RB016.91	c	CHPY 2		34.35	31.59	34.97	0.04	0	0	0	0.08	0	0	101.08
RB016.91	c	CHPY 3		34.3	31.49	34.7	0.04	0	0	0	0.07	0	0	100.64
RB016.91	c	CHPY 4		34.3	31.69	34.89	0.05	0	0	0	0	0	0	101.01
RB016.91	c	CHPY 5		33.43	30.13	33.83	0.05	0	0	0	0	0	0	97.53
RB016.91	c	CHPY 6	ASS CASS	34.62	31.43	35.06	0.05	0	0	0	0.09	0	0	101.31
RB016.91	c	CHPY 7		34.7	31.61	35.15	0.05	0	0	0	0	0	0	101.63
RB088.91	cotton	PY 3	INCL	38.03	34.06	26.67	0.15	0.83	0	0	0.15	0	0	99.89
RB088.91	cotton	CHPY 1		34.42	31.12	34.6	0.05	0	0	0	0.09	0	0	100.31

SLIDE NR	LODE	POINT	DESCR.	S	Fe	Cu	Co	Ni	Zn	Mn	As	Pb	Ag	TOTAL
RB088.91	cotton	CHPY 2		34.28	31.46	34.99	0	0	0	0	0	0	0	100.87
RB088.91	cotton	CHPY 3		34.3	31.55	35.04	0.04	0	0	0	0	0	0	101.04
RB088.91	cotton	CHPY 4		34.02	31.2	34.77	0.04	0	0	0	0.07	0	0	100.13
RB088.91	cotton	CHPY 5		34.34	31.24	35.02	0.04	0	0	0	0	0	0	100.73
RB088.91	cotton	CHPY 6		33.97	31.15	35.01	0.04	0	0	0	0	0	0	100.22
RB088.91	cotton	CHPY 7		33.66	31.5	34.8	0.05	0	0	0	0.07	0	0	100.1
RB088.91	cotton	CHPY 8		34.01	31.21	34.67	0.06	0	0	0	0	0	0	100.03
RB115.91	b	CHPY 1.1		34.05	30.97	34.56	0.06	0	0	0	0.08	0	0	99.78
RB115.91	b	CHPY	VEIN IN PY	34.15	31.8	33.48	0.14	0.05	0	0	0.09	0	0	99.76
RB115.91	b	CHPY 3		33.86	31.74	34.22	0.04	0	0	0	0	0	0	100.18
RB115.91	b	CHPY 4		33.82	31.55	34.5	0.05	0	0	0	0	0	0	100.02
RB115.91	b	CHPY 5		33.894	31.161	34.615	0.034	0	0	0	0	0	0	99.798
RB115.91	b	CHPY 6		33.84	31.173	34.429	0.036	0	0	0	0	0	0	99.715
RB115.91	b	CHPY 7		33.233	31.089	34.493	0.053	0	0	0	0.112	0	0	99.113
RB161.91	c	PY 11	CHPY INCL	38.6	35.8	23.82	0.2	0.18	0	0	0.07	0.17	0	98.89

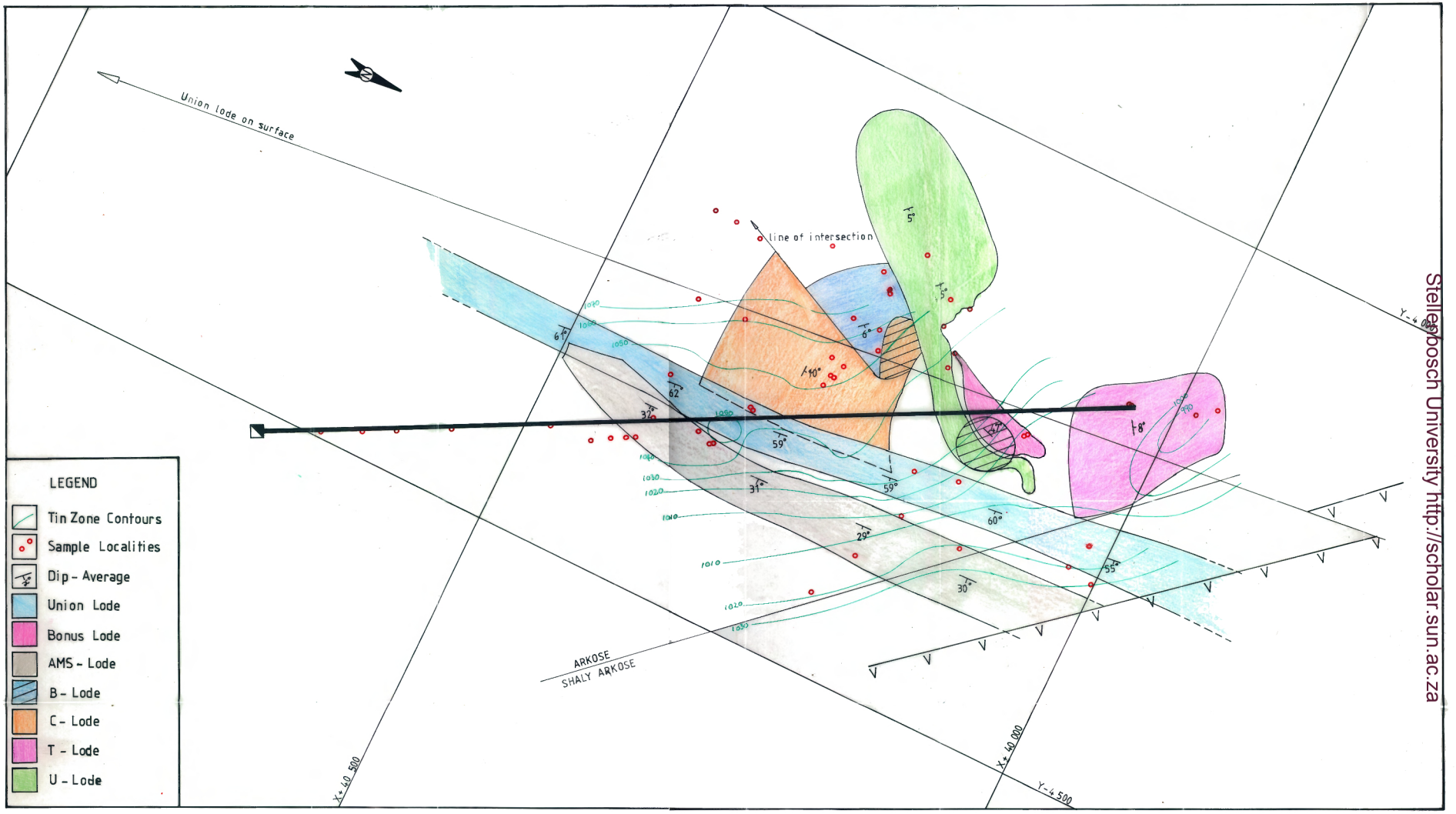

ROOIBERG NAD MINE
Extent of Ore Lodes
1 : 2 500
February 1991